

# Manufacturing Cost Analysis of 100 and 250 kW Fuel Cell Systems for Primary Power and Combined Heat and Power Applications

Prepared by:  
Battelle Memorial Institute  
505 King Avenue  
Columbus, OH 43201

Prepared for:  
U.S. Department of Energy  
DOE Contract No. DE-EE0005250

January 2017

Acknowledgment: This material is based upon work supported by the U.S. Department of Energy under DOE Contract Number DE-EE0005250.

Disclaimer: This report was prepared as an account of work sponsored by an agency of the United States Government. Neither the United States Government nor any agency thereof, nor any of their employees, makes any warranty, express or implied, or assumes any legal liability or responsibility for the accuracy, completeness, or usefulness of any information, apparatus, product, or process disclosed, or represents that its use would not infringe privately owned rights. Reference herein to any specific commercial product, process, or service by trade name, trademark, manufacturer, or otherwise does not necessarily constitute or imply its endorsement, recommendation, or favoring by the United States Government or any agency thereof. The views and opinions of authors expressed herein do not necessarily state or reflect those of the United States Government or any agency thereof.

This report is a work prepared for the United States Government by Battelle. In no event shall either the United States Government or Battelle have any responsibility or liability for any consequences of any use, misuse, inability to use, or reliance upon the information contained herein, nor does either warrant or otherwise represent in any way the accuracy, adequacy, efficacy, or applicability of the contents hereof.

## Acknowledgments

Funding and support of this work by the U.S. Department of Energy, Fuel Cell Technologies Office, is gratefully acknowledged.

## Collaborators

The following have provided assistance in the form of design inputs, cost inputs, design review and manufacturing review. Their valuable assistance is greatly appreciated.

- National Renewable Energy Laboratory (NREL)
- Hydrogenics
- Ballard
- Nexceris
- Johnson Matthey/Catacel
- Strategic Analysis
- US Hybrid
- dPoint Technologies
- Panasonic
- Advanced Power Associates
- Ideal Power
- Innovatek
- Zahn Electronics
- Watt Fuel Cell
- Vicor Power
- SMA-America
- Outback Power Technologies
- Tranter
- API Heat Transfer
- Dry Coolers
- Cain Industries

Battelle would also like to thank Tom Benjamin for strengthening the report through his thorough review.

## Executive Summary

Fuel cell power systems may be beneficially used to offset all or a portion of grid-purchased electrical power and supplement on-site heating or cooling requirements. For this application, the fuel of choice is usually pipeline natural gas or on-site propane storage. These fuel sources generally have much higher reliability than utility electric power, being less subject to damage-related outages, and can therefore provide for some continued operation in the event of grid outage – performing both primary power and back-up power functions. Battelle evaluated low-temperature polymer electrolyte membrane (LTPEM) fuel cell systems and solid oxide fuel cell (SOFC) systems for use as continuous power (primary power) and as a source for auxiliary heating in combined heat and power (CHP) configurations. The power levels considered for this portion of the project were 100 kilowatts (kW) and 250. A significant primary-power/CHP commercial market has not yet developed in this size range; however, our analysis suggests an attractive business opportunity under the right conditions. Indeed, FuelCell Energy, Bloom, and Doosan are approaching the primary power market with three different fuel cell technologies (molten carbonate, solid oxide, and phosphoric acid, respectively) and are achieving some market penetration. Based on the installed applications from these companies, we believe that fuel cell systems of this size will primarily serve medium to large commercial buildings, data centers, product distribution centers, and light industrial fabrication/manufacturing sites. We also suggest that utility operators and municipality-operated power companies may find these systems attractive for distributed generation and electric power islanding support.

In the absence of a developed market and publicly available system configuration information, Battelle's evaluation included the definition of representative systems that could serve this market. The representative system concepts were subjected to detailed cost evaluation based on industry feedback and the application of standard design for manufacturing and assembly analysis methods, including the application of the Boothroyd Dewhurst, Inc. Design for Manufacture and Assembly (DFMA®) software for specific hardware and assembly evaluation. A sensitivity analysis was performed to evaluate the influence of high cost/custom subassemblies and components with a high degree of cost uncertainty. Commercially available components and commodity materials generally have a low level of variability and do not significantly impact the overall economics. Because some of the commercially available balance of plant (BOP) hardware for systems in this range is commonly configured for different operating conditions (typically higher pressure), some assumptions are required regarding customization of hardware such as heat exchangers.

The evaluation shows that the highest cost category for these systems is the BOP hardware directly related to connecting to the grid – the inverter. For this evaluation we selected recently developed hybrid inverters which incorporate a separate direct current input/output (I/O) port for connection to batteries. These inverters, while initially more expensive than a more conventional inverter, eliminate the need for a direct current/direct current (DC/DC) converter to match battery voltage as we have used in prior system analyses. Eliminating the DC/DC converter saves significant cost though the power electronics still represent the highest cost system component. Hybrid inverters are relatively new technology developed primarily for solar applications, and as such, their costs, particularly for higher volumes, are not well defined. Therefore, while the selection of the hybrid inverter does represent some uncertainty, the benefit is so clear for both fuel cell and solar installations that we believe some version of hybrid inverter will be available for fuel cell systems.

Heat exchangers, particularly high-temperature heat exchangers, also represent a major portion of the BOP. For the PEM system the most expensive heat exchanger was the steam superheater/reformate

cooler. Our cost for this heat exchanger was based on a commercially available heat exchanger that is oversized for the application and is hence probably more expensive than necessary. A designed-to-purpose heat exchanger may offer notable savings.

PEM stack costs were less than 18% of overall system cost for all sizes and production volumes considered – averaging 14% at the higher production volumes. SOFC stacks, however, represented a notably larger fraction of overall costs (~25-29%) as a result of a much simpler BOP.

A sensitivity analysis of some of the major cost contributors shows the potential for further cost reductions through design-to-purpose engineering for some high cost items, especially for heat exchangers. Unlike prior studies, we found the price of platinum to have a minor overall impact on the PEM system cost. This primarily results from the relatively small overall contribution of the stack to system costs at this size. As noted above, a significant cost benefit at the system level was achieved by using a hybrid converter in place of a DC/DC converter and separate DC/AC inverter. Although not specifically considered in the sensitivity analysis, we outline a possible method of directly connecting batteries in parallel with the fuel cell that may be satisfactory for some applications, providing another path to cost reduction.

A life cycle cost analysis was performed for a nominal commercial installation requiring electrical power and additional heating or cooling energy input. With or without a supplemental heat requirement, the analysis showed a significant positive return on investment (ROI) for locations where electricity prices are high and natural gas prices are low. For applications with a need for supplemental space or process heating the number of attractive geographic installation sites increases. The analysis considered the utility costs for specific states, finding several to be attractive for fuel cell installations. However, when the overall gas and electricity cost averages for the US were considered, the ROI was not good until high production volumes are reached suggesting that additional capital cost reduction is needed to achieve widespread acceptance.

Our analysis shows that the stack costs, while a significant portion of the overall system costs, may not be the most critical area in need of development for achieving attractive initial costs. Instead, engineering activities focused on addressing cost reductions for power electronics (all systems) and heat exchangers (primarily PEM systems) are appropriate. SOFC systems were found to have better ROI than PEM systems based on initial costs and overall efficiency, however, the lifetime for SOFC stacks has not yet been demonstrated to the necessary level under deployed operating conditions.

# Table of Contents

	Page
<b>Acknowledgments</b> .....	<b>i</b>
<b>Executive Summary</b> .....	<b>ii</b>
<b>1. Introduction</b> .....	<b>1</b>
<b>2. Approach</b> .....	<b>1</b>
<b>3. Market Analysis</b> .....	<b>3</b>
3.1 Market Requirements and Desired Features .....	6
3.2 Technology Selection .....	7
3.3 Market Analysis Conclusion .....	7
<b>4. System Specifications</b> .....	<b>8</b>
4.1 General Description .....	8
4.2 Nominal Metrics .....	9
4.3 System Sizing and Operation .....	11
4.4 System Configuration .....	13
4.4.1 PEM System .....	14
4.4.2 SOFC System .....	17
4.5 Electrical System .....	19
4.5.1 Overview .....	19
4.5.2 On-Grid Operation .....	20
4.5.3 Off-Grid Operation .....	21
4.5.4 System Configurations .....	22
4.5.5 Thermal Management .....	26
4.5.6 Wiring and Ancillary Components .....	27
<b>5. Manufacturing Cost Analysis</b> .....	<b>27</b>
5.1 System Cost Scope .....	27
5.2 System Cost Approach .....	27
5.2.1 System Manufacturing Cost Assumptions .....	28
5.2.2 Machine Costs .....	28
5.2.3 Material Costs .....	29
5.3 PEM System Manufacturing Costs .....	29
5.3.1 PEM Stack Manufacturing Process .....	31
5.3.2 PEM Systems BOP Manufacturing Cost Assessment .....	42
5.3.3 PEM BOP Cost Assumptions .....	48
5.3.4 PEM System Assembly and Learning Curve Assumptions .....	52
5.3.5 PEM CHP System Testing .....	52
5.3.6 PEM Capital Cost Assumptions .....	53
5.4 SOFC System Manufacturing Costs .....	54
5.4.1 SOFC Stack Manufacturing Process .....	56
5.4.2 SOFC Systems BOP Manufacturing Cost Assessment .....	70
5.4.3 SOFC BOP Cost Assumptions .....	73
5.4.4 SOFC System Assembly and Learning Curve Assumptions .....	77
5.4.5 SOFC System Testing .....	77

5.4.6 SOFC Capital Cost Assumptions .....	78
5.5 Electrical System Cost Assumptions.....	79
5.5.1 DC/DC and DC/AC Power Electronics.....	79
5.5.2 Controller and Sensors.....	80
5.5.3 Protection and Interconnects .....	81
5.5.4 Electrical Cost Summary .....	83
<b>6. Limitations of the Analysis .....</b>	<b>83</b>
6.1 PEM Manufacturing Costs .....	83
6.1.1 PEM Stack Manufacturing Costs .....	84
6.1.2 PEM BOP Hardware Costs .....	85
6.2 SOFC Manufacturing Costs .....	85
6.2.1 SOFC Stack Manufacturing Costs .....	85
6.2.2 SOFC BOP Hardware Costs .....	86
<b>7. Cost Analysis Results .....</b>	<b>87</b>
7.1 PEM CHP Systems .....	87
7.2 SOFC CHP Systems.....	92
7.3 Future Cost Reduction .....	96
<b>8. Sensitivity Analysis .....</b>	<b>97</b>
8.1 PEM System.....	97
8.2 SOFC System .....	100
<b>9.0. Life Cycle Cost Analyses of Fuel Cells.....</b>	<b>102</b>
9.1 Introduction.....	102
9.2 Scenarios Evaluated .....	102
9.3 Results	105
9.4 Conclusions.....	113
<b>10.0. Conclusions.....</b>	<b>113</b>
10.1 System Cost Summary .....	113
10.2 Value Proposition .....	119
10.3 Sensitivity and Future Market Impact.....	120
<b>Appendix A-1: Machine Rate with Make-Buy Calculations.....</b>	<b>A-1-1</b>
<b>Appendix A-2: Material Cost Learning Curve Calculations .....</b>	<b>A-2-1</b>
<b>Appendix A-3: Assembly Cost Learning Curve Calculations.....</b>	<b>A-3-1</b>
<b>Appendix A-4: PEM Production Facility Estimation .....</b>	<b>A-4-1</b>
<b>Appendix A-5: PEM End Plate Manufacturing Process .....</b>	<b>A-5-1</b>
<b>Appendix A-6: PEM Platinum Catalyst Coating Process .....</b>	<b>A-6-1</b>
<b>Appendix A-7: PEM MEA Hot Pressing Process .....</b>	<b>A-7-1</b>
<b>Appendix A-8: PEM Seal Injection Molding Process.....</b>	<b>A-8-1</b>
<b>Appendix A-9: PEM Bipolar Plate Compression Molding Process.....</b>	<b>A-9-1</b>
<b>Appendix A-10: PEM Stack Testing and Conditioning Process.....</b>	<b>A-10-1</b>
<b>Appendix A-11: SOFC Production Facility Estimation.....</b>	<b>A-11-1</b>

**Appendix A-12: SOFC Ceramic Slurry Production Process ..... A-12-1**

**Appendix A-13: SOFC Anode Blanking Process ..... A-13-1**

**Appendix A-14: SOFC Screen Printing Process Ceramic Screen Printing Process ..... A-14-1**

**Appendix A-15: SOFC Kiln Firing Process ..... A-15-1**

**Appendix A-16: SOFC Sintering Process ..... A-16-1**

**Appendix A-17: SOFC Final Trim Process ..... A-17-1**

**Appendix A-18: SOFC Interconnect Production Process ..... A-18-1**

**Appendix A-19: SOFC Picture Frame Production Process ..... A-19-1**

**Appendix A-20: SOFC Glass-Ceramic Sealant Production Process ..... A-20-1**

**Appendix A-21: SOFC Stack Brazing Process ..... A-21-1**

**Appendix A-22: SOFC Tape Casting Process ..... A-22-1**

**Appendix A-23: SOFC Testing and Conditioning Process ..... A-23-1**

**Appendix A-24: SOFC End Plate Manufacturing Process ..... A-24-1**

**Appendix A-25: Mesh Production Process ..... A-25-1**

**Appendix A-26: Laser Welding Process ..... A-26-1**

List of Tables

	Page
Table 4-1. Nominal Design Basis.....	10
Table 5-1. General Process Cost Assumptions.....	28
Table 5-2. PEM Fuel Cell Design Parameters.....	30
Table 5-3. PEM MEA Material Cost Summary - 100 kW and 250 kW.....	34
Table 5-4. PEM MEA Cost Summary - 100 kW and 250 kW.....	34
Table 5-5. PEM End Plate Cost Summary - 100 kW and 250 kW.....	36
Table 5-6. PEM Anode Bipolar Plate Cost Summary - 100 kW and 250 kW.....	36
Table 5-7. PEM Cathode Bipolar Plate Cost Summary – 100 kW and 250 kW.....	37
Table 5-8. PEM Anode and Cooling Seal Cost Summary - 100 kW and 250 kW.....	37
Table 5-9. PEM Cathode Seal Cost Summary – 100 and 250 kW Systems.....	38
Table 5-10. PEM Stack Assembly Costs - 100 kW and 250 kW Systems.....	38
Table 5-11. PEM Stack Testing and Conditioning Cost Summary - 100 kW and 250 kW.....	39
Table 5-12. PEM Stack Component Cost Summary - 100 kW and 250 kW.....	40
Table 5-13. PEM Stack Manufacturing Cost Summary - 100 kW and 250 kW.....	40
Table 5-14. PEM Reformer Sizing Parameters.....	44
Table 5-15. PEM Reformer Dimensional Summary.....	45
Table 5-16. PEM System Reformer Cost Summary - 100 kW and 250 kW.....	45
Table 5-17. PEM Shift/PrOx Reactor Sizing Recommendations.....	46
Table 5-18. PEM Shift/PrOx Reactor Dimensional Summary.....	46
Table 5-19. Shift and PrOx Reactor Manufacturing Costs.....	48
Table 5-20. PEM BOP Cost Summary for 100-kW and 250-kW Systems.....	49
Table 5-21. PEM System Assembly Costs - 100 kW and 250 kW.....	52
Table 5-22. PEM System Testing Cost Summary - 100 kW and 250 kW.....	52
Table 5-23. Summary of PEM Capital Cost Assumptions.....	53



Table 5-24. PEM Capital Cost Summary - 100 kW and 250 kW .....	54
Table 5-25. SOFC Fuel Cell Design Parameters.....	55
Table 5-26. SOFC Ceramic Cell Cost Summary—100 kW and 250 kW .....	60
Table 5-27. SOFC End Plate Cost Summary - 100 kW and 250 kW.....	61
Table 5-28. SOFC Interconnect Cost Summary - 100 kW and 250 kW .....	62
Table 5-29. SOFC Anode Frame Cost Summary - 100 kW and 250 kW .....	63
Table 5-30. SOFC Picture Frame Cost Summary - 100 kW and 250 kW .....	63
Table 5-31. SOFC Cathode Frame Cost Summary - 100 kW and 250 kW .....	64
Table 5-32. SOFC Laser Welding Cost Summary - 100 kW and 250 kW .....	64
Table 5-33. SOFC Ceramic-Glass Sealing Cost Summary - 100 kW and 250 kW .....	65
Table 5-34. SOFC Anode Mesh Cost Summary - 100 kW and 250 kW .....	65
Table 5-35. SOFC Cathode Mesh Cost Summary - 100 kW and 250 kW.....	66
Table 5-36. SOFC Stack Assembly Cost Summary - 100 kW and 250 kW .....	66
Table 5-37. SOFC Stack Brazing Cost Summary - 100 kW and 250 kW.....	67
Table 5-38. SOFC Stack Testing and Conditioning Cost Summary - 100 kW and 250 kW .....	67
Table 5-39. SOFC Stack Component Cost Summary - 100 kW and 250 kW .....	68
Table 5-40. SOFC Stack Manufacturing Cost Summary - 100 kW and 250 kW .....	68
Table 5-41. SOFC Reformer Sizing Parameters .....	72
Table 5-42. SOFC Reformer Dimensional Summary .....	72
Table 5-43. SOFC System Reformer Cost Summary - 100 kW and 250 kW .....	73
Table 5-44. SOFC BOP Cost Summary for 100-kW and 250-kW Systems .....	74
Table 5-45. SOFC System Assembly Costs - 100 kW and 250 kW .....	77
Table 5-46. SOFC System Testing Cost Summary - 100 kW and 250 kW .....	77
Table 5-47. Summary of SOFC Capital Cost Assumptions .....	78
Table 5-48. SOFC Capital Cost Summary - 100 kW and 250 kW .....	78
Table 5-49. DC/DC Converter Cost per Watt.....	80
Table 5-50. DC/AC Inverter Cost per Watt .....	80
Table 5-51. Hybrid DC/AC Inverter Cost per Watt.....	80
Table 5-52. Controller and Sensors Cost.....	81
Table 5-53. Minimum Battery Requirements .....	81
Table 5-54. Battery Cost per System.....	82
Table 5-55. Load Bank Cost per System .....	82
Table 5-56. Electrical Cost Summary .....	83
Table 6-1. PEM Manufacturing Processes Evaluated .....	84
Table 6-2. SOFC Manufacturing Processes Evaluated .....	86
Table 7-1. Cost Summary for 100-kW PEM CHP Fuel Cell System .....	90
Table 7-2. Cost Summary for 250-kW PEM CHP Fuel Cell System .....	91
Table 7-3. Cost Summary for 100-kW CHP SOFC Fuel Cell System .....	94
Table 7-4. Cost Summary for 250-kW CHP SOFC Fuel Cell System .....	95
Table 9-1. Cost Basis for California .....	104
Table 9-2. Operating Costs for California .....	104
Table 9-3. Annual Cash Flows, IRR and Payback Period (100-kW SOFC system with waste heat recovery).....	106
Table 9-4. Annual Cash Flows, IRR and Payback Period (100-kW PEM system without waste heat recovery).....	107
Table 9-5. IRR and Payback for Installations in California .....	108
Table 9-6. IRR Summary for Installations in California .....	109
Table 9-7. IRR and Payback for Installations in New York State.....	110
Table 9-8. IRR and Payback for Installations Based on Overall US Energy Costs .....	111
Table 9-9: Direct Utility Price Comparison <sup>2</sup> .....	112

Table 10-1. PEM System Cost.....	116
Table 10-2. SOFC System Cost.....	116
Table 10-3. IRR in California Based on Average Commercial Rates .....	119

## List of Figures

	Page
Figure 2-1. Battelle’s cost analysis approach. ....	2
Figure 3-1. Total CHP installed sites by system size.....	4
Figure 3-2. Total CHP installed capacity by technology. ....	5
Figure 3-3. Current number of CHP installations by technology.....	5
Figure 4-1. Notional load curve for illustration. ....	12
Figure 4-2. High-level fuel cell system outline. ....	13
Figure 4-3. Representative multi-stack PEM CHP system. ....	15
Figure 4-4. Representative SOFC CHP system. ....	18
Figure 4-5. DC/DC converter electrical system schematic. ....	23
Figure 4-6. Hybrid inverter electrical system schematic. ....	24
Figure 4-7. Directly-connected battery system schematic. ....	25
Figure 4-8. PEM fuel cell polarization curve with battery state of charge. ....	26
Figure 5-1. PEM fuel cell stack manufacturing process.....	32
Figure 5-2. PEM MEA configuration for 780 cm <sup>2</sup> active area. ....	33
Figure 5-3. PEM end plate size.....	35
Figure 5-4. Breakdown of 100-kW system – 60-kW fuel cell costs and production volume trends. ....	41
Figure 5-5. Breakdown of 250-kW system – 50-kW fuel cell costs and production volume trends. ....	41
Figure 5-6. Catacel SSR <sup>®</sup> schematic diagram after patent no. 7,501,102. ....	43
Figure 5-7. Three-tube 100-kW reformer configuration. ....	43
Figure 5-8. Seven-tube 250-kW reformer configuration. ....	44
Figure 5-9a. Shift/PrOx reactor configuration. ....	47
Figure 5-9b. Shift/PrOx reactor typical dimensions. ....	47
Figure 5-10. 100-kW PEM BOP cost distribution.....	50
Figure 5-11. 250-kW PEM BOP cost distribution.....	50
Figure 5-12. 100-kW PEM BOP cost volume trends. ....	51
Figure 5-13. 250-kW PEM BOP cost volume trends. ....	51
Figure 5-14. Detail assembly of SOFC cell.....	56
Figure 5-15. Cell repeat unit showing function of major components.....	57
Figure 5-16. SOFC stack manufacturing process.....	58
Figure 5-17. SOFC cell size.....	59
Figure 5-19. 100-kW SOFC stack cost volume trends. ....	69
Figure 5-20. 250-kW SOFC stack cost volume trends. ....	69
Figure 5-21. Catacel SSR <sup>®</sup> schematic diagram after patent no. 7,501,102. ....	70
Figure 5-22. Three-tube 100-kW reformer configuration. ....	71
Figure 5-23. Seven-tube 250-kW reformer configuration. ....	71
Figure 5-24. 100-kW SOFC BOP cost distribution.....	75
Figure 5-25. 250-kW SOFC BOP cost distribution.....	75
Figure 5-26. 100-kW SOFC BOP cost volume trends. ....	76
Figure 5-27. 250-kW SOFC BOP cost volume trends. ....	76
Figure 7-1. 100-kW PEM system costs at 1,000 units per year.....	88
Figure 7-2. 250-kW PEM system costs at 1,000 units per year.....	88
Figure 7-3. 100-kW PEM cost volume trends. ....	90
Figure 7-4. 250-kW PEM cost volume trends. ....	91

Figure 7-5. Cost per kilowatt for 100-kW and 250-kW PEM system.....	92
Figure 7-6. 100-kW SOFC system costs at 1,000 units per year. ....	93
Figure 7-7. 250-kW SOFC system costs at 1,000 units per year. ....	93
Figure 7-8. 100-kW SOFC cost volume trends. ....	94
Figure 7-9. 250-kW SOFC cost volume trends. ....	95
Figure 7-10. Cost per kilowatt for 100-kW and 250-kW SOFC system. ....	96
Figure 8-1. PEM sensitivity analysis: 100-kW system cost – 1,000 production volume.....	99
Figure 8-2. PEM sensitivity analysis: 100-kW system cost – 10,000 production volume.....	99
Figure 8-3. SOFC sensitivity analysis: 100-kW system cost – 1,000 production volume.....	101
Figure 8-4. SOFC sensitivity analysis: 100-kW system cost – 10,000 production volume.....	101
Figure 9-1. IRR heat map for a 100-kW SOFC system with waste heat recovery at various costs of electricity and natural gas.....	112
Figure 9-2. Payback heat map for a 100-kW SOFC system with waste heat recovery at various costs of electricity and natural gas.....	113
Figure 10-1. PEM system costs at 1,000 units per year. ....	114
Figure 10-2. SOFC system costs at 1,000 units per year. ....	114
Figure 10-3. Net system installed cost (after mark-up).....	118
Figure 10-4. Final system cost of energy delivered (thermal and electric). ....	118
Figure 10-5. Total system cost of energy delivered including an absorption chiller. ....	119

## 1. Introduction

Battelle is conducting manufacturing cost assessments of fuel cells for stationary and non-automotive applications to identify the primary cost drivers impacting successful product commercialization. Battelle, under a five-year cooperative agreement with the Department of Energy's (DOE's) Fuel Cell Program, will provide an independent assessment of fuel cell manufacturing costs at various volumes and alternative system designs. This report provides cost estimates for the manufacture of 100-kW and 250-kW fuel cell systems for combined heat and power (CHP) and primary power applications. Both polymer electrolyte membrane (PEM) fuel cell stacks and solid oxide fuel cell (SOFC) stacks are considered. This report identifies the manufacturing costs of fuel cell systems using scale-appropriate manufacturing processes at annual production volumes of 100, 1,000, 10,000 and 50,000 units. The manufacturing volumes were defined by DOE and are used for all systems being evaluated within the overall project. For 100-kW and larger systems, the higher manufacturing volumes would represent a significant fraction of the new power generating capacity brought on line in a typical year. Thus, the higher volumes represent a mature market with fuel cells drawing market share from the gas turbine systems that now dominate new generation capacity. In such a market, we believe utilities and municipal power companies will find fuel cells advantageous for distributed generation to enable islanding and localized damage response.

The system designs were defined based on Battelle's fuel cell system integration expertise and were refined through discussion with industry partners. The report presents our representative designs for both SOFC and PEM systems, including the basic sizing and configuration design assumptions. For SOFC systems we elected to analyze planer configurations as these seem to be preferred over tubular configurations by the active companies working at this size range (100 to 250 kW). Key components of the example designs were evaluated using manufacturing processes modeled with the Boothroyd Dewhurst, Inc. Design for Manufacture and Assembly (DFMA®) software. Costs of the system, sub-system, and specific components were determined by obtaining quotes from candidate manufacturers and the main cost drivers were identified through a sensitivity analysis. The sensitivity analysis includes the costs of some of the more expensive components and those for which the included cost is less certain. A summary of possible opportunities for cost reduction is included. Because balance of plant (BOP) hardware for the scale of equipment required for 100- and 250-kW systems is typically manufactured at a few to perhaps as many as a few hundred units/year, the assumptions for the higher production volumes must be understood to reflect engineering judgement as to the level of cost reduction possible through specific design for mass-manufacturing that would necessarily occur to support the higher volume production rates.

## 2. Approach

Battelle's cost analysis methodology is a four-step approach (Figure 2-1):

- Step 1—Market Assessment
- Step 2—System Design
- Step 3—Cost Modeling
- Step 4—Sensitivity Analysis/Life Cycle Cost Analysis

This approach has been successfully applied to previous cost analyses developed by Battelle.<sup>1,2</sup>

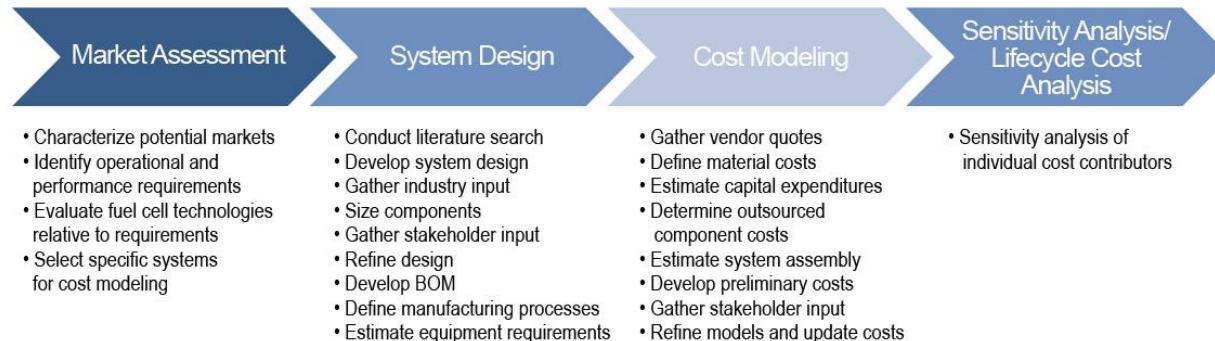


Figure 2-1. Battelle's cost analysis approach.

The first step in our methodology, **Market Assessment**, assures that we have selected the right fuel cell type and appropriate production volumes to meet market requirements. In this step, Battelle identified the operational and performance requirements (e.g., hours of operation, frequency, expected lifetime) of the target application and market. Using this information, we defined an assessment of the user requirements for a fuel cell product. For this phase of the project Battelle completed a quick survey of the market through dialogue with industry to estimate the number of potential units in the market and the expected market growth for fuel cells in CHP and primary power applications in the 100-kW to 250-kW range. This information formed the basis for selecting the system design and fuel cell types best suited to meet user requirements and the appropriate production volumes to consider in the modeling exercise.

Step 2, **System Design**, began with a literature review of fuel cell designs for CHP and primary power applications including component design and manufacturing processes. Possible improvements in system design and manufacturing were identified and incorporated into the example systems. From these results, the basic construction and operational parameters for a fuel cell stack and system were defined, along with potential improvements. The fuel cell system design did not focus on an individual manufacturer's designs, but was instead representative of typical design based on literature and Battelle's engineering expertise. The stack and system design were vetted with industry stakeholders to ensure feasibility of the design, identify possible improvements, and determine current and alternative manufacturing approaches. The finalized design and projected improvements were consolidated to form the basis for developing the bill of materials (BOM). Decisions were then made about which components would be manufactured internally and which would be outsourced. For internally manufactured components (including applicable BOP components), manufacturing processes and production equipment were defined in detail.

In Step 3, **Cost Modeling**, Battelle gathered vendor quotes for material costs, production equipment and outsourced components. Where necessary, custom manufacturing process models were defined and parametrically modeled based on knowledge of the machine, energy and labor requirements for the individual steps that comprise the custom process. The sequence of actions required to assemble the components and test the final fuel cell system was developed and analyzed for cost reduction

<sup>1</sup> Battelle. 2011. The High Volume Manufacture Cost Analysis of 5 kW Direct Hydrogen Polymer Electrolyte Membrane (PEM) Fuel Cell for Backup Power Applications. Contract No. DE-FC36GO13110.

<sup>2</sup> H. Stone, K. Mahadevan, K. Judd, H. Stein, V. Contini, J. Myers, J. Sanford, J. Amaya, and D. Paul. 2006. Economics of Stationary Proton Exchange Membrane Fuel Cells, Interim Report. Contract No. DE-FC36GO13110.

opportunities through component consolidation and process optimization. Manufacturing quality control requirements were based on input from equipment vendors and Battelle's experience with product manufacturing. Outsourced component costs were estimated through vendor quotes. Mathematical functions for scaling factors were developed to estimate the changes to outsourced components and material costs as a function of production volumes when vendor quotes for higher volumes were not available. These were derived using engineering rules of thumb and estimates from other manufacturing processes and considered impacts on system design.

Using the DFMA<sup>®</sup> software, component costs calculated from both custom and library manufacturing processes and the outsourced components were incorporated into the assembly and test sequence models to determine the final cost of producing the fuel cell systems. The output of the DFMA<sup>®</sup> models was also used to calculate production line utilization. The calculated value determined the number of individual process lines required to support various product demand levels. The manufacturing capital cost model is based on the number of process lines required. We assumed that capital equipment expenditures for production would be amortized over a 20-year period and that the annual amortized cost would be distributed over the production volume for that year. The financial assumptions that were used are consistent with the DOE Hydrogen Analysis (H<sub>2</sub>A) model. Total fuel cell system costs including capital expenditures were then estimated for the baseline system and projected improvements. Details of these costing calculations appear in Appendices A-1 through A-26.

The **Sensitivity Analysis** (Step 4) was then performed to determine which design parameters or assumptions have the most effect upon the stack and system cost. Single factor sensitivity analyses were performed and helped determine the impact of individual parameters on system costs. Based on these results, Battelle outlined possible design optimization approaches to reduce the total fuel cell system cost and total cost of ownership.

A preliminary life cycle cost analysis was developed for the systems evaluated in this portion of the overall project. Life cycle analyses are necessarily tied to specific applications. For this study, we considered installations of alternative fuel cell power generation in the range of 100 kW to 1 MW of total power requirements. Most installations depend on the fuel cell system to reduce demand charges and overall electrical power costs and to provide back-up power in the event of grid outage. We believe that using the waste heat may be a decision factor in selecting a fuel cell power system even for those applications where the primary interest is reduced grid power demand or back-up power during grid outage. The waste heat may be used directly for space or water heating (e.g. hotels, conference centers) or indirectly to provide cooling through adsorption chillers (e.g. data and communication centers). Therefore, we consider some hypothetical installations where the heat may be used to reduce overall energy consumption.

### 3. Market Analysis

The fuel cell primary power and CHP markets in the United States are young, although the use of fuel cell primary power and CHP has been growing over the past 20 years. The market is served by three primary companies, each taking different approaches in their market offerings. None of the companies directly align with the systems examined in this report (specifically, 100- and 250-kW PEM and SOFC CHP systems), although similar market needs are served. FuelCell Energy offers large primary power and CHP systems in the 250-kW operating range, utilizing a Molten Carbonate Fuel Cell (MCFC) system. Doosan (ClearEdge/UTC Power) serves the market with its PureCell<sup>®</sup> Phosphoric Acid CHP system, providing 440 kW of power as well as substantial usable heat. The final primary market player, Bloom



Energy, utilizes SOFC technology to produce power in 200+ kW systems which can be grouped to produce larger quantities of power. FuelCell Energy's modules can also be grouped for higher power output. Unlike the other market competitors, Bloom Energy does not offer CHP systems. Each of these fuel cell systems serves several markets, and while few systems on the market align within the constraints of this study (100- and 250-kW PEM/SOFC CHP systems), they cater to similar markets; therefore, they were used as guidance when market requirements and criteria were evaluated. Each of these systems may be operated in parallel to provide larger quantities of power, if required, based on the end user's demands.

Nationally, over 54% of all CHP installations (including those powered by both fuel cells and traditional hydrocarbon fuels) are under 1 megawatt (MW) (Figure 3-1).<sup>3</sup> Fuel cell installations make up approximately 3% of all CHP installations and less than 0.1% of all energy (total megawatts) provided by CHP systems (Figure 3-2 and Figure 3-3).<sup>3</sup> Over 90% of existing fuel cell CHP systems are installed in three states: California (62% of total installations and 67% of the total installed megawattage), Connecticut (17% of total installations and 15% of the total installed megawattage), and New York (14% of total installations and 12.0% of the total installed megawattage).

According to Grandview Research, small- and micro-scale systems accounted for over 15% of all CHP installations in 2014 and are expected to witness significant growth rates of over 8% from 2015 to 2022. Reciprocating engines accounted for 54% of the total installations, followed by turbine and microturbine with 26% and 9% of total installations, respectively.<sup>3</sup>

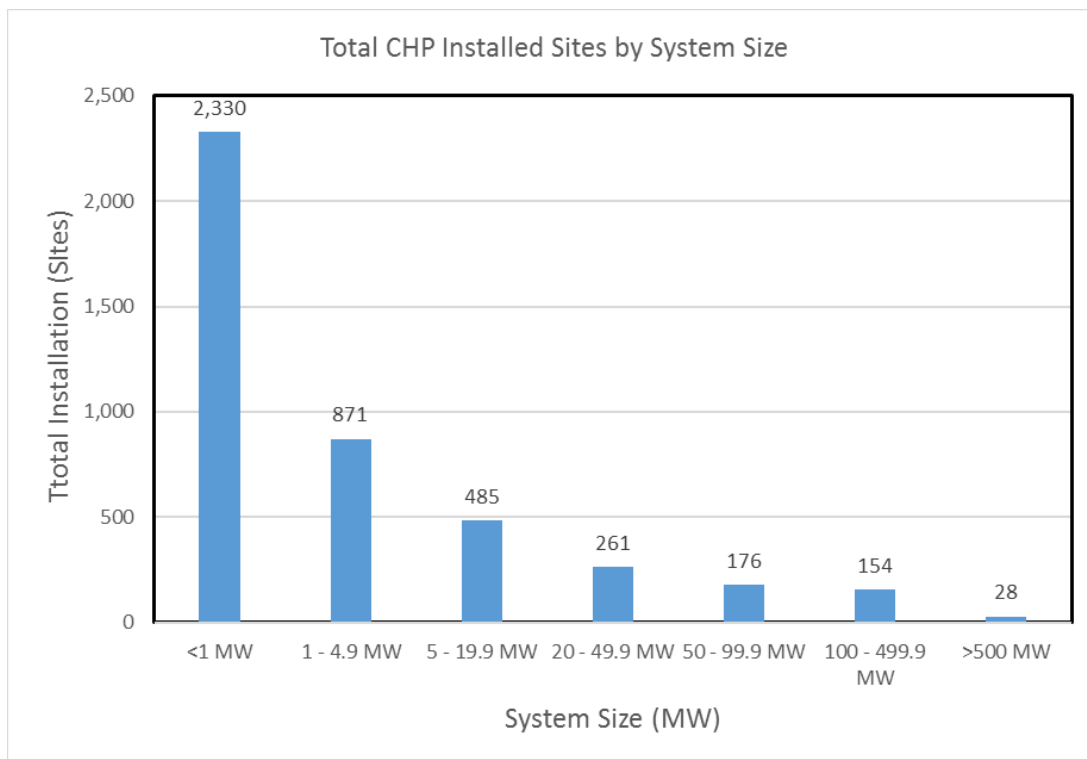


Figure 3-1. Total CHP installed sites by system size

<sup>3</sup> U.S. DOE Combined Heat and Power Database. Accessed December 2016. <https://doe.icfwebservices.com/chpdb/about>

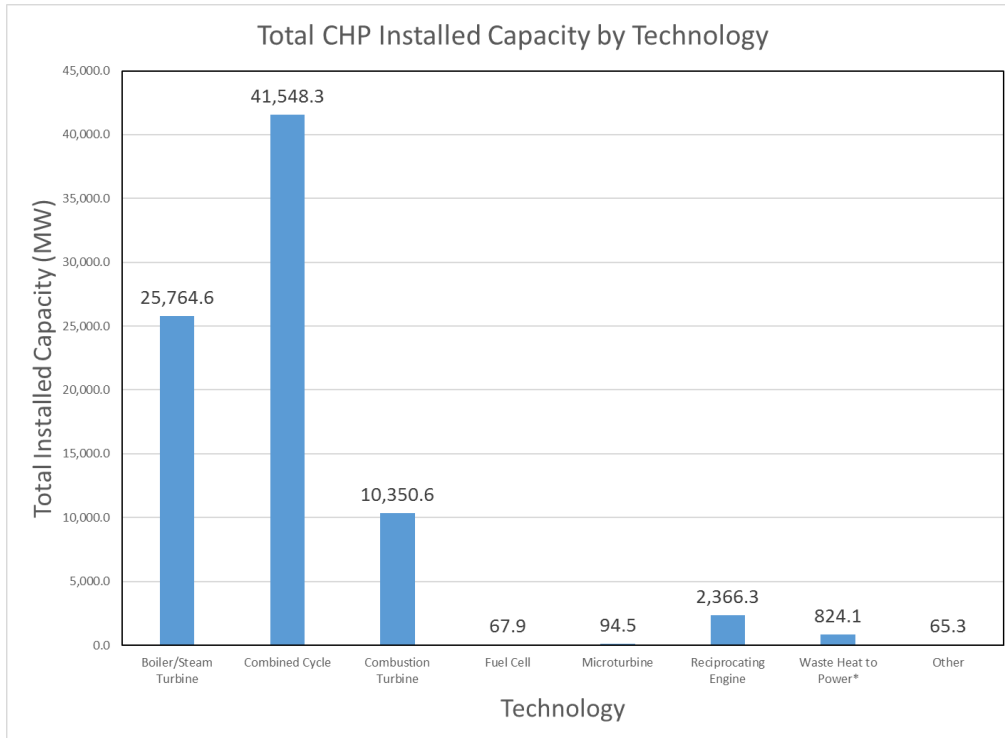


Figure 3-2. Total CHP installed capacity by technology.

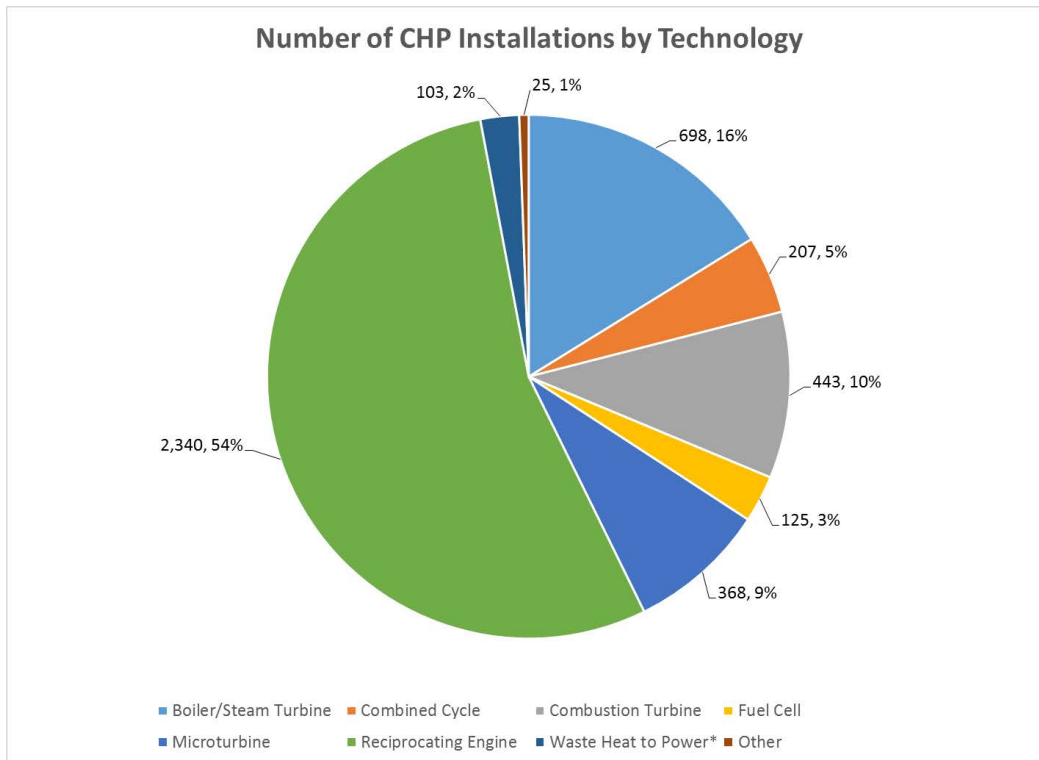


Figure 3-3. Current number of CHP installations by technology.



### 3.1 Market Requirements and Desired Features

In addition to the above-mentioned guidance of fuel cell primary power or CHP markets, Battelle used past experience with providing services to market sectors that could potentially benefit from a high-efficiency CHP system. Although we considered primary power as an option, the economics are more attractive if the rejected heat from the fuel cell system can offset other energy use on site; hence, the focus was primarily on CHP applications. A notable exception for primary power is remote telecom operations. Some systems for this application are being installed, although most of that emphasis is overseas (e.g., in India).

Primary power and CHP applications will typically use readily available gaseous fuel—primarily pipeline natural gas with some potential use of propane or anaerobic digester biogas, though the cost benefits are typically less for propane than for natural gas. To be attractive, particularly for an emerging technology like fuel cells, the savings compared to grid electricity must be significant: anecdotally, the payback period must be less than or equal to 2 years, per personal communications with the president of a national restaurant chain. To provide for more attractive ROIs, many manufacturers are offering Purchase Power Agreements (PPAs) through which the customer does not need to invest in the capital equipment of the fuel cell system, but rather agrees to purchase power at an established rate for a given period of time<sup>4</sup>.

Many of the early CHP installations will likely be at locations with significant heat loads that can be served by the heat rejected by the fuel cell system. For example, large restaurants, hotels, and resorts have significant water-heating loads with desired water temperatures near 135°F (57°C) for washing applications (hands, dishes, linens, showers). Restaurants are also subject to significant electric demand charges, so offsetting the peaks which naturally occur at meal times can have notable economic benefit. Both PEM and SOFC systems can support the hot-water demand at either restaurants or hotels. Typical water-heating applications include gas-fired storage-type water heaters. For sterilization, a booster heater is typically used to heat water from 135°F to 180°F (82°C). An SOFC system could support the higher temperature water, while a PEM system would provide only the 135°F water. Alternate applications could include locations with significant cooling load (e.g., data centers). By utilizing heat rejected from the fuel processor to increase the temperature of the coolant for a PEM system, the cooling water can be used to drive an absorption chiller.

A significant consideration for CHP and primary power systems is the nature of the utility grid connection. Some CHP installations are connected to the grid to primarily provide heat and partially offset base power but depend on the grid for transient management and starting. If the grid goes down, so do these systems. In discussions with some potential end users, we found that back-up operation during grid outage is considered to be a significant benefit. This seems to be a basis for at least some of the Bloom installations. We believe it is relevant in particular for restaurants, grocery stores, and warehouses (refrigeration); hotels and hospitals (emergency egress/elevators, restaurant refrigeration); medium commercial/industrial (critical process continuation); large schools or universities (heating); and data centers (back-up power, cooling) even if all business/normal operations cannot be continued during the outage. Grid connection and operation during grid outages asserts significant influence on system design. With the grid available, the fuel cell system can be operated at steady-state power appropriate for the application. When the grid is not available, a back-up power system must effectively follow applied load and respond to transients, for example refrigeration compressor operation, and thus requires appropriate electrical energy storage: typically batteries. Because site use during a power outage will vary

---

<sup>4</sup> <http://www.bloomenergy.com/fuel-cell-purchase-options/>, <http://www.doosanfuelcell.com/en/services/financial.do>

significantly from normal use, a CHP system serving as back-up power must be able to operate with lower heat load—perhaps with no heat load in some cases. Thus, the fuel cell cooling system must be configured to manage rejected heat with or without a CHP heating load.

### 3.2 Technology Selection

Three fuel cell technology operations were considered: low-temperature PEM (LTPEM), high-temperature PEM (HTPEM), and SOFC. In discussions with several knowledgeable stakeholders, it became clear that HTPEM was unlikely to achieve reasonable lifetimes and certainly not the necessary 40,000-hour life. Although a few companies remain committed to HTPEM, BASF has discontinued commercial production of the polybenzimidazole (PBI) membrane material, and future commercial deployment in the CHP market is unlikely. Therefore, this technology was not actively considered for this project.

SOFC and PEM have different operating characteristics and may, therefore, serve different segments of the CHP/primary power market. SOFC systems will be less expensive than PEM because of the reformat clean-up hardware required for PEM systems and the lower use of precious metals. However, where off-grid operation is expected to occur with some frequency, the relatively slow load-following capability of SOFC may result in a higher cost for energy storage required to allow transient management. LTPEM stack technology is relatively mature and will benefit from future cost reductions achieved by the automotive industry—though the lifetime requirements are much higher for CHP, so automotive cost targets are not relevant to CHP. LTPEM is well suited to load management in off-grid conditions; however, transients are not as fast for a reformer-based system as for a stored hydrogen system, so additional energy storage in the form of lead acid batteries is required. The demonstrated durability of LTPEM systems is approaching 40,000 hours. SOFC durability lags but may eventually reach the same level.

LTPEM stacks will typically be operated at 60°C to 70°C for long life and are only appropriate for low-temperature CHP. However, in a reformer-based system, some heat is recovered from intermediate cooling within the fuel processor and from the reformer exhaust, enabling delivered temperatures to exceed 70°C. In SOFC CHP systems, delivered temperature may be higher since the stack operates at over 650°C. Recuperative heat exchangers are typically employed to improve electrical efficiency by reducing uncontrolled heat lost, but temperatures in excess of 200°C should be achievable with SOFC systems.

### 3.3 Market Analysis Conclusion

Both SOFC and LTPEM have potential applications in the CHP market. The system sizes considered in this report are appropriate for large applications, including hotels, commercial buildings, and a wide variety of light industrial applications. Demonstrated durability for LTPEM stacks is considerably higher than for SOFC and load following for applications that experience significant load swings is superior. The greater flexibility of LTPEM will be beneficial for restaurant and some other applications at smaller scales where a greater exposure to uncontrolled operating conditions exists and where individual loads may represent a greater fraction of the total load. SOFC will ultimately be less expensive, operate at higher efficiency, and be capable of serving higher-temperature thermal loads. At this point in the development of the CHP/primary power market, there is no reason to downselect to a single technology.

## 4. System Specifications

This section provides a general description of the systems selected for analysis. Both SOFC and LTPEM were considered. The systems analyzed are representative of potential system configurations but do not reflect any specific commercial system. They reflect Battelle's judgment on an appropriate balance between efficiency and cost and between proven and developing technology. In conversations with fuel cell stack manufacturers, we concluded that 100-kW and larger single stacks would not be the preferred approach. This is particularly true for SOFC systems, where the entire stack must be scrapped if it includes a defect found either in factory testing or during a warranty period in the field. For PEM systems, it is generally possible to repair a defective stack, but the cost and manufacturing uncertainty associated with the larger components discouraged single-stack approaches. Hence, the systems considered for this analysis incorporate multiple PEM stacks at 50 or 60 kW per stack. The SOFC systems evaluated used 30-kW rated stacks essentially equivalent to the stacks used in our 2017 report<sup>5</sup> on smaller-sized CHP systems. The choice of multiple stack systems has significant impact on the overall analysis because production volumes of specific stack components quickly reach threshold quantities where significant automation is appropriate. The use of multiple stacks also impacts overall system design and operation, potentially affording operational flexibility. However, incorporating the hardware necessary to allow operation of a subset of the stacks in order to achieve partial load or damage recovery would represent a significant cost adder and was not considered in this analysis; the stacks are assumed to be balanced at the factory and remain so during their lifetime.

### 4.1 General Description

This report concerns primary power and CHP applications—that is, stationary systems that provide electrical power and may or may not export thermal energy to some form of process or space heating. For CHP applications, the systems may be sized to match a specific heat load or a specific electrical load. With few exceptions, either one or both of the loads will be variable and the variations may or may not be in phase. That is, the heat load may be high when the electrical load is low or vice-versa.

A key assumption for the systems evaluated in this study is that the utility grid is available, so the fuel cell system is offsetting grid power and, in some cases, excess power generated may be exported onto the grid. This assumption allows the fuel cell system to be operated to meet a specific heat demand or to be operated at an optimum condition for offsetting grid power at the owner's discretion. However, a key benefit of a fuel cell CHP system is continued operation of at least critical loads during periods of grid outage. This may be particularly important (and in fact may be the primary reason for the purchase of a CHP system) for some applications with critical power requirements, including commercial buildings, health service facilities, server/telecom sites, and critical industrial operations. Therefore, the designs considered include features to enable off-grid operation—most importantly, battery support for transients and load management. However, we did not take credit for off-grid operation when analyzing the life cycle costs, which could vary widely between applications.

For many applications there will be some form of “hard-start” electrical hardware such as refrigeration or air conditioning compressors. These devices have very high power demand for a short period as the system is coming up to speed. Inrush current can be six to ten times the normal run current. The duration may only be a few cycles (AC power assumed) to a few seconds, but the power must be available. If the

---

<sup>5</sup> Battelle. 2017. “Manufacturing Cost Analysis of 1, 5, 10, and 25 kW Fuel Cell Systems for Primary Power and Combined Heat and Power Applications.” DOE Contract No. DE-EE0005250.

voltage decreases due to the heavy current draw, the high-load period may be extended due to slower motor spin-up, which may also damage the motors if the voltage sag is extreme. For a grid-connected system, these transients are not applied to the fuel cell but are instead handled by the grid.

The opposite situation arises if a heavy load is turned off: the sudden drop in current may cause a sharp increase in voltage. With the grid available, the voltage spike is largely absorbed by the grid. The specifics of these transients will vary widely with application, with some installations having few, if any, spikes while others may experience frequent and significant spikes. Systems at the 100-kW and larger scale are likely to be at least partially custom engineered systems. The specifics of spike management would likely be customized to the application. In developing the system design, we assumed that load picks and drops will be limited to 20% of nominal capacity; however, we have included capability to handle starting loads of up to five times nominal for a period not exceeding 5 seconds.

During a grid outage, the primary objective is to meet the critical load (heat and/or power); efficiency is somewhat less important. Since grid outages in the United States occur infrequently and typically have durations less than 1 week, our system designs favor lower first cost over high efficiency during outages. We did not include the capability for black start—that is, off-grid starting from a cold condition—as the CHP systems are intended for near continuous operation. CHP systems would therefore be expected to be in operation when a grid outage occurs.

## 4.2 Nominal Metrics

Table 4-1 shows the performance objectives considered as the example designs were being developed. Table 4-2 provides details on the fuel cell stack design for the PEM systems, and Table 4-3 provides details on the fuel cell stack design for the SOFC systems. Tables 4-1, 4-2, and 4-3 are based on our judgment regarding typical and representative specifications and requirements; they are not based on any specific system nor do they constitute recommendations for specific hardware. The overall efficiency associated with the PEM system assumes that waste heat is recovered at a usable temperature of ~80°C to 100°C. This temperature is higher than would be achieved in a direct hydrogen system because some high-quality heat is recovered from the fuel processing system. The extended lifetime target of 50,000 hours results in stacks that are operated more conservatively (e.g., 0.4 amps per square centimeter [cm<sup>2</sup>]) than automotive or material-handling installations. Based on conversations with PEM stack manufacturers, they suggest that this current density is appropriate for reformate versus hydrogen as the fuel.

**Table 4-1. Nominal Design Basis**

Metric/Feature	Objective
Input, Fuel	Utility Natural Gas or Propane (>30 psig preferred)
Input, Air	Ambient air (-20° to 50°C)
Input, Other	N/A
Output	480 3-phase VAC
Net Power Output	100, 250 kW
System Efficiency (electrical)	
PEM	30%
SOFC	40%
System Efficiency Overall (including heat delivered)	
PEM	80%
SOFC	90%
System Life	50,000 hours
System Maintenance Interval (filter change: sulfur trap, air filter, fuel filter)	1 year
Grid Connection	Yes, local and/or utility
Operate off-grid	Yes, critical load back-up
Start off-grid	No

**Table 4-2. PEM Fuel Cell Design Parameters**

Parameter	100 kW	250 kW
Power Density (W/cm <sup>2</sup> )	0.27	
Full Load Current Density (A/cm <sup>2</sup> )	0.4	
Full Load Cell Voltage (VDC)	0.68	
Active Area Per Cell (cm <sup>2</sup> )	780	780
System Net Power (kW)	100	250
System Gross Power (kW)	120	300
Number and Size of Stacks per System	2 x 60 kW (gross)	6 x 50 kW (gross)
Number of Cells per stack (#)	283	236
Nominal Stack Open Circuit Voltage (VDC)	283	236
Full Load Stack Voltage (VDC)	192	160

**Table 4-3. SOFC Fuel Cell Design Parameters**

Parameter	100 kW	250 kW
Cell Power Density (W/cm <sup>2</sup> )	0.28	
Full Load Cell Current Density (A/cm <sup>2</sup> )	0.4	
Full Load Cell Voltage (VDC)	0.7	
Active Area Per Cell (cm <sup>2</sup> )	414	414
System Net Power (kW, continuous)	100	250
System Gross Power (kW, continuous)	120	300
Number and Size of Stacks per System	4 x 30 kW (gross)	10 x 30 kW (gross)
Number of Cells per Stack(#)	259	259
Nominal Stack Open Circuit Voltage (VDC)	285	285
Full Load Stack Voltage (VDC)	181	181
Cell Design	Planar, Anode supported	

### 4.3 System Sizing and Operation

Grid outage conditions apply some constraints on system size and design. For our analysis, we assumed the CHP system has a 2:1 turndown ratio for both heat and power. In the absence of the grid to provide additional power or accept excess power, the fuel cell system should be sized to cover critical loads but not over-power the on-site electrical system when power usage drops.

Figure 4-1 shows a notional load curve (red) along with solid horizontal lines representing the peak, minimum, and critical loads and dashed horizontal lines representing possible fuel cell designs discussed below. Critical loads are safety or process critical loads (e.g., elevator power and stairwell/exit lighting for commercial, operational minimums for industrial processes) that should be available at all times, though they may not be continuous. As shown in Figure 4-1, the critical load is shown above the red load curve for a significant portion of the time, representing loads such as refrigeration which operate intermittently but which must be available when needed. The illustrated load curve does not include transient (surge) power required for compressor starting or voltage spikes caused by switch opening to turn off high power loads. Those issues are addressed separately.

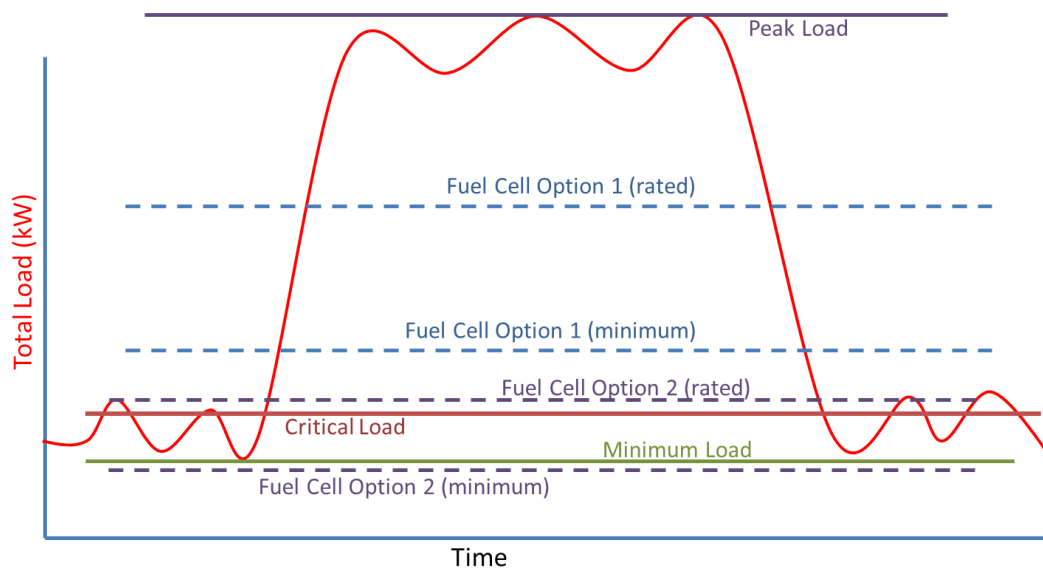


Figure 4-1. Notional load curve for illustration.

With the grid available and power export allowed, the fuel cell system may be sized to meet either the heat load or some selected fraction of the total electrical load. So long as the grid is available, the fuel cell is assumed to be operated continuously and at steady near-full load, with the grid providing any load power beyond the fuel cell rating and absorbing any excess power generated. Two options for fuel cell sizing are illustrated in Figure 4-1. Both options are shown at rated power and at minimum power (approximately 50% turndown).

- Option 1 is sized to cover a significant portion of the total load during the high load portion of the day.
- Option 2 is sized so that the power at fuel cell minimum is less than the minimum load expected for the system.

In Figure 4-1, purchased power is represented by the area under the load curve and above the fuel cell rated power. Any demand charge would be based on the maximum difference between load curve and fuel cell power. Option 1 would clearly make a significant change in both purchased power and demand charges. When the fuel cell power is above the load curve, power is assumed to be exported to the grid. The fuel cell power might be reduced to minimum during low-load conditions unless an attractive power purchase arrangement is in place with the utility for those times. If the grid is not available (during a grid outage or if power exporting is not allowed), the difference between the minimum fuel cell output power and load must be rejected to ambient in some way (e.g., an air-cooled resistor bank). Storage of the excess power from the fuel cell could be considered, but storage would add significant cost, space, and weight requirements, making the economics site-specific. As illustrated in Figure 4-1, under Option 1 significant power must be either stored by some means (not considered here), rejected, or returned to the grid during a significant portion of the day, even at minimum power. For occasional grid outages, the excess power wasted might represent an acceptable cost of maintaining operation and reducing demand/power charges over the remainder of the year. For instances in which grid export is disallowed



by regulation or the absence of a utility agreement, the “wasted” energy represents a significant and likely unacceptable cost.

Option 2 offsets significantly less of the overall load for the profile in Figure 4-1 but still maintains sufficient power to handle the critical loads continuously. In fact, as shown it may be larger than needed to cover the critical loads since some of the intermittent load might be addressed with energy storage (e.g., batteries, which are required to manage start/stop transients for off grid operation). As illustrated, the minimum fuel cell power level is below the overall minimum load power—an intentional design choice. Thus, it should not be necessary to export or dump power at any time with this configuration, and the cost of power export hardware or power dump hardware can be avoided. For applications in which the difference between peak load and minimum load is much less significant than illustrated, Option 2 may be very attractive because it will offset a greater portion of the average load without requiring power export or dump while still maintaining the ability to operate critical loads during grid outage. Applications with near-constant heat or power load are well suited to the Option 2 approach— that is, sizing the system to meet minimum demand at the lowest steady-state operating condition.

Since the sizing is typically specific to the load profile of the application, we assume that a nominal resistor bank will be provided (and included in the cost of installation) for most applications to allow sizing based on normal, grid-available operation (Option 1 above).

#### 4.4 System Configuration

Figure 4-2 is a high-level schematic of a CHP fuel cell system. The fuel of choice for CHP applications is natural gas. For 100-kW and larger systems, the available natural gas pressure is assumed to be 30 pounds per square inch gauge (psig) or greater. An auxiliary natural gas compressor would be required if the supply pressure is less than 10 psig for the PEM system and less than 30 psig for the SOFC system. At 100 kW and above, we expect an industrial/commercial natural gas supply and therefore have not included a compressor. Propane is an acceptable fuel, although some modifications to the system may be required to accommodate propane due to the higher density and volumetric heating value of the fuel. Generally propane will be available at 30 psig or greater from the tank (at ambient temperatures of greater than 0°F).

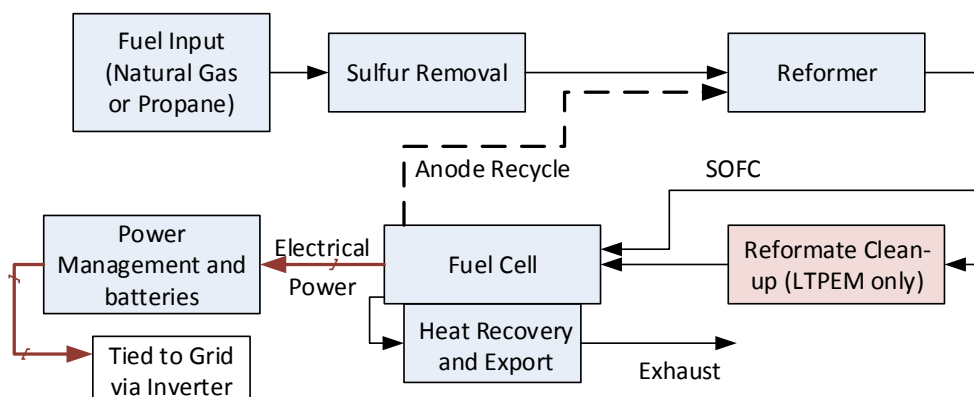


Figure 4-2. High-level fuel cell system outline.



Both propane and natural gas typically contain mercaptan odorant, a sulfur-bearing compound. While generally present in low levels, even low levels of sulfur are damaging to the catalyst in the reformer and fuel cell, so sulfur removal is included in all systems considered.

The key differentiating factor between SOFC and PEM is the composition of the anode inlet stream. PEM systems prefer pure hydrogen. However, some PEM stacks can be designed to operate on reformat so long as the carbon monoxide (CO) content of the gas is low (<50 parts per million [ppm]). We have based our systems on reformat-capable PEM stacks in order to avoid the high cost of hydrogen purification. SOFC stacks can accommodate percentage levels of CO and methane (CH<sub>4</sub>) in the reformat, so they require minimal reformat clean-up and tolerate less-effective reforming so long as the higher hydrocarbons that may be present in natural gas are reformed to methane. Excess methane and/or percent levels of higher hydrocarbons in the reformat reaching an SOFC stack can lead to carbon deposition on the stack anode, capacity loss, and eventual failure.

As indicated by the dashed line in Figure 4-2, the anode and/or cathode exhaust from the fuel cell (SOFC or PEM) may be routed to the reformer for energy and water recovery. While both systems use steam reforming in order to achieve high efficiency, the details of how the fuel cell exhaust energy is recovered for each differ significantly. Water produced appears primarily on the cathode side for PEM systems and on the anode side for SOFC systems. For SOFC systems, some of the anode exhaust is directed to the reformer, where the water content (as steam) directly interacts with the input fuel to achieve steam reforming. For efficient operation of PEM systems, particularly open anode (once-through anode) systems, the residual heating value in the anode effluent is recovered by combusting this gas in a separate burner to heat the reformer. Water is condensed from the combustion and cathode exhausts and re-vaporized for use as steam in the reformer. The energy required to vaporize the water for PEM systems is a factor in the overall system efficiency being lower for PEM than for SOFC.

Other features of the overall system configuration that differentiate SOFC from PEM are discussed below.

#### 4.4.1 PEM System

A schematic of the multi-stack PEM system configuration used for this costing study is shown in Figure 4-3. The major subassemblies are:

- Fuel supply, including: fuel filter, fuel flow management (control valve), and sulfur sorption reactor.
- Fuel processor, including steam generator, reformer, and reformat CO removal reactors (two shift and two preferential oxidation [PrOx]), along with several heat exchangers. All of these components are typically hot, albeit at different temperatures; integrating them reduces heat loss and improves system efficiency.
- Air supply, including filter, three blowers (combustion, PrOx, and cathode), and recuperative cathode humidifier.
- Cooling and heat export system, including several heat exchangers operating on low-electrical-conductivity water/glycol coolant and a CHP load heat exchanger that couples the fuel cell coolant system to the external thermal (heat) load. The heating load is assumed to be independent of the fuel cell system—that is, the fuel cell system cannot adjust the external heat load, it can only respond to it. Low conductivity glycol coolant is required for the PEM stack to avoid shorting the stack. A different configuration using conventional automotive antifreeze for the other heat exchangers is possible but would add another cooling loop and pump along with additional control hardware.

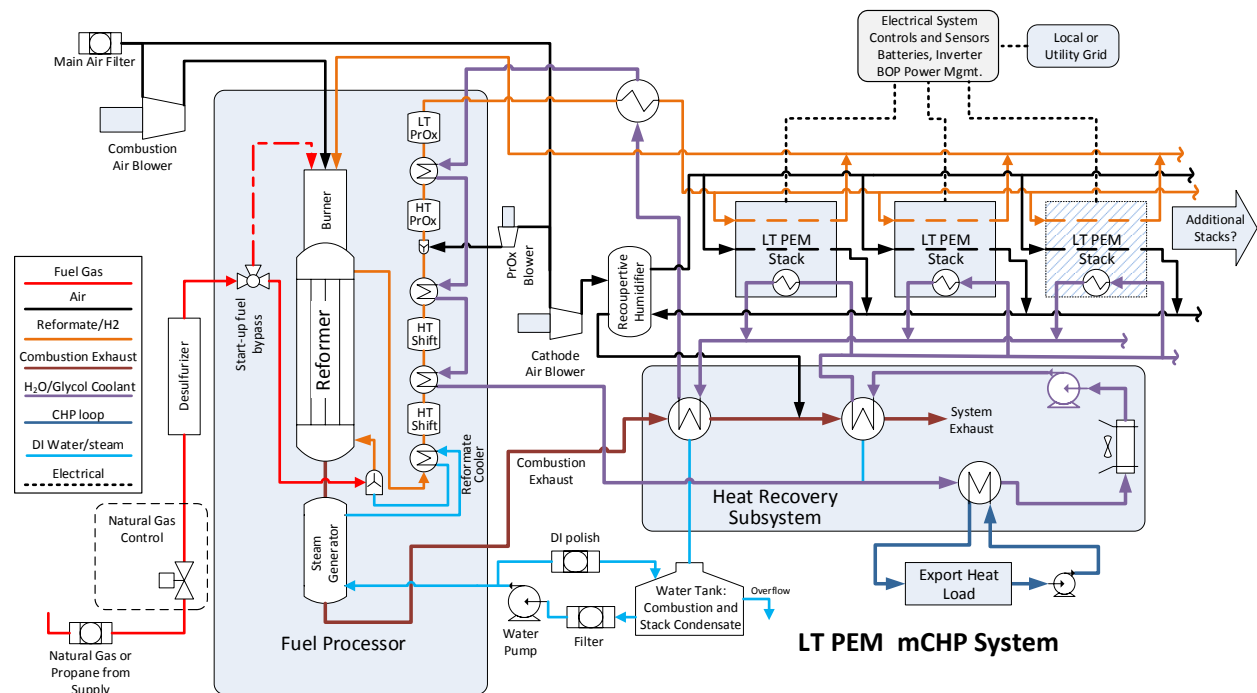


Figure 4-3. Representative multi-stack PEM CHP system.

- Electrical system, including batteries, resistor bank, overall controls, and voltage/current management. The electrical system also includes the grid connection electronics (inverter and any required physical disconnects.) Additional detail, including a schematic of the electrical subsystem, appears in Section 4.5. The electrical system is similar for both PEM and SOFC, though the energy storage required is larger for the SOFC and the voltages vary somewhat depending on system size.
- Multi-stack assembly, including manifolds and electrical connections. Figure 4-3 shows that the stacks are parallel for anode, cathode, and coolant flows. Figure 4-3 suggests that the stacks are electrically parallel. However, to achieve the voltage preferred by the power electronics typically used in this size range, the stacks will be paired in series. For the 100-kW system, there are two 60-kW stacks in series. For the 250-kW system, there are six 50-kW stacks arranged in pairs in series, yielding three parallel sets. Cell active area is the same for all PEM stacks so the 50-kW stacks have a lower output voltage.

As shown in Figure 4-3, fuel enters the system and passes immediately through a sulfur sorption trap to remove mercaptan odorant and any other sulfur compounds present. The sulfur sorbent is considered a consumable and, if space permits, would typically be designed for a 1- or 2-year replacement cycle based on local conditions of sulfur in the gas. For start-up, desulfurized fuel is routed directly to the reformer burner and combusted to preheat the reformer and steam generator (vaporizer) directly. Once combustion gas temperature at the vaporizer is adequate ( $\sim 150^{\circ}\text{C}$ ), water is started and the system is preheated by flowing steam through the downstream reactors. Once the system is adequately preheated, fuel is diverted from the start-up burner and mixed with hot steam before being routed to the reformer. Upon leaving the reformer, the reformat is cooled by steam from the vaporizer to approximately  $350^{\circ}\text{C}$  before entering the high-temperature shift reactor. A water-cooled heat exchanger reduces the reformat temperature between the high-temperature and low-temperature shift reactors and before the PrOx

reactor. Additional heat exchangers reduce the temperature between the high-temperature and low-temperature shift reactors and after the PrOx reactors. The shift and PrOx reactors are packaged with the reformer to minimize heat loss. Reformate leaving the final PrOx reactor will be cooled to stack operating temperature—typically ~60°C.

The cathode air entering the stack is humidified by adsorbing water across a membrane (or via enthalpy wheel or some other form of recuperative humidifier) from the stack cathode exhaust. Anode exhaust is routed to the reformer burner. Stack fuel utilization is adjusted to balance the system so that the anode exhaust has sufficient energy content to support reforming. Because the anode effluent is burned to provide the energy to support the reforming process, the system must be balanced to avoid overheating the reformer while providing adequate reformate for the fuel cell load. The large number of heat exchangers and reactors in the PEM system represent significant thermal inertia. Therefore, the reformer is expected to respond slowly to load changes due to both thermal lag and system control stability requirements. In considering system dynamic design, we allowed for up to 15 minutes for the 100-kW system to respond to a 25% of nominal load change; 25 minutes was allowed for the 250-kW system.

A low-electrical-conductivity glycol/water mixture is used to cool the PEM stack. Coolant should enter the stack at about 50°C. As shown in Figure 4-3, coolant leaving the circulating pump is preheated slightly by the final combustion exhaust. This preheating serves to condense some residual water out of the combustion exhaust for reuse in the system. After the stack, the glycol coolant is directed to the initial combustion gas condenser, where the coolant temperature is increased above the stack operating temperature by combustion gases and where the initial condensation of water from the combustion exhaust occurs. After passing through the initial condenser, the coolant is routed to the pre-stack reformate cooler and then to the shift and PrOx reactor heat exchangers. This somewhat arbitrary heat exchanger sequence was developed based on a simplified ChemCad® model of the PEM system that allowed several heating and cooling scenarios to be considered. Of the systems evaluated, this configuration provided the highest temperature coolant to the CHP system. An important feature of a reformer-based PEM fuel cell system is that the waste heat can be provided at a temperature significantly above the stack temperature. A second coolant loop could be used to deliver even higher-temperature waste heat by separating the stack cooling from fuel processor cooling, which would allow lower coolant flow and higher delivered temperature from the fuel processor. However, for many CHP applications the additional cost of this approach is not needed, so it was not considered in the costing analysis. The PEM system is equipped with a radiator on the stack coolant loop to reject any heat not absorbed by the CHP system. Since the coolant loop is required to maintain system temperatures, especially the stack temperature, the radiator must be sized to reject all heat from the system if a CHP thermal load is not present. A smaller radiator might be specified for systems with known continuous CHP load. Because the temperature of the coolant to the export heat exchanger is projected to be less than 90°C, it is not necessary to bypass the export heat exchanger if little or no CHP load is present. For this analysis, all heat exchangers are assumed to be counter-flow heat exchangers (typically either tube-in-tube or plate frame type) with the exception of the radiator, which is automotive-style cross-flow.

Figure 4.3 includes high-temperature and low-temperature shift reactors and high-temperature and low-temperature PrOx reactors. This follows advice from a shift/PrOx catalyst supplier to cool between reactors. Based on the advice of the catalyst supplier, the shift and PrOx reactors are ceramic monoliths coated with an appropriate catalyst and housed within stainless steel ducts. The monoliths are available in various diameters and in two lengths (full: ~6 inch and half: ~3 inch). The lead CO and PrOx reactors include one monolith each for the 100-kW system. The trailing CO and PrOx reactors include

1.5 monoliths. For the 250-kW system, the lead reactors include 2.5 monoliths and the trailing reactors include 4 monoliths each. Additional information on these reactors is included in Section 5.

#### 4.4.2 SOFC System

A schematic of the multi-stack SOFC system used in our cost analysis is shown in Figure 4-4. The major subassemblies are:

- Fuel supply, including the fuel filter, fuel flow management (control valve), and sulfur sorption reactor. Because the SOFC system uses an eductor for anode gas recirculation, natural gas pressure must be 30 psig or greater for all systems.
- Fuel processor, including natural gas/anode recirculation eductor/mixer, preheater/reformer, and tail gas combustor.
- Air supply, including filter and two blowers (start-up and primary cathode) and recuperative cathode preheater. The start-up blower is used as a secondary cathode blower to achieve full stack load.
- Heat export system, including an exhaust gas to CHP heat exchanger and a bypass valve combination to manage the heat delivered to the CHP system. The heating load is assumed to be independent of the fuel cell system—that is, the fuel cell system cannot adjust the external heat load, it can only respond to it. Therefore, the valve system provides for diverting high-temperature exhaust gas away from the CHP system if required to avoid overheating the CHP fluid.
- Electrical system, including batteries, overall controls, and voltage/current management. The electrical system also includes the grid connection electronics (inverter and any required physical disconnects.) Additional detail, including a schematic of the electrical subsystem, is included in Section 4.5. The electrical system is essentially identical for either PEM or SOFC, with minor variations associated with the additional energy storage needed for SOFC transient management.
- Multi-stack assembly, including manifolds and electrical connections. Figure 4-4 shows that the stacks are parallel for anode and cathode flows. Figure 4-4 shows two pairs of series-connected stacks to yield a high voltage. The stack pairs are electrically parallel so that the current is shared between stack pairs. For the 100-kW system, there are four 30-kW stacks as illustrated in Figure 4-4. For the 250-kW system, there are ten 30-kW stacks arranged as series pairs, yielding five parallel sets.

The schematic of Figure 4-4 is notably simpler than Figure 4-3:

- No shift or PrOx reactors are required, no PrOx blower or PrOx heat exchanger is needed.
- No recuperative humidifier is required.
- No steam generator is required.
- No special glycol cooling loop is required.
- Several heat exchangers are not needed.
- No water supply subsystem is required.

The relative simplicity of an SOFC system is attractive from a cost perspective. The higher quality heat also facilitates SOFC use in a broader range of applications.

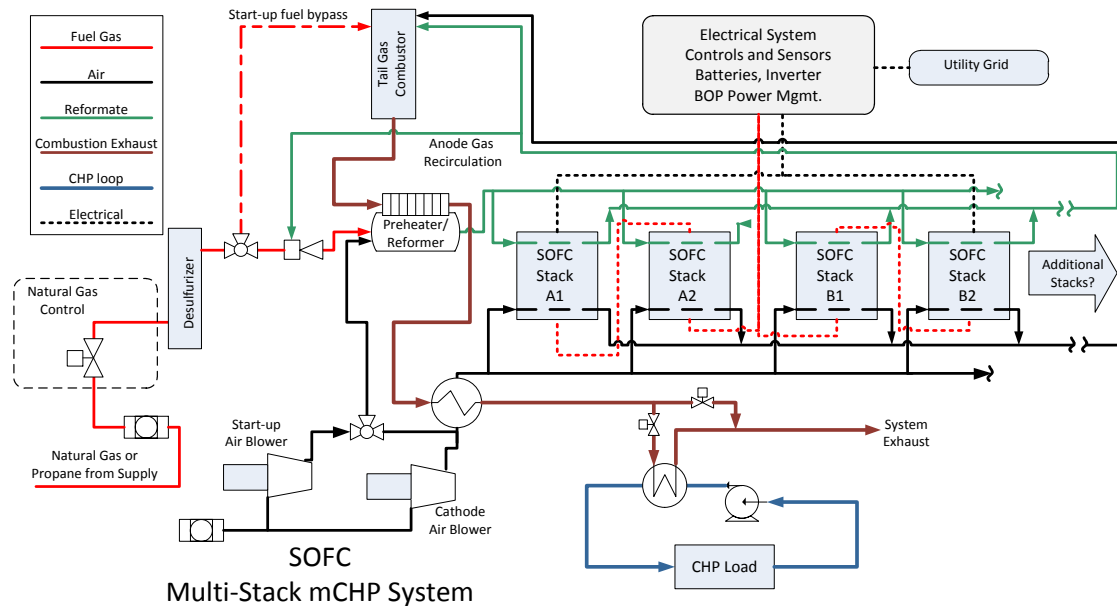


Figure 4-4. Representative SOFC CHP system.

As shown in Figure 4-4, the fuel is first passed through an absorber identical to the one used for the PEM system to remove sulfur. Fuel would be routed directly to the tail gas combustor for start-up, where it is burned with cathode air to preheat the cathode indirectly via the cathode recuperative heat exchanger. The combustion products also preheat the reformer in preparation for the catalytic partial oxidation (CPOx) mode during the next phase of start-up. As the stack assembly warms above  $\sim 100^{\circ}\text{C}$ , the fuel is moved to the preheater/reformer, where it is burned in CPOx mode to continue heating from both the anode and cathode sides of the stack. Combustion is completed in the tail gas burner for indirect heating of the reformer and preheating of the anode. Careful control of flow rates and burner temperatures is necessary to heat the stack uniformly. When fuel is initially routed to the preheater/reformer, anode exit gas begins recirculating to mix with the fuel. Initial recirculation will be limited because the fuel flow for start-up will be significantly lower than for final operation, causing the aspirator used to operate significantly off-design.

As the stack heats and fuel can be increased, more anode recirculation will occur. Current draw can begin at a stack temperature determined by the manufacturer. The start-up blower will be reduced and eventually turned off to transition the reformer into steam reforming mode using water in the recirculated anode for reforming and heat from the tail gas burner to support the endothermic reaction. Once the stack reaches operating temperature, full power may be drawn from the stack. As shown in Figure 4-4, the start-up air blower output may be diverted to combine with the primary cathode blower. This is more economical than having a full-size cathode blower and a start-up blower that is seldom used. Stack and other system temperatures are managed by fuel and cathode air flow. Anode recirculation is passive and depends on the design of the aspirator. There is a potential for limiting the available stack turndown if insufficient steam is recirculated to support reforming. In developing our system performance estimates, we assume that the aspirator will be sized for approximately 50% load with the higher fraction of recirculation at full load being generally beneficial. Alternatively, a hot gas blower might be used to

provide greater turndown in exchange for additional cost and operating complexity. We did not include this option in our cost estimates.

Residual heat from the cathode is available to the CHP load as soon as the system has warmed sufficiently—typically before actually drawing power from the stack. Unlike the PEM system, the CHP system is not expected to cool the stack. Stack cooling depends primarily on cathode air flow, so additional heat can be directed to the heat load by increasing cathode air flow. To prevent the hot cathode outlet from overheating the CHP system at times of low demand, provision is made in the system to bypass cathode air directly to exhaust. Therefore, system exhaust may be hot and appropriate safety precautions and exit locations requirements must be defined and observed. Routing of the hot exhaust is outside the scope of this study.

The ability of an SOFC system to follow electrical load is somewhat restricted because long-term reliability requires that thermal ramp-rates be limited. Thus, an SOFC system will typically operate at near-full load, with the grid either making up any unmet requirement or accepting any excess power. If the grid is not available, the SOFC system will need to keep running at or above its minimum power output, even if the power must be dumped to an air-cooled resistor bank. A hot standby condition is plausible but somewhat difficult for SOFC because of the sensitivity of the stack to internal temperature gradients. Generally, the SOFC stack will remain on and above minimum power to provide for critical loads and any other loads that may be within the overall capability of the stack. Generated power in excess of the available load will be rejected through an air-cooled resistor bank.

Because transients are slower for the SOFC system than for the PEM system, the energy storage requirements are greater. The load pick/drop assumption for off-grid operations is the same for both systems—20% maximum single pick. However, the SOFC system is assumed to require a significantly longer time to respond to the load pick (or drop) while maintaining stack health and control system stability. We assume that a 20% load change would require approximately 30 minutes to re-establish steady state for the 100-kW system and 45 minutes for the 250-kW system. Thus, the battery and resistor bank subsystems are larger for the SOFC system than for the PEM system.

## 4.5 Electrical System

### 4.5.1 Overview

The electrical system provides the interface between the fuel cell stack and the local electric utility grid as well as providing auxiliary power for system components and, when hybridized with batteries, the capability for operation during grid outages. All systems considered in this cost study assume that a utility grid is available and that for normal operation, the fuel cell system will use the grid to manage start-up and load changes. To provide for critical load continuance during grid outage, the systems considered include battery capacity to allow rapid electrical load changes while limiting the speed of the fuel cell system response to achieve stable and reliable long-term operation. The batteries are maintained on trickle charge when the grid is available.

The main challenge in designing a fuel cell system for off-grid operation is matching the stack variable voltage over the desired load range with the battery system while keeping it in an acceptable range for the direct current/alternating current (DC/AC) inverter. The most straightforward design is to have a DC/DC converter between the fuel cell and battery bus to keep the stack output voltage in a proper range for the battery and the DC/AC inverter. However, a DC/DC converter adds a significant cost to the system. Another option is to use a three-port hybrid converter. Hybrid converters are an emerging



technology that is more economical than discrete components. These converters are designed to integrate energy sources and storage. A three-port inverter includes two bidirectional DC ports—one for the primary source and one for the storage source—with an additional bidirectional AC port that ties the system to the grid. The currently available three-port inverters are designed and marketed for solar photovoltaic (PV) applications. However, a fuel cell system can be configured to provide comparable input voltages that would allow three-port inverters to be used. Three-port inverters are more expensive than simple inverters; however, they are less expensive than a DC/DC converter followed by an independent DC/AC inverter.

An off-grid fuel cell system could be designed with a simple wide-input-range DC/AC inverter (these are typically used for solar systems) by directly connecting the battery in parallel with the fuel cell if the battery voltage can be matched to the fuel cell output. This is somewhat problematic as most battery chemistries have a preferred voltage range that is narrower than a typical fuel cell polarization curve. For this report, we have assumed the use of a three-port inverter as the base cost assumption. In Section 4.5.3, we suggest a means to directly connect batteries to the fuel cell output and DC/AC inverter input as a possible future cost reduction approach appropriate for some applications requiring wide turndown for off-grid operation.

#### 4.5.2 On-Grid Operation

The primary objectives of the fuel cell CHP system are to provide process or space heat and offset a portion of the power purchased from the utility grid. When connected to the grid, the fuel cell system does not need to respond to equipment starting spikes or sudden load drops or pickups—the grid is available and on the downstream side of the inverter, so the fuel cell is isolated from transients. Typical operation of a fuel cell CHP system would be to match a required heat load with any power generated, offsetting grid-purchased power. Alternatively, the fuel cell can be operated at near-full power to offset a greater portion of utility power, particularly during periods when high demand charges might apply (e.g., when facility electrical loads are high). For on-grid operation, the fuel cell is operated at a power level chosen by the system operator subject to any agreements in place with the utility for power buy-back if the fuel cell power exceeds facility usage.

If the grid is considered to be always present when the fuel cell is operating, no energy storage or rapid transient response is needed by the fuel cell system, greatly simplifying the electrical system. The only major components necessary are a DC/AC inverter configured to accept the fuel cell input voltage range and an appropriate disconnect switch on the AC power.

Commercially available DC/AC grid-tied inverters in the 100- to 500-kW power range are primarily designed for solar PV systems with input voltages in the 300- to 1,000-volts DC (VDC) range. They are typically unidirectional (DC to AC only) because there is no need to route power back to the solar array. The same conditions apply for fuel cell operation. However, solar inverters include features intended to optimize solar power output based on transient solar conditions which may interfere with their direct use by fuel cell systems. Based on phone conversations with hybrid inverter manufacturers, the production costs associated with solar inverters are representative even if some features must be revised so long as the input voltages remain within the inverter-allowed operating range. While some features of the solar inverters (e.g., power optimization for variable solar incident radiation) are not required for fuel cells, these are apparently minor variations on the overall inverter cost, so the fuel cell versions will be comparable. Fuel cell systems may be designed to have a voltage that matches commercially available solar inverters. So long as there is no need for off-grid operation, the inverter is the major cost driver

within the power electronics area. If off-grid operation is desired (as it typically will be), additional storage and interface requirements will add significant cost.

### 4.5.3 Off-Grid Operation

Section 4.3 describes the system sizing and operation options for off-grid applications. Off-grid operation is seen as a key feature of a CHP system to enable continued critical operations when the grid is down for some, typically brief, period of time. For off-grid operation, the fuel cell CHP system must respond to transient conditions that are usually out of the control of the operator—for example, equipment starts and stops, or increases or decreases in heat load. Electrical transients may be near instantaneous, while changes in heat load will generally be slower. The system schematics in Sections 4.4.1 and 4.4.2 (Figures 4-3 and 4-4) show provisions for dumping excess heat from the system if a rapid drop in heat load occurs. Rapid heat load pick-ups cannot significantly exceed the ability of the system to increase power. However, most process or space heating applications will ramp more slowly than the fuel cell system. Within limits, the fuel cell system operator may choose to reduce electrical power while increasing fuel flow rate to push more heat to the CHP load. Heat-load-following algorithms would typically be programmed on system installation.

The more challenging load changes are electrical, as these occur very quickly and frequently include short-duration spikes of many times the nominal equipment power rating (starting compressor motors, for example). While a PEM fuel cell operated on compressed hydrogen can respond quickly (within a few seconds), a reformer-based fuel cell is limited by the thermal inertia of the reformer and support hardware. An SOFC fuel cell stack cannot respond as quickly as a PEM stack without potentially damaging the stack due to thermal expansion issues. As mentioned in Section 4.4.2, an SOFC system is not burdened with as many heat exchangers or secondary reactors as a PEM system; however, the higher temperatures make response times slow, and since the stack is not repairable if damaged, transients are typically slow to minimize the potential for thermal stress damage to the stack.

For this analysis, we have assumed that a PEM system can respond to a change that is 25% of nominal load change within 15 minutes for the 100-kW system (a change from a 50-kW to a 75-kW load) and within 25 minutes for the 250-kW system. The SOFC system is assumed to require roughly twice as long to respond to equivalent load changes—30 minutes and 45 minutes for 100-kW and 250-kW systems, respectively. With these assumed constraints on system response, an electrical energy storage system (battery bank) is required to manage the load. The batteries must provide at least sufficient amount of stored energy to accommodate a single 25% load step up, and preferably two 25% steps up in succession.

The energy storage requirements may be relaxed in some cases where system controls and facility operation permit the demand-side management of loads and where no single load represents more than (for example) 5% of the nominal power. As will be shown Section 5, energy storage costs make up a noticeable percentage of the system installation costs. Furthermore, the batteries represent an ongoing cost as their lifetimes, particularly if deeply cycled frequently, may be shorter than the presumed life of the fuel cell system. Some systems which have frequent high-power spikes associated with equipment starting may benefit from ultracapacitors in place of, or in coordination with, battery storage. These would be specialized applications and are not considered in this report.

There are three possible methods for connecting a battery assembly to a fuel cell system. All relate to methods of managing the voltage associated with the energy storage so that the batteries are neither overcharged nor undercharged. The most conventional is to place a DC/DC converter on the output of



the fuel cell to regulate the voltage on the battery bus to match that of the battery system. Emerging hybrid DC/AC inverters that incorporate one or more auxiliary bidirectional DC ports represent a lower-cost approach to managing the voltage to the batteries. In some cases, it is possible that the batteries may be connected directly to the output of the fuel cell and operate in parallel with it. This option represents the lowest-cost approach but brings significant uncertainty associated with battery life and overall system management. Directly connected batteries would not be appropriate for all applications and would require application specific engineering in most cases. All three approaches are described below. Because three-port hybrid inverters are commercially available, would serve a wide range of potential system configurations, and cost less than a high-power DC/DC converter + DC/AC inverter configuration, they were chosen as the basis for our cost analysis.

#### 4.5.4 System Configurations

Commercially available high-power, grid-tied inverters are primarily designed for PV systems. Generally, these inverters are not appropriate for fuel cell systems due to design features used to maximize solar power under varying insolation (incident solar radiation) conditions. However, several solar inverter manufacturers indicated that they are able to design appropriate inverters to meet fuel cell requirements and that at production volumes, inverter costs for fuel cell systems would be similar to those for their solar systems. Because of the widely varying voltage experienced from a PV array, solar inverters (and, by extension, fuel cell inverters) are designed to accommodate a wide range of voltage input while maintaining regulated AC voltage on the output. The 100-kW and 250-kW high-power solar inverters typically have an input voltage range of 300 VDC to 600 VDC. Given that fuel cells can be configured to have a comparable operating voltage variance from peak to minimum power, basic solar inverter design should accommodate fuel cell voltage input. Therefore, with an AC grid available, batteries are not required and the fuel cell could be directly connected to the inverter input. However, the inverter must be capable of limiting output to match the input power available from the fuel cell, as the reformer responds to load changes slowly. This should be no more difficult than applying design and control features to maximize power from a solar array; therefore, we have used quotes for solar inverters (both simple DC/AC and hybrid/three-port inverters) as the basis for our cost estimating.

Lead acid batteries are used for energy storage. Lead acid batteries are widely available, relatively inexpensive, and well understood. They tolerate rapid charge and discharge cycles well and achieve acceptable lifetimes when properly managed. For lead acid batteries, the battery management system (BMS) can be relatively simple. State of charge is reasonably well represented by battery open-circuit voltage or by a polarization curve of voltage versus current. The BMS regulates charging rate based on the implied state of charge, dropping to a trickle charge as battery voltage increases. The BMS also limits the minimum terminal voltage difference by tripping the system should the battery terminal voltage become too low, indicating excess current draw for the state of charge of the battery.

Other energy storage options exist. Lithium ion (LI) batteries have a high energy/power density relative to other battery technologies, but they cost more than lead acid batteries for an equivalent amount of energy storage and require a more sophisticated BMS. For mobile/transportation applications, LI batteries are attractive due to their low weight and small footprint, but for stationary applications the minimal premium for smaller size and weight is not enough to overcome the cost advantage enjoyed by lead acid batteries. Ultracapacitors are also an option, particularly for high-surge power applications. The main drawback of ultracapacitor technology is limited energy density. This limitation can be overcome by hybridization with either lead acid or LI batteries. For this study, we assumed that lead acid batteries alone would be sufficient to manage the transients; alternative technologies were not considered.

#### 4.5.4.1 DC/DC Converter System

Figure 4-5 shows a basic electrical configuration with a DC/DC converter. Fuel cell output voltage and current are regulated by the DC/DC converter to maintain a relatively constant voltage at the battery terminals. Typically, the battery bus voltage is maintained at a level that yields a relatively high state of charge (80% or greater) on the batteries. However, the DC/DC converter is also managed to prevent drawing excessive power from the fuel cell if adequate hydrogen (or reformat) is not available due to the state of the reformer (during load increases, for example). Limiting the output current of the DC/DC converter causes the batteries to accept additional load as they will increase current as the bus voltage drops below the voltage associated with their state of charge. The battery voltage will decrease as the battery state of charge decreases.

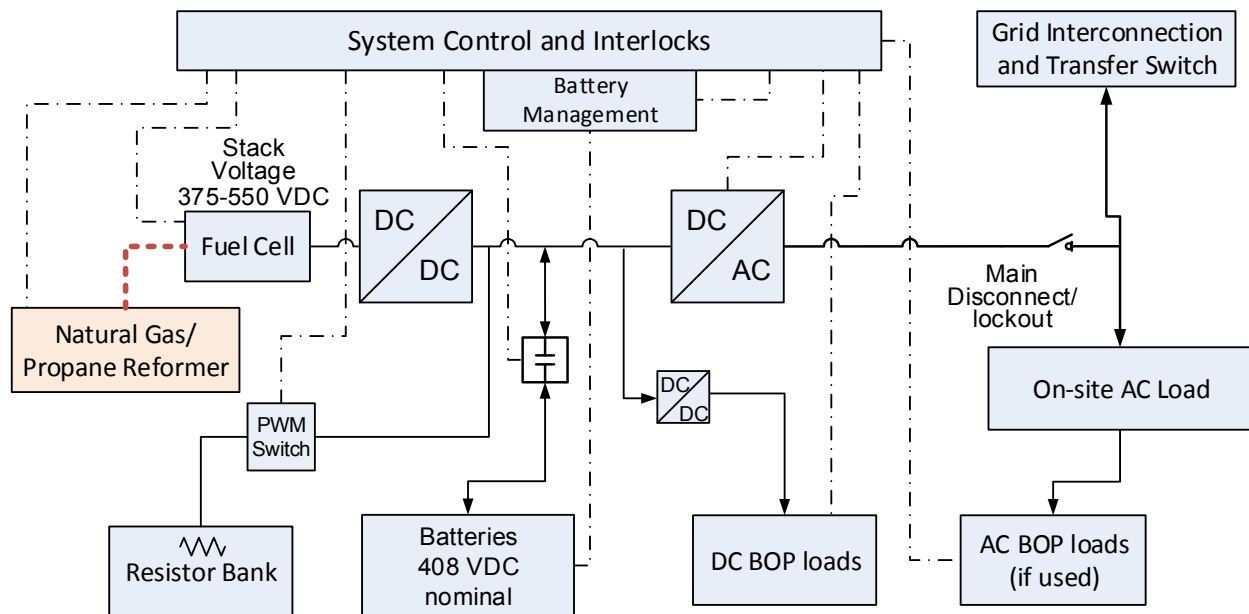


Figure 4-5. DC/DC converter electrical system schematic.

For load decreases, the reformer may be presented with excess reformat returning from the fuel cell anode, which can easily result in overheating the reformer and its support hardware. To address this condition, an actively managed resistor bank is necessary to dump some power as the reformer decreases reformat output. The resistor bank is managed to keep the fuel cell fuel utilization high while the reformer output decreases by applying an auxiliary load to the DC/DC converter to prevent overvoltage/overcharging of the batteries.

A secondary DC/DC converter is required to power the control electronics and miscellaneous support equipment in the system. The DC bus is assumed to be ~400 VDC for both the 100-kW and 250-kW systems. Most of the equipment is 24 VDC, so we have included a 400/24 DC/DC converter rated for 10% of nominal load for 100 kW and 250 kW. Buck converters, such as the one used for auxiliary power, are well defined, consist of minimal components, and can be very efficient at high power levels. The range of equipment available for 24 VDC is generally good, so the controls will typically include internal DC/DC converters to achieve the tightly regulated voltage required for the sensing electronics and

hardware. These “brick” converters, which have a relatively wide input voltage range, are typically included in the cost of the control hardware and would usually accept a supply voltage of 24 VDC nominal or 120 VAC, depending on the system design; both are available for a typical system.

For grid-connected service, the DC/AC inverter may allow charging the batteries if the fuel cell is not able to provide adequate power or is off-line for maintenance or some other reason. As indicated in Figure 4-5, the battery bus voltage is nominally 408 VDC, corresponding to thirty-four 12-volt batteries in series. A similar battery bank assembly is used for all three system configurations, with higher power batteries being used for the 250-kW system. The specific number of batteries used for the directly connected option is varied to match the stack output voltage range.

#### 4.5.4.2 Hybrid DC/AC Inverter System

Figure 4-6 shows a system schematic based on using a hybrid DC/AC inverter to provide interface between the fuel cell, batteries, and AC bus. Two companies were contacted that utilize recently developed technology to integrate a secondary high power DC/DC input/output (I/O) port into the primary DC/AC inverter specifically for connection to storage systems operating in parallel with the primary power source (typically solar for the currently available hybrid inverters). The main DC-to-AC inverter is configured for a wide input voltage range associated with solar (or fuel cell applications). The batteries (or other storage media) connect to an auxiliary port that is bidirectional for charging the batteries. A hybrid system provides flexibility on battery configuration, allowing the nominal battery voltage to be significantly different from the primary bus voltage. Since series-connected batteries result in lower current and smaller conductors for equivalent power, we have assumed that the batteries would be configured to operate near the fuel cell bus voltage. A similar battery bank assembly is used for all three system configurations, with higher power batteries being used for the 250-kW system.

An additional feature that may be required for the hybrid converters is a means to adjust the balance between the batteries and the fuel cell so that excess power is not drawn from the fuel cell during transients as the fuel processor ramps up. This feature would seem to be comparable to the load optimization feature for solar; therefore, we assume the cost would be comparable.

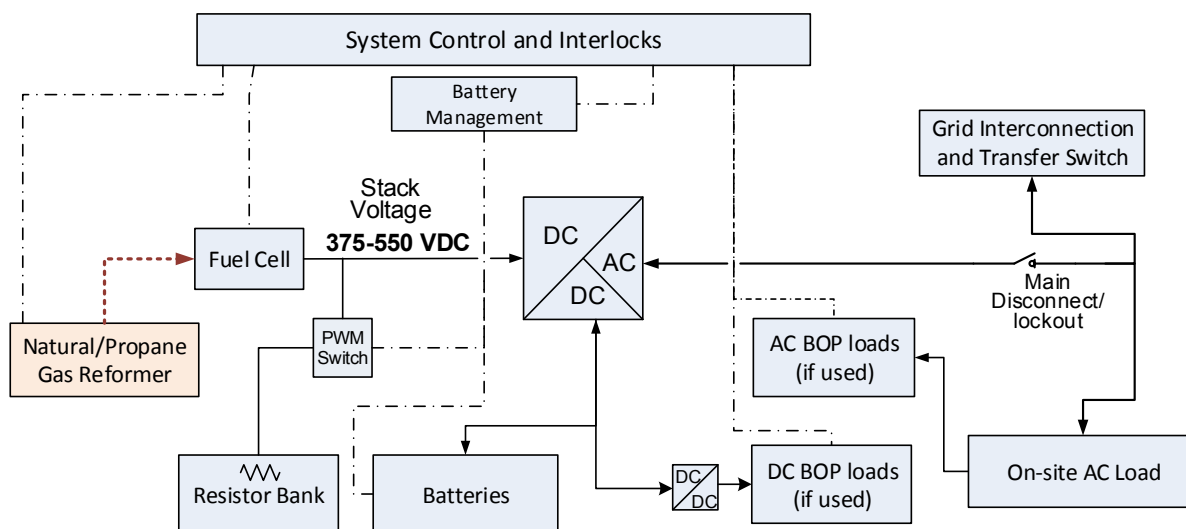


Figure 4-6. Hybrid inverter electrical system schematic.

#### 4.5.4.3 Direct Connect Battery System

Figure 4-7 is an electrical system schematic that includes a direct connection between batteries and the fuel cell output; no DC/DC converter is used. This approach is based on allowing the battery state of charge to vary with system load. When system load is high, the battery state of charge is low. Conversely, when system load is low, battery state of charge is high. The argument for this approach is that load changes that occur from low to high (equipment starting) require the batteries to provide significant energy while the fuel processor and fuel cell ramp up. Thus, battery state of charge should be high when load increases are expected—that is, when system power is overall low. Similarly, when the system load is high, significant increases in load are unlikely, but significant decreases in load are expected as equipment turns off. In that case, the batteries should be in a low state of charge to absorb the extra power produced by the fuel cell while the reformer ramps down.

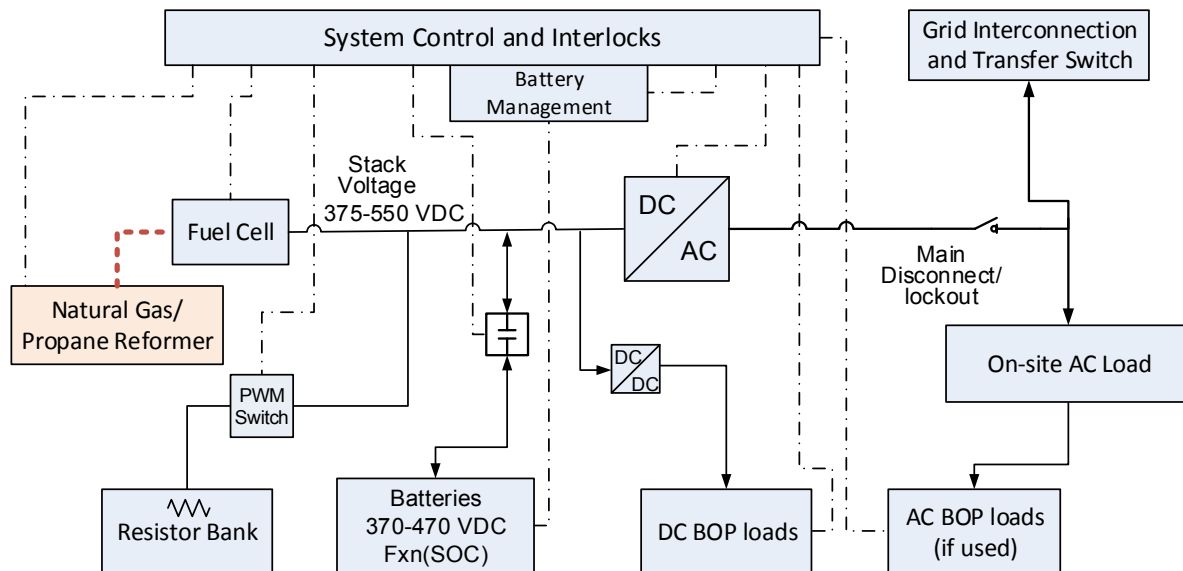


Figure 4-7. Directly-connected battery system schematic.

Figure 4-8 shows a typical PEM fuel cell polarization curve (extrapolated to the stack full power conditions for the 60-kW fuel cell stacks used for 100-kW PEM<sup>6</sup>). Also shown on the graph are the gross power from a single fuel cell stack and the state of charge of a set of 17 (in this case) lead acid batteries represented by the stack voltage at each power level. For this illustration, the state of charge of a nominal 12-volt battery is presumed to be linear from 10.5 VDC at 0% state of charge to 13.8 VDC at maximum charge. Voltage above 13.8 VDC may be acceptable if the voltage does not exceed that usually used for trickle-charging the batteries. However, Figure 4-8 shows that the fuel cell will output excessive voltage at low power. Therefore, as power drops below ~35% of nominal, action should be taken to protect the batteries from excess voltage. For extreme conditions (system trip), the batteries should be disconnected from the fuel cell outlet bus until the fuel cell can be fully taken off-line. Alternatively, the resistor bank may be used to dump power as fuel cell voltage approaches the fully charged limit.

<sup>6</sup> Hydrogenics HyPM HD30 performance curve from: [http://www.hydrogenics.com/docs/default-source/pdf/2-3-1-hypm\\_hd30\\_one-pager\\_en\\_a4\\_rev00.pdf?sfvrsn=2](http://www.hydrogenics.com/docs/default-source/pdf/2-3-1-hypm_hd30_one-pager_en_a4_rev00.pdf?sfvrsn=2)

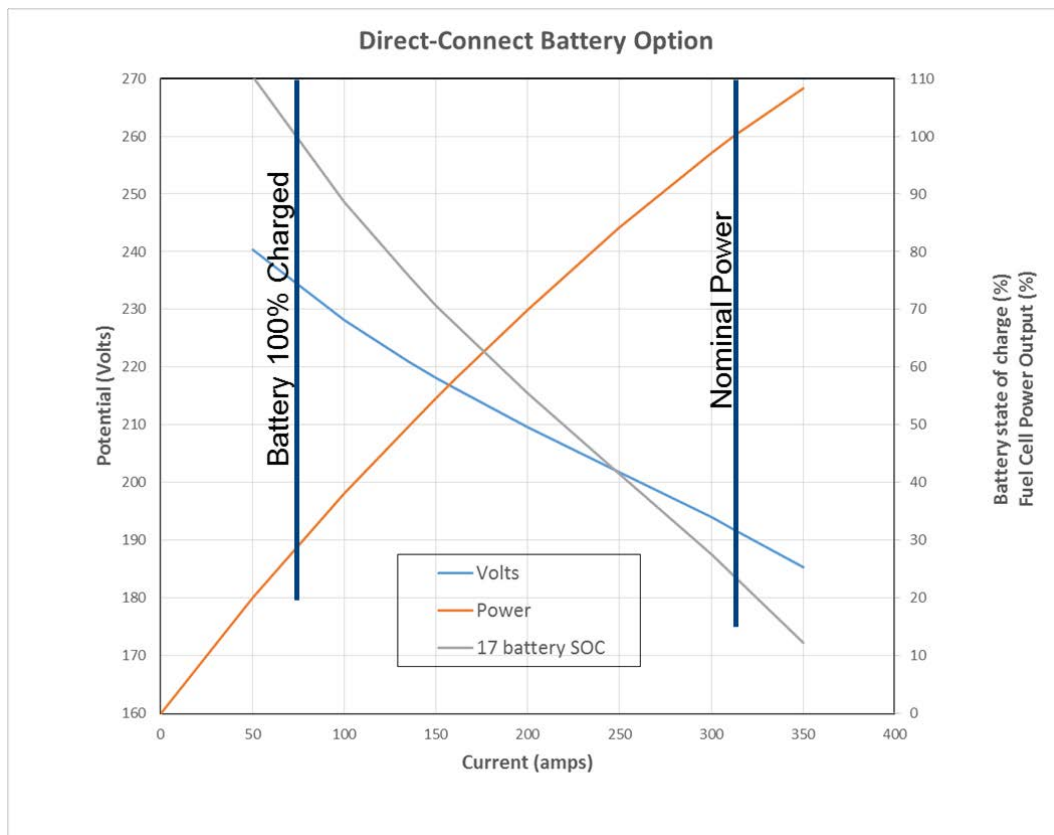


Figure 4-8. PEM fuel cell polarization curve with battery state of charge.

For the system in Figure 4-8, a bidirectional DC/AC inverter is preferred to ensure that the batteries are maintained in a relatively high state of charge during a fuel cell outage. The illustration in Figure 4-8 is for a single fuel cell stack matched with a set of 17 batteries. However, to achieve the appropriate voltages for typical solar-derivative inverters, we assume that two stacks will be connected electrically in series and will be matched with a series connected set of 34 nominally 12-volt batteries. Although not explicitly shown in the schematic, appropriate disconnects are required for personnel safety given the high voltages associated with this system.

Although illustrated here for PEM, a similar approach is possible for SOFC. However, in both cases significant engineering and testing is needed to confirm successful operation over the life of the fuel cell and battery assembly, as both may experience changes with age that could result in a mismatch in the state of charge versus nominal power. Because of the uncertainty, we have chosen not to include this case in the base costing but rather consider it as possible improvement in the sensitivity analysis.

#### 4.5.5 Thermal Management

Most power management electronics are 90% efficient or better—typically on the order of 95%. However, this still represents a significant heat load. At the output power of interest here, the power electronics are typically liquid-cooled, though air-cooled versions are available. If liquid-cooled power electronics are specified, thermal management hardware may be integrated with the main cooling loop and the heat

recovered for CHP purposes. For this analysis, we assumed that the heat associated with the power electronics would not be recovered for CHP purposes and that any heat rejection hardware would be included in the price of the equipment. Recovery of some electronics heat would further boost the temperature of the coolant reaching the CHP heat exchanger, representing both an improvement in net overall efficiency and higher-quality heat for CHP purposes.

#### 4.5.6 Wiring and Ancillary Components

Wiring, connectors, support hardware, and other minor components of the electrical system were addressed as a 5% addition to pre-markup cost.

## 5. Manufacturing Cost Analysis

### 5.1 System Cost Scope

As outlined in Section 4, two different fuel cell technologies with their associated BOP characteristics were considered. Due to the significant differences in stack fabrication and BOP hardware, the two technologies are considered separately (Sections 5.3 and 5.4). In addition to the stack for each technology, Battelle also developed a representative design for the fuel processing hardware and used DFMA<sup>®</sup> analysis on some components for each system. The electrical system is the same for both systems; therefore, it is costed as a stand-alone section and then incorporated into the total system costs for both technologies.

### 5.2 System Cost Approach

The manufacturing cost analysis approach includes:

- Developing cost estimates for each component and/or outsourced subassembly
- Designing a set of discrete steps to assemble the components into higher-level subassemblies and then into the final overall system
- Defining a burn-in and test sequence for the subassemblies and overall assembly and any statistical processes that might be used for higher volume manufacturing
- Establishing a representative manufacturing line configuration, including material handling and assembly machinery
- Evaluating capital, operation, supply, and maintenance costs for the representative manufacturing line

The estimated manufacturing cost was developed from the above factors, which were adjusted to the specifics of the system and production volumes.

Component and assembly costs were calculated from both custom models and the DFMA<sup>®</sup> library of manufacturing process models provided with the Boothroyd Dewhurst software. The specifics of the subsystem/component costs are shown in Appendices A-6 through A-26. Purchased components were incorporated into the assembly sequence models to determine the assembly cost for each size and production volume. The final cost of producing the fuel cell systems includes a testing and burn-in sequence for the overall system. The output of the manufacturing models was also used to calculate the

number of individual assembly stations or production lines required to support various product demand levels. From this, manufacturing equipment utilization was calculated and used to determine machine rates for the various manufacturing processes. The manufacturing capital cost model is also based on the number of process lines required, which provides the basis for calculating factory floor space and personnel requirements. We assumed that capital equipment expenditures for production would be amortized over a 20-year period (see Appendix A-1) and that the annual amortized cost would be distributed over the production volume for that year. Total system costs including capital expenditures were then estimated for the baseline system and projected improvements.

Because each system considered in this analysis incorporates multiple stacks (anywhere from 2 to 10 discrete stacks), stack production volumes increase rapidly, reaching 500,000 stacks/year for the 250-kW SOFC systems at 50,000 systems/year. Since each stack includes over 200 cells, stack component manufacturing volumes quickly reach millions of units/year even at relatively low system shipment levels (in excess of 2 million cells for one thousand 250-kW SOFC units shipped.) These high volumes affect the cost estimation process, and very few stack-related operations are considered to occur as outsourced supply.

At the 100-kW to 250-kW scale, most purchased components (e.g., heat exchangers) are not mass produced. In fact, for many of the purchased components, the manufacturer (or perhaps more accurately engineer/fabricator) typically sells less than 10 of any specific item in a year. Thus, achieving reliable high-volume cost quotes or rough order-of-magnitude (ROM) estimates was very difficult, and in many cases impossible. In order to establish the relative importance of the various purchased components, we used the best available quotes and conventional extrapolation methods (see Appendix A-2) to estimate higher production volume costs. It is likely that substantial redesign of many of the low-production-volume components would be required for significantly larger-volume purchases. Designs specific to larger-volume production would enable additional automation and more rapid cost reduction than we could confidently include in this analysis.

### 5.2.1 System Manufacturing Cost Assumptions

General process cost assumptions are presented in Table 5-1.

**Table 5-1. General Process Cost Assumptions**

Process Category	Assumed value
Energy cost	\$0.07/kWh
Labor cost	\$45.00/hr
Overall plant efficiency	85.00%

### 5.2.2 Machine Costs

The basic machine rate equation used in this analysis is a function of equipment capital costs, labor and energy costs, and utilization. To provide for easy comparison between various cost studies, Battelle followed the machine cost protocols described in James et al. (2014)<sup>7</sup>. Appendix A-1 provides details of

<sup>7</sup> B.D. James, A.B. Spisak, and W.G. Colella, 2014, "Design for Manufacturing and Assembly (DFMA®) Cost Estimates of Transportation Fuel Cell Systems," *ASME Journal of Manufacturing Science and Engineering*, New York, NY: ASME, Volume 136, Issue 2, p. 024503.



our machine rate calculations for the various production processes used to manufacture the CHP systems.

For each production line or machine station, utilization is calculated as the fraction of the total available time required to produce the required annual volume of systems. We assume that total available manufacturing time consists of three 8-hour shifts per day for 250 days per year, or 6,000 hours per year. The total required machine time is the product of the number of systems to be produced and the time required to produce the required components for each system. The number of machines required is calculated as:

$$\text{No. of machines} = \text{roundup} (\text{total required machine time} / 6,000)$$

For each machine, utilization is calculated as the fraction of the total available time required to produce the required annual volume of stacks:

$$\text{Utilization} = \text{total required machine time} / (6,000 \times \text{No. of machines})$$

The base (100% utilization) machine rate is divided by the utilization to determine the machine rate used to produce the components for that level of system production.

At low utilizations, job shops may make parts at a lower cost because their machines are used by multiple customers. This is particularly true for flexible Computer Numerically Controlled (CNC) tooling that can be applied to diverse industries. Additional job shop costs include the profit charged by the job shop and any overhead incurred by the manufacturer as a result of contract administration, shipping, and incoming parts inspection. For consistency across all types of tooling, we assume a job shop will base its cost on 65% machine utilization overall and 40% markup for profit plus overhead when calculating its rate. Refer to Appendix A-1 for details of the job shop machine rate calculations and the details of the make vs. buy decision.

### 5.2.3 Material Costs

Material cost on a per-unit basis (e.g., per kilogram, per square meter) tends to decrease with increasing purchase volumes, due primarily to the manufacturer's ability to produce larger volumes of material from a single production run setup. Material cost estimates at various discrete purchase volumes can be estimated for intermediate volumes using a learning curve analysis. Refer to Appendix A-2 for details of the analysis and learning curve parameters for the various materials used in the CHP system manufacturing process.

## 5.3 PEM System Manufacturing Costs

A PEM system, as described in Section 4, includes multiple fuel cell stacks and the BOP (fuel processor, support hardware, fuel and air supply, controls and sensors, and electrical equipment). This section discusses the stack manufacturing process used to achieve the design specifications in Table 5-2, followed by consideration of custom-fabricated BOP components, and finally by a summary of subassemblies created from commercially available hardware. As noted in Section 4, in order to achieve appropriate voltages and overall system power, the fuel cells are arranged in pairs connected in series: two 60-kW stacks yielding 120 kW gross for the 100-kW systems, and six 50-kW stacks in three pairs yielding 300 kW gross for the 250-kW system. The only difference in the stacks is the number of cells – 283 to yield 60 kW and 236 to yield 50 kW. The number of cells affects the stack voltage and impacts some aspects of the BOP—primarily the electrical power management and energy storage components.



**Table 5-2. PEM Fuel Cell Design Parameters**

Parameter	100-kW System	250-kW System
Power Density (W/cm <sup>2</sup> )	0.27	
Current Density (A/cm <sup>2</sup> )	0.4	
Cell Voltage (VDC)	0.68	
Active Area Per Cell (cm <sup>2</sup> )	780	780
System Net Power (kW)	100	250
System Gross Power (kW)	120	300
Number and Size of Stacks per System	2 x 60 kW (gross)	6 x 50 kW (gross)
Number of Cells per stack (#)	283	236
Full Load Stack Voltage (VDC)	192	160
Membrane Base Material	PFSA, 0.2mm thick, PTFE reinforced	
Catalyst Loading	0.4 mg Pt/cm <sup>2</sup> (total) Cathode is 2:1 relative to Anode	
Catalyst Application	Catalyst ink applied with selective slot die coating deposition, heat dried, decal transfer	
Gas diffusion layer (GDL) Base Material	Carbon paper 0.2 mm thick	
GDL Construction	Carbon paper dip-coated with PTFE for water management	
Membrane electrode assembly (MEA) Construction	Hot press and die cut	
Seals	1 mm silicone, injection molded	
Stack Assembly	Hand assembled, Machined pressed before tie rod installation	
Bipolar Plates	Graphite composite, compression molded	
End Plates	Sand cast and machined A356 aluminum	

### 5.3.1 PEM Stack Manufacturing Process

Each stack consists of end plates, bipolar plates, seals, and membrane electrode assemblies (MEAs). Figure 5-1 shows the manufacturing process in flow chart format. The four branches leading to stack assembly are:

- End plate fabrication
- Bipolar plate fabrication
- Gasket/seal fabrication
- MEA fabrication

Only the primary manufacturing and assembly processes are shown. As indicated in Figure 5-1 and Table 5-2, a stack consists of two end plates and the appropriate number of repeat units. Repeat units include:

- One MEA
- One each cathode and anode bipolar plate
  - The anode and cathode plates are stacked back to back to provide coolant flow channels)
- Seals between each item (three seals per each repeat unit).

#### ***5.3.1.1 PEM Stack Component Size and MEA Manufacturing Setup***

MEA components for both the 60-kW and 50-kW stacks (100-kW and 250-kW systems, respectively) are identical and have 780 cm<sup>2</sup> active area. Using a length-to-width ratio of 1.3, the active cell size was determined to be 245.0 millimeters (mm)— by 318.4 mm. Using a 30-mm margin on all sides to allow for gas channels and tie rod holes, the overall cell size was determined to be 305 mm by 378.4 mm. The primary dimension of 245 mm was selected to optimize usage from standard roll width material.

The cell configuration is shown in Figure 5-2.

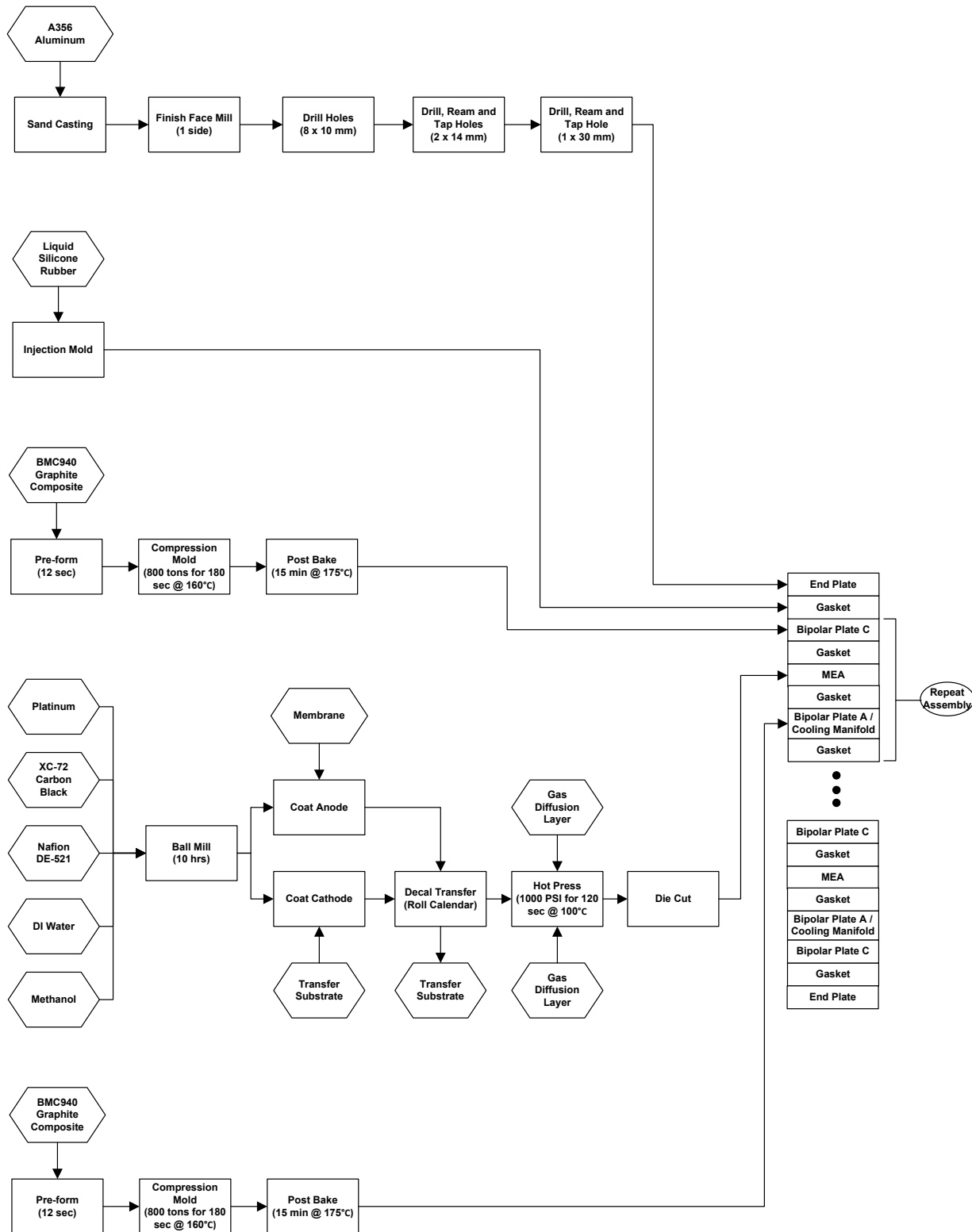


Figure 5-1. PEM fuel cell stack manufacturing process.

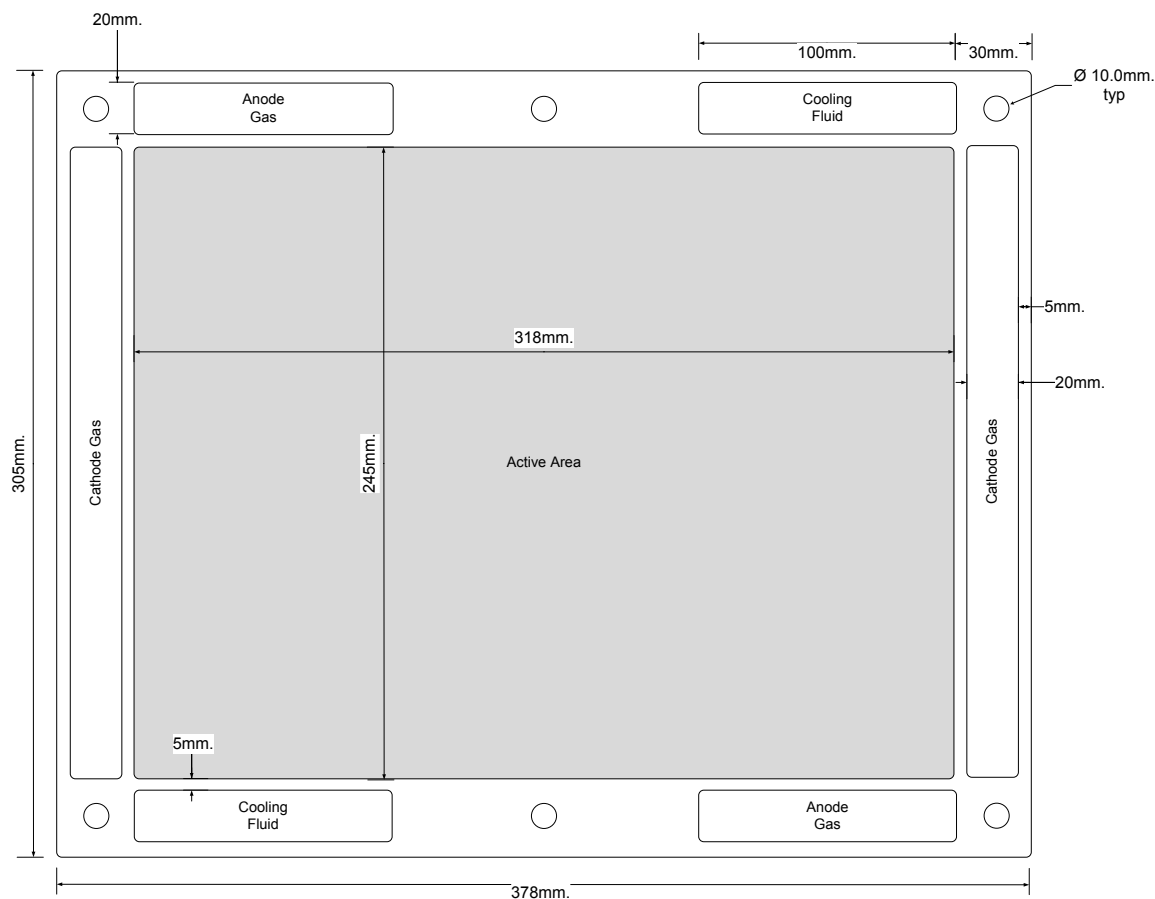


Figure 5-2. PEM MEA configuration for 780 cm<sup>2</sup> active area.

### 5.3.1.2 PEM Membrane Electrode Assembly (MEA)

The MEA is built up in layers starting with the hydrated membrane. The components of the catalyst ink are ball-milled into a uniform suspension. The anode layer is selective slot-die-coated directly on the hydrated membrane and dried. The cathode layer, meanwhile, is slot-die-coated onto a transfer substrate and dried. The coated membrane and transfer substrate layers are heated and roll pressed, then the transfer substrate is peeled away from the cathode layer following pressing. The catalyst-loaded membrane is then hot pressed between two gas diffusion layers (GDLs) and die cut to final cell dimensions. The catalysts and GDLs are applied only to the active area. The die-cutting process includes cutouts for the manifolds as shown in Figure 5-2. Details of the analysis are shown in Appendices A-7 (catalyst application) and A-8 (GDL application). For all production volumes, the component reject rate was assumed to be 2.5% for catalyst production, 2.5% for catalyst application, 3.0% for decal transfer, 0.5% for hot pressing, and 3.0% for die cutting. The MEA material cost summary is provided in Table 5-3, and the part production cost summary is given in Table 5-4.

**Table 5-3. PEM MEA Material Cost Summary - 100 kW and 250 kW**

	60-kW Stack (100-kW System)				50-kW Stack (250-kW System)			
	100	1,000	10,000	50,000	100	1,000	10,000	50,000
Catalyst	\$15.06	\$14.44	\$14.08	\$13.92	\$14.77	\$14.27	\$13.98	\$13.88
Membrane	\$6.70	\$4.06	\$2.93	\$2.93	\$5.48	\$3.32	\$2.93	\$2.93
GDL	\$17.02	\$4.96	\$3.44	\$3.44	\$10.42	\$3.44	\$3.44	\$3.44
Transfer Substrate	\$0.14	\$0.03	\$0.03	\$0.03	\$0.06	\$0.03	\$0.03	\$0.03
<b>Total Material Cost</b>	<b>\$38.92</b>	<b>\$23.49</b>	<b>\$20.47</b>	<b>\$20.31</b>	<b>\$30.74</b>	<b>\$21.06</b>	<b>\$20.37</b>	<b>\$20.27</b>

**Table 5-4. PEM MEA Cost Summary - 100 kW and 250 kW**

	60-kW Stack (100-kW System)				50-kW Stack (250-kW System)			
	100	1,000	10,000	50,000	100	1,000	10,000	50,000
Material	\$38.92	\$23.49	\$20.47	\$20.31	\$30.74	\$21.06	\$20.37	\$20.27
Labor	\$0.76	\$0.76	\$0.76	\$0.76	\$0.76	\$0.76	\$0.76	\$0.76
Machine	\$1.20	\$0.88	\$0.49	\$0.41	\$1.19	\$0.71	\$0.44	\$0.39
Scrap	\$1.12	\$0.65	\$0.56	\$0.56	\$0.87	\$0.58	\$0.56	\$0.56
Tooling	\$0.26	\$0.15	\$0.15	\$0.14	\$0.21	\$0.15	\$0.15	\$0.14
<b>Part Total</b>	<b>\$42.25</b>	<b>\$25.93</b>	<b>\$22.42</b>	<b>\$22.18</b>	<b>\$33.77</b>	<b>\$23.26</b>	<b>\$22.28</b>	<b>\$22.11</b>
# per Stack	283	283	283	283	236	236	236	236
<b>Stack Total</b>	<b>\$11,957.66</b>	<b>\$7,338.04</b>	<b>\$6,346.17</b>	<b>\$6,276.45</b>	<b>\$7,969.40</b>	<b>\$5,490.05</b>	<b>\$5,257.39</b>	<b>\$5,218.78</b>

Although the cells are identical for the 60-kW and 50-kW stacks, the higher volume production associated with the 50-kW stacks used for the 250-kW system (six stacks/system versus two) results in material and labor cost savings. Note that the membrane and GDLs dominate the cost at low volume, becoming much less important at high production rates, where catalyst cost becomes the dominant factor. Because of the precious metal content of the catalyst cost, it does not reduce as quickly with production volume as do those of the other materials. In fact, a potential concern is that the high production volumes, particularly for the larger systems, could cause increases in catalyst cost. While some recycling programs to reclaim the catalyst from retired fuel cells do exist, they still lack the availability and robustness of other precious metal programs, such as those in place for automotive catalytic converters. Additionally, due to the nature of PEM fuel cell construction, recovering high-value materials would likely be easier than is the case for catalytic converters.

### 5.3.1.3 PEM End Plates

The end plates are the same length and width as the MEA with the exception of the tie-rod projection on either end of the end plates. Six tie rods pass through the MEA to provide alignment (note round holes in Figure 5-2). Each end plate has three reamed and tapped holes for mounting fuel, cooling, and air connectors, as shown schematically in Figure 5-3. The large hole and entrance transition are for the air. The others are cooling and fuel. The end plates are identical: they must be oriented correctly in assembly. Correct orientation would be confirmed by assembly fixture position based on the large air inlet hole.



**Table 5-5. PEM End Plate Cost Summary - 100 kW and 250 kW**

	60-kW Stack (100-kW System)				50-kW Stack (250-kW System)			
	100	1,000	10,000	50,000	100	1,000	10,000	50,000
Material	\$9.15	\$9.03	\$9.03	\$9.03	\$9.03	\$9.03	\$9.03	\$9.03
Labor	\$7.94	\$5.76	\$5.54	\$5.52	\$6.32	\$5.60	\$5.52	\$5.52
Machine	\$28.40	\$20.59	\$9.48	\$5.41	\$22.61	\$20.01	\$9.51	\$4.04
Scrap	\$0.23	\$0.18	\$0.12	\$0.10	\$0.19	\$0.17	\$0.12	\$0.09
Tooling	\$9.89	\$0.99	\$0.20	\$0.12	\$3.30	\$0.33	\$0.13	\$0.11
Part Total	<b>\$55.62</b>	<b>\$36.54</b>	<b>\$24.37</b>	<b>\$20.18</b>	<b>\$41.46</b>	<b>\$35.14</b>	<b>\$24.32</b>	<b>\$18.79</b>
# per Stack	2	2	2	2	2	2	2	2
Total Cost per Stack	<b>\$111.23</b>	<b>\$73.08</b>	<b>\$48.73</b>	<b>\$40.35</b>	<b>\$82.91</b>	<b>\$70.28</b>	<b>\$48.64</b>	<b>\$37.59</b>

### 5.3.1.4 PEM Bipolar Plates

The bipolar plates are a compression-molded, graphite/thermoset-polymer composite material. While the use of stainless steel bipolar plates is a common practice for many applications requiring low weight and cost per kilowatt (such as automotive applications), industry feedback still supports the use of graphite material for applications focused on long lifetime expectations. The material is preformed into the approximate rectangular shape of the plate, then compressed into final shape in a 1,000-ton press at 160°C for 230 seconds. Two plates are formed during each machine cycle. The anode plate includes the cooling channels (two-sided plate) and is roughly twice as thick as the cathode plate. However, processing time is considered to be equivalent for both plates. Following molding, the plates are removed from the molds and baked at 175°C for 15 minutes. The process scrap rate was assumed to be 2.5% based on conversations with industry leaders. Details of the analysis are shown in Appendix A-10. The bipolar plate cost summary is provided in Tables 5-6 and 5-7.

**Table 5-6. PEM Anode Bipolar Plate Cost Summary - 100 kW and 250 kW**

	60-kW Stack – 100-kW System				50-kW Stack – 250-kW System			
	100	1,000	10,000	50,000	100	1,000	10,000	50,000
Material	\$1.46	\$1.46	\$1.46	\$1.46	\$1.46	\$1.46	\$1.46	\$1.46
Labor	\$0.97	\$0.97	\$0.97	\$0.97	\$0.97	\$0.97	\$0.97	\$0.97
Machine	\$3.05	\$1.84	\$1.84	\$1.82	\$2.24	\$1.92	\$1.82	\$1.82
Scrap	\$0.14	\$0.11	\$0.11	\$0.11	\$0.12	\$0.11	\$0.11	\$0.11
Tooling	\$0.59	\$0.43	\$0.41	\$0.41	\$0.46	\$0.41	\$0.41	\$0.41
Part Total	<b>\$6.22</b>	<b>\$4.82</b>	<b>\$4.80</b>	<b>\$4.77</b>	<b>\$5.26</b>	<b>\$4.88</b>	<b>\$4.78</b>	<b>\$4.77</b>
# per Stack	284	284	284	284	237	237	237	237
Total Cost per Stack	<b>\$1,766.21</b>	<b>\$1,368.44</b>	<b>\$1,361.86</b>	<b>\$1,354.77</b>	<b>\$1,246.04</b>	<b>\$1,156.45</b>	<b>\$1,131.73</b>	<b>\$1,130.03</b>



**Table 5-7. PEM Cathode Bipolar Plate Cost Summary – 100 kW and 250 kW**

	60-kW Stack – 100-kW System				50-kW Stack – 250-kW System			
	100	1,000	10,000	50,000	100	1,000	10,000	50,000
Material	\$0.98	\$0.98	\$0.98	\$0.98	\$0.98	\$0.98	\$0.98	\$0.98
Labor	\$0.97	\$0.97	\$0.97	\$0.97	\$0.97	\$0.97	\$0.97	\$0.97
Machine	\$3.05	\$1.84	\$1.84	\$1.82	\$2.24	\$1.92	\$1.82	\$1.82
Scrap	\$0.13	\$0.10	\$0.10	\$0.10	\$0.11	\$0.10	\$0.10	\$0.10
Tooling	\$0.59	\$0.43	\$0.41	\$0.41	\$0.46	\$0.41	\$0.41	\$0.41
Part Total	<b>\$5.72</b>	<b>\$4.32</b>	<b>\$4.29</b>	<b>\$4.27</b>	<b>\$4.76</b>	<b>\$4.38</b>	<b>\$4.27</b>	<b>\$4.27</b>
# per Stack	284	284	284	284	237	237	237	237
Total Cost per Stack	<b>\$1,624.09</b>	<b>\$1,226.32</b>	<b>\$1,219.74</b>	<b>\$1,212.66</b>	<b>\$1,127.44</b>	<b>\$1,037.85</b>	<b>\$1,013.13</b>	<b>\$1,011.43</b>

### 5.3.1.5 PEM Seals

The seals are injection-molded from two-part liquid silicone rubber (LSR) material using a four-cavity tool-steel mold. The component reject rate was assumed to be 0.5%. Details of the analysis are shown in Appendix A-9. The seal cost summary is provided in Tables 5-8 and 5-9. With the configuration shown in Figure 5-2, the seal between anode bipolar plate and the anode side of the MEA is identical to the seal between the back-to-back bipolar plates; the installed orientation is simply reversed. Thus, a single tool may be used for two of the three seals, increasing equipment utilization for the anode/cooling seal production. The seals require an orientation feature (e.g., a tab) to provide external evidence that the seals are correctly installed.

**Table 5-8. PEM Anode and Cooling Seal Cost Summary - 100 kW and 250 kW**

	60-kW Stack (100-kW System)				50-kW Stack (250-kW System)			
	100	1,000	10,000	50,000	100	1,000	10,000	50,000
Material	\$0.32	\$0.31	\$0.31	\$0.31	\$0.32	\$0.31	\$0.31	\$0.31
Labor	\$0.02	\$0.02	\$0.02	\$0.02	\$0.02	\$0.02	\$0.02	\$0.02
Machine	\$0.03	\$0.03	\$0.00	\$0.00	\$0.03	\$0.03	\$0.00	\$0.00
Scrap	\$0.00	\$0.00	\$0.00	\$0.00	\$0.00	\$0.00	\$0.00	\$0.00
Tooling	\$0.23	\$0.14	\$0.13	\$0.13	\$0.19	\$0.14	\$0.13	\$0.13
Part Total	<b>\$0.61</b>	<b>\$0.50</b>	<b>\$0.46</b>	<b>\$0.46</b>	<b>\$0.55</b>	<b>\$0.49</b>	<b>\$0.46</b>	<b>\$0.46</b>
# per Stack	566	566	566	566	472	472	472	472
Total Cost per Stack	<b>\$343.36</b>	<b>\$283.64</b>	<b>\$262.52</b>	<b>\$262.00</b>	<b>\$261.76</b>	<b>\$233.36</b>	<b>\$218.65</b>	<b>\$218.47</b>

**Table 5-9. PEM Cathode Seal Cost Summary – 100 and 250 kW Systems**

	60-kW Stack (100-kW System)				50-kW Stack (250-kW System)			
	100	1,000	10,000	50,000	100	1,000	10,000	50,000
Material	\$0.31	\$0.30	\$0.29	\$0.29	\$0.30	\$0.29	\$0.29	\$0.29
Labor	\$0.02	\$0.02	\$0.02	\$0.02	\$0.02	\$0.02	\$0.02	\$0.02
Machine	\$0.03	\$0.03	\$0.00	\$0.00	\$0.03	\$0.02	\$0.00	\$0.00
Scrap	\$0.00	\$0.00	\$0.00	\$0.00	\$0.00	\$0.00	\$0.00	\$0.00
Tooling	\$0.33	\$0.10	\$0.09	\$0.09	\$0.13	\$0.10	\$0.09	\$0.09
Part Total	<b>\$0.68</b>	<b>\$0.44</b>	<b>\$0.41</b>	<b>\$0.41</b>	<b>\$0.48</b>	<b>\$0.44</b>	<b>\$0.41</b>	<b>\$0.41</b>
# per Stack	285	285	285	285	238	238	238	238
Total Cost per Stack	<b>\$193.39</b>	<b>\$124.85</b>	<b>\$116.13</b>	<b>\$115.75</b>	<b>\$113.54</b>	<b>\$104.30</b>	<b>\$96.77</b>	<b>\$96.58</b>

### 5.3.1.6 PEM Stack Assembly

The stack components are assembled as defined in Figure 5-1. Pressure is applied to the completed stack using a hydraulic press, and the tie rods are installed to complete the stack assembly. Tie rod costs were estimated to be \$174.00 per stack and gas fittings were estimated to be \$304.00 per stack before applying learning curve analysis. Stack assembly times were estimated using the DFMA<sup>®</sup> software. After applying learning curve analysis to the assembly times and multiplying by the standard labor rate of \$45.00/hour, the average stack assembly costs were calculated as shown in Table 5-10. Details of the analysis appear in Appendix A-3.

**Table 5-10. PEM Stack Assembly Costs - 100 kW and 250 kW Systems**

	60-kW Stack (100-kW System)				50-kW Stack (250-kW System)			
	100	1,000	10,000	50,000	100	1,000	10,000	50,000
Material	\$438.23	\$409.78	\$383.18	\$365.62	\$424.42	\$396.87	\$371.11	\$354.10
Labor	\$187.62	\$166.36	\$164.23	\$164.05	\$144.29	\$138.34	\$137.74	\$137.69
Total Cost per Stack	<b>\$625.85</b>	<b>\$576.14</b>	<b>\$547.42</b>	<b>\$529.67</b>	<b>\$568.71</b>	<b>\$535.21</b>	<b>\$508.85</b>	<b>\$491.79</b>

### 5.3.1.7 PEM Stack Testing and Conditioning

Following assembly, the PEM stack is tested and conditioned to determine its fitness for installation into the system. Based on industry input, the total test time is assumed to be 2.5 hours. Stack testing requires connection to appropriate sources for air, hydrogen, and cooling and to an appropriately controlled load bank. Although these are reformate stacks, stack testing may be accomplished for this purpose with hydrogen to avoid the cost and complexity of mixed gases. The anode outlet is blocked for burn-in and power testing. Anode flow conditions may be tested with nitrogen before and after the test, thus purging the stack of hydrogen before it is moved to the system assembly area. The testing process is reportedly

subject to a fairly high failure rate, probably due to the immaturity of the production processes for stacks being produced currently. We have assumed a failure rate of 5% for this analysis (lower than the industry reported values, but still high for a mature production process) regardless of production volume. Stacks failing the test are reworked by disassembling the stack, replacing the defective part, and reassembling the stack. The cost of the rework is included in the scrap cost. Details of the analysis are shown in Appendix A-11. The stack testing and conditioning costs were calculated as shown in Table 5-11. The high stack failure rate would usually be expected to come down as higher volumes are reached and additional automation and quality control measures are instituted. In the absence of information on why the stack failure rates are high, we have to assume that the rate does not change with production volume. There is a sharp drop in machine cost per stack that occurs as production volumes change from 100 to 1,000 units/year; this reflects the low utilization rate in the case of the 100-unit volumes, and the assumption that all stack testing is performed in-house.

**Table 5-11. PEM Stack Testing and Conditioning Cost Summary - 100 kW and 250 kW**

	60-kW Stack (100-kW System)				50-kW Stack (250-kW System)			
	100	1,000	10,000	50,000	100	1,000	10,000	50,000
Material	\$80.53	\$38.68	\$20.94	\$20.93	\$50.39	\$24.39	\$17.65	\$17.65
Labor	\$90.34	\$88.10	\$87.88	\$87.86	\$85.78	\$85.15	\$85.09	\$85.08
Machine	\$592.18	\$31.70	\$20.90	\$20.90	\$177.01	\$20.90	\$20.90	\$20.90
Scrap	\$40.16	\$8.34	\$6.83	\$6.83	\$16.48	\$6.87	\$6.51	\$6.51
Tooling	\$0.00	\$0.00	\$0.00	\$0.00	\$0.00	\$0.00	\$0.00	\$0.00
Part Total	<b>\$803.22</b>	<b>\$166.82</b>	<b>\$136.54</b>	<b>\$136.51</b>	<b>\$329.66</b>	<b>\$137.30</b>	<b>\$130.15</b>	<b>\$130.13</b>
# per Stack	1	1	1	1	1	1	1	1
Total Cost per Stack	<b>\$803.22</b>	<b>\$166.82</b>	<b>\$136.54</b>	<b>\$136.51</b>	<b>\$329.66</b>	<b>\$137.30</b>	<b>\$130.15</b>	<b>\$130.13</b>

### 5.3.1.8 PEM Stack Cost Summary

Total stack manufacturing costs are summarized in Tables 5-12 and 5-13 and illustrated in Figures 5-4 and 5-5.

**Table 5-12. PEM Stack Component Cost Summary - 100 kW and 250 kW**

	60-kW Stack – 100-kW System				50-kW Stack – 250-kW System			
	100	1,000	10,000	50,000	100	1,000	10,000	50,000
MEA	\$11,957.66	\$7,338.04	\$6,346.17	\$6,276.45	\$7,969.40	\$5,490.05	\$5,257.39	\$5,218.78
Anode / Cooling Gasket	\$343.36	\$283.64	\$262.52	\$262.00	\$261.76	\$233.36	\$218.65	\$218.47
Cathode Gasket	\$193.39	\$124.85	\$116.13	\$115.75	\$113.54	\$104.30	\$96.77	\$96.58
Anode Bipolar Plate	\$1,766.21	\$1,368.44	\$1,361.86	\$1,354.77	\$1,246.04	\$1,156.45	\$1,131.73	\$1,130.03
Cathode Bipolar Plate	\$1,624.09	\$1,226.32	\$1,219.74	\$1,212.66	\$1,127.44	\$1,037.85	\$1,013.13	\$1,011.43
End plates	\$111.23	\$73.08	\$48.73	\$40.35	\$82.91	\$70.28	\$48.64	\$37.59
Assembly Hardware	\$438.23	\$409.78	\$383.18	\$365.62	\$424.42	\$396.87	\$371.11	\$354.10
Assembly Labor	\$187.62	\$166.36	\$164.23	\$164.05	\$144.29	\$138.34	\$137.74	\$137.69
Test and Conditioning	\$803.22	\$166.82	\$136.54	\$136.51	\$329.66	\$137.30	\$130.15	\$130.13
<b>Total Cost per Stack</b>	<b>\$17,425.01</b>	<b>\$11,157.34</b>	<b>\$10,039.11</b>	<b>\$9,928.16</b>	<b>\$11,699.45</b>	<b>\$8,764.80</b>	<b>\$8,405.29</b>	<b>\$8,334.81</b>

**Table 5-13. PEM Stack Manufacturing Cost Summary - 100 kW and 250 kW**

	60-kW Stack – 100-kW System				50-kW Stack – 250-kW System			
	100	1,000	10,000	50,000	100	1,000	10,000	50,000
Material	\$12,512.36	\$8,066.68	\$7,164.71	\$7,102.49	\$8,547.08	\$6,202.16	\$6,007.15	\$5,965.32
Labor	\$1,078.73	\$1,046.33	\$1,043.15	\$1,042.87	\$894.79	\$885.55	\$884.61	\$884.53
Machine	\$2,743.48	\$1,392.51	\$1,228.66	\$1,183.89	\$1,585.47	\$1,157.30	\$1,011.68	\$984.86
Scrap	\$434.30	\$254.20	\$226.47	\$224.31	\$277.56	\$195.92	\$188.57	\$187.56
Tooling	\$656.15	\$397.62	\$376.12	\$374.59	\$394.55	\$323.87	\$313.28	\$312.55
<b>Part Total</b>	<b>\$17,425.01</b>	<b>\$11,157.34</b>	<b>\$10,039.11</b>	<b>\$9,928.16</b>	<b>\$11,699.45</b>	<b>\$8,764.80</b>	<b>\$8,405.29</b>	<b>\$8,334.81</b>
Stacks/System	2	2	2	2	6	6	6	6
<b>Total Cost per System</b>	<b>\$34,850.03</b>	<b>\$22,314.67</b>	<b>\$20,078.22</b>	<b>\$19,856.31</b>	<b>\$70,196.72</b>	<b>\$52,588.83</b>	<b>\$50,431.76</b>	<b>\$50,008.86</b>

Breakdowns of stack cost volume trends appear in Figures 5-4 and 5-5.

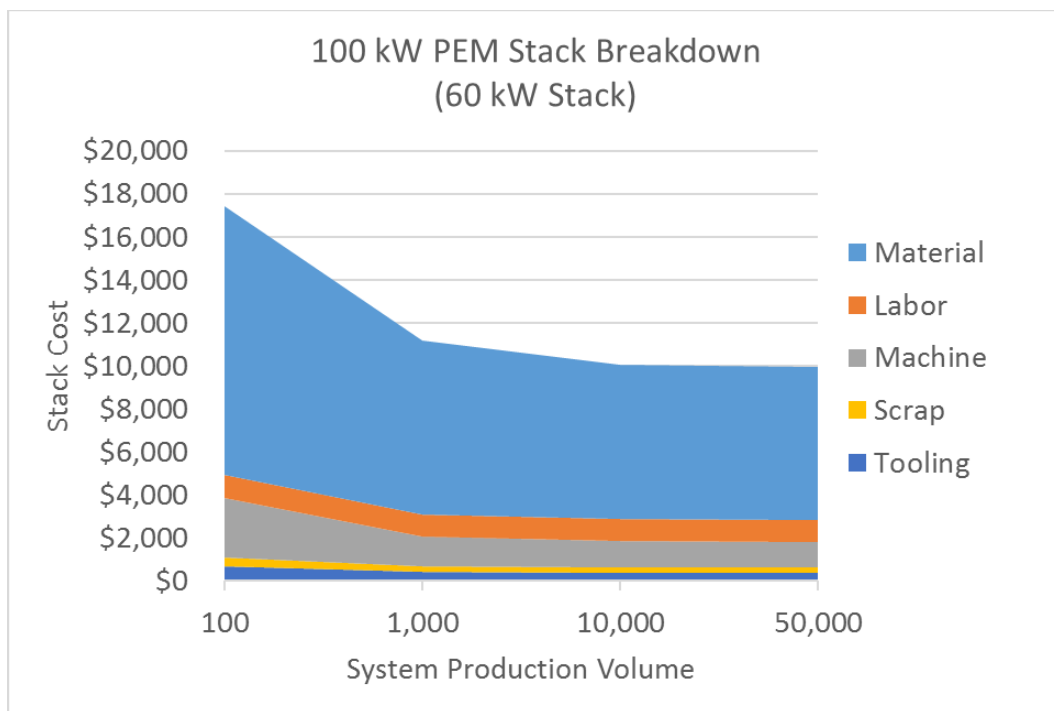


Figure 5-4. Breakdown of 100-kW system – 60-kW fuel cell costs and production volume trends.

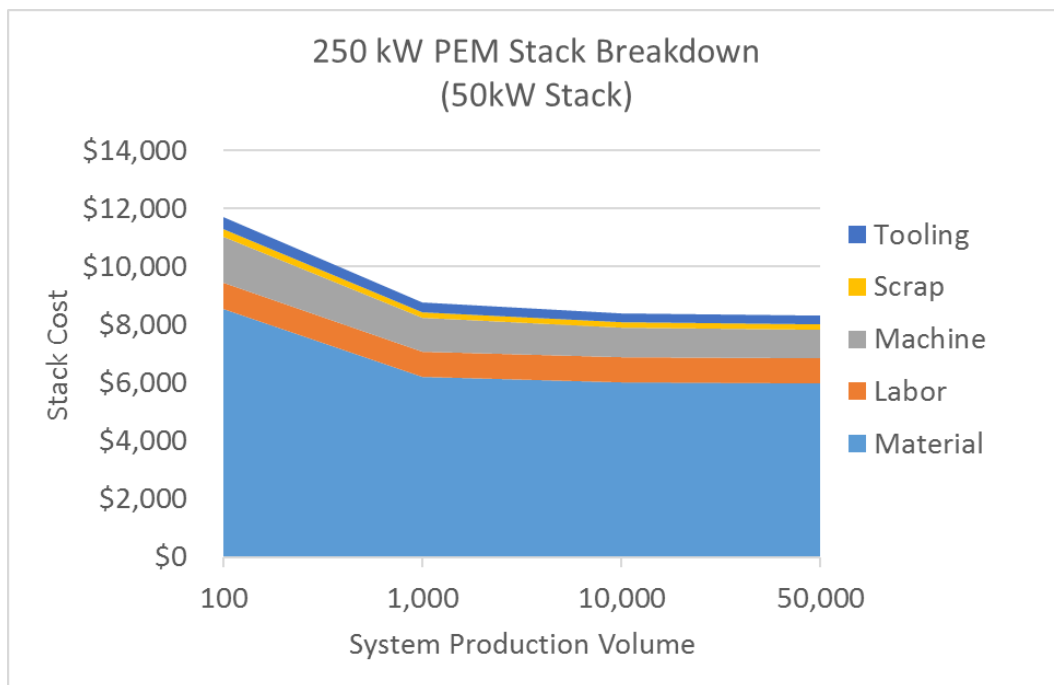


Figure 5-5. Breakdown of 250-kW system – 50-kW fuel cell costs and production volume trends.

### 5.3.2 PEM Systems BOP Manufacturing Cost Assessment

Fuel processing systems for natural gas and propane, the fuels of choice for primary power and CHP applications, tend to be unique to each manufacturer with very little detailed information available to the public. To provide a basis for costing, representative fuel processing systems were designed by Battelle based on experience with smaller systems and conversations with various component suppliers. The Battelle-designed fuel processing systems were modeled with ChemCad® to define operating temperatures, pressures, heat loads, and other performance metrics. The ChemCad® model outputs were used to specify some items for commercial quotes and to define performance criteria for other non-standard components that were assumed to be fabricated in-house. Fabricated components were modeled using DFMA® software. For the PEM system, fabricated items included: the reformer, steam generator, and water gas shift (WGS) and PrOx reactors. The reformate burner was based on a commercially available burner. While we recognize that some additional modifications will be required to manage the high-hydrogen/low-BTU wet anode gas, we believe that the final cost, after non-recurring engineering, should be representative. The heat exchangers shown in Figure 4-3 were quoted for one-off delivery by several heat exchanger manufacturers, as they have no experience with the higher production volumes evaluated in this study. Only one heat exchanger manufacturer was able to provide quotes for more than 1,000 units/order.

The reformer concept pricing was based on a reformer design patented by Catacel Corporation (now part of Johnson Matthey). The patent describes a single-tube, single-burner configuration suitable for systems up to approximately 25 kW. For the 100- and 250-kW versions described here, Battelle envisioned a multiple-tube, single-burner configuration. The steam generator is integrated with the reformer as a coil of finned tubing surrounding the multi-tube assembly and directly using the combustion gas from the reformer. The shift and PrOx reactors are pipe reactors using catalyst-coated ceramic monoliths. Additional detail on these components is included below.

#### 5.3.2.1 PEM Steam Reformer

To provide a basis for DFMA® analysis, we assumed that the steam reformer would be based on the design of the Catacel SSR® catalytic steam reformer (Figure 5-6). Figure 5-6 is based on a figure from Catacel patent no. 7,501,102. Design of the reformer used for Battelle's report on smaller fuel cell systems<sup>8</sup> was accomplished with guidance on sizing provided informally by Catacel. The reformer consists of a stack of catalyst-coated (CC) fans or stages and is scaled primarily by increasing the number of stages in the stack but also by adjusting the stage diameter. However, extending the number of stages to accommodate a 100-kW or larger system results in an unacceptably long device and likely an excessive pressure drop. Expanding the diameter of the reformer core would result in degraded internal heat transfer performance for the CC fans. Because the reforming reaction is endothermic, the fans are cooled by the reaction, leading to reduced reaction rates near the center of the fans if the diameter is too large. For this report, we developed an alternative design that packages several reformer cores within a single housing served by a single burner. The reformer cores are the same diameter as used previously for 5-, 10-, and 25-kW reformers.

---

<sup>8</sup> Battelle 2015. "Manufacturing Cost Analysis of 1, 5, 10, and 25 kW Fuel Cell Systems for Primary Power and Combined Heat and Power Applications." Report to DOE. DOE contract no. DE-EE0005250.

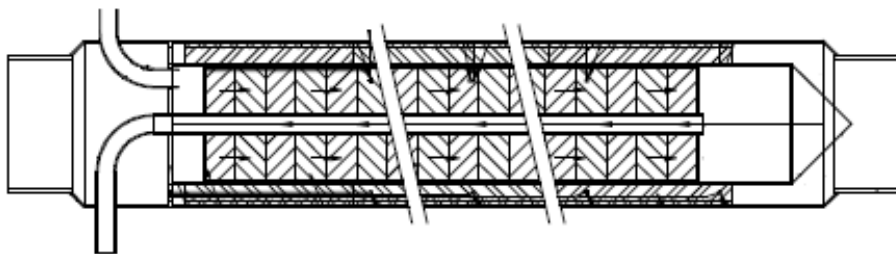


Figure 5-6. Catacel SSR<sup>®</sup> schematic diagram after patent no. 7,501,102.

Figure 5-7 shows the conceptual reformer configuration for a 100-kW system, and Figure 5-8 shows the reformer configuration for a 250-kW system. The reformer tube lengths and overall length are the same for both systems. The number of tubes and overall diameter are increased for the 250-kW system. In both systems the steam/fuel-reformate flow through the CC fan stack is opposite the combustion gas flow. Reformate flows to the exit manifold through a central tube within the CC fan stack.

Also illustrated in Figures 5-7 and 5-8 is a steam generator coil wrapped around the reformer and heated by the effluent combustion gas from the reformer. Integrating the steam generator in this way reduces both cost and heat loss compared to a separate steam generator. The steam generator coil is assumed to be a 25.4-mm outside diameter (OD) tube with 9.5-mm tall stainless steel fins continuously wound and brazed to the tube. Although shown as a loosely wound coil in Figures 5-7 and 5-8, for costing purposes the coils were assumed to be closely wound—that is, with the fin tips contacting adjacent fins on each coil and the coil occupying the available length.

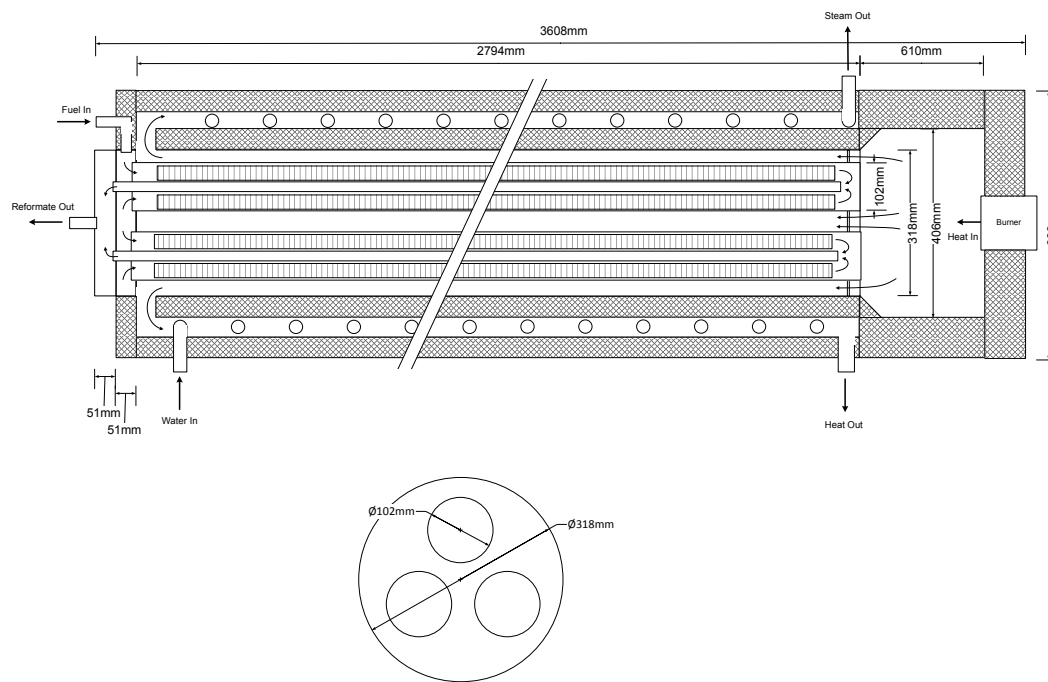


Figure 5-7. Three-tube 100-kW reformer configuration.



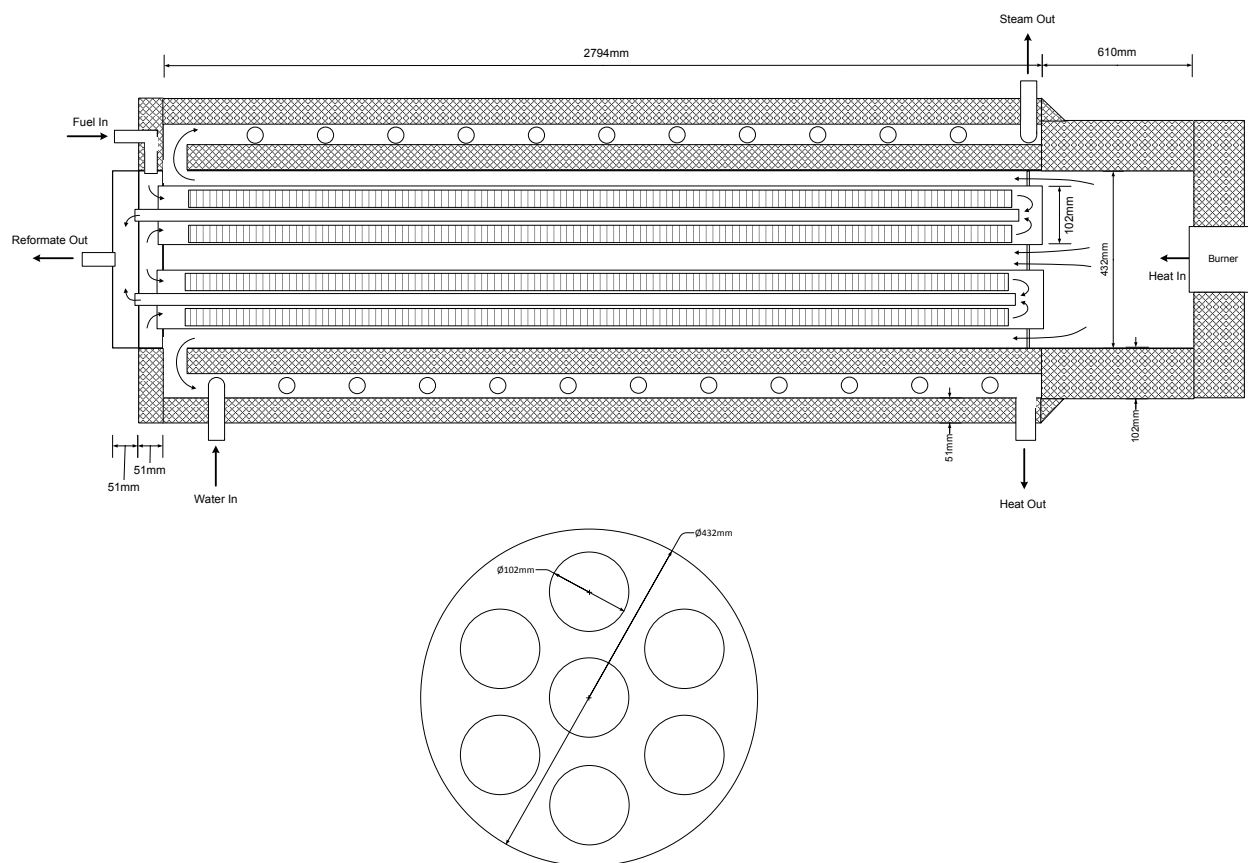


Figure 5-8. Seven-tube 250-kW reformer configuration

The required catalyst-coated surface area for each of the reformers is calculated based on a catalyst content of approximately 3,850 cm<sup>2</sup> per kilowatt as used by Catacel in its SSR<sup>®</sup> design. For the systems under consideration, we started with the reformer sizing parameters shown in Table 5-14.

Table 5-14. PEM Reformer Sizing Parameters

System Size (kW)	Approximate Reformer Size	Target Catalyst Area (cm <sup>2</sup> )
100	3 tubes @ 2663 cm active fan length	3@1.62x10 <sup>5</sup> = 4.62x10 <sup>5</sup> total
250	7 tubes @ 2663 cm active fan length	7@1.62 x10 <sup>5</sup> = 1.16x10 <sup>6</sup> total

Each reformer tube includes 168 CC fans. Using fixed fan dimensions and the target coated areas listed in Table 5-14, we established the final reformer dimensions for each system as shown in Table 5-15. The tubes and housings are rolled and welded from high alloy or stainless steel sheets. Appropriate locating features are assumed to be incorporated into the tube to position the CC fans. The fans and associated separator washers are loaded into the tubes prior to the end plates being welded on and before the tubes are welded into the tube sheet. The center tubes are inserted through the inlet tube sheet and through the CC fan stack before the assembly is welded into the overall shell. The reactor cost summary is shown in Table 5-16.

**Table 5-15. PEM Reformer Dimensional Summary**

Dimension	100 kW	250 kW
Overall Diameter (mm) Includes steam generator and insulation	609	724
Overall Length. (mm)	3,710	3,710
Flow Stages	3 tubes @ 168 = 504	7 tubes @ 168 = 1,176
Final Catalyst Area (cm <sup>2</sup> )	485,300	1,132,365

**Table 5-16. PEM System Reformer Cost Summary - 100 kW and 250 kW**

	100-kW PEM System				250-kW PEM System			
	100	1,000	10,000	50,000	100	1,000	10,000	50,000
Material	\$1,605.38	\$1,487.43	\$1,399.48	\$1,345.74	\$2,633.88	\$2,490.28	\$2,387.14	\$2,321.71
Process	\$2,048.19	\$1,166.09	\$1,075.30	\$1,008.81	\$4,657.94	\$2,669.29	\$2,287.13	\$2,213.28
Scrap	\$182.68	\$132.68	\$123.74	\$117.73	\$364.59	\$257.98	\$233.71	\$226.75
Tooling	\$2,077.17	\$207.72	\$41.54	\$29.08	\$3,864.15	\$386.41	\$77.28	\$54.10
Manufactured Parts	\$5,913.42	\$2,993.91	\$2,640.06	\$2,501.36	\$11,520.56	\$5,803.96	\$4,985.27	\$4,815.84
Catalyst	\$43.61	\$40.15	\$37.02	\$35.02	\$98.69	\$90.91	\$83.88	\$72.32
Purchased Parts	\$843.01	\$843.01	\$843.01	\$843.01	\$1,823.07	\$1,823.07	\$1,823.07	\$1,823.07
Assembly	\$621.25	\$496.19	\$483.69	\$482.58	\$1,434.65	\$1,145.87	\$1,116.99	\$1,114.42
Total Cost per System	\$7,421.29	\$4,373.27	\$4,003.79	\$3,861.97	\$14,876.96	\$8,863.81	\$8,009.20	\$7,825.64

### 5.3.2.2 PEM Shift and PrOx Reactors

To provide a basis for DFMA<sup>®</sup> analysis, we assumed the shift and PrOx reactors would be designed as cylindrical containers sized to hold the appropriate volume of catalyst material as determined based on the required gas hourly space velocity for the reactors. Although originally conceived as pipe reactors with granulated or pelletized catalyst, a major automotive catalyst supplier provided recommendations for sizing and cost estimating using catalyst-coated ceramic monoliths. The supplier suggested using cylindrical catalyst monoliths that were ~5.66 inches (144 mm) in diameter and 6 inches (152 mm) long. Equivalent “half” monoliths at 3 inches (76 mm) long are also available. By selecting appropriate catalysts and varying the precious metal type and loading, they suggested that the shift and PrOx reactors could be made to be essentially the same size (and, we assume, essentially the same cost, though they provided only an overall cost, not a reactor-specific cost). The cost estimates were compared to catalyst cost/quantity (or equivalently, space velocity) recommendations from other sources, including pelletized catalysts, and were found to be somewhat lower but not radically different. These reactors also compare reasonably well to the costs of automotive catalytic converters. This follows because the monoliths and catalyst coating methodology were developed for automotive applications. The costs were rounded up to account for unknowns, including the preliminary nature of the estimates and the dependence on precious metal pricing. Generally, we have found that precious metal content is typically less than half of the cost

of the catalyst, whether for a granulated, pelletized, or coated monolith; however, precious metal costs are enough of the catalyst cost to notably change the cost if metal prices change significantly. When considering the production of 10,000 to 50,000 large systems/year, the total quantity of catalyst required could in fact push precious metal prices higher. As noted for the fuel cell catalyst, a robust recycling program would alleviate most of this concern. Because these reactors have significant commonality with automotive catalytic converters, a recycling process is already in place. Shift and PrOx reactor sizing is shown in Table 5-17.

**Table 5-17. PEM Shift/PrOx Reactor Sizing Recommendations**

System Size (kW)	Shift Reactor Monoliths (total)	PrOx Reactor Monoliths (total)
100	5	5
250	12.5	12.5

The supplier also recommended that each reactor be split into two sections with a heat exchanger between. The 100-kW reactors (both shift and PrOx) were divided into two reactors with 2.5 monolith assemblies in each followed by a heat exchanger. For the 250-kW assembly, the lead reactor includes 6 monoliths and the trailing reactor (after the heat exchanger) includes 6.5 monoliths. The 250-kW system uses the same overall can size for all shift and PrOx reactors. The reactor dimensions for each system are shown in Table 5-18.

**Table 5-18. PEM Shift/PrOx Reactor Dimensional Summary**

Dimension	100 kW	250 kW
Shift Diameter (OD-cm)	152.5	152.5
Shift Length (each reactor) (mm) (2 required)	1170	1930
PrOx Diameter (OD-mm)	152.5	152.5
PrOx Length (each reactor) (mm) (2 required)	1170	1930

Example reactor configurations, applicable to either shift or PrOx, are shown in Figure 5-9a and Figure 5-9b. As shown, the reactors are designed with a low-included-angle conical inlet to distribute the flow across the face of the catalyst. The choice of conical inlet rather than screens or other distribution features was enabled by the relatively large scale of the system: space was considered less valuable than overall cost and pressure drop. The shift reactor operates at modest temperatures and low pressure, allowing the use of 18 gauge 316L stainless steel sheet for the primary container construction. The cylindrical shell was formed by stamping two identical clamshell halves. The catalyst monoliths are wrapped with compliant high-temperature felt and placed between the two clamshells, which are then welded together. The outlet cap could be incorporated with the stamping; however, for our analysis it was fabricated separately and welded to the clamshell halves as the last process in reactor assembly. The outlet caps are formed by stamping circular disks and welding a short tubing section to the disk before the disk is welded to the clamshells. The reactor cost summaries are shown in Table 5-19.

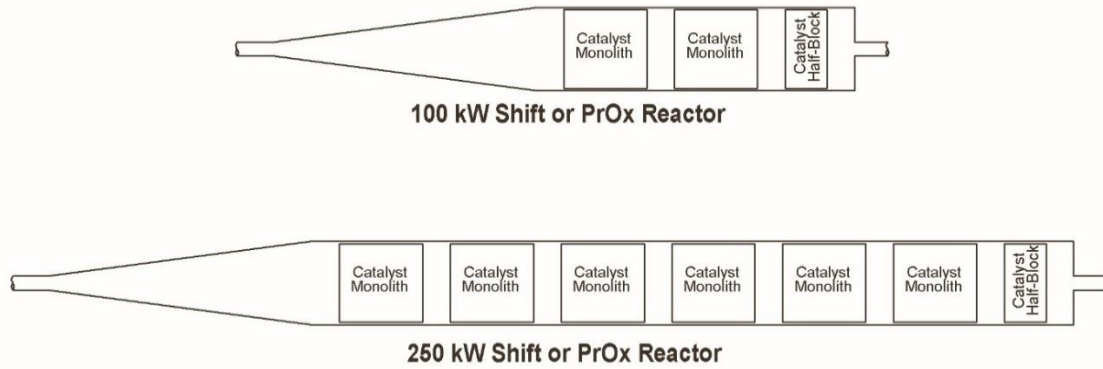


Figure 5-9a. Shift/PrOx reactor configuration.

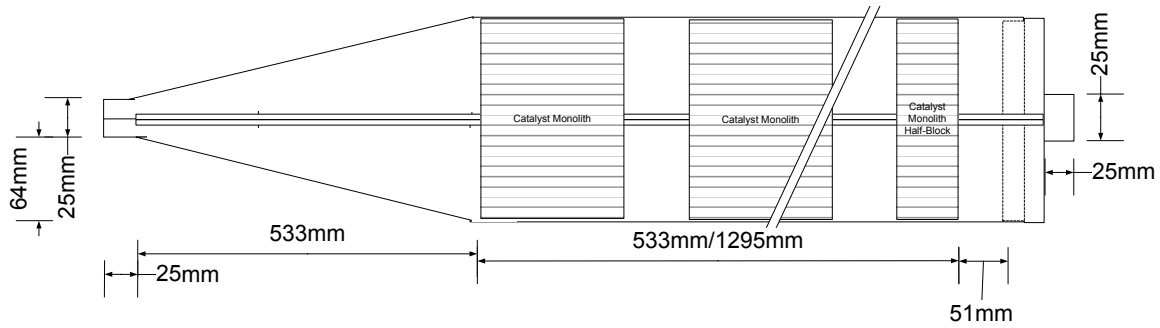


Figure 5-9b. Shift/PrOx reactor typical dimensions.

**Table 5-19. Shift and PrOx Reactor Manufacturing Costs**

	100 kW				250 kW			
	100	1,000	10,000	50,000	100	1,000	10,000	50,000
Material	\$96.69	\$94.47	\$94.10	\$94.10	\$183.86	\$181.65	\$181.27	\$181.27
Process	\$12.50	\$94.47	\$94.10	\$94.10	\$39.43	\$181.65	\$181.27	\$181.27
Scrap	\$5.46	\$9.45	\$9.41	\$9.41	\$11.16	\$18.16	\$18.13	\$18.13
Tooling	\$82.46	\$8.25	\$0.82	\$0.16	\$157.86	\$15.79	\$1.58	\$0.32
Manufactured Parts	\$197.11	\$206.64	\$198.44	\$197.78	\$392.31	\$397.24	\$382.25	\$380.99
Catalyst	\$4,566.73	\$3,784.36	\$3,136.02	\$2,750.00	\$10,982.76	\$9,101.18	\$7,541.96	\$6,756.75
Purchased Parts	\$13.39	\$13.39	\$13.39	\$13.39	\$26.71	\$26.71	\$26.71	\$26.71
Assembly	\$7.43	\$5.94	\$5.79	\$5.77	\$12.35	\$9.87	\$9.62	\$9.60
Reactor Cost	\$4,784.67	\$4,010.33	\$3,353.63	\$2,966.94	\$11,414.13	\$9,535.00	\$7,960.53	\$7,174.04
# per System	4	4	4	4	4	4	4	4
Total Cost per System	\$19,138.69	\$16,041.31	\$13,414.53	\$11,867.77	\$45,656.52	\$38,139.99	\$31,842.13	\$28,696.16

### 5.3.3 PEM BOP Cost Assumptions

The costs associated with the BOP components are tabulated in Table 5-20. Figures 5-10 through 5-13 compare component costs at a subcategory level similar to the system schematic. At a production rate of 1,000 systems a year, the BOP hardware is estimated to cost in excess of \$147,000 for each 100-kW system. The cost increases to over \$235,000 for a 250-kW system at the same production volume. These BOP costs are ~\$1,470/kW and ~\$940/kW, respectively. This compares to \$126/kW and \$110/kW for the fuel cell stacks for these systems. System overall cost is more sensitive to the assumptions applied to the BOP components than those applied to the stack. Many component costs, including most sensors and regulators, remain the same regardless of system size, and are therefore similar to costs presented in the FY14 primary power and CHP study.<sup>9</sup> Furthermore, these costs do not vary significantly with system size. Power electronics for grid connection and off grid operation, as well as fuel processor equipment, comprise the majority of the BOP costs, and these do scale significantly with capacity.

A category titled “Additional Work Estimate” is included to capture small contingencies not specifically itemized in this report. These include components such as heat sinks and fans for additional electrical cooling, supplementary temperature or pressure sensors, and any extra assembly hardware. This estimate is based on a 20% buffer to the electrical subsystem cost and a 10% buffer to all remaining hardware.

<sup>9</sup> Battelle. 2015. “Manufacturing Cost Analysis of 1, 5, 10, and 25 kW Fuel Cell Systems for Primary Power and Combined Heat and Power Applications.” Report to DOE. DOE contract no. DE-EE0005250.

**Table 5-20. PEM BOP Cost Summary for 100-kW and 250-kW Systems**

System	Component Description	Annual Production of 100kW PEM Systems				Annual Production of 250kW PEM Systems			
		(100)	(1,000)	(10,000)	(50,000)	(100)	(1,000)	(10,000)	(50,000)
Fuel Supply	Nat. Gas Filter	\$ 97	\$ 81	\$ 68	\$ 57	\$ 305	\$ 254	\$ 241	\$ 178
	Natural Gas Control Valve	\$ 4,561	\$ 3,882	\$ 3,397	\$ 3,154	\$ 4,501	\$ 3,830	\$ 3,352	\$ 3,112
	Natural Gas Flowmeter	\$ 1,697	\$ 1,619	\$ 1,416	\$ 1,214	\$ 1,697	\$ 1,619	\$ 1,416	\$ 1,214
	Desulfurizer	\$ 2,427	\$ 1,457	\$ 1,269	\$ 1,142	\$ 4,855	\$ 3,424	\$ 3,027	\$ 2,724
	3-way valve	\$ 1,320	\$ 1,247	\$ 1,174	\$ 1,174	\$ 3,521	\$ 3,325	\$ 3,130	\$ 3,130
Water Supply	Reformer Water Pump	\$ 2,011	\$ 1,910	\$ 1,810	\$ 1,709	\$ 2,011	\$ 1,910	\$ 1,810	\$ 1,709
	Recovered Water Tank	\$ 51	\$ 38	\$ 30	\$ 30	\$ 95	\$ 71	\$ 57	\$ 57
	Water filter	\$ 37	\$ 34	\$ 34	\$ 34	\$ 60	\$ 56	\$ 56	\$ 56
	Di Polisher	\$ 144	\$ 137	\$ 130	\$ 123	\$ 144	\$ 137	\$ 130	\$ 123
	Water flow meter	\$ 1,098	\$ 976	\$ 976	\$ 976	\$ 1,030	\$ 970	\$ 970	\$ 970
Fuel Processor	Reformer	\$ 7,421	\$ 4,373	\$ 4,004	\$ 3,862	\$ 14,877	\$ 8,864	\$ 8,009	\$ 7,826
	Burner	\$ 4,750	\$ 4,500	\$ 4,275	\$ 4,168	\$ 5,700	\$ 5,400	\$ 5,130	\$ 5,002
	WGS & PrOx Reactors	\$ 19,139	\$ 16,041	\$ 13,415	\$ 11,868	\$ 45,657	\$ 38,140	\$ 31,842	\$ 28,696
	Superheater	\$ 24,306	\$ 23,091	\$ 21,936	\$ 21,497	\$ 28,229	\$ 26,818	\$ 25,477	\$ 24,967
Air Supply	Air Filter	\$ 510	\$ 479	\$ 447	\$ 415	\$ 1,177	\$ 1,108	\$ 1,039	\$ 970
	Combustion Air Blower	\$ 3,049	\$ 2,818	\$ 2,586	\$ 2,471	\$ 3,696	\$ 3,416	\$ 3,136	\$ 2,996
	Combustion Air Flowmeter	\$ 1,493	\$ 1,405	\$ 1,317	\$ 1,229	\$ 1,493	\$ 1,405	\$ 1,317	\$ 1,229
	PrOx blower	\$ 805	\$ 770	\$ 735	\$ 717	\$ 2,961	\$ 2,730	\$ 2,499	\$ 2,383
	PrOx Flowmeter	\$ 1,493	\$ 1,405	\$ 1,317	\$ 1,229	\$ 1,493	\$ 1,405	\$ 1,317	\$ 1,229
	Cathode Air Blower	\$ 3,049	\$ 2,818	\$ 2,586	\$ 2,471	\$ 3,696	\$ 3,416	\$ 3,136	\$ 2,996
	Cathode Air Flowmeter	\$ 1,493	\$ 1,405	\$ 1,317	\$ 1,229	\$ 1,493	\$ 1,405	\$ 1,317	\$ 1,185
	Recuperative Humidifier	\$ 498	\$ 376	\$ 285	\$ 248	\$ 1,245	\$ 966	\$ 712	\$ 619
Heat Recovery	WGS Outlet Cooler 1	\$ 2,948	\$ 2,653	\$ 2,388	\$ 2,268	\$ 4,412	\$ 3,971	\$ 3,574	\$ 3,395
	WGS Outlet Cooler 2	\$ 2,948	\$ 2,653	\$ 2,388	\$ 2,268	\$ 4,412	\$ 3,971	\$ 3,574	\$ 3,395
	First Combustion Condenser	\$ 3,870	\$ 3,483	\$ 3,135	\$ 2,978	\$ 4,964	\$ 4,467	\$ 4,020	\$ 3,819
	Second Combustion Condenser	\$ 5,490	\$ 4,941	\$ 4,447	\$ 4,225	\$ 7,683	\$ 6,915	\$ 6,223	\$ 5,912
	PrOx Outlet Cooler 1	\$ 5,335	\$ 4,801	\$ 4,321	\$ 4,105	\$ 7,984	\$ 7,185	\$ 6,467	\$ 6,143
	PrOx Outlet Cooler 2	\$ 5,335	\$ 4,801	\$ 4,321	\$ 4,105	\$ 7,984	\$ 7,185	\$ 6,467	\$ 6,143
	CHP Export Exchanger	\$ 4,860	\$ 4,374	\$ 3,937	\$ 3,740	\$ 5,512	\$ 4,960	\$ 4,464	\$ 4,241
	Radiator	\$ 5,957	\$ 5,659	\$ 5,376	\$ 5,268	\$ 12,513	\$ 11,888	\$ 11,293	\$ 11,067
Power Electronics	Glycol Pump	\$ 698	\$ 629	\$ 556	\$ 509	\$ 752	\$ 676	\$ 598	\$ 548
	Hybrid Inverter	\$ 42,000	\$ 33,600	\$ 26,400	\$ 21,600	\$ 96,000	\$ 75,000	\$ 57,000	\$ 45,000
	Batteries	\$ 5,690	\$ 5,464	\$ 5,269	\$ 5,060	\$ 11,765	\$ 11,298	\$ 10,897	\$ 10,465
	Resistor Bank	\$ 2,000	\$ 1,610	\$ 1,289	\$ 1,030	\$ 4,026	\$ 3,220	\$ 2,577	\$ 2,061
Control and Instrumentation	Grid Interconnect Switch	\$ 1,204	\$ 1,084	\$ 975	\$ 878	\$ 2,645	\$ 2,381	\$ 2,142	\$ 1,928
	Control Module	\$ 719	\$ 647	\$ 582	\$ 565	\$ 719	\$ 647	\$ 582	\$ 565
	Thermocouples	\$ 228	\$ 192	\$ 168	\$ 168	\$ 304	\$ 256	\$ 224	\$ 224
	H2S sensor	\$ 243	\$ 219	\$ 210	\$ 204	\$ 243	\$ 219	\$ 210	\$ 204
	Anode/cathode Pressure Sensor	\$ 452	\$ 406	\$ 364	\$ 354	\$ 1,356	\$ 1,218	\$ 1,092	\$ 1,062
Assembly Comp	Assorted Plumbing/Fittings	\$ 10,285	\$ 9,350	\$ 8,415	\$ 7,575	\$ 16,095	\$ 14,630	\$ 13,165	\$ 11,850
	Assembly Hardware	\$ 1,030	\$ 935	\$ 840	\$ 755	\$ 1,610	\$ 1,465	\$ 1,320	\$ 1,190
	Frame and Housing	\$ 3,085	\$ 2,805	\$ 2,525	\$ 2,275	\$ 4,835	\$ 4,395	\$ 3,955	\$ 3,560
+	Additional Work Estimate	\$ 15,100	\$ 13,700	\$ 12,300	\$ 11,100	\$ 24,300	\$ 22,100	\$ 19,900	\$ 17,900
	<b>TOTAL BOP COST</b>	\$ 200,924	\$ 174,868	\$ 154,728	\$ 142,047	\$ 350,048	\$ 298,714	\$ 258,865	\$ 234,045

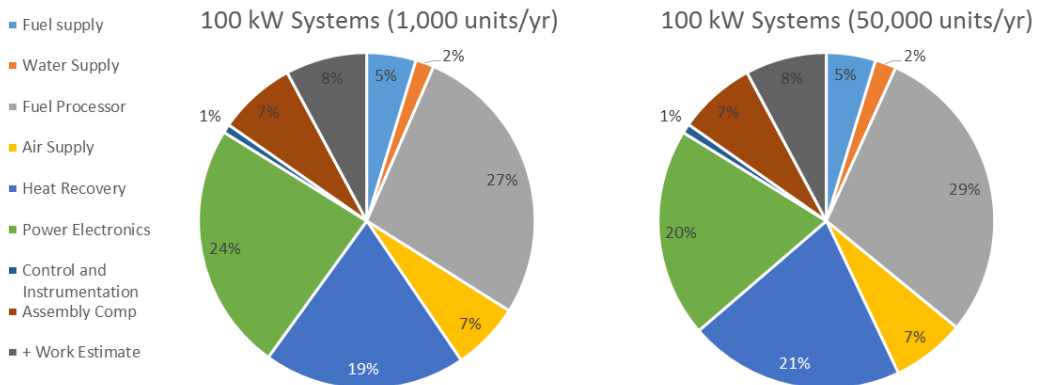


Figure 5-10. 100-kW PEM BOP cost distribution.

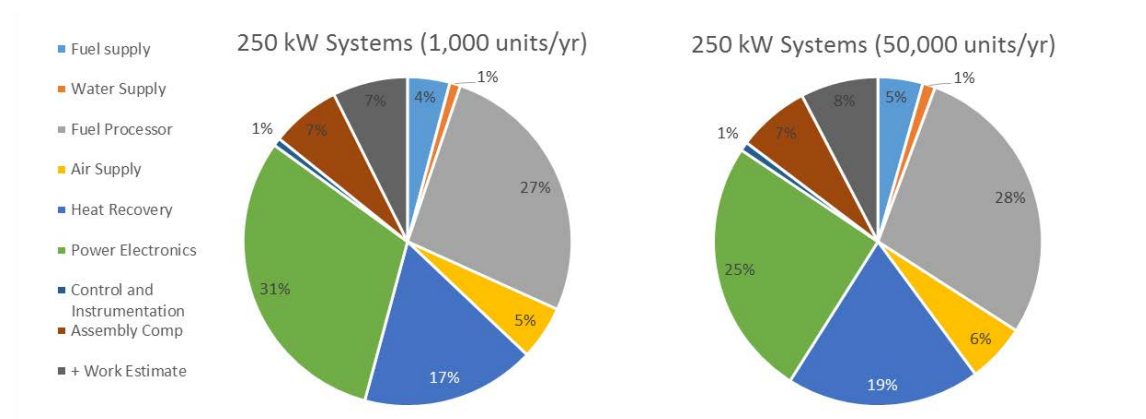


Figure 5-11. 250-kW PEM BOP cost distribution.



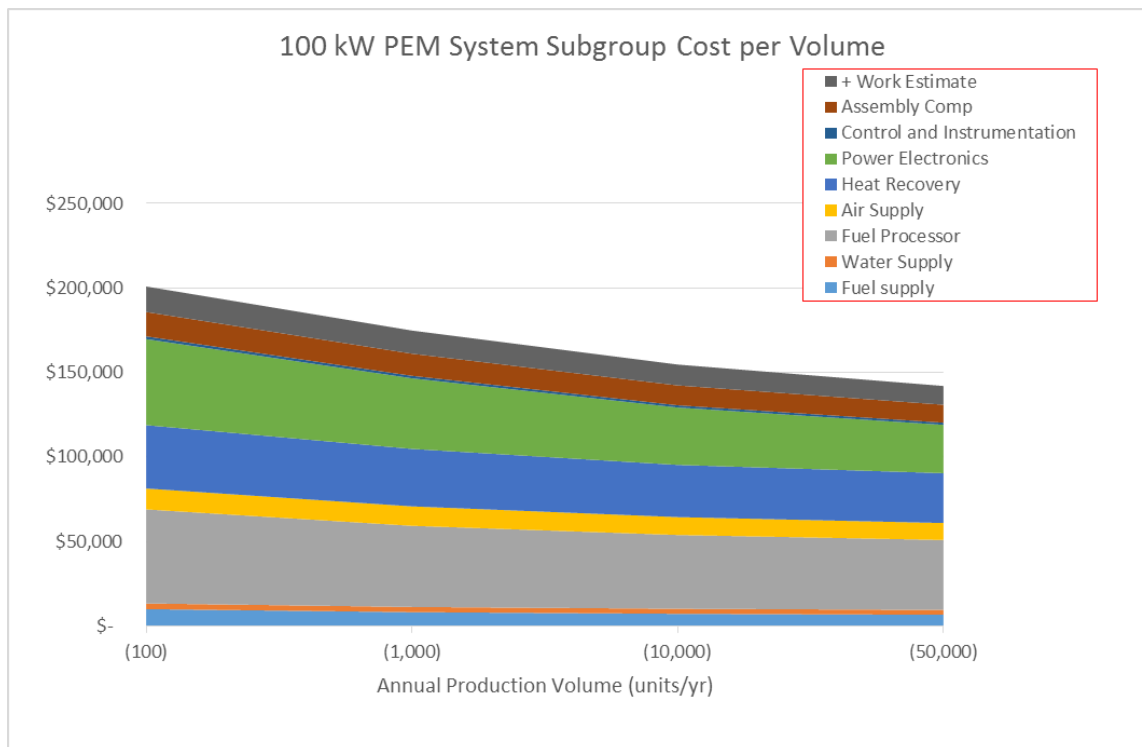


Figure 5-12. 100-kW PEM BOP cost volume trends.

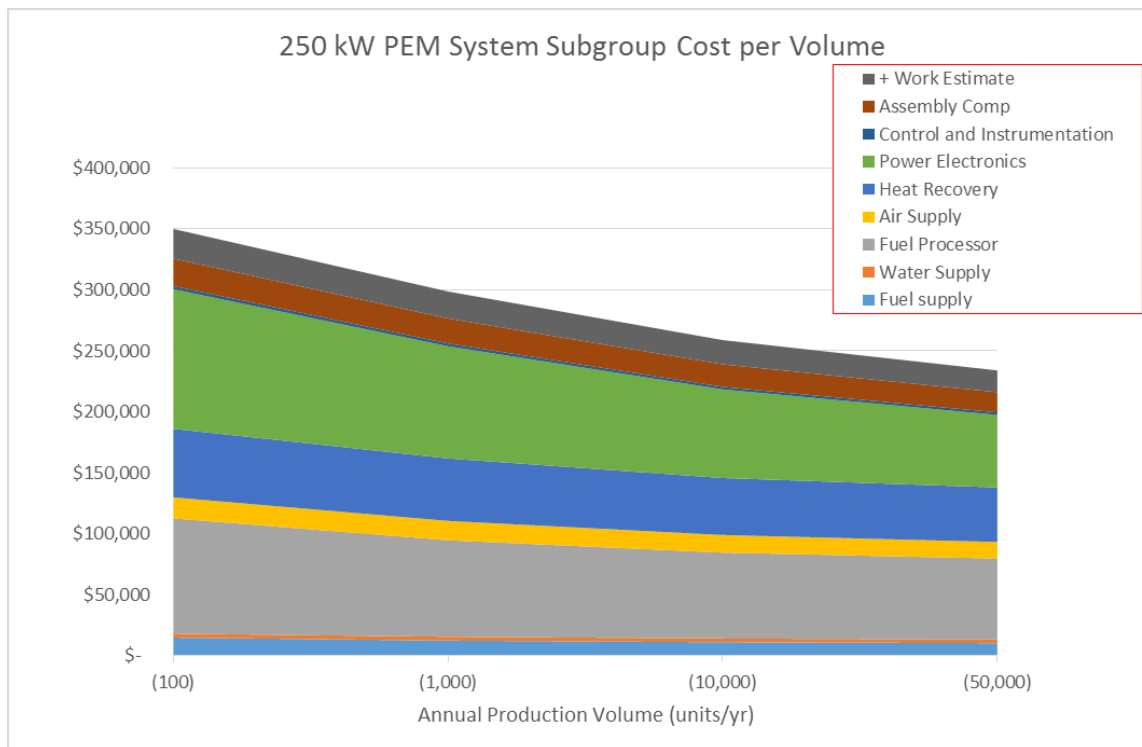


Figure 5-13. 250-kW PEM BOP cost volume trends.

### 5.3.4 PEM System Assembly and Learning Curve Assumptions

The system assembly hardware costs are accounted for in the BOP cost calculations. System assembly times were estimated using the DFMA<sup>®</sup> software. After applying learning curve analysis to the assembly times and multiplying by the standard labor rate of \$45.00/hour, the average system assembly costs were calculated as shown in Table 5-21. Details of the learning curve analysis appear in Appendix A-3.

**Table 5-21. PEM System Assembly Costs - 100 kW and 250 kW**

	100-kW System				250-kW System			
	100	1,000	10,000	50,000	100	1,000	10,000	50,000
Material	\$0.00	\$0.00	\$0.00	\$0.00	\$0.00	\$0.00	\$0.00	\$0.00
Labor	\$246.26	\$157.10	\$149.28	\$148.59	\$280.99	\$179.25	\$170.33	\$169.55
Total Cost per System	<b>\$246.26</b>	<b>\$157.10</b>	<b>\$149.28</b>	<b>\$148.59</b>	<b>\$280.99</b>	<b>\$179.25</b>	<b>\$170.33</b>	<b>\$169.55</b>

### 5.3.5 PEM CHP System Testing

Following assembly, the CHP system is tested and conditioned to determine its fitness for installation in the field. The total test time is assumed to be 2.5 hours. Systems failing test are reworked by disassembly, replacement of the defective part, and reassembly. The failure rate is assumed to be 3%. The failure cost is treated as 3% of the testing cost, which roughly accounts for the cost of disassembly, part replacement, and reassembly of the defective portion of the system. System failure costs are included in the scrap costs. Details of the analysis are the same as stack testing and conditioning shown in Appendix A-11. The system testing costs were calculated as shown in Table 5-22. There is a sharp drop in machine cost per system that occurs as production volumes change from 100 to 1,000 systems/year; this reflects the low utilization rate in the case of the 100-system volumes, and the assumption that all system testing is performed in-house.

**Table 5-22. PEM System Testing Cost Summary - 100 kW and 250 kW**

	60-kW Stack – 100-kW System				50-kW Stack – 250-kW System			
	100	1,000	10,000	50,000	100	1,000	10,000	50,000
Material	\$2.27	\$2.25	\$2.25	\$2.25	\$5.62	\$5.62	\$5.62	\$5.62
Labor	\$217.33	\$214.70	\$214.44	\$214.41	\$635.90	\$633.70	\$633.47	\$633.46
Machine	\$1,181.46	\$60.49	\$43.78	\$43.78	\$1,053.34	\$131.35	\$131.35	\$131.35
Scrap	\$43.33	\$8.58	\$8.06	\$8.05	\$52.42	\$23.84	\$23.83	\$23.83
Tooling	\$0.00	\$0.00	\$0.00	\$0.00	\$0.00	\$0.00	\$0.00	\$0.00
Part Total	<b>\$1,444.39</b>	<b>\$286.02</b>	<b>\$268.52</b>	<b>\$268.50</b>	<b>\$1,747.28</b>	<b>\$794.50</b>	<b>\$794.27</b>	<b>\$794.25</b>
# per System	1	1	1	1	1	1	1	1
Total Cost per System	<b>\$1,444.39</b>	<b>\$286.02</b>	<b>\$268.52</b>	<b>\$268.50</b>	<b>\$1,747.28</b>	<b>\$794.50</b>	<b>\$794.27</b>	<b>\$794.25</b>

### 5.3.6 PEM Capital Cost Assumptions

Table 5-23 summarizes the cost assumptions for the components that make up the total PEM capital cost.

**Table 5-23. Summary of PEM Capital Cost Assumptions**

Capital Cost	Unit Cost	Assumption/Reference
Construction Cost	\$250/ft <sup>2</sup>	Includes Electrical Costs (\$50/sq ft). Total plant area based on line footprint plus 1.5x line space for working space, offices, shipping, etc. Varies with anticipated annual production volumes
Expected lifetime of capital equipment	20 years	
Discount Rate	7%	Guidance for govt project cost calculations per OMB Circular 94
Forklift Cost	\$30,000	With extra battery and charger.
Crane Cost	\$7,350	Assumes 1 ton capacity jib crane with hoist
Real Estate Cost	\$125,000/acre	Assumes vacant land, zoned industrial Columbus, OH
Contingency Margin	10%	Assumed 10% additional work estimate

Production line use was estimated to determine the number of individual process lines required to support various product demand levels. This information, along with equipment cost quotes, was used to determine production line equipment costs. The production facility estimation is based on the floor area required for production equipment, equipment operators, and support personnel. Guidelines used for this analysis were developed by Prof. Jose Ventura at Pennsylvania State University and are detailed in Appendix A-4. Capital cost summaries appear in Table 5-24. A production line in Table 5-24 refers to the equipment needed to produce a subcomponent or to assemble an entire system from components produced on support production lines. For example, bipolar plate production requires a hot press and a post-press heat treating oven. Because each pair (press and oven) can only produce ~27 parts/hour, a significant number of bipolar plate production lines are required (e.g., 869 bipolar plate production lines to produce 50,000 of the 250-kW systems/year).

**Table 5-24. PEM Capital Cost Summary - 100 kW and 250 kW**

	60-kW Stack – 100-kW System				50-kW Stack – 250-kW System			
	100	1,000	10,000	50,000	100	1,000	10,000	50,000
Production Lines	4	4	17	83	4	5	24	117
Factory Total Construction Cost	\$472,263	\$472,263	\$1,900,263	\$9,308,856	\$472,263	\$599,463	\$2,650,475	\$13,222,678
Forklifts	\$12,000	\$12,000	\$51,000	\$249,000	\$12,000	\$15,000	\$72,000	\$351,000
Cranes	\$14,700	\$14,700	\$62,475	\$305,025	\$14,700	\$18,375	\$88,200	\$429,975
Real Estate	\$47,151	\$47,151	\$87,427	\$244,571	\$47,151	\$49,862	\$100,317	\$329,393
Contingency	\$54,611	\$54,611	\$210,116	\$1,010,745	\$54,611	\$68,270	\$291,099	\$1,433,305
<b>Total Capital Cost</b>	<b>\$600,725</b>	<b>\$600,725</b>	<b>\$2,311,281</b>	<b>\$11,118,197</b>	<b>\$600,725</b>	<b>\$750,970</b>	<b>\$3,202,091</b>	<b>\$15,766,351</b>
Equivalent Annual Capital Cost	\$56,704	\$56,704	\$218,169	\$1,049,479	\$56,704	\$70,886	\$302,255	\$1,488,232
Annual Capital Cost per Stack	<b>\$567.04</b>	<b>\$56.70</b>	<b>\$21.82</b>	<b>\$20.99</b>	<b>\$567.04</b>	<b>\$70.89</b>	<b>\$30.23</b>	<b>\$29.76</b>

## 5.4 SOFC System Manufacturing Costs

An SOFC system as described in Section 4 includes multiple fuel cell stacks and the BOP (fuel processor, support hardware, fuel and air supply, controls and sensors, and electrical equipment). This section discusses the stack manufacturing process required to achieve the design specifications in Table 5-25, followed by consideration of custom-fabricated components, and finally by a summary of subassemblies created from commercially available hardware. As noted in Section 4, in order to achieve appropriate voltages and overall system power, the fuel cells are arranged in electrically-series-connected pairs: four 30-kW stacks (2 series-connected pairs in parallel) yielding 120 kW gross for the 100-kW systems and ten 30-kW stacks (5 series-connected pairs in parallel) yielding 300 kW gross for the 250-kW system. The stacks used for the 100-kW and 250-kW systems are identical in size and cell count. The per stack component costs are shown in Table 5-26 through Table 5-39. The final Table 5-40 shows the costs for a complete system. As for the PEM system, the increase in the total number of cell components required for the 250-kW system results in lower cost per part compared to the 100-kW system.

**Table 5-25. SOFC Fuel Cell Design Parameters**

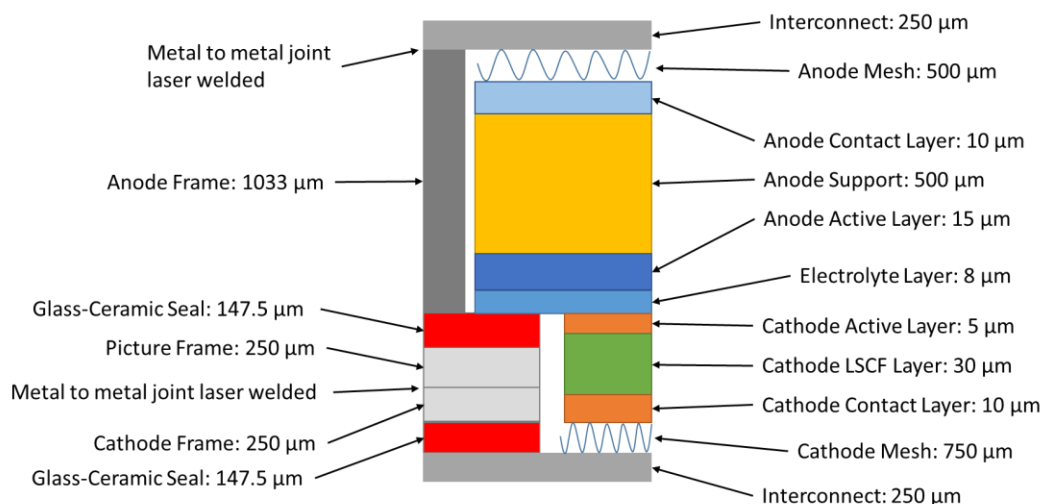
Parameter	100 kW	250 kW
Cell Power Density (W/cm <sup>2</sup> )	0.28	
Cell Current Density (A/cm <sup>2</sup> )	0.4	
Cell Voltage (VDC)	0.7	
Active Area Per Cell (cm <sup>2</sup> )	414	414
System Net Power (kW, continuous)	100	250
System Gross Power (kW, continuous)	120	300
Number and Size of Stacks per System	4 x 30 kW (gross)	10 x 30 kW (gross)
Number of Cells (#)	259	259
Stack Open Circuit Voltage (VDC)	285	285
Full Load Stack Voltage (VDC)	181	181
Cell Design	Planar, Anode supported	
Anode Material	Ni-8YSZ, 500 μm thick (2 layers 250 μm thick)	
Anode Application	Tape cast, kiln fire	
Anode Active Layer Material	Ni-YSZ, 15 μm thick	
Anode Active Layer Application	Screen Print, kiln fire	
Anode Contact Layer Material	Ni-YSZ, 10 μm thick	
Anode Contact Layer Application	Screen Print, kiln fire	
Electrolyte Material	8YSZ, 8 μm thick	
Electrolyte Application	Screen print, kiln fire	
Cathode Active Layer Material	YSZ/LSM, 5 μm thick	
Cathode Active Layer Application	Screen Print, kiln fire	
Cathode Material	LSCF, 30 μm thick	
Cathode Application	Screen Print, kiln fire	
Cathode Contact Layer Material	LSM/YSZ, 10 μm thick	
Cathode Contact Layer Application	Screen Print, kiln fire	
Seals	Wet application bonded glass/ceramic	
Stack Assembly	Hand Assembled, tie rods, furnace brazed	
Interconnects	Ferritic Stainless Steel (SS-441) with Perovskite coating, 2-3 μm thick	
Anode/Cathode Spacer Frames	Ferritic Stainless Steel (SS-441)	
Anode/Cathode Mesh	Corrugated expanded foil (SS-441)	
End Plates	Sand Cast and Machined Hastelloy X	

### 5.4.1 SOFC Stack Manufacturing Process

The SOFC fuel cell stack consists of two end plates and the appropriate number of repeat units. Repeat units include:

- One interconnect and anode frame (these may be integrated into a single piece)
- One cell (anode, electrolyte, cathode) and picture frame (the picture frame supports the entire periphery of the electrolyte)
- Cathode frame
- One cathode mesh and one anode mesh
  - The anode and cathode meshes sandwich the cell to provide flow cavities and a compliant electrical path from the cell to the interconnects
- Seals between each frame, the cell, and interconnect

Figures 5-14 and 5-15 illustrate the layer configuration and orientation. Figure 5-16 shows the stack manufacturing process. This study focuses only on the primary manufacturing and assembly processes shown in Figures 5-14, 5-15, and 5-16, and in Table 5-25.



Note: Not to scale; parts depicted as shown for clarity.

Figure 5-14. Detail assembly of SOFC cell.

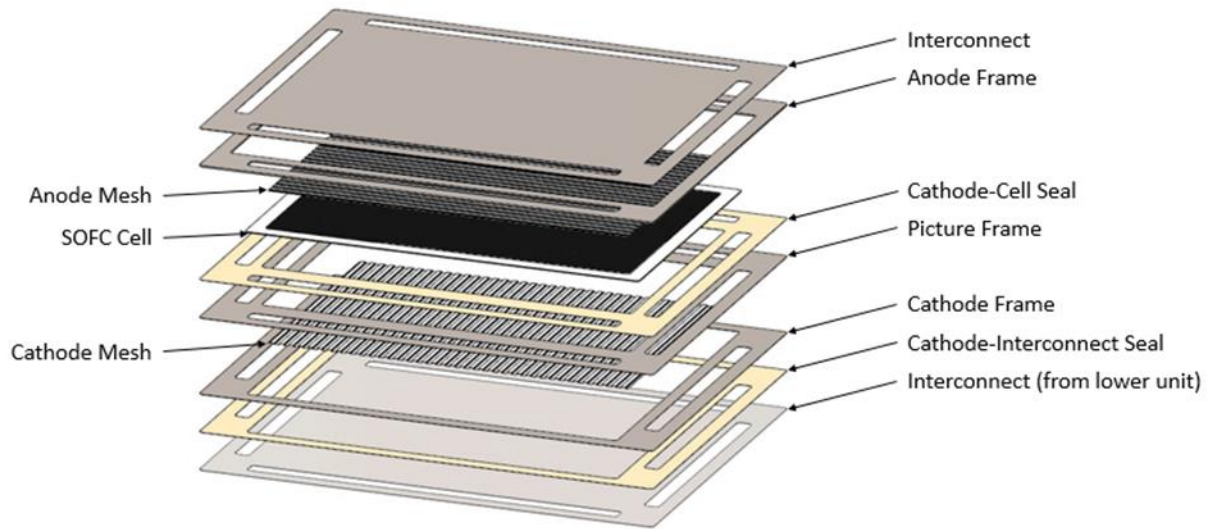


Figure 5-15. Cell repeat unit showing function of major components.



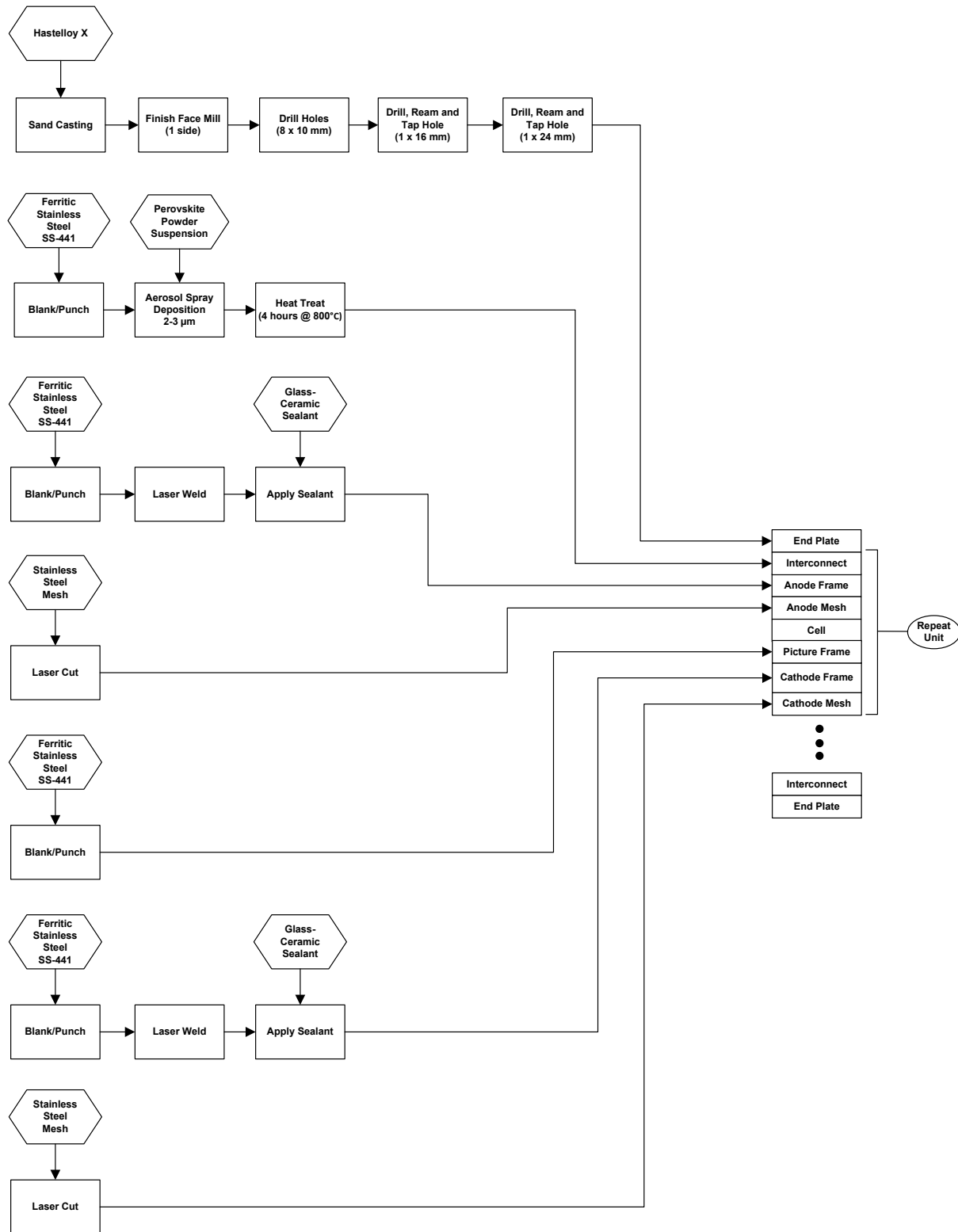


Figure 5-16. SOFC stack manufacturing process.

#### 5.4.1.1 SOFC Stack Component Size and Ceramic Cell Manufacturing Setup

Ceramic cell assemblies for the 30-kW stacks (used in both the 100-kW and 250-kW systems) are assumed to have a 414-cm<sup>2</sup> active area. Using a length-to-width ratio of 1.5, the active cell size was determined to be 167 mm by 248 mm. Using a 10-mm margin on all sides to allow for sealing to the picture frame, the overall cell size was determined to be 187 mm by 268 mm.

The SOFC cell size is shown in Figure 5-17.

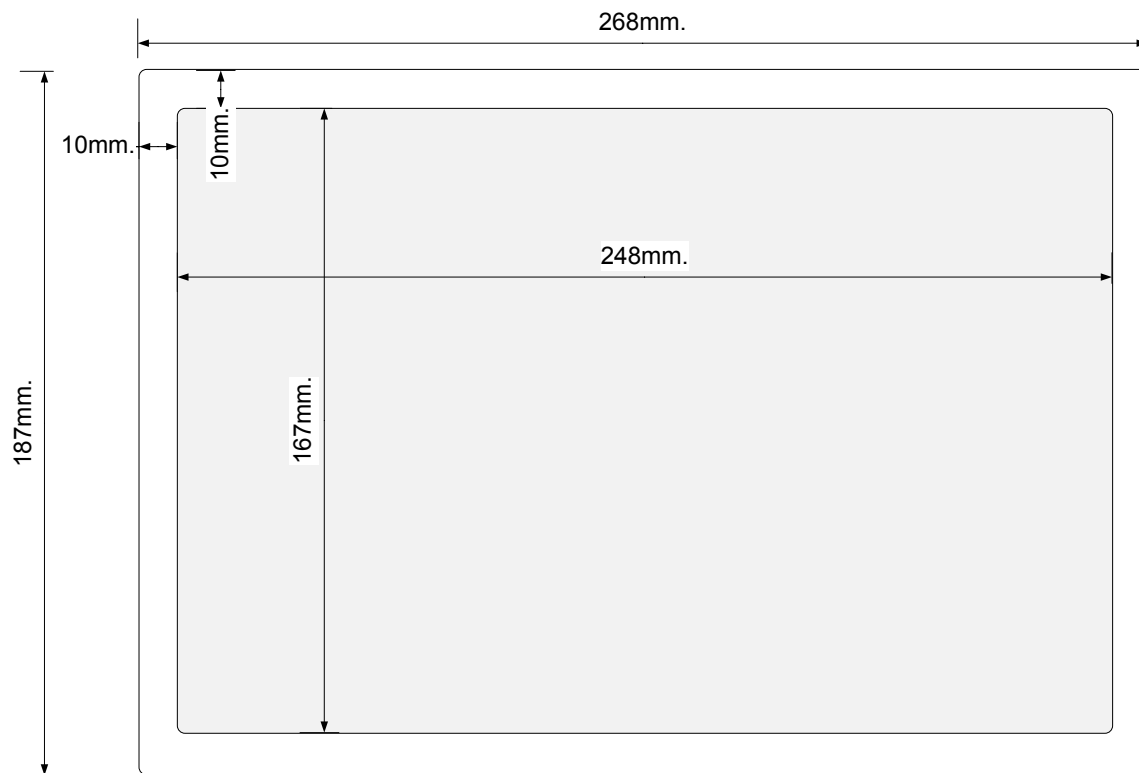


Figure 5-17. SOFC cell size.

#### 5.4.1.2 SOFC Ceramic Cell

The ceramic cell is built up in layers. Each layer starts as an aqueous ceramic slurry that is ball-milled into a uniform suspension as detailed in Appendix A-12. The anode support is created by tape casting as detailed in Appendix A-22, and blanking as detailed in Appendix A-13. Subsequent layers are screen printed onto the anode support, as detailed in Appendix A-14. All layers are infrared-conveyor-dried following application, and then kiln-fired, as detailed in Appendix A-15. The cell is sintered twice, following application of the electrolyte layer to anode active layer and anode support and following application of the final cathode layer, as detailed in Appendix A-16. The cell is then trimmed to final configuration as detailed in Appendix A-17. The resulting ceramic cell costs are shown in Table 5-26.

**Table 5-26. SOFC Ceramic Cell Cost Summary—100 kW and 250 kW**

	30-kW Stack – 100-kW System				30-kW Stack – 250-kW System			
	100	1,000	10,000	50,000	100	1,000	10,000	50,000
Material	\$5.36	\$5.11	\$5.04	\$5.03	\$5.24	\$5.06	\$5.03	\$5.02
Labor	\$3.87	\$3.85	\$3.85	\$3.85	\$3.86	\$3.85	\$3.85	\$3.85
Machine	\$8.43	\$3.92	\$2.76	\$2.63	\$5.43	\$3.04	\$2.65	\$2.62
Scrap	\$0.54	\$0.39	\$0.36	\$0.35	\$0.44	\$0.37	\$0.35	\$0.35
Tooling	\$0.14	\$0.14	\$0.14	\$0.14	\$0.14	\$0.14	\$0.14	\$0.14
Part Total	<b>\$18.33</b>	<b>\$13.42</b>	<b>\$12.15</b>	<b>\$12.01</b>	<b>\$15.11</b>	<b>\$12.47</b>	<b>\$12.03</b>	<b>\$11.98</b>
# per Stack	259	259	259	259	259	259	259	259
Total Cost per Stack	<b>\$4,748.70</b>	<b>\$3,475.98</b>	<b>\$3,147.06</b>	<b>\$3,110.03</b>	<b>\$3,912.28</b>	<b>\$3,228.67</b>	<b>\$3,115.22</b>	<b>\$3,103.48</b>

### 5.4.1.3 SOFC End Plates

The end plates overhang the stack by 30 mm on all sides to accommodate six of the eight tie rods that press and hold the stack together. The tie rods are insulated from the end plates by ceramic shoulder bushings. A sheet of ceramic material protects the tie rods from contact by the interconnects. The end plate has two reamed and tapped holes for mounting fuel and exhaust gas connectors as shown in Figure 5-18. The end plates are identical top and bottom with the orientation managed by the assembly fixture and a visual alignment feature on one side (detail not shown).

The process selected to produce the end plates was sand casting Hastelloy X. Following cooling, the cast plate is moved to a CNC drilling center to face one side, drill and ream the eight tie rod holes, and drill, ream and tap the gas connector holes as needed. The end plate cost analysis is detailed in Appendix A-24, and summarized in Table 5-27.

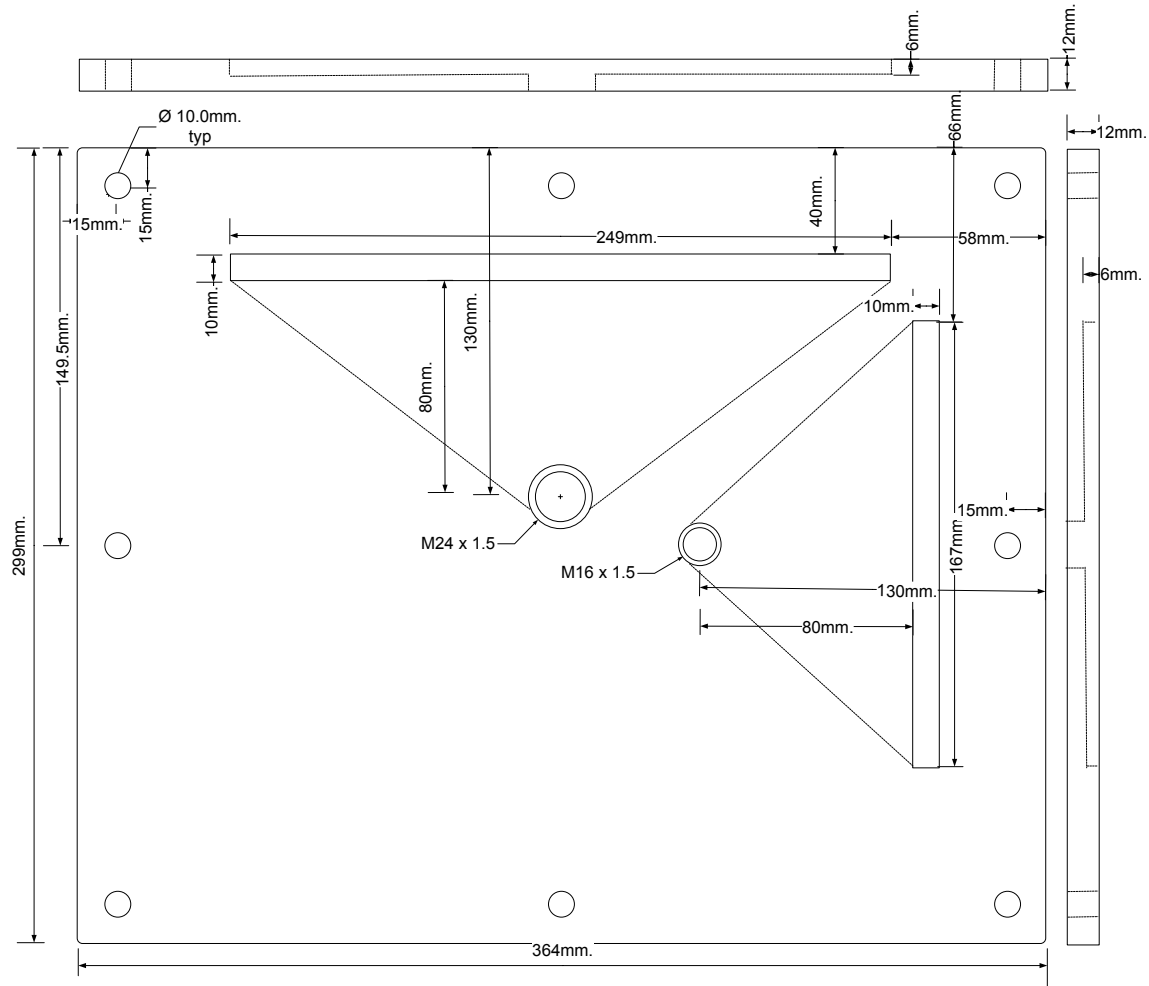


Figure 5-18. SOFC end plate size.

Table 5-27. SOFC End Plate Cost Summary - 100 kW and 250 kW

	30-kW Stack – 100-kW System				30-kW Stack – 250-kW System			
	100	1,000	10,000	50,000	100	1,000	10,000	50,000
Material	\$212.77	\$212.77	\$212.77	\$212.77	\$212.77	\$212.77	\$212.77	\$212.77
Labor	\$28.15	\$27.10	\$26.99	\$26.98	\$27.45	\$27.03	\$26.98	\$26.98
Machine	\$105.44	\$61.37	\$32.84	\$30.94	\$105.44	\$42.35	\$30.94	\$30.94
Scrap	\$1.74	\$1.51	\$1.37	\$1.36	\$1.74	\$1.42	\$1.36	\$1.36
Tooling	\$3.76	\$0.38	\$0.11	\$0.09	\$1.50	\$0.15	\$0.09	\$0.08
Part Total	<b>\$351.87</b>	<b>\$303.13</b>	<b>\$274.09</b>	<b>\$272.15</b>	<b>\$348.90</b>	<b>\$283.72</b>	<b>\$272.15</b>	<b>\$272.14</b>
# per Stack	2	2	2	2	2	2	2	2
Total Cost per Stack	<b>\$703.74</b>	<b>\$606.26</b>	<b>\$548.18</b>	<b>\$544.29</b>	<b>\$697.81</b>	<b>\$567.44</b>	<b>\$544.30</b>	<b>\$544.28</b>

#### 5.4.1.4 SOFC Interconnects

The interconnects are manufactured from 0.25-mm-thick ferritic stainless steel (SS-441) sheet. The material is stamped into a rectangular blank, then laser-cut to provide the anode and cathode gas path openings. For all volumes, the process scrap rate for the stamping operation was assumed to be 0.5%. Following laser cutting, the interconnects are spray-coated with a perovskite material. The coated interconnects are heat treated at 1,000°C for 4 hours. Details of the analysis are shown in Appendix A-18. The interconnect cost summary is provided in Table 5-28.

**Table 5-28. SOFC Interconnect Cost Summary - 100 kW and 250 kW**

	30-kW Stack – 100-kW System				30-kW Stack – 250-kW System			
	100	1,000	10,000	50,000	100	1,000	10,000	50,000
Material	\$0.90	\$0.73	\$0.70	\$0.70	\$0.82	\$0.70	\$0.70	\$0.70
Labor	\$0.37	\$0.37	\$0.37	\$0.37	\$0.37	\$0.37	\$0.37	\$0.37
Machine	\$2.23	\$1.06	\$0.36	\$0.36	\$1.84	\$0.59	\$0.37	\$0.35
Scrap	\$0.13	\$0.08	\$0.05	\$0.05	\$0.11	\$0.06	\$0.05	\$0.05
Tooling	\$0.19	\$0.12	\$0.12	\$0.12	\$0.15	\$0.13	\$0.12	\$0.12
Part Total	<b>\$3.81</b>	<b>\$2.36</b>	<b>\$1.60</b>	<b>\$1.60</b>	<b>\$3.29</b>	<b>\$1.84</b>	<b>\$1.61</b>	<b>\$1.59</b>
# per Stack	259	259	259	259	259	259	259	259
Total Cost per Stack	<b>\$987.20</b>	<b>\$610.15</b>	<b>\$413.44</b>	<b>\$413.34</b>	<b>\$852.26</b>	<b>\$476.71</b>	<b>\$417.52</b>	<b>\$410.81</b>

#### 5.4.1.5 SOFC Frames

The SOFC repeat unit contains three frames as illustrated in Figures 5-14 and 5-15:

- The anode frame supports the interconnect on the anode side and provides space for the anode and anode mesh
- The picture frame supports the entire periphery of the electrolyte and is sealed (weld or glass seal) to the anode frame
- The cathode frame supports the interconnect on the cathode side and provides space for the cathode mesh

The anode, picture, and cathode frames are manufactured from 1.033-mm, 0.25-mm, and 0.25-mm-thick ferritic stainless steel (SS-441) sheet respectively. The material is stamped into a rectangular blank, then punched to provide the required gas path openings and active area relief. For all volumes, the process scrap rate for the stamping operation was assumed to be 0.5%. Details of the analysis are shown in Appendix A-19. The frame cost summaries are provided in Tables 5-29, 5-30, and 5-31. The tooling cost differences are primarily the result of different configurations resulting in different total shearing lengths of the tooling.

**Table 5-29. SOFC Anode Frame Cost Summary - 100 kW and 250 kW**

	30-kW Stack – 100-kW System				30-kW Stack – 250-kW System			
	100	1,000	10,000	50,000	100	1,000	10,000	50,000
Material	\$1.18	\$1.18	\$1.18	\$1.18	\$1.18	\$1.18	\$1.18	\$1.18
Labor	\$0.02	\$0.02	\$0.02	\$0.02	\$0.02	\$0.02	\$0.02	\$0.02
Machine	\$0.04	\$0.04	\$0.01	\$0.01	\$0.04	\$0.04	\$0.01	\$0.01
Scrap	\$0.01	\$0.01	\$0.01	\$0.01	\$0.01	\$0.01	\$0.01	\$0.01
Tooling	\$0.20	\$0.13	\$0.13	\$0.13	\$0.16	\$0.13	\$0.13	\$0.13
Part Total	<b>\$1.45</b>	<b>\$1.38</b>	<b>\$1.35</b>	<b>\$1.35</b>	<b>\$1.41</b>	<b>\$1.38</b>	<b>\$1.35</b>	<b>\$1.34</b>
# per Stack	259	259	259	259	259	259	259	259
Total Cost per Stack	<b>\$375.44</b>	<b>\$356.24</b>	<b>\$349.34</b>	<b>\$348.40</b>	<b>\$364.39</b>	<b>\$356.71</b>	<b>\$349.24</b>	<b>\$347.87</b>

**Table 5-30. SOFC Picture Frame Cost Summary - 100 kW and 250 kW**

	30-kW Stack – 100-kW System				30-kW Stack – 250-kW System			
	100	1,000	10,000	50,000	100	1,000	10,000	50,000
Material	\$0.29	\$0.29	\$0.29	\$0.29	\$0.29	\$0.29	\$0.29	\$0.29
Labor	\$0.02	\$0.01	\$0.01	\$0.01	\$0.02	\$0.01	\$0.01	\$0.01
Machine	\$0.03	\$0.02	\$0.01	\$0.00	\$0.02	\$0.02	\$0.01	\$0.00
Scrap	\$0.00	\$0.00	\$0.00	\$0.00	\$0.00	\$0.00	\$0.00	\$0.00
Tooling	\$0.24	\$0.16	\$0.16	\$0.16	\$0.19	\$0.16	\$0.16	\$0.16
Part Total	<b>\$0.57</b>	<b>\$0.49</b>	<b>\$0.47</b>	<b>\$0.47</b>	<b>\$0.52</b>	<b>\$0.49</b>	<b>\$0.47</b>	<b>\$0.46</b>
# per Stack	259	259	259	259	259	259	259	259
Total Cost per Stack	<b>\$148.53</b>	<b>\$125.93</b>	<b>\$121.30</b>	<b>\$120.61</b>	<b>\$135.53</b>	<b>\$126.49</b>	<b>\$121.18</b>	<b>\$120.25</b>

**Table 5-31. SOFC Cathode Frame Cost Summary - 100 kW and 250 kW**

	30-kW Stack – 100-kW System				30-kW Stack – 250-kW System			
	100	1,000	10,000	50,000	100	1,000	10,000	50,000
Material	\$0.28	\$0.28	\$0.28	\$0.28	\$0.28	\$0.28	\$0.28	\$0.28
Labor	\$0.02	\$0.01	\$0.01	\$0.01	\$0.02	\$0.01	\$0.01	\$0.01
Machine	\$0.03	\$0.02	\$0.01	\$0.00	\$0.02	\$0.02	\$0.01	\$0.00
Scrap	\$0.00	\$0.00	\$0.00	\$0.00	\$0.00	\$0.00	\$0.00	\$0.00
Tooling	\$0.18	\$0.12	\$0.12	\$0.12	\$0.15	\$0.12	\$0.12	\$0.12
Part Total	<b>\$0.51</b>	<b>\$0.44</b>	<b>\$0.42</b>	<b>\$0.42</b>	<b>\$0.47</b>	<b>\$0.44</b>	<b>\$0.42</b>	<b>\$0.42</b>
# per Stack	259	259	259	259	259	259	259	259
Total Cost per Stack	<b>\$131.12</b>	<b>\$113.67</b>	<b>\$109.04</b>	<b>\$108.38</b>	<b>\$121.07</b>	<b>\$114.08</b>	<b>\$108.94</b>	<b>\$108.02</b>

#### 5.4.1.6 SOFC Laser Welding

To minimize the requirement for glass ceramic seals and reduce any potential for leaks, certain sets of metallic components are penetration-laser-welded together prior to assembly. Specifically, the anode frame is joined to the interconnect and the cathode frame is joined to the cell picture frame. The laser path tracks inside the frame perimeter and outside any closed gas ports. Details of the analysis are shown in Appendix A-26. The sealing cost summary is provided in Table 5-32.

**Table 5-32. SOFC Laser Welding Cost Summary - 100 kW and 250 kW**

	30-kW Stack – 100-kW System				30-kW Stack – 250-kW System			
	100	1,000	10,000	50,000	100	1,000	10,000	50,000
Material	\$0.00	\$0.00	\$0.00	\$0.00	\$0.00	\$0.00	\$0.00	\$0.00
Labor	\$0.19	\$0.19	\$0.19	\$0.19	\$0.19	\$0.19	\$0.19	\$0.19
Machine	\$0.95	\$0.13	\$0.13	\$0.13	\$0.27	\$0.13	\$0.13	\$0.13
Scrap	\$0.01	\$0.00	\$0.00	\$0.00	\$0.00	\$0.00	\$0.00	\$0.00
Tooling	\$0.00	\$0.00	\$0.00	\$0.00	\$0.00	\$0.00	\$0.00	\$0.00
Part Total	<b>\$1.15</b>	<b>\$0.32</b>	<b>\$0.32</b>	<b>\$0.32</b>	<b>\$0.46</b>	<b>\$0.32</b>	<b>\$0.32</b>	<b>\$0.32</b>
# per Stack	259	259	259	259	259	259	259	259
Total Cost per Stack	<b>\$298.00</b>	<b>\$83.75</b>	<b>\$83.75</b>	<b>\$83.75</b>	<b>\$119.20</b>	<b>\$83.75</b>	<b>\$83.75</b>	<b>\$83.75</b>

#### 5.4.1.7 SOFC Ceramic-Glass Sealing

A ceramic-glass sealant is applied between the cell, picture frame, and interconnect prior to assembling onto the stack. The primary components are lanthanum oxide and borosilicate glass in an organic solvent paste. The paste is applied as a 0.25-mm bead using a robotic applicator. The scrap rate was assumed to be 3.0%. Details of the analysis are shown in Appendix A-20. The sealing cost summary is provided in Table 5-33.

**Table 5-33. SOFC Ceramic-Glass Sealing Cost Summary - 100 kW and 250 kW**

	30-kW Stack – 100-kW System				30-kW Stack – 250-kW System			
	100	1,000	10,000	50,000	100	1,000	10,000	50,000
Material	\$0.78	\$0.64	\$0.64	\$0.64	\$0.68	\$0.64	\$0.64	\$0.64
Labor	\$0.41	\$0.41	\$0.41	\$0.41	\$0.41	\$0.41	\$0.41	\$0.41
Machine	\$2.07	\$0.10	\$0.10	\$0.09	\$0.10	\$0.10	\$0.09	\$0.09
Scrap	\$0.10	\$0.04	\$0.04	\$0.04	\$0.04	\$0.04	\$0.04	\$0.04
Tooling	\$0.00	\$0.00	\$0.00	\$0.00	\$0.00	\$0.00	\$0.00	\$0.00
Part Total	<b>\$3.36</b>	<b>\$1.18</b>	<b>\$1.18</b>	<b>\$1.17</b>	<b>\$1.22</b>	<b>\$1.18</b>	<b>\$1.17</b>	<b>\$1.17</b>
# per Stack	259	259	259	259	259	259	259	259
Total Cost per Stack	<b>\$869.39</b>	<b>\$306.61</b>	<b>\$306.61</b>	<b>\$303.10</b>	<b>\$315.90</b>	<b>\$306.61</b>	<b>\$303.10</b>	<b>\$303.10</b>

#### 5.4.1.8 SOFC Mesh

Each cell has an anode and cathode mesh that each act as an electrical conduit between the electrodes and the interconnect while allowing sufficient space for gas flow over the cell surface. They are created from 0.08-mm stainless steel that has been expanded and corrugated to the proper height: 0.5 mm for the anode and 0.75 mm for the cathode. The material is then laser-cut to final dimension. Details of the analysis are shown in Appendix A-25. The mesh cost summaries are provided in Tables 5-34 and 5-35.

**Table 5-34. SOFC Anode Mesh Cost Summary - 100 kW and 250 kW**

	30-kW Stack – 100-kW System				30-kW Stack – 250-kW System			
	100	1,000	10,000	50,000	100	1,000	10,000	50,000
Material	\$0.93	\$0.66	\$0.57	\$0.57	\$0.81	\$0.57	\$0.57	\$0.57
Labor	\$0.11	\$0.11	\$0.11	\$0.11	\$0.11	\$0.11	\$0.11	\$0.11
Machine	\$0.12	\$0.06	\$0.03	\$0.03	\$0.12	\$0.04	\$0.03	\$0.03
Scrap	\$0.01	\$0.00	\$0.00	\$0.00	\$0.01	\$0.00	\$0.00	\$0.00
Tooling	\$0.00	\$0.00	\$0.00	\$0.00	\$0.00	\$0.00	\$0.00	\$0.00
Part Total	<b>\$1.16</b>	<b>\$0.83</b>	<b>\$0.71</b>	<b>\$0.71</b>	<b>\$1.04</b>	<b>\$0.72</b>	<b>\$0.71</b>	<b>\$0.71</b>
# per Stack	259	259	259	259	259	259	259	259
Total Cost per Stack	<b>\$300.59</b>	<b>\$214.34</b>	<b>\$183.38</b>	<b>\$183.38</b>	<b>\$269.07</b>	<b>\$186.37</b>	<b>\$183.97</b>	<b>\$183.26</b>



**Table 5-35. SOFC Cathode Mesh Cost Summary - 100 kW and 250 kW**

	30-kW Stack – 100-kW System				30-kW Stack – 250-kW System			
	100	1,000	10,000	50,000	100	1,000	10,000	50,000
Material	\$0.94	\$0.67	\$0.58	\$0.58	\$0.82	\$0.58	\$0.58	\$0.58
Labor	\$0.11	\$0.11	\$0.11	\$0.11	\$0.11	\$0.11	\$0.11	\$0.11
Machine	\$0.12	\$0.06	\$0.03	\$0.03	\$0.12	\$0.04	\$0.03	\$0.03
Scrap	\$0.01	\$0.00	\$0.00	\$0.00	\$0.01	\$0.00	\$0.00	\$0.00
Tooling	\$0.00	\$0.00	\$0.00	\$0.00	\$0.00	\$0.00	\$0.00	\$0.00
Part Total	<b>\$1.18</b>	<b>\$0.84</b>	<b>\$0.72</b>	<b>\$0.72</b>	<b>\$1.05</b>	<b>\$0.73</b>	<b>\$0.72</b>	<b>\$0.72</b>
# per Stack	259	259	259	259	259	259	259	259
Total Cost per Stack	<b>\$304.43</b>	<b>\$217.06</b>	<b>\$185.73</b>	<b>\$185.73</b>	<b>\$272.44</b>	<b>\$188.74</b>	<b>\$186.33</b>	<b>\$185.61</b>

#### 5.4.1.9 SOFC Stack Assembly

The stack components are assembled as detailed in Figure 5-16. Pressure is applied to the completed stack using a hydraulic press, and the tie rods are installed to complete the stack assembly. Tie rod costs were estimated to be \$117.40 per stack and gas fittings were estimated to be \$110.84 per stack before applying learning curve analysis. Stack assembly times were estimated using the DFMA® software. After applying learning curve analysis to the assembly times and multiplying by the standard labor rate of \$45.00/hour, the average stack assembly costs were calculated as detailed in Appendix A-3 and summarized in Table 5-36.

**Table 5-36. SOFC Stack Assembly Cost Summary - 100 kW and 250 kW**

	30-kW Stack – 100-kW System				30-kW Stack – 250-kW System			
	100	1,000	10,000	50,000	100	1,000	10,000	50,000
Material	\$206.93	\$193.50	\$181.00	\$172.75	\$201.46	\$188.42	\$176.25	\$168.22
Labor	\$200.31	\$188.20	\$186.99	\$186.88	\$192.23	\$187.39	\$186.91	\$186.86
Total Cost per Stack	<b>\$407.24</b>	<b>\$381.70</b>	<b>\$367.98</b>	<b>\$359.63</b>	<b>\$393.70</b>	<b>\$375.81</b>	<b>\$363.16</b>	<b>\$355.08</b>

#### 5.4.1.10 SOFC Stack Brazing

Following assembly, the stack is furnace brazed to cure the ceramic-glass sealant. The component scrap rate following brazing was assumed to be 0.5%. Details of the analysis are shown in Appendix A-21. The stack brazing cost summary is provided in Table 5-37.

**Table 5-37. SOFC Stack Brazing Cost Summary - 100 kW and 250 kW**

	30-kW Stack – 100-kW System				30-kW Stack – 250-kW System			
	100	1,000	10,000	50,000	100	1,000	10,000	50,000
Material	\$25.92	\$22.62	\$22.62	\$22.62	\$24.00	\$22.62	\$22.62	\$22.62
Labor	\$6.37	\$6.25	\$6.24	\$6.24	\$6.29	\$6.24	\$6.24	\$6.24
Machine	\$47.14	\$47.14	\$25.81	\$19.43	\$47.14	\$36.45	\$19.43	\$19.43
Scrap	\$2.46	\$2.35	\$1.69	\$1.49	\$2.39	\$2.02	\$1.49	\$1.49
Tooling	\$0.00	\$0.00	\$0.00	\$0.00	\$0.00	\$0.00	\$0.00	\$0.00
Part Total	<b>\$81.88</b>	<b>\$78.37</b>	<b>\$56.37</b>	<b>\$49.79</b>	<b>\$79.83</b>	<b>\$67.33</b>	<b>\$49.79</b>	<b>\$49.79</b>
# per Stack	1	1	1	1	1	1	1	1
Total Cost per Stack	<b>\$81.88</b>	<b>\$78.37</b>	<b>\$56.37</b>	<b>\$49.79</b>	<b>\$79.83</b>	<b>\$67.33</b>	<b>\$49.79</b>	<b>\$49.79</b>

#### 5.4.1.11 SOFC Stack Testing and Conditioning

Following assembly, the stack is placed on a test stand and subjected to a 6-hour test and conditioning cycle to assess its fitness for installation into a system. The cycle consists of a 2-hour warm-up, 2 hours at full power, and a 2-hour cool-down using a hydrogen/nitrogen fuel mixture. The test reject rate was assumed to be 5.0%. Since it is not possible to disassemble the brazed stack, a failed stack is considered to be scrap, resulting in relatively high scrap costs associated with this task. Details of the analysis are shown in Appendix A-23. The stack testing and conditioning summary is provided in Table 5-38.

**Table 5-38. SOFC Stack Testing and Conditioning Cost Summary - 100 kW and 250 kW**

	30-kW Stack – 100-kW System				30-kW Stack – 250-kW System			
	100	1,000	10,000	50,000	100	1,000	10,000	50,000
Material	\$244.87	\$157.01	\$157.01	\$157.01	\$193.72	\$157.01	\$157.01	\$157.01
Labor	\$157.76	\$157.76	\$157.76	\$157.76	\$157.76	\$157.76	\$157.76	\$157.76
Machine	\$273.53	\$25.87	\$25.87	\$25.87	\$86.70	\$25.87	\$25.87	\$25.87
Scrap	\$528.02	\$363.72	\$326.99	\$323.74	\$419.56	\$337.86	\$324.59	\$322.94
Tooling	\$0.00	\$0.00	\$0.00	\$0.00	\$0.00	\$0.00	\$0.00	\$0.00
Part Total	<b>\$1,204.18</b>	<b>\$704.37</b>	<b>\$667.64</b>	<b>\$664.39</b>	<b>\$857.75</b>	<b>\$678.51</b>	<b>\$665.24</b>	<b>\$663.59</b>
# per Stack	1	1	1	1	1	1	1	1
Total Cost per Stack	<b>\$1,204.18</b>	<b>\$704.37</b>	<b>\$667.64</b>	<b>\$664.39</b>	<b>\$857.75</b>	<b>\$678.51</b>	<b>\$665.24</b>	<b>\$663.59</b>

### 5.4.1.12 SOFC Stack Cost Summary

Total SOFC stack component and manufacturing costs are summarized in Tables 5-39 and 5-40.

**Table 5-39. SOFC Stack Component Cost Summary - 100 kW and 250 kW**

	30-kW Stack – 100-kW System				30-kW Stack – 250-kW System			
	100	1,000	10,000	50,000	100	1,000	10,000	50,000
Ceramic Cells	\$4,748.70	\$3,475.98	\$3,147.06	\$3,110.03	\$3,912.28	\$3,228.67	\$3,115.22	\$3,103.48
Interconnects	\$987.20	\$610.15	\$413.44	\$413.34	\$852.26	\$476.71	\$417.52	\$410.81
Anode Frame	\$375.44	\$356.24	\$349.34	\$348.40	\$364.39	\$356.71	\$349.24	\$347.87
Anode Mesh	\$300.59	\$214.34	\$183.38	\$183.38	\$269.07	\$186.37	\$183.97	\$183.26
Cathode Frame	\$131.12	\$113.67	\$109.04	\$108.38	\$121.07	\$114.08	\$108.94	\$108.02
Cathode Mesh	\$304.43	\$217.06	\$185.73	\$185.73	\$272.44	\$188.74	\$186.33	\$185.61
Picture Frame	\$148.53	\$125.93	\$121.30	\$120.61	\$135.53	\$126.49	\$121.18	\$120.25
Laser Weld	\$298.00	\$83.75	\$83.75	\$83.75	\$119.20	\$83.75	\$83.75	\$83.75
Glass Ceramic Sealing	\$869.39	\$306.61	\$306.61	\$303.10	\$315.90	\$306.61	\$303.10	\$303.10
End Plates	\$703.74	\$606.26	\$548.18	\$544.29	\$697.81	\$567.44	\$544.30	\$544.28
Assembly Hardware	\$206.93	\$193.50	\$181.00	\$172.75	\$201.46	\$188.42	\$176.25	\$168.22
Assembly Labor	\$200.31	\$188.20	\$186.99	\$186.88	\$192.23	\$187.39	\$186.91	\$186.86
Stack Brazing	\$81.88	\$78.37	\$56.37	\$49.79	\$79.83	\$67.33	\$49.79	\$49.79
Test and Conditioning	\$1,204.18	\$704.37	\$667.64	\$664.39	\$857.75	\$678.51	\$665.24	\$663.59
<b>Total Cost per Stack</b>	<b>\$10,560.45</b>	<b>\$7,274.43</b>	<b>\$6,539.82</b>	<b>\$6,474.81</b>	<b>\$8,391.23</b>	<b>\$6,757.23</b>	<b>\$6,491.73</b>	<b>\$6,458.88</b>

**Table 5-40. SOFC Stack Manufacturing Cost Summary - 100 kW and 250 kW**

	30-kW Stack – 100-kW System				30-kW Stack – 250-kW System			
	100	1,000	10,000	50,000	100	1,000	10,000	50,000
Material	\$3,661.24	\$3,270.06	\$3,188.52	\$3,175.69	\$3,462.83	\$3,201.26	\$3,181.03	\$3,169.02
Labor	\$1,742.40	\$1,722.03	\$1,720.05	\$1,719.87	\$1,728.84	\$1,720.76	\$1,719.92	\$1,719.84
Machine	\$4,159.24	\$1,600.06	\$1,003.83	\$957.00	\$2,404.96	\$1,189.82	\$967.38	\$948.96
Scrap	\$741.54	\$507.28	\$452.99	\$448.29	\$585.66	\$468.78	\$449.44	\$447.19
Tooling	\$256.04	\$175.00	\$174.43	\$173.96	\$208.94	\$176.62	\$173.96	\$173.86
<b>Part Total</b>	<b>\$10,560.45</b>	<b>\$7,274.43</b>	<b>\$6,539.82</b>	<b>\$6,474.81</b>	<b>\$8,391.23</b>	<b>\$6,757.23</b>	<b>\$6,491.73</b>	<b>\$6,458.88</b>
# per System	4	4	4	4	10	10	10	10
<b>Total Cost per System</b>	<b>\$42,241.82</b>	<b>\$29,097.72</b>	<b>\$26,159.27</b>	<b>\$25,899.23</b>	<b>\$83,912.25</b>	<b>\$67,572.34</b>	<b>\$64,917.28</b>	<b>\$64,588.83</b>

SOFC stack cost volume trends are shown in Figures 5-19 and 5-20.

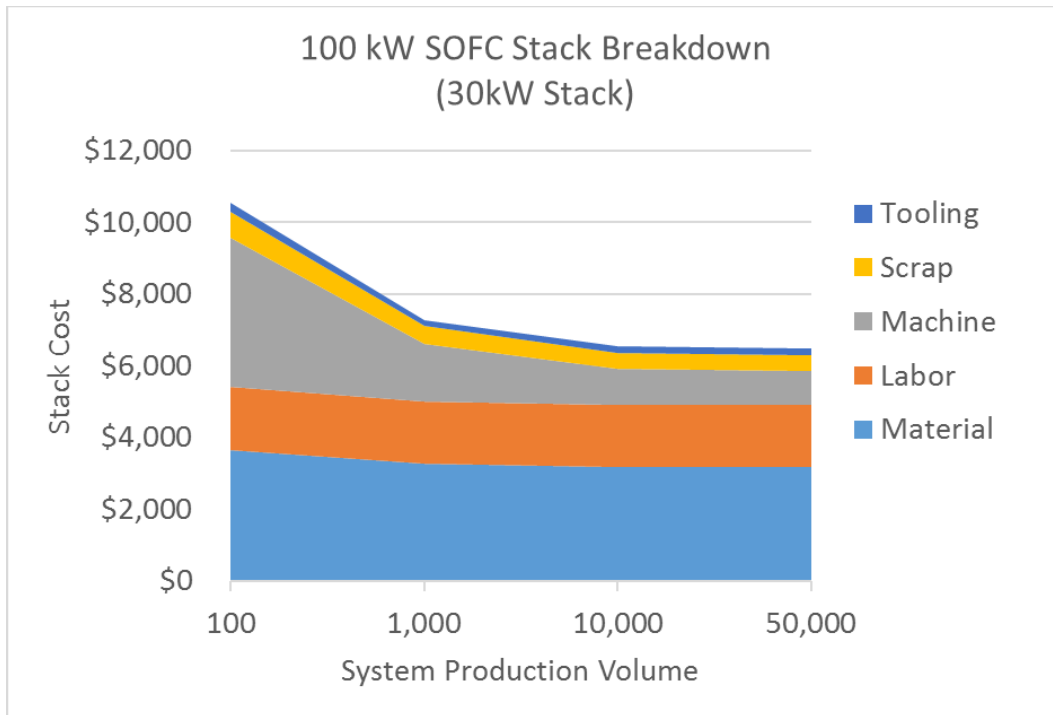


Figure 5-19. 100-kW SOFC stack cost volume trends.

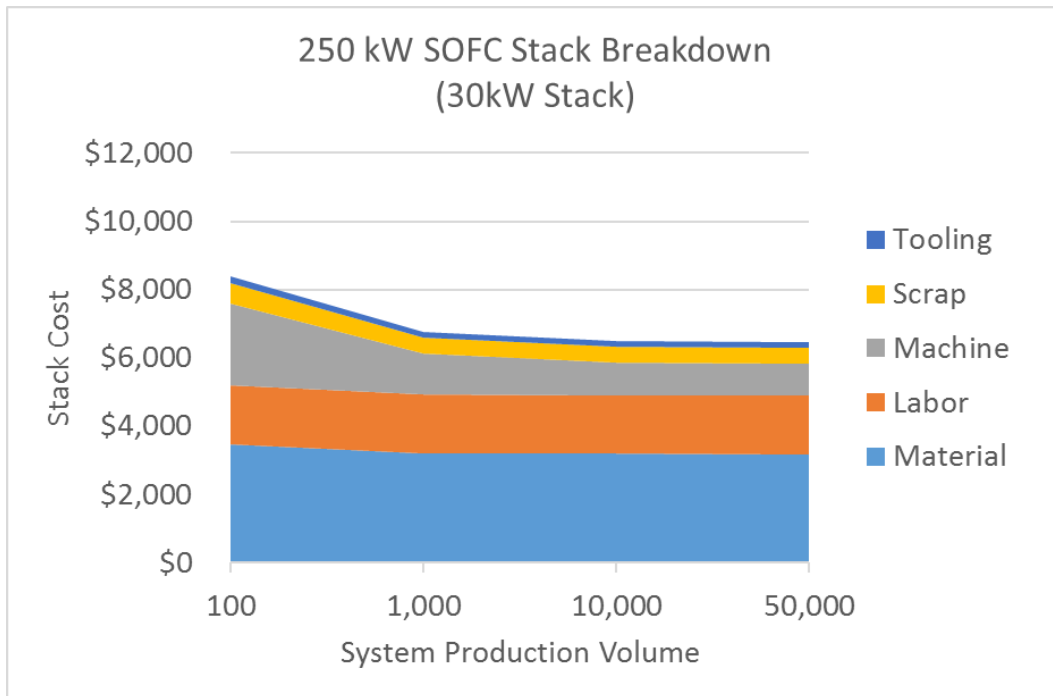


Figure 5-20. 250-kW SOFC stack cost volume trends.

## 5.4.2 SOFC Systems BOP Manufacturing Cost Assessment

Fuel processing systems for natural gas and propane, the fuels of choice for primary power and CHP applications, tend to be unique to each manufacturer with very little detailed information available. To provide a basis for costing, representative fuel processing systems were designed by Battelle based on experience with smaller systems and on conversations with various component suppliers. The Battelle-designed fuel processing systems were modeled with ChemCad® to define operating temperatures, pressures, heat loads, and other performance metrics. The ChemCad® model outputs were used to specify some items for commercial quotes and to define performance criteria for other non-standard components that were assumed to be fabricated in-house. Fabricated components were modeled using DFMA® software. For the SOFC system, only the reformer was considered to be designed and built in-house.

### 5.4.2.1 SOFC Steam Reformer

To provide a basis for DFMA® analysis, we assumed the steam reformer would be based on the design of the Catacel SSR® catalytic steam reformer (Figure 5-21). Figure 5-21 is based on a figure from Catacel patent no. 7,501,102. Design of the reformer used for Battelle's report on smaller fuel cell systems<sup>10</sup> was accomplished with guidance on sizing provided informally by Catacel. The reformer consists of a stack of CC fans or stages and is scaled primarily by increasing the number of stages in the stack but also by adjusting stage diameter. However, extending the number of stages to accommodate a 100-kW or larger system results in an unacceptably long device and likely excess pressure drop. Expanding the diameter of the reformer core, on the other hand, would result in degraded internal heat transfer performance for the CC fans. Because the reforming reaction is endothermic, the fans are cooled by the reaction, leading to reduced reaction rates near the center of the fans if the diameter is too large. For this report, we developed an alternative design which packages several reformer cores within a single housing served by a single burner. The reformer cores are the same diameter as used previously for the 5-, 10-, and 25-kW reformers.

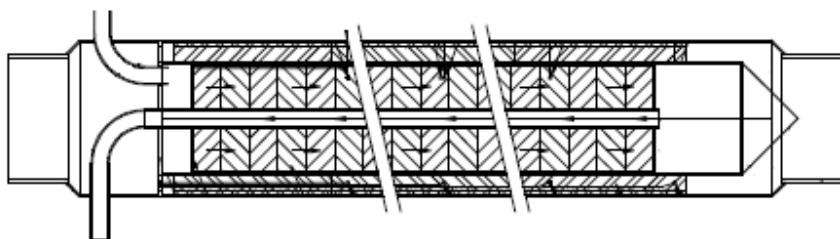


Figure 5-21. Catacel SSR® schematic diagram after patent no. 7,501,102.

<sup>10</sup> Battelle 2015. "Manufacturing Cost Analysis of 1, 5, 10, and 25 kW Fuel Cell Systems for Primary Power and Combined Heat and Power Applications." Report to DOE. DOE contract no. DE-EE0005250.

Figure 5-22 shows the conceptual reformer configuration for a 100-kW system, and Figure 5-23 shows the reformer configuration for a 250-kW system. The reformer tube lengths and overall length are the same for both systems. The number of tubes and overall assembly diameter are increased for the 250-kW system. In both systems, the steam/fuel-reformate flow through the CC fan stack is opposite the combustion gas flow. Reformate flows to the exit manifold through a central tube within the CC fan stack.

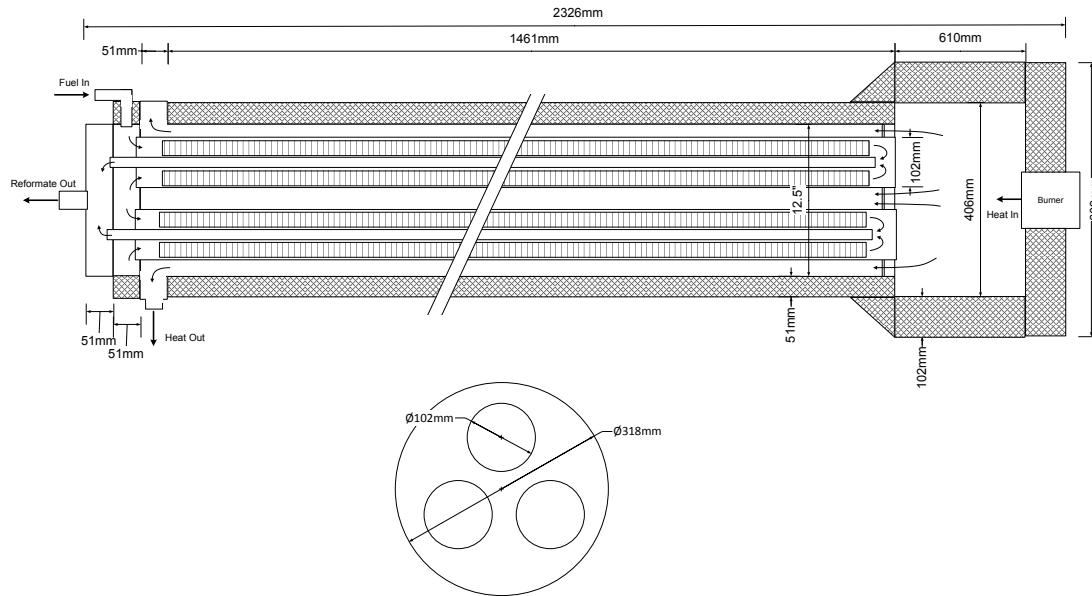


Figure 5-22. Three-tube 100-kW reformer configuration.

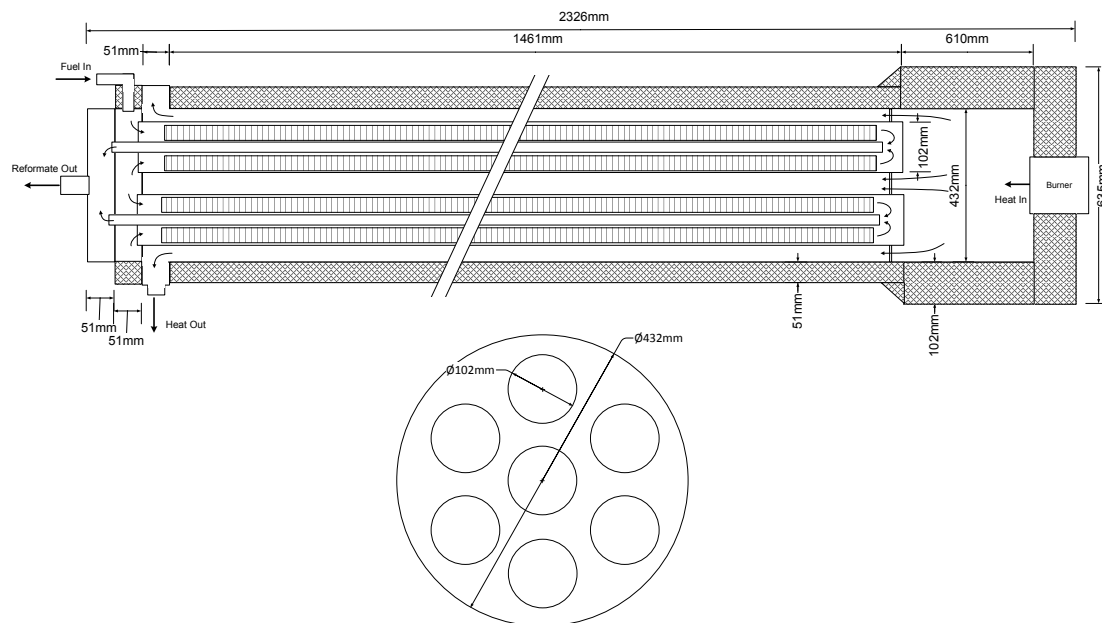


Figure 5-23. Seven-tube 250-kW reformer configuration.

The required catalyst-coated surface area for each reformer is calculated based on a catalyst content of approximately 1,925 cm<sup>2</sup> per kilowatt. This value is half that used by Catacel in its SSR<sup>®</sup> design for PEM systems because some methane breakthrough is acceptable, and in fact desirable, for SOFC stack cooling from internal reforming. An additional factor in the downsizing is the higher electrical efficiency of the SOFC system. For the systems under consideration, we started with the reformer sizing parameters shown in Table 5-41.

**Table 5-41. SOFC Reformer Sizing Parameters**

System Size (kW)	Approximate Reformer Size	Target Catalyst Area (cm <sup>2</sup> )
100	3 tubes @ 1,331 cm active fan length	3@0.81x10 <sup>5</sup> = 2.43x10 <sup>5</sup> total
250	7 tubes @ 1,331 cm active fan length	7@0.81 x10 <sup>5</sup> = 5.67x10 <sup>5</sup> total

Each reformer tube includes 168 CC fans. Using fixed fan dimensions and the target coated areas listed in Table 5-41, we established the final reformer dimensions for each system as shown in Table 5-42. The tubes and housings are rolled and welded from high alloy or stainless steel sheet. Appropriate locating features are assumed to be incorporated into the tube to position the CC fans. The fans and separator washers are loaded into the tubes prior to the endplates being welded on and before the tubes are welded into the tube sheet. The center tubes are inserted through the inlet tube sheet and through the CC fan stack before the assembly is welded into the overall shell. The reformer cost summary is shown in Table 5-43.

**Table 5-42. SOFC Reformer Dimensional Summary**

Dimension	100 kW	250 kW
Overall Diameter (mm)	609	635
Overall Length (mm)	2,326	2,326
Flow Stages	3 tubes @ 168 = 504	7 tubes @ 168 = 1,176
Final Catalyst Area (cm <sup>2</sup> )	232,550	565,950

**Table 5-43. SOFC System Reformer Cost Summary - 100 kW and 250 kW**

	100-kW SOFC System				250-kW SOFC System			
	100	1,000	10,000	50,000	100	1,000	10,000	50,000
Material	\$633.31	\$567.08	\$540.19	\$525.59	\$993.85	\$937.90	\$919.92	\$909.11
Process	\$1,026.93	\$585.89	\$585.89	\$505.71	\$2,333.63	\$1,604.52	\$1,158.38	\$1,125.13
Scrap	\$83.01	\$57.65	\$56.30	\$51.57	\$166.37	\$127.12	\$103.92	\$101.71
Tooling	\$1,844.96	\$184.50	\$36.90	\$25.83	\$3,481.09	\$348.11	\$69.62	\$48.74
Manufactured Parts	\$3,588.21	\$1,395.11	\$1,219.27	\$1,108.69	\$6,974.95	\$3,017.64	\$2,251.84	\$2,184.69
Catalyst	\$22.36	\$20.58	\$18.97	\$17.93	\$50.59	\$46.59	\$42.96	\$40.64
Purchased Parts	\$79.71	\$79.71	\$79.71	\$79.71	\$87.10	\$87.10	\$87.10	\$87.10
Assembly	\$379.39	\$303.03	\$295.39	\$294.71	\$747.40	\$596.96	\$581.91	\$570.13
Total Cost per System	\$4,069.68	\$1,798.42	\$1,613.33	\$1,501.04	\$7,860.04	\$3,748.28	\$2,963.81	\$2,882.56

### 5.4.3 SOFC BOP Cost Assumptions

The costs associated with the BOP components are tabulated in Table 5-44. Figures 5-24 and 5-25 compare component costs at a subcategory level similar to the system schematic. A category titled “Additional Work Estimate” is included to capture any small contingencies not specifically itemized in this report. This includes components such as heat sinks and fans for additional electrical cooling, supplementary temperature or pressure sensors, and any extra assembly hardware. This estimate is based on a 20% buffer to the electrical subsystem cost, and a 10% buffer to all remaining hardware.

Aside from the reformer, BOP items are assumed to be commercially available; therefore, quotes or budgetary pricing was used.



**Table 5-44. SOFC BOP Cost Summary for 100-kW and 250-kW Systems**

System	Component Description	Annual Production of 100kW SOFC Systems				Annual Production of 250kW SOFC Systems			
		(100)	(1,000)	(10,000)	(50,000)	(100)	(1,000)	(10,000)	(50,000)
Fuel Supply	Nat. Gas Filter	\$ 97	\$ 81	\$ 68	\$ 60	\$ 342	\$ 266	\$ 251	\$ 188
	Natural Gas Control Valve	\$ 1,788	\$ 1,453	\$ 1,229	\$ 1,182	\$ 2,619	\$ 2,287	\$ 1,997	\$ 1,816
	Desulfurizer	\$ 2,427	\$ 1,457	\$ 1,269	\$ 1,142	\$ 4,855	\$ 3,424	\$ 3,027	\$ 2,724
	3-way valve	\$ 137	\$ 115	\$ 97	\$ 86	\$ 137	\$ 115	\$ 97	\$ 86
Fuel Processor	Ejector	\$ 592	\$ 545	\$ 501	\$ 472	\$ 1,113	\$ 1,023	\$ 941	\$ 887
	Reformer/Burner	\$ 4,070	\$ 1,798	\$ 1,613	\$ 1,501	\$ 7,860	\$ 3,748	\$ 2,964	\$ 2,883
	Tail gas Burner	\$ 3,583	\$ 3,350	\$ 3,133	\$ 2,989	\$ 5,374	\$ 5,025	\$ 4,699	\$ 4,484
Air Supply	Air Filter	\$ 510	\$ 479	\$ 479	\$ 479	\$ 1,020	\$ 958	\$ 958	\$ 958
	Start-up Air Blower	\$ 961	\$ 854	\$ 758	\$ 698	\$ 3,049	\$ 2,818	\$ 2,586	\$ 2,586
	Start-up Air Flowmeter	\$ 1,493	\$ 1,405	\$ 1,317	\$ 1,229	\$ 1,493	\$ 1,405	\$ 1,317	\$ 1,229
	Start-up Diverter Valve	\$ 241	\$ 204	\$ 172	\$ 152	\$ 241	\$ 204	\$ 172	\$ 152
	Cathode Air Blower	\$ 961	\$ 854	\$ 758	\$ 698	\$ 3,049	\$ 2,818	\$ 2,586	\$ 2,586
	Cathode Air Flowmeter	\$ 1,493	\$ 1,405	\$ 1,317	\$ 1,229	\$ 1,493	\$ 1,405	\$ 1,317	\$ 1,229
Heat Recovery	Cathode Recuperator	\$ 18,800	\$ 17,580	\$ 16,439	\$ 15,685	\$ 28,200	\$ 26,369	\$ 24,658	\$ 23,528
	System Exhaust Valves	\$ 241	\$ 204	\$ 172	\$ 152	\$ 241	\$ 204	\$ 172	\$ 152
	CHP Export Exchanger	\$ 2,016	\$ 1,915	\$ 1,819	\$ 1,783	\$ 5,416	\$ 5,145	\$ 4,888	\$ 4,790
Power Electronics	Hybrid Inverter	\$ 42,000	\$ 33,600	\$ 26,400	\$ 21,600	\$ 96,000	\$ 75,000	\$ 57,000	\$ 45,000
	Batteries	\$ 5,690	\$ 5,464	\$ 5,269	\$ 5,060	\$ 11,765	\$ 11,298	\$ 10,897	\$ 10,465
	Resistor Bank	\$ 2,000	\$ 1,610	\$ 1,289	\$ 1,030	\$ 4,026	\$ 3,220	\$ 2,577	\$ 2,061
	Grid Interconnect Switch	\$ 1,204	\$ 1,084	\$ 975	\$ 878	\$ 2,645	\$ 2,381	\$ 2,142	\$ 1,928
Control and Instrumentation	Control Module	\$ 719	\$ 647	\$ 582	\$ 565	\$ 719	\$ 647	\$ 582	\$ 565
	Thermocouples	\$ 228	\$ 192	\$ 168	\$ 168	\$ 304	\$ 256	\$ 224	\$ 224
	H2S sensor	\$ 243	\$ 219	\$ 210	\$ 204	\$ 243	\$ 219	\$ 210	\$ 204
	Anode/cathode Pressure Sensor	\$ 904	\$ 812	\$ 728	\$ 708	\$ 2,260	\$ 2,030	\$ 1,820	\$ 1,770
Assembly Comp	Assorted Plumbing/Fittings	\$ 3,365	\$ 3,060	\$ 2,755	\$ 2,480	\$ 5,510	\$ 5,010	\$ 4,510	\$ 4,060
	Assembly Hardware	\$ 335	\$ 305	\$ 275	\$ 250	\$ 550	\$ 500	\$ 450	\$ 405
	Frame and Housing	\$ 1,005	\$ 915	\$ 825	\$ 745	\$ 1,650	\$ 1,500	\$ 1,350	\$ 1,215
+	Additional Work Estimate	\$ 6,400	\$ 5,800	\$ 5,200	\$ 4,700	\$ 11,400	\$ 10,400	\$ 9,400	\$ 8,500
	<b>TOTAL BOP COST</b>	\$ 103,503	\$ 87,405	\$ 75,818	\$ 67,927	\$ 203,575	\$ 169,675	\$ 143,793	\$ 126,677

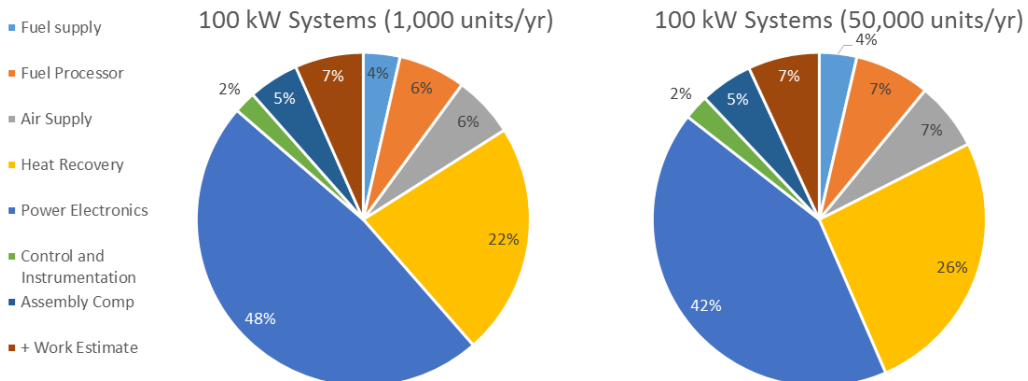


Figure 5-24. 100-kW SOFC BOP cost distribution.

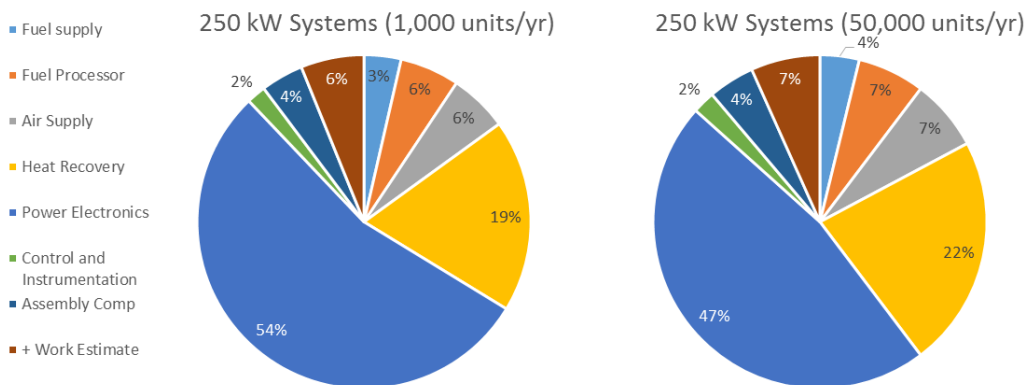


Figure 5-25. 250-kW SOFC BOP cost distribution.

Figures 5-26 and 5-27 show SOFC BOP cost trends across the annual production volumes studied.

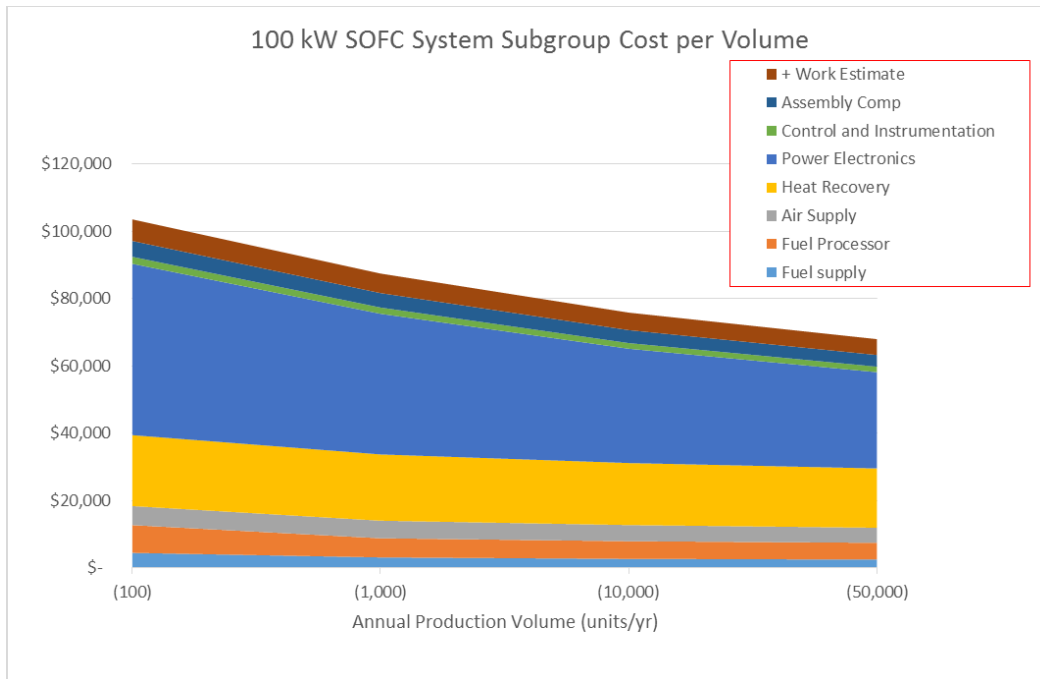


Figure 5-26. 100-kW SOFC BOP cost volume trends.

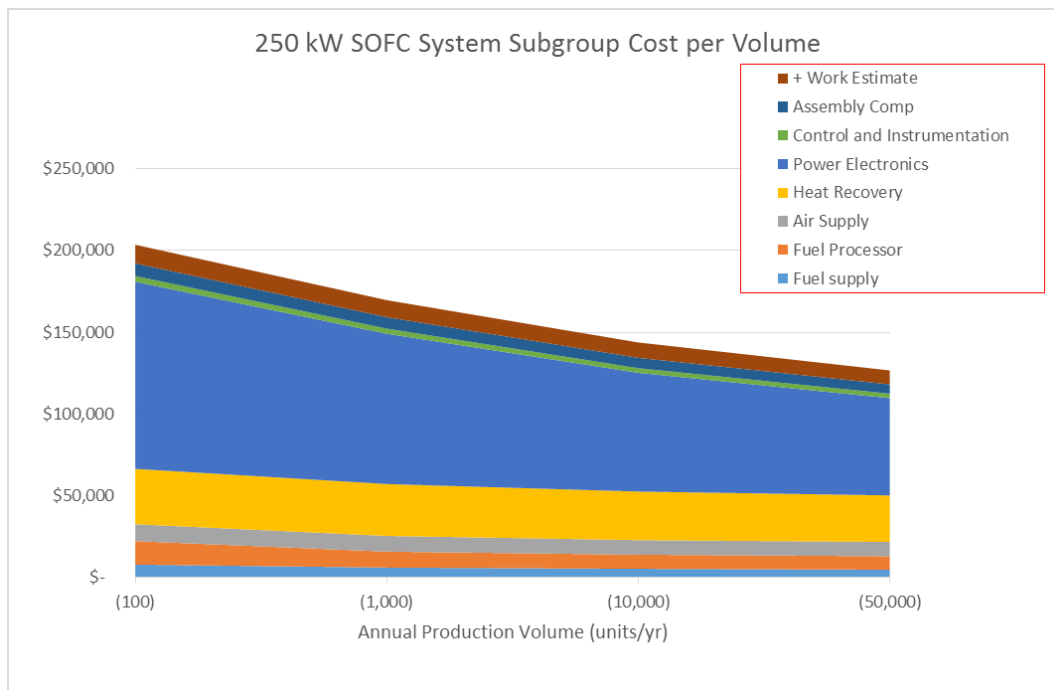


Figure 5-27. 250-kW SOFC BOP cost volume trends.

#### 5.4.4 SOFC System Assembly and Learning Curve Assumptions

The system assembly hardware costs are accounted for in the BOP cost calculations. System assembly times were estimated using the DFMA<sup>®</sup> software. After applying learning curve analysis to the assembly times and multiplying by the standard labor rate of \$45.00/hour, the average system assembly costs were calculated as detailed in Appendix A-3 and summarized in Table 5-45.

**Table 5-45. SOFC System Assembly Costs - 100 kW and 250 kW**

	30-kW Stack – 100-kW System				30-kW Stack – 250-kW System			
	100	1,000	10,000	50,000	100	1,000	10,000	50,000
Material	\$0.00	\$0.00	\$0.00	\$0.00	\$0.00	\$0.00	\$0.00	\$0.00
Labor	\$163.66	\$104.40	\$99.21	\$98.75	\$203.62	\$129.90	\$123.43	\$122.86
<b>Total Cost per System</b>	<b>\$163.66</b>	<b>\$104.40</b>	<b>\$99.21</b>	<b>\$98.75</b>	<b>\$203.62</b>	<b>\$129.90</b>	<b>\$123.43</b>	<b>\$122.86</b>

#### 5.4.5 SOFC System Testing

Following assembly, the CHP system is tested and conditioned to determine its fitness for installation in the field. Total test time is assumed to be 6 hours. The cycle consists of a 2-hour warm-up, 2 hours at full power, and a 2-hour cool-down. The test reject rate was assumed to be 5.0%. The system testing costs were calculated as shown in Table 5-46.

**Table 5-46. SOFC System Testing Cost Summary - 100 kW and 250 kW**

	30-kW Stack – 100-kW System				30-kW Stack – 250-kW System			
	100	1,000	10,000	50,000	100	1,000	10,000	50,000
Material	\$85.77	\$85.77	\$85.77	\$85.77	\$214.43	\$214.43	\$214.43	\$214.43
Labor	\$108.45	\$107.26	\$107.16	\$107.15	\$109.25	\$107.77	\$107.65	\$107.63
Machine	\$1,172.72	\$51.76	\$49.75	\$49.75	\$1,172.72	\$51.76	\$49.75	\$49.75
Scrap	\$13.81	\$2.47	\$2.45	\$2.45	\$15.12	\$3.78	\$3.76	\$3.76
Tooling	\$0.00	\$0.00	\$0.00	\$0.00	\$0.00	\$0.00	\$0.00	\$0.00
<b>Part Total</b>	<b>\$1,380.75</b>	<b>\$247.27</b>	<b>\$245.14</b>	<b>\$245.13</b>	<b>\$1,511.51</b>	<b>\$377.74</b>	<b>\$375.58</b>	<b>\$375.57</b>
# per System	1	1	1	1	1	1	1	1
<b>Total Cost per System</b>	<b>\$1,380.75</b>	<b>\$247.27</b>	<b>\$245.14</b>	<b>\$245.13</b>	<b>\$1,511.51</b>	<b>\$377.74</b>	<b>\$375.58</b>	<b>\$375.57</b>

### 5.4.6 SOFC Capital Cost Assumptions

Table 5-47 summarizes the cost assumptions for the components that make up the total capital cost.

**Table 5-47. Summary of SOFC Capital Cost Assumptions**

Capital Cost	Unit Cost	Assumption/Reference
Construction Cost	\$250/ft <sup>2</sup>	Includes Electrical Costs (\$50/sq ft). Total plant area based on line footprint plus 1.5x line space for working space, offices, shipping, etc. Varies with anticipated annual production volumes
Expected lifetime of capital equipment	20 years	
Discount Rate	7%	Guidance for govt project cost calculations per OMB Circular 94
Forklift Cost	\$30,000	With extra battery and charger
Crane Cost	\$7,350	Assumes 1 ton capacity jib crane with hoist
Real Estate Cost	\$125,000/acre	Assumes vacant land, zoned industrial Columbus, OH
Contingency Margin	10%	Assumed 10% additional work estimate

Machine utilization was used to determine the number of machines required to support various product demand levels. This information, along with equipment cost quotes, was used to determine production line equipment costs. The production facility estimation is based on the floor area required for production equipment, equipment operators, and support personnel. Guidelines used for this analysis were developed by Prof. Jose Ventura at Pennsylvania State University, and are detailed in Appendix A-5. Capital cost breakdown appears in Table 5-48. As was the case for the PEM estimates, a production line refers to the set of equipment necessary to produce a component, subassembly, or system.

**Table 5-48. SOFC Capital Cost Summary - 100 kW and 250 kW**

	30-kW Stack – 100-kW System				30-kW Stack – 250-kW System			
	100	1,000	10,000	50,000	100	1,000	10,000	50,000
Production Lines	7	40	334	1,641	13	86	810	4,016
Factory Total Construction Cost	\$642,665	\$5,633,885	\$46,309,334	\$226,715,727	\$1,631,795	\$12,113,154	\$112,653,830	\$559,666,277
Forklifts	\$21,000	\$120,000	\$1,002,000	\$4,923,000	\$39,000	\$258,000	\$2,430,000	\$12,048,000
Cranes	\$25,725	\$147,000	\$1,227,450	\$6,030,675	\$47,775	\$316,050	\$2,976,750	\$14,758,800
Real Estate	\$50,769	\$180,239	\$1,001,904	\$4,379,683	\$82,697	\$313,877	\$2,261,675	\$10,411,973
Contingency	\$74,016	\$608,112	\$4,954,069	\$24,204,909	\$180,127	\$1,300,108	\$12,032,225	\$59,688,505
<b>Total Capital Cost</b>	<b>\$814,175</b>	<b>\$6,689,237</b>	<b>\$54,494,756</b>	<b>\$266,253,994</b>	<b>\$1,981,394</b>	<b>\$14,301,189</b>	<b>\$132,354,480</b>	<b>\$656,573,555</b>
Equivalent annual capital cost	\$76,852	\$631,417	\$5,143,919	\$25,132,493	\$187,030	\$1,349,931	\$12,493,327	\$61,975,899
<b>Annual Capital Cost per Stack</b>	<b>\$192.13</b>	<b>\$157.85</b>	<b>\$128.60</b>	<b>\$125.66</b>	<b>\$187.03</b>	<b>\$134.99</b>	<b>\$124.93</b>	<b>\$123.95</b>

## 5.5 Electrical System Cost Assumptions

The cost for the electrical system is primarily driven by the power electronics (DC/DC converter and DC/AC inverter.) These components are somewhat more expensive for CHP and primary power applications than for back-up power because of safety and performance requirements applied by the utility to devices connected to the grid. The system controller and sensors comprise the next largest portion of the cost. Protective devices and interconnecting components comprise the remainder of the electrical system cost.

### 5.5.1 DC/DC and DC/AC Power Electronics

Most of the commercially available DC/DC converters rated for continuous use are suitable for fuel cell applications assuming appropriate control interface features to allow the converter to be used to assist with system management. Specifically, the converter is typically coordinated with the reformer/fuel cell through the control system to limit current draw in relationship to the fuel flow to the reformer to avoid overloading the stack. Since most converters include some form of control interface, no cost was assumed to be associated with this feature. The input to the converters was required to accommodate the range of voltage for the specific fuel cell stack being served. Stack output voltage is variable with stack loading and number of cells. Output voltage was assumed to be ~400 VDC for both 100- and 250-kW systems. The converters have been sized based on 120% of the nominal output of the system size to allow for parasitic loads and short-term overload. For example, for the 100-kW system, a 120-kW power converter was selected.

Most of the commercially available grid-tie DC/AC inverters are designed for PV systems and may not be directly applicable to fuel cells due to their incorporation of specific features for maximizing power output from a variable solar input. However, several solar inverter manufacturers noted that they could design an appropriate inverter for fuel cells. They expected the cost of fuel cell inverters to be similar to if not less than PV inverters since designing an inverter for a fuel cell is less complicated. Design simplification results from relatively steady input at known voltage which removes the need for maximum power point tracking system control, which is needed to manage solar arrays. The simplification is somewhat offset by the larger conductor size and heat management required for the higher current associated with the lower input voltage likely with a fuel cell system. For cost estimating, we assumed that PV inverter costs would be representative. Inverters are sized based on 120% of the nominal output of the system size to allow for parasitic loads and short-term overload.

Recently, hybrid DC/AC inverters have been developed to integrate a secondary high-power DC/DC port into the primary DC/AC inverter specifically for connection to storage systems operating in parallel with the primary power source (typically solar for the existing commercial products). The cost is comparable to that of a single DC/AC inverter.

The DC/DC, DC/AC, and hybrid DC/AC hardware costs are estimated based on the costs of similar hardware already in limited production that were obtained from the manufacturers. These costs were blended with costs for systems appropriate for PV systems currently being produced in high volume. The PV systems operate at somewhat higher voltage, but are a reasonable approximation for the necessary systems. The cost breakdown for increasing power and increasing production volumes on a cost-per-watt basis is shown for the DC/DC converter (Table 5-49), the DC/AC inverter (Table 5-50), and the DC/AC hybrid inverter (Table 5-51). Note that the hybrid inverter costs are considered to be significantly uncertain since current production levels and field experience are limited.

**Table 5-49. DC/DC Converter Cost per Watt**

System Size	100 units (\$/W)	1,000 units (\$/W)	10,000 units (\$/W)	50,000 units (\$/W)
100 kW	\$0.32	\$0.23	\$0.19	\$0.14
250 kW	\$0.29	\$0.21	\$0.17	\$0.13

**Table 5-50. DC/AC Inverter Cost per Watt**

System Size	100 units (\$/W)	1,000 units (\$/W)	10,000 units (\$/W)	50,000 units (\$/W)
100 kW	\$0.31	\$0.25	\$0.20	\$0.16
250 kW	\$0.28	\$0.22	\$0.18	\$0.14

**Table 5-51. Hybrid DC/AC Inverter Cost per Watt**

System Size	100 units (\$/W)	1,000 units (\$/W)	10,000 units (\$/W)	50,000 units (\$/W)
100 kW	\$0.35	\$0.28	\$0.22	\$0.18
250 kW	\$0.32	\$0.25	\$0.19	\$0.15

We received estimates from one company for hybrid inverters that were significantly lower than for conventional inverters at higher production volumes. In the absence of corroborating estimates, we believe it unlikely that the companies fabricating hybrid inverters will sell them at substantially reduced prices compared to conventional inverters already on the market; therefore, we have used the current price quote for the hybrid inverter and applied an 80% discount rate for higher volumes. This brings the hybrid inverters near to, but not below, conventional inverters on a cost-per-watt basis.

### 5.5.2 Controller and Sensors

The system controller cost was estimated based on previous efforts completed at Battelle and original equipment manufacturer (OEM) automotive electronic control unit (ECU) costs. We assumed that the system controller is a custom circuit card assembly built around a micro-controller that handles the specific needs of the system. Because of the similarity to an automotive ECU, the system controller would probably have some of the same features as an automotive ECU; as such, the cost of OEM ECUs was used to estimate the higher quantity cost of the controller. The current sensor and voltage sense circuitry are readily available, so the cost for those components could be identified via the internet. The costs are summarized in Table 5-52.

**Table 5-52. Controller and Sensors Cost**

Component	Cost per System (\$/System)							
	100-kW System (Annual Production)				250-kW System (Annual Production)			
	100	1,000	10,000	50,000	100	1,000	10,000	50,000
Control Module	\$719	\$647	\$582	\$565	\$719	\$647	\$582	\$565
Thermocouples	\$228	\$192	\$168	\$168	\$304	\$256	\$224	\$224
H <sub>2</sub> S Sensor	\$243	\$219	\$210	\$204	\$243	\$219	\$210	\$204
Anode/Cathode Pressure Sensor	\$452	\$406	\$364	\$354	\$1,356	\$1,218	\$1,092	\$1,062

### 5.5.3 Protection and Interconnects

The contactors and fuses used in this size of fuel cell application typically require high current and high DC voltage ratings. The number of manufacturers that supply these types of devices is somewhat limited. Therefore, the costs used in this study for these components is an average of the component costs obtained from the internet and quoted prices from authorized distributors of the products. The cost for the connectors and other interconnection cable was estimated to be 10% of the overall system electrical costs.<sup>11</sup>

#### 5.5.3.1 Batteries

Energy storage is required to provide critical load support during grid outages. As outlined in Section 4, the batteries were sized for direct connection to provide 25% of nominal power. An alternative design approach might include sizing the batteries to provide near-full-operational power for the high-power portion of the day, followed by recharging at night. Battery costs were obtained from battery manufacturers on the basis of the design required to provide 25% nominal power for 20 minutes for PEM fuel cells and 40 minutes for SOFC. Table 5-53 shows the minimum requirements of the battery. For costing purposes, both PEM fuel cells and SOFC use the same battery assembly. However, the assumption is that the PEM batteries will experience a 50% discharge (50% remaining charge) during a typical outage event, whereas SOFC batteries will experience an ~80% discharge associated with the same event. The battery capacity is shown in Table 5-53. The batteries specified were 12V, 58 amp-hr at C/100 hr-rate for a 100-kW system, and 12V, 137 amp-hr at C/100 hr-rate for a 250-kW system.

**Table 5-53. Minimum Battery Requirements**

System Size (kw)	Battery Rating		Battery Voltage
	kW-hr	Amp-hr	VDC
100	21	58	370
250	52	137	370

<sup>11</sup> Battelle. 2011. The High Volume Manufacture Cost Analysis of 5 kW Direct Hydrogen Polymer Electrolyte (PEM) Membrane Fuel Cell for Backup Power Applications. Report to the DOE. DOE Contract No. DE-FC36-03GO13110.



Nominally, thirty-four 12-volt batteries connected in series are used for both the SOFC and PEM systems. The costs are shown in Table 5-54.

**Table 5-54. Battery Cost per System**

Battery Power (kW)	100 units	1,000 units	10,000 units	50,000 units
100	\$5,690	\$5,464	\$5,269	\$5,060
250	\$11,765	\$11,298	\$10,897	\$10,465

### 5.5.3.2 Load Bank

The resistor bank is required in case of load decrease to dump some excess power as the reformer decreases reformat output. During a load decrease, excess reformat from the fuel cell anode can result in overheating the reformer and its support hardware if power ramp rate is not controlled. The resistor bank combined with a pulse-width-modulated (PWM) switch has been designed to handle a load reduction of 25% of nominal power for a battery that was fully charged. Table 5-55 shows the cost of the load bank system.

**Table 5-55. Load Bank Cost per System<sup>12</sup>**

Resistor Bank Power (kW)	100 units	1,000 units	10,000 units	50,000 units
25 (100-kW system)	\$2,000	\$1,610	\$1,289	\$1,030
50 (250-kW system)	\$4,026	\$3,220	\$2,577	\$2,061

### 5.5.3.3 Transfer Switch

The fuel cell system is designed to produce power in the absence of the utility grid, so it requires a transfer switch to rapidly disconnect the fuel cell system from the grid and from unnecessary loads when the grid goes down or brown-out conditions are encountered. The cost of the transfer switch varies based on the switching current and whether it is single-phase or three-phase. The same transfer switch that is used for battery back-up power could be used for a fuel cell system. The situation could be more complex if there are several power sources on site. For most light commercial installations, this would not be the case; however, for 100-kW and larger systems, secondary sources (e.g., reciprocating-engine-driven generators) would potentially be present in commercial and industrial buildings. Some large commercial installations such as hotels and hospitals may have multiple back-up power sources that would require coordination or that might use a single transfer switch.

<sup>12</sup> Load bank costs sized based off 25% of the system net power output.

## 5.5.4 Electrical Cost Summary

Table 5-56 provides a summary of the costs associated with the electrical power system and support components (including controls and sensors). Overall costs are dominated by the inverter. We note that while these costs are high, the power management costs would be substantially greater if a DC/DC converter were used between the stack and inverter. Hybrid inverters represent an emerging technology which offers significant overall cost reduction to fuel cell systems that require a managed interface with energy storage, including batteries and ultracapacitors.

**Table 5-56. Electrical Cost Summary**

Component	Cost per System (\$/System)							
	100-kW System (Annual Production)				250-kW System (Annual Production)			
	100	1,000	10,000	50,000	100	1,000	10,000	50,000
Hybrid Inverter <sup>13</sup>	\$42,000	\$33,600	\$26,400	\$21,600	\$96,000	\$75,000	\$57,000	\$45,000
Batteries	\$5,690	\$5,464	\$5,269	\$5,060	\$11,765	\$11,298	\$10,897	\$10,465
Resistor Bank	\$2,000	\$1,610	\$1,289	\$1,030	\$4,026	\$3,220	\$2,577	\$2,061
Grid Interconnect Switch	\$1,204	\$1,084	\$975	\$878	\$2,645	\$2,381	\$2,142	\$1,928
Control Module	\$719	\$647	\$582	\$565	\$719	\$647	\$582	\$565
Thermocouples	\$228	\$192	\$168	\$168	\$304	\$256	\$224	\$224
H <sub>2</sub> S sensor	\$243	\$219	\$210	\$204	\$243	\$219	\$210	\$204
Anode/cathode Pressure Sensor	\$452	\$406	\$364	\$354	\$1,356	\$1,218	\$1,092	\$1,062
Total Cost per System	\$52,536	\$43,221	\$35,258	\$29,859	\$117,058	\$94,238	\$74,725	\$61,509

## 6. Limitations of the Analysis

The analytical approach employed here was to create a generic system that is representative of current industry technology and practice. The generic system is made from the merged non-proprietary input from multiple industry representatives and is defined at a high level. There are numerous tradeoffs to be considered when choosing a specific design feature or system specification characteristic. Since the decisions made to define the design and specification are the basis for the cost analysis, it is worthwhile to explicitly consider the impact and limitations of, as well as the justification for, the choices made.

### 6.1 PEM Manufacturing Costs

Many fuel cell cost studies focus on stack manufacturing costs with little or no consideration of the BOP necessary to support the stack. However, stack fabrication techniques and materials for both PEM and SOFC stacks have advanced so that stack cost is no longer the majority of a system cost—in fact, stack

<sup>13</sup> Hybrid inverter sized based on system gross power, 120 kW and 300 kW for the 100-kW and 250-kW systems, respectively.

costs may represent only about 20% of the overall cost. In no case did stack costs for this study exceed 30% of the overall system cost. This stresses the importance of the BOP design and component selection. Based on past experience and industry input, reasonable choices regarding the overall system design were selected: a limitation of this analysis is dependence on representative system designs, not field tested hardware.

### 6.1.1 PEM Stack Manufacturing Costs

Stack costs are based on the use of high-volume processes (i.e., roll-to-roll) to fabricate the MEA. These processes include catalyst deposition, decal transfer, and hot pressing. Individual MEA stack components are die-cut following hot pressing. The assumption of the use of roll-to-roll processes for low annual production volumes could result in artificially low stack cost estimates at these production levels since the specialized machinery may not yet be available and minimum purchase quantities for roll-to-roll materials would not be justified for small production volumes. Because of the power levels associated with this study and the number of stacks per system, the number of MEA units is relatively high, so this limitation is less of a concern for this study than for previous lower-power studies.

Alternative and innovative manufacturing techniques were not evaluated. Industry feedback indicates that the techniques used for the cost analysis are consistent with existing processes used by stack component manufacturers. One possible exception is with the bipolar plates, for which some manufacturers use compression-molded graphite composite material and others use stamped and coated metal material. For this analysis, graphite composite bipolar plates were chosen due to longevity concerns associated with the CHP application. Table 6-1 summarizes the manufacturing processes that were evaluated.

**Table 6-1. PEM Manufacturing Processes Evaluated**

Process	Method Evaluated	Alternatives Not Evaluated
Catalyst deposition	Selective Slot die coating with decal transfer	Tape casting Nanostructure Thin Film
	Single head slot die with decal transfer (not chosen)	Dual head slot die Multi-pass slot die
	Screen printing (not chosen)	
	Spray coating (not chosen)	
Bipolar plate	Compression molding	Die stamping and coating (metal plates)
MEA forming	Ruler blade die cutting	Laser cutting
Gasket/seal forming	Injection molding	Laser cutting
	Die cutting (not chosen)	
End plate	Sand casting + final machining	Stamping, welding
	Die Casting (not chosen)	
	Machine from block (not chosen)	

The cost analysis assumed that membrane and GDL materials were purchased in roll form. This could result in slightly higher stack cost compared to in-house production of these materials. However, the membrane and GDL materials are manufactured using complex, highly specialized, multi-step processes.<sup>14</sup> Consequently, in-house production may not be justified until yearly volumes reach the larger production volumes considered here. However, for consistency with prior reports, we assumed that both membrane and GDL materials would be purchased materials for all production volumes.

## 6.1.2 PEM BOP Hardware Costs

BOP costs are strongly influenced by the cost of the electrical equipment, namely the hybrid DC/AC inverter and grid connection hardware. Three-port hybrid inverters are a relatively new technology currently in early commercial production for solar PV systems with battery support. They represent a significant savings compared to the discrete components for DC/DC conversion followed by DC/AC inversion that have historically been used for grid-connected CHP and back-up power systems. Because they are relatively new to the market and only available from two companies, the long-term cost picture for hybrid inverters is somewhat uncertain; however, they are believed to be attractive pieces of equipment. The costs included here reflect quotes adjusted to different volumes and sizes using typical scaling and volume production factors; we did not evaluate the core costs associated with the power electronics and controls to determine if significant cost savings might be available. In our life cycle cost analysis, we have taken no credit for critical load maintenance, but we believe that back-up power is a valuable feature of any type of on-site generation system.

Heat exchangers make up another significant cost category, especially for the PEM system. The PEM heat exchangers were scaled on the basis of a ChemCad<sup>®</sup> model of the system and assumed to be sized appropriately for their designed load heat duty. These heat exchangers represent an area of uncertainty in the development of the system costs. Typical off-the-shelf (OTS) heat exchangers carry pressure ratings that are much greater than required for the PEM CHP systems considered here. Although efforts were made to work with suppliers to identify the lowest-cost heat exchangers capable of meeting system requirements, a full DFMA<sup>®</sup> analysis was not conducted for these items, and significant potential exists for their associated costs to decrease with a design-to-purpose engineering effort.

Blower selection depends significantly on system pressure drop at design flow rate. Absent an actual design, we presumed modest pressure drop. As pressure requirements increase, either through the cathode or through the combustion system for the reformer, blower requirements may increase notably with an attendant increase in cost. In most cases, the system designer has some leeway in the design to minimize pressure drop.

## 6.2 SOFC Manufacturing Costs

### 6.2.1 SOFC Stack Manufacturing Costs

Stack costs are based on the use of typical manufacturing processes for the construction of the individual cells. These include creation of the supporting anode, cell blanking, ceramic layer deposition, kiln firing and sintering (Table 6-2).

---

<sup>14</sup> B.D. James, J.A. Kalinoski, and K.N. Baum. 2010. *Mass Production Cost Estimation for Direct H<sub>2</sub> PEM Fuel Cell Systems for Automotive Applications: 2010 Update*. NREL Report No. SR-5600-49933. Directed Technologies, Inc. Available at [http://www1.eere.energy.gov/hydrogenandfuelcells/pdfs/dti\\_80kW\\_fc\\_system\\_cost\\_analysis\\_report\\_2010.pdf](http://www1.eere.energy.gov/hydrogenandfuelcells/pdfs/dti_80kW_fc_system_cost_analysis_report_2010.pdf)

**Table 6-2. SOFC Manufacturing Processes Evaluated**

Process	Method Evaluated	Alternatives Not Evaluated
Ceramic deposition	Screen printing	Plasma spray coating
	Tape casting	
Interconnect	Sheet metal stamping, laser etching	Laser cutting, water jet cutting, chemical etching
	Spray deposition coating	CVD/PVD
Sealing	Bead deposition	Screen printing, tape casting
Picture frame	Sheet metal stamping	Laser cutting, water jet cutting.
End plate	Sand casting + final machining	Stamping, welding
	Die Casting (not chosen)	
	Machine from block (not chosen)	

Alternative and innovative manufacturing techniques were not evaluated. Based on industry feedback, the techniques used for the cost analysis are consistent with existing processes used by SOFC stack component manufacturers.

### 6.2.2 SOFC BOP Hardware Costs

The SOFC BOP associated with stack support is considerably simpler than for PEM, leading to lower cost. However, as for PEM, the design chosen is the result of Battelle’s engineering judgment tempered by industry input rather than of analysis of existing commercial systems. The BOP related to heat recovery is also simpler for SOFC than for PEM and can yield higher-quality heat. However, the high-temperature materials and components that are required may partially offset the cost savings achieved through simplicity.

As for the PEM system, SOFC BOP hardware cost estimates are strongly influenced by electrical system components. The same limitations mentioned for the PEM analysis apply for SOFC. The SOFC system may include additional energy storage (batteries) to compensate for the relatively slow response of the stack to changes in electrical load. Since the specifics of a grid outage are not defined, for this analysis we assumed that the batteries will be the same for either technology. However, the SOFC batteries may be subjected to deeper discharge events during rapid electrical transients with the system off grid.

The BOP estimates for SOFC assume that lower effectiveness reforming is adequate since some methane introduced to the stack will be reformed *in situ*, benefiting stack thermal management. We assumed that a reformer approximately half the size of a similar-scale PEM reformer would be satisfactory. Appropriate scaling of the reformer to satisfy the specific requirements set by a stack manufacturer could result in higher or lower costs. Similarly, we assume anode recirculation using an eductor. Performance of the eductor could impact overall system performance and efficiency and will likely limit turndown to 2:1 for the SOFC. Alternative methods, such as high-temperature, blower-recirculated anode gas, could provide better turndown if desired for some applications, but high-temperature blowers represent a significantly higher initial expense and have an unknown life. Proven high-temperature blowers for anode recirculation do not seem to exist at this scale, so they were not considered for this analysis.

BOP hardware cost estimates included here exhibit limited cost savings at high volume. This results from the specialized nature of the BOP components, particularly the expense of the higher-temperature materials necessary to achieve adequate lifetime.

Bulk commodity materials used in much of the hardware have relatively fixed costs unless purchased at very low quantities, where prices are very high. Conversely, certain specialty components (e.g., fuel reformers and compact heat exchangers) required to meet the rigorous specifications of the CHP system are currently custom-designed and are not available at high volumes. The volume discounts applied were based on general scaling parameters that may not reflect the benefits of industry standardization and/or more specific design efforts yielding lower overall costs.

## 7. Cost Analysis Results

In this section we provide an overall view of system costs. To provide insight into the cost drivers that may be unique to primary power and CHP, we have broken out system costs into six categories associated with different aspects of operation and production:

- Total Stack Manufacturing
- Fuel, Water (PEM only), and Air Supply Components
- Fuel Processor Components
- Heat Recovery Components
- Power Electronic, Control, and Instrumentation Components
- Assembly Components and Additional Work Estimate

These categories allow comparison across system sizes and technologies.

### 7.1 PEM CHP Systems

This section presents the results of the analyses of four manufacturing volumes for 100- and 250-kW CHP PEM fuel cell systems, including fuel cell stack, BOP, and overall system costs. Figures 7-1 and 7-2 show the distribution of costs for each size for a production volume of 1,000 units/year. The largest contributor to the overall cost for both 100- and 250-kW systems is the power electronics and controls category. The primary cost within this category, representing 78% to 80% of the total category, is the hybrid (three-port) inverter. However, it is important to note for both the PEM and SOFC systems that this category would make up a much larger percentage of the overall costs if a more conventional DC/DC converter and single-function DC/AC inverter were used. This will be considered further in Section 8. Although the fuel cell stack is the second largest category, it represents only ~11 to 17% of the overall system cost. Although considered separately, the fuel processor and heat recovery categories are significantly intertwined as several of the heat recovery components are integral to management of the fuel processor. The combined categories represent 36% to 44% of the system cost, the higher percentage applying to the smaller (100 kW) system.

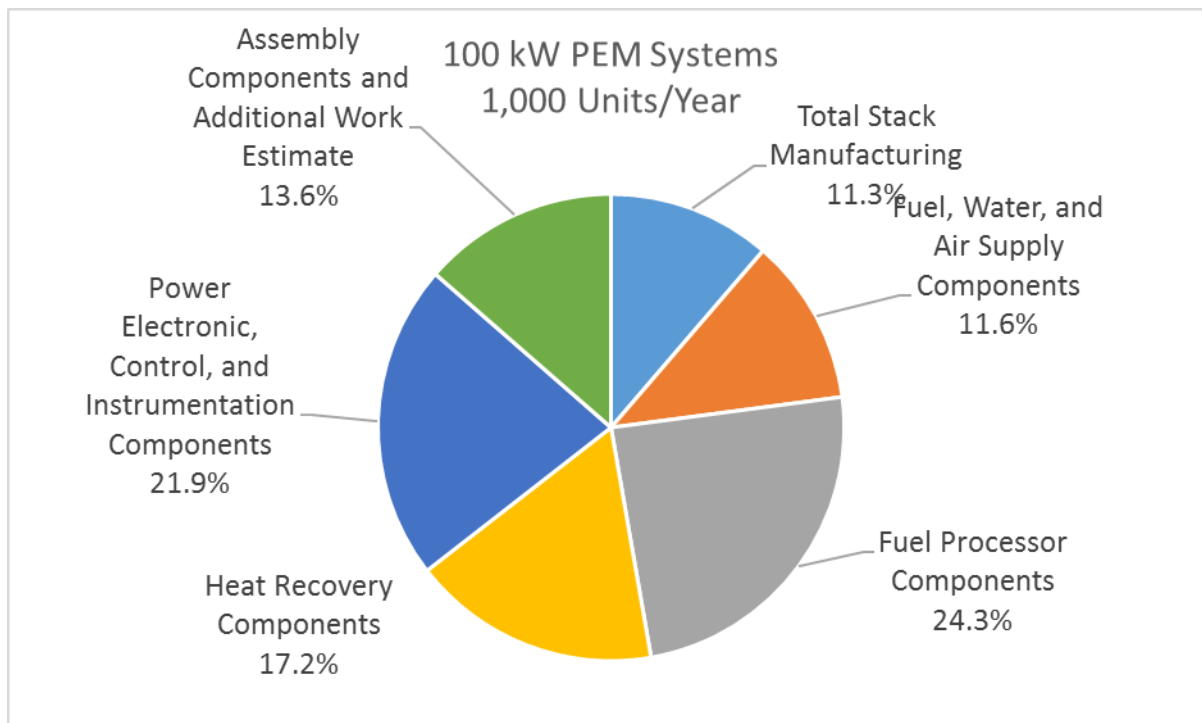


Figure 7-1. 100-kW PEM system costs at 1,000 units per year.

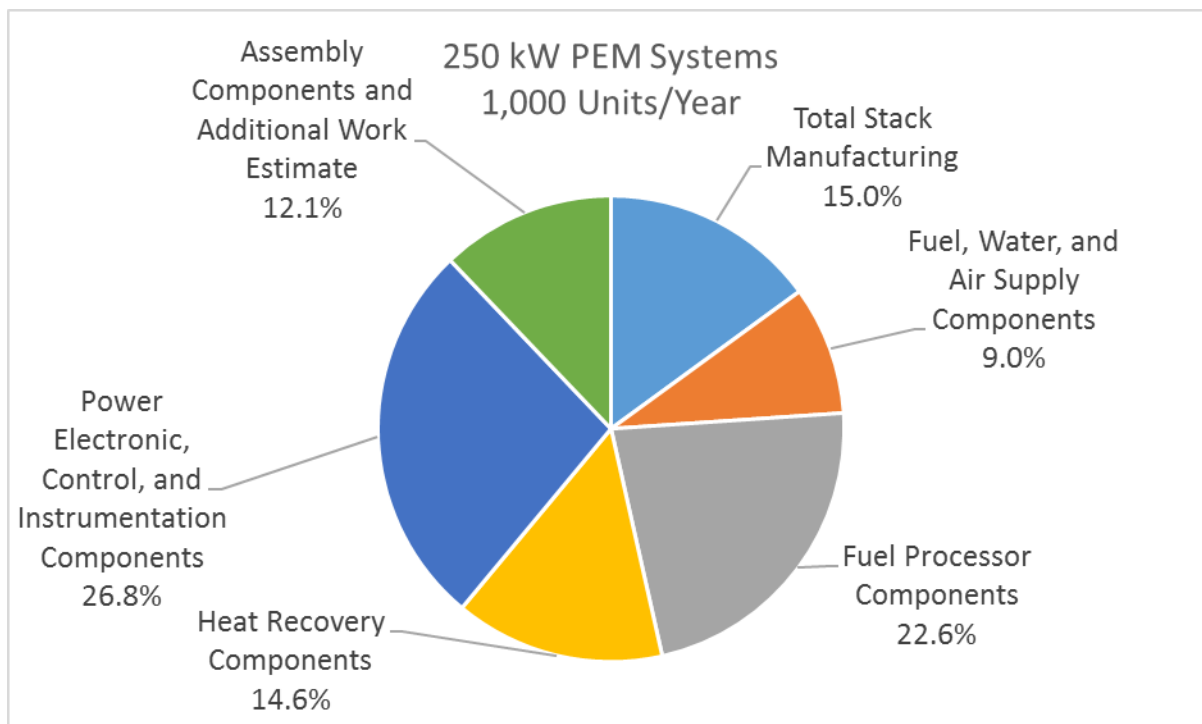


Figure 7-2. 250-kW PEM system costs at 1,000 units per year.

Since the fuel cell stacks dictate much of the equipment and space capital costs, all capital costs are captured in the “total stack manufacturing” category. Furthermore, the manufacturing capital cost (the investment required to produce the systems) is relatively small on a per-system basis even for a limited number of units, accounting for only 0.24% of total system cost at the most. Capital costs are assumed to be amortized over the projected lifetime of the machine or 20 years, whichever is shorter. The number of stacks required for all but the lowest volume production rates considered for this report results in most fabrication work being done in-house with the attendant capital expenditures necessary to obtain and commission the production machinery. Stack and system testing is incorporated into the stack and assembly categories, respectively. All systems and production volumes assume that stack and final system testing and evaluation will be done in-house as a quality control measure. The cost of dedicated test equipment is rolled into the capital investment.

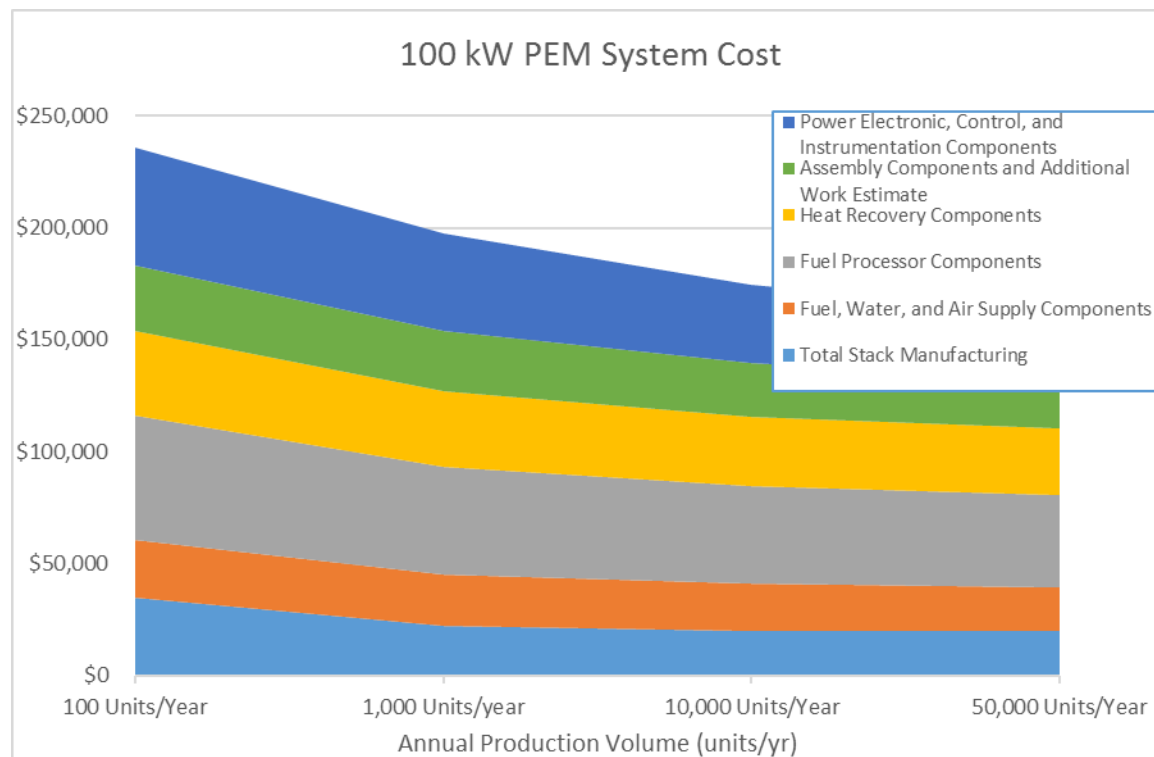
Tables 7-1 and 7-2 provide the estimated costs for each size and production volume. Figures 7-3 and 7-4 graphically show the pre-markup cost trend with increasing manufacturing volume that is represented in Tables 7-1 and 7-2. A 50% markup was used based on discussions with industry to cover overhead and profit and to remain consistent with past reports.

Figure 7-5 shows the cost per kilowatt (excluding mark-up) for each size and each production volume. As expected, there is benefit to increased total production and system size on a cost-per-kW<sub>net</sub> basis. The trends in Figure 7-5 influence the life cycle cost analysis of Section 9. When considering a 5-year life for the system, the higher-production-rate, larger-capacity systems offer attractive payback periods because they are able to generate electrical power at rates competitive with or lower than utility rates in many locations.



**Table 7-1. Cost Summary for 100-kW PEM CHP Fuel Cell System**

Description	100 Units/Yr	1,000 Units/Yr	10,000 Units/Yr	50,000 Units/Yr
Total Stack Manufacturing	\$34,850	\$22,315	\$20,078	\$19,856
Fuel, Water, and Air Supply Components	\$25,832	\$22,857	\$20,894	\$19,622
Fuel Processor Components	\$55,616	\$48,005	\$43,629	\$41,395
Heat Recovery Components	\$37,440	\$33,994	\$30,868	\$29,466
Power Electronic, Control, and Instrumentation Components	\$52,536	\$43,221	\$35,258	\$29,859
Assembly Components and Additional Work Estimate	\$29,500	\$26,790	\$24,080	\$21,705
Total system cost, pre-markup	\$235,774	\$197,183	\$174,807	\$161,904
System cost per kW <sub>net</sub> , pre-markup	\$2,358	\$1,972	\$1,748	\$1,619
Sales markup	50%	50%	50%	50%
Total system cost, with markup	\$353,661	\$295,774	\$262,210	\$242,856
System cost per kW <sub>net</sub> , with markup	\$3,537	\$2,958	\$2,622	\$2,429



*Figure 7-3. 100-kW PEM cost volume trends.*

**Table 7-2. Cost Summary for 250-kW PEM CHP Fuel Cell System**

Description	100 Units/Yr	1,000 Units/Yr	10,000 Units/Yr	50,000 Units/Yr
Total Stack Manufacturing	\$70,197	\$52,589	\$50,432	\$50,009
Fuel, Water, and Air Supply Components	\$35,472	\$31,447	\$28,662	\$26,881
Fuel Processor Components	\$94,462	\$79,221	\$70,458	\$66,491
Heat Recovery Components	\$56,215	\$51,218	\$46,680	\$44,665
Power Electronic, Control, and Instrumentation Components	\$117,058	\$94,238	\$74,725	\$61,509
Assembly Components and Additional Work Estimate	\$46,840	\$42,590	\$38,340	\$34,500
Total system cost, pre-markup	\$420,245	\$351,303	\$309,297	\$284,054
System cost per kW <sub>net</sub> , pre-markup	\$1,681	\$1,405	\$1,237	\$1,136
Sales markup	50%	50%	50%	50%
Total system cost, with markup	\$630,367	\$526,954	\$463,945	\$426,081
System cost per kW <sub>net</sub> , with markup	\$2,521	\$2,108	\$1,856	\$1,704

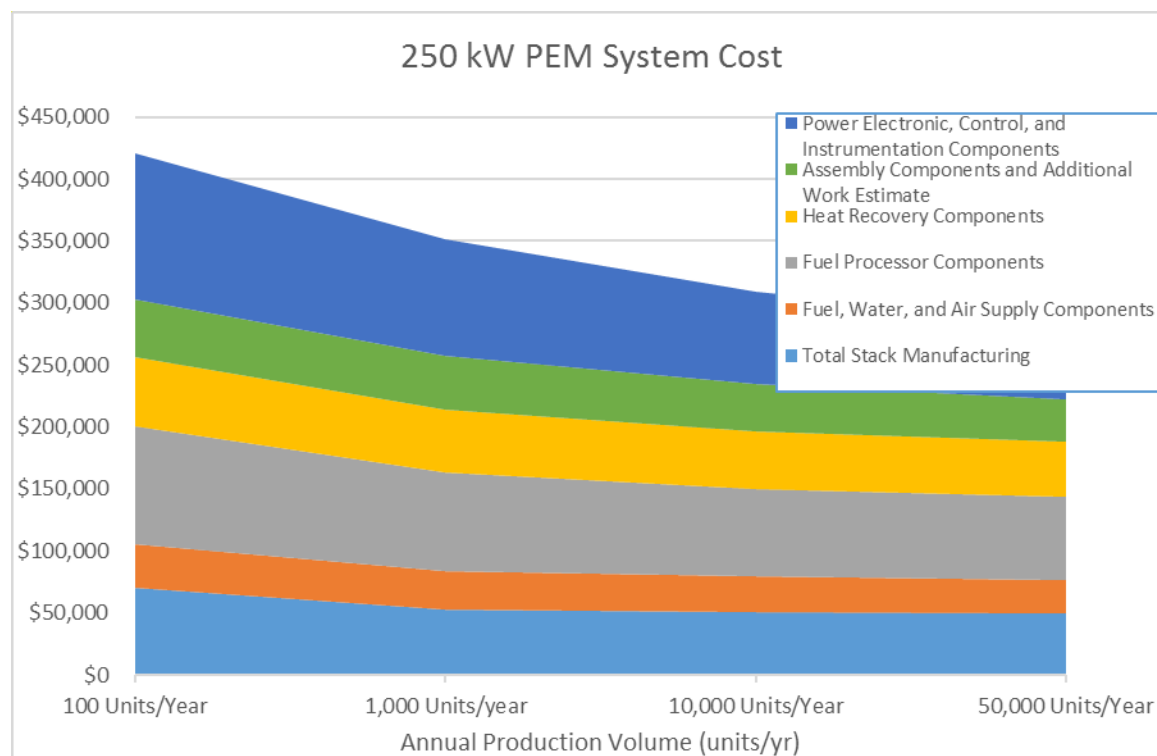


*Figure 7-4. 250-kW PEM cost volume trends.*

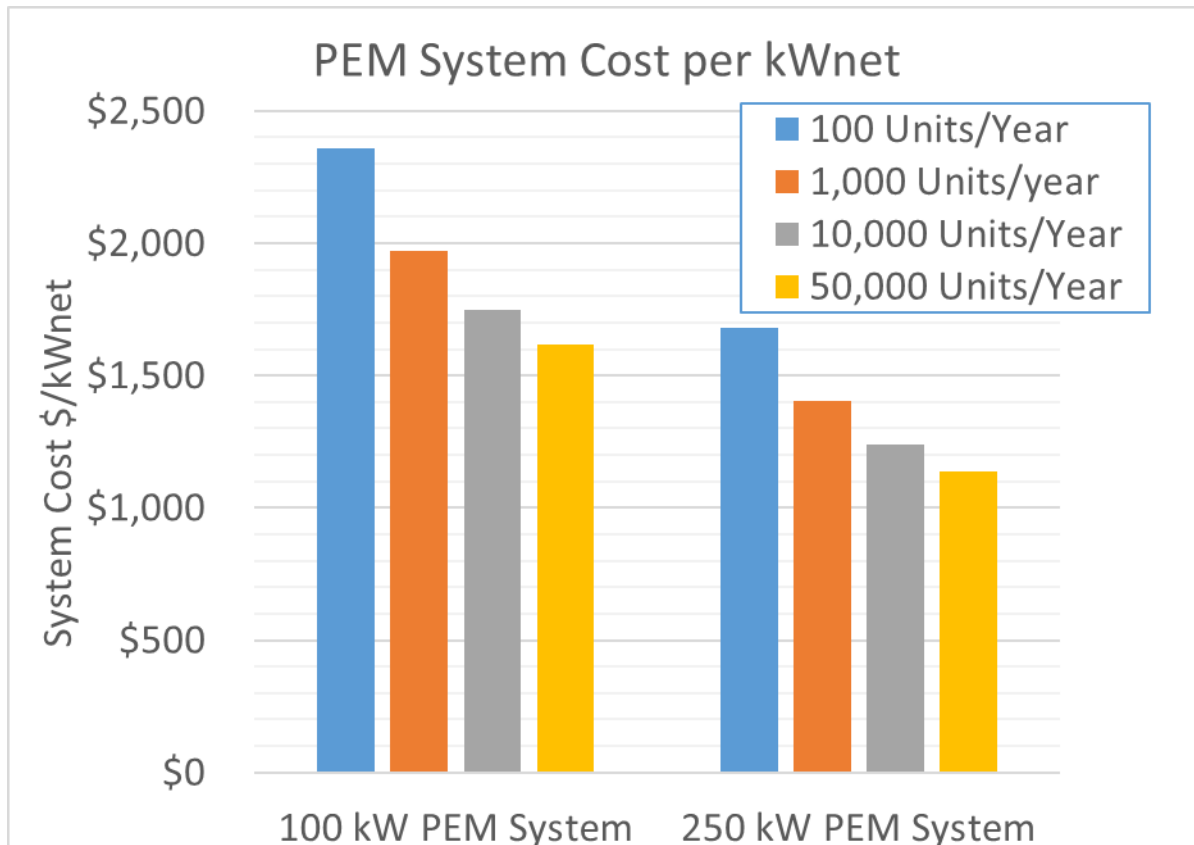


Figure 7-5. Cost per kilowatt for 100-kW and 250-kW PEM system.

## 7.2 SOFC CHP Systems

This section presents the results of the analyses of four manufacturing volumes for 100- and 250-kW CHP SOFC systems, separated into the categories listed above. Figures 7-6 and 7-7 show the distribution of costs for both system sizes at a production volume of 1,000 units/year. The notable difference from the PEM systems is that the SOFC system costs are dominated by the fuel cell stack production and electronic equipment; primarily, the three-port hybrid inverter as highlighted in Section 5 of this study.

Since the fuel cell stacks dictate much of the equipment and space capital costs, all capital costs are captured in the “total stack manufacturing” category. Furthermore, the manufacturing capital cost (the investment required to produce the systems) is relatively small on a per-system basis even for limited numbers of units, accounting for 0.13% of total system cost at the most. Capital costs are assumed to be amortized over the projected lifetime of the machine or 20 years, whichever is shorter. As is the case with PEM systems, most production volumes involved in SOFC system construction benefit from in-house production facilities with the attendant capital expenditures necessary to obtain and commission the machinery. This is somewhat more important for SOFC systems as the cells are fabricated from raw materials (e.g., YSZ) rather than purchased semi-finished materials (e.g., GDL carbon paper) as they are for PEM systems. All systems and sizes assume that final testing, evaluation, and burn-in (if required) will

be done in-house as a quality control measure. Hence, the cost of dedicated test equipment is also rolled into the capital investment for all sizes and volumes.

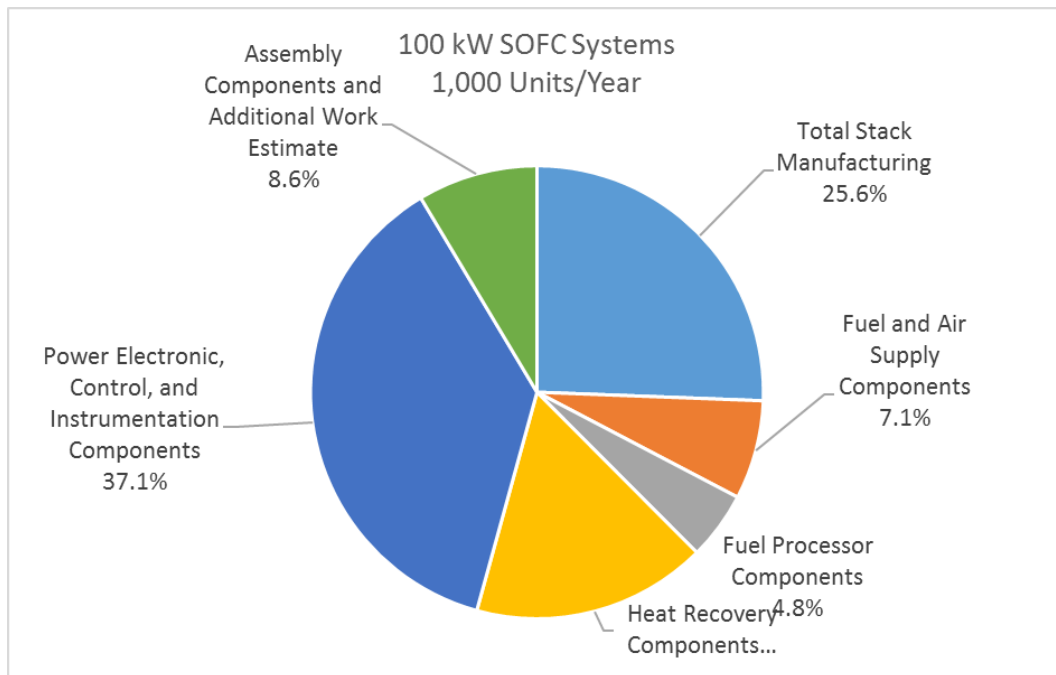


Figure 7-6. 100-kW SOFC system costs at 1,000 units per year.

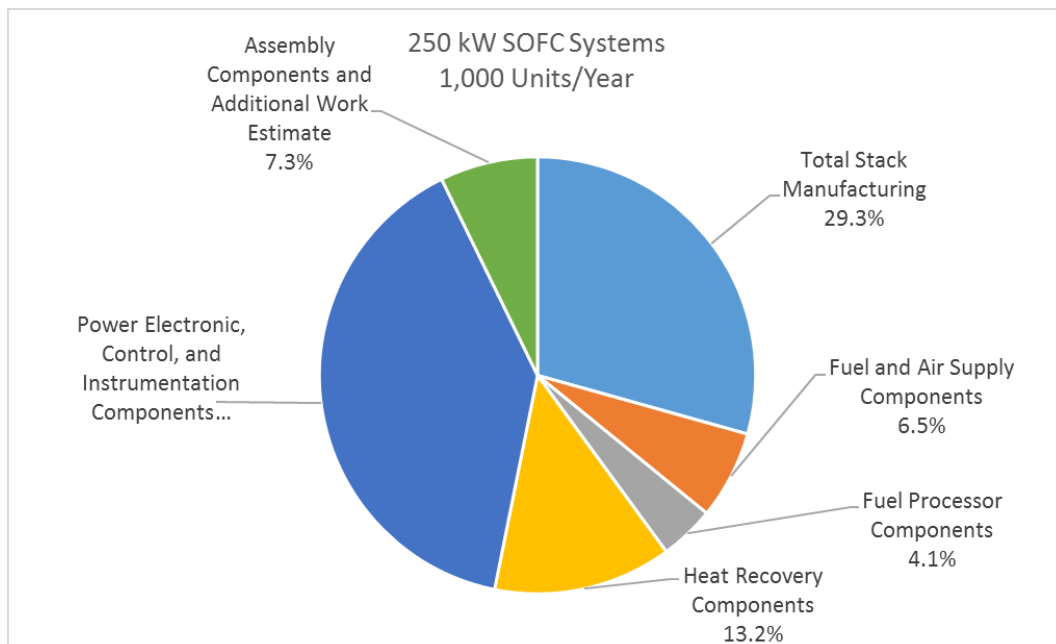


Figure 7-7. 250-kW SOFC system costs at 1,000 units per year.

Tables 7-3 and 7-4 provide the estimated cost values. Figures 7-8 and 7-9 show the pre-markup cost trend with increasing manufacturing volume that is represented in Tables 7-3 and 7-4.

**Table 7-3. Cost Summary for 100-kW CHP SOFC Fuel Cell System**

Description	100 Units/Yr	1,000 Units/Yr	10,000 Units/Yr	50,000 Units/Yr
Total Stack Manufacturing	\$44,555	\$30,081	\$27,017	\$26,746
Fuel and Air Supply Components	\$10,108	\$8,306	\$7,465	\$6,956
Fuel Processor Components	\$8,245	\$5,693	\$5,247	\$4,962
Heat Recovery Components	\$21,057	\$19,698	\$18,430	\$17,621
Power Electronic, Control, and Instrumentation Components	\$52,988	\$43,627	\$35,622	\$30,213
Assembly Components and Additional Work Estimate	\$11,105	\$10,080	\$9,055	\$8,175
Total system cost, pre-markup	\$148,058	\$117,486	\$102,835	\$94,673
System cost per kW <sub>net</sub> , pre-markup	\$1,481	\$1,175	\$1,028	\$947
Sales markup	50%	50%	50%	50%
Total system cost, with markup	\$222,087	\$176,229	\$154,252	\$142,009
System cost per kW <sub>net</sub> , with markup	\$2,221	\$1,762	\$1,543	\$1,420

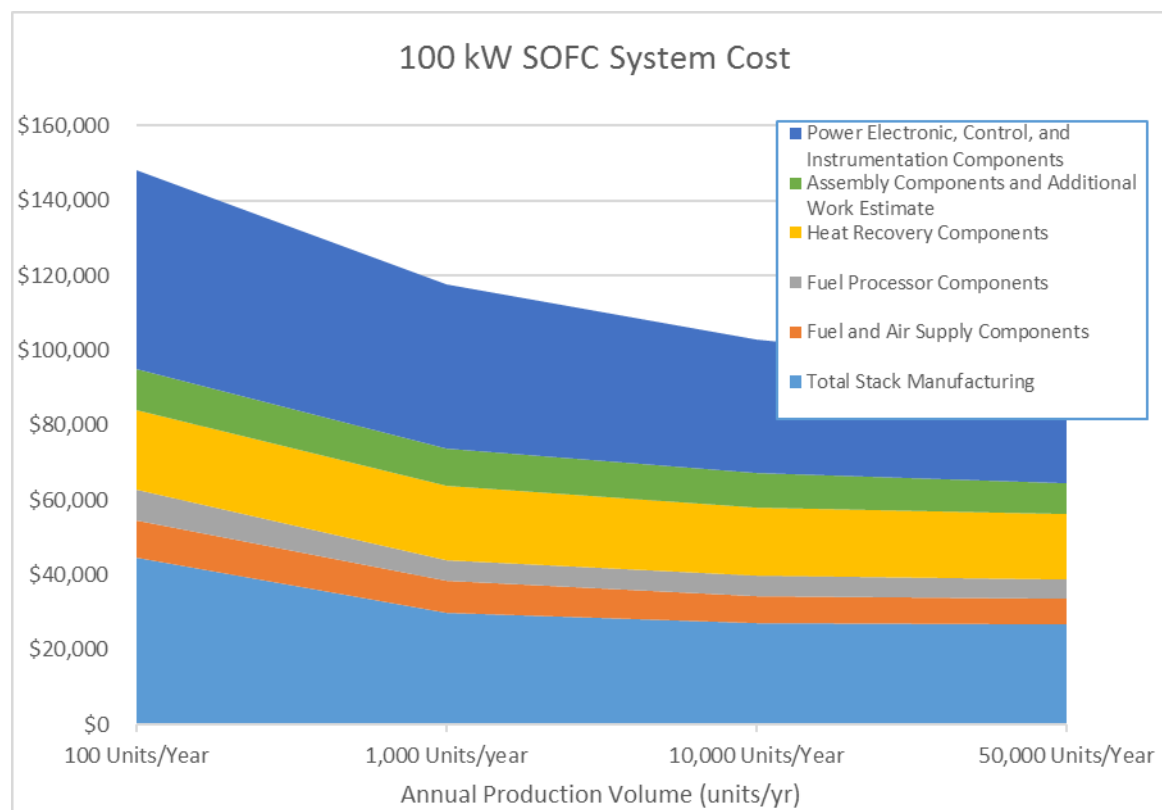


Figure 7-8. 100-kW SOFC cost volume trends.

**Table 7-4. Cost Summary for 250-kW CHP SOFC Fuel Cell System**

Description	100 Units/Yr	1,000 Units/Yr	10,000 Units/Yr	50,000 Units/Yr
Total Stack Manufacturing	\$87,497	\$70,430	\$66,665	\$66,327
Fuel and Air Supply Components	\$18,298	\$15,700	\$14,309	\$13,556
Fuel Processor Components	\$14,347	\$9,797	\$8,604	\$8,253
Heat Recovery Components	\$33,857	\$31,718	\$29,718	\$28,470
Power Electronic, Control, and Instrumentation Components	\$117,962	\$95,050	\$75,453	\$62,217
Assembly Components and Additional Work Estimate	\$19,110	\$17,410	\$15,710	\$14,180
Total system cost, pre-markup	\$291,072	\$240,105	\$210,458	\$193,004
System cost per kW <sub>net</sub> , pre-markup	\$1,164	\$960	\$842	\$772
Sales markup	50%	50%	50%	50%
Total system cost, with markup	\$436,608	\$360,157	\$315,686	\$289,505
System cost per kW <sub>net</sub> , with markup	\$1,746	\$1,441	\$1,263	\$1,158

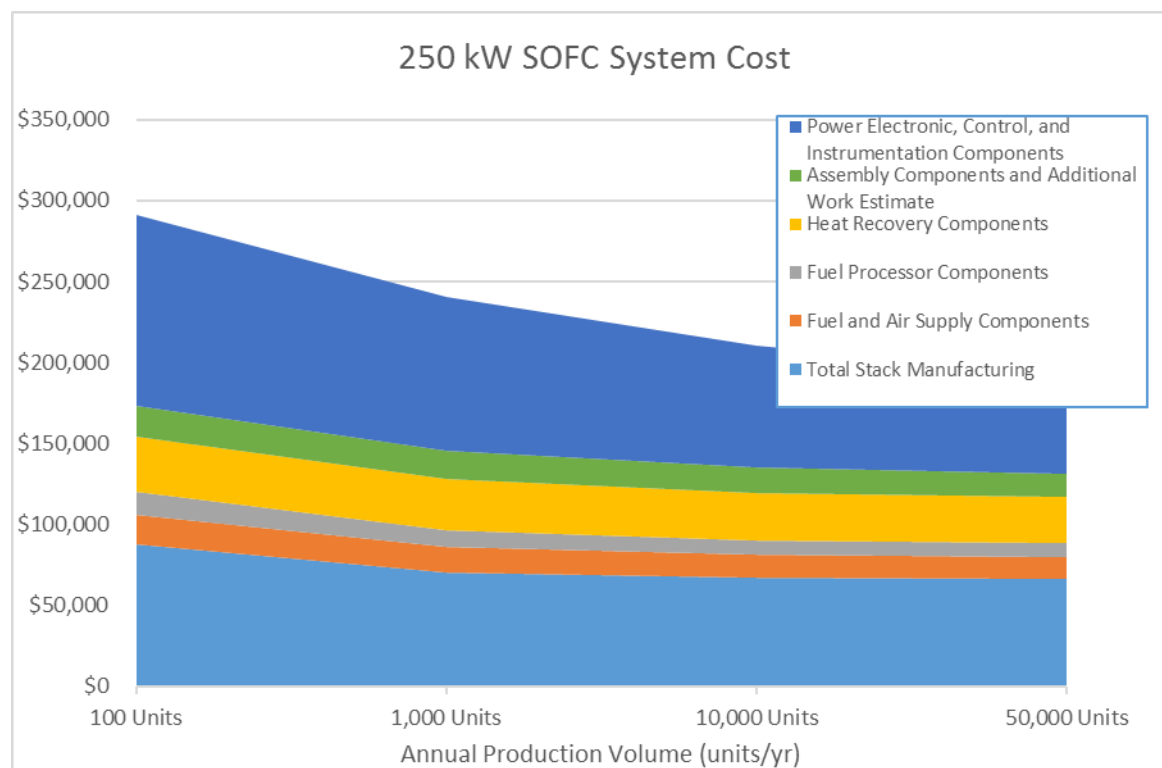


Figure 7-9. 250-kW SOFC cost volume trends.

Figure 7-10 shows the cost per kilowatt (excluding mark-up) for each size and each production volume. As expected, there is benefit to increased total production and system size on cost-per-kW capacity. The trends in Figure 7-10 figure into the life cycle cost analysis. When considering a 5-year life for the system, the higher-production-rate, larger systems offer attractive payback periods because they are able to generate electrical power at rates competitive with or lower than utility rates. The cost analysis does not place any value on grid outage response, though that may be a significantly beneficial factor in many locations.

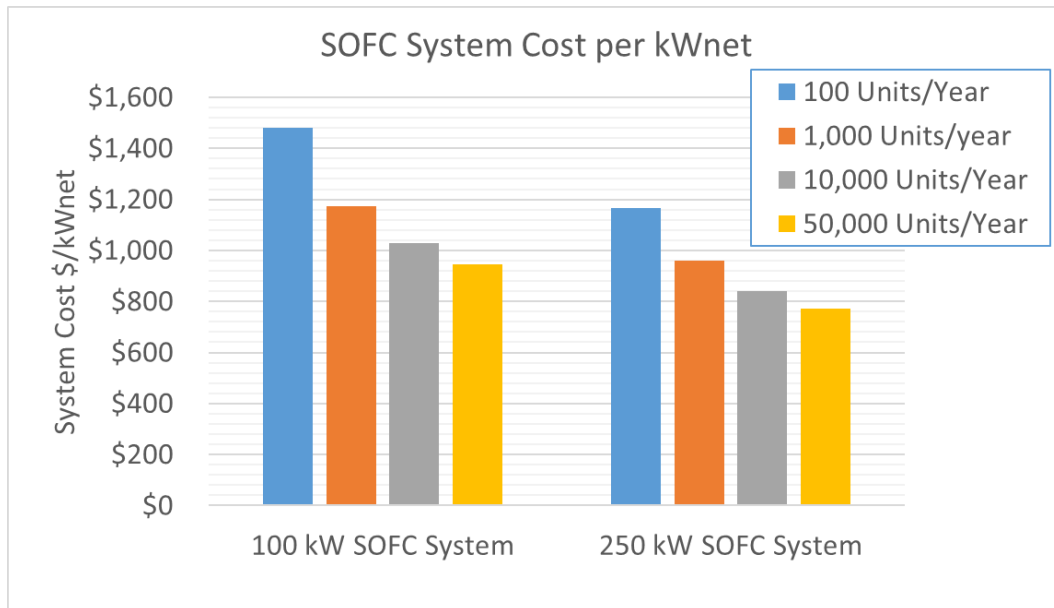


Figure 7-10. Cost per kilowatt for 100-kW and 250-kW SOFC system.

### 7.3 Future Cost Reduction

The items below are potential areas for product or manufacturing improvement. Additional work and discussion is provided in Section 8 (Sensitivity Analysis). Because of the strong influence of the BOP on overall system costs, BOP hardware is clearly a topic of interest for cost reduction.

Before considering specific cost reduction areas, it is appropriate to note that neither the PEM nor SOFC systems analyzed here have been optimized for cost. Neither design specifically reflects installed equipment and is therefore amenable to improvement. Further, specific applications or installations will apply different constraints and afford different opportunities in system design. A significant opportunity for cost reduction likely exists in modifications to the system schematics to eliminate components by integrating hardware components with one another or by drawing on advances in technology that eliminate the need for some hardware. The first place to look for cost improvement is in the details of the system configuration, giving attention to potential simplification and function integration. For example, a low-cost hydrogen purification membrane technology could potentially eliminate the PrOx reactor, PrOx air blower, and associated heat exchanger and control hardware, reducing costs in three of the primary categories considered (control hardware savings would be minimal).

A review of the cost tables (Section 5) and the sensitivity analysis (Section 8) shows that power electronics are major contributors to the overall cost. The costs presented here assume that a hybrid (three- or four-port) inverter has replaced discrete DC/DC and DC/AC hardware. An additional cost reduction may be available in some cases by using batteries connected directly in parallel with the fuel cell stack. However, the savings associated with incorporating a battery in parallel are not as notable as savings associated with incorporating the hybrid inverter, and there is greater risk and/or engineering required to match the system to the application. If the system is to be operated only with the grid present, and if an appropriate power purchase agreement is in place to allow the sale of excess power to the utility, the costs of the batteries can be avoided and some savings is potentially available by having a single-purpose inverter in place of the hybrid inverter.

As the sensitivity analysis of Section 8 shows, additional BOP improvements (e.g., lower cost, designed-to-purpose heat exchangers, blowers) have the potential to impact cost. Blowers are sensitive to overall system pressure drop, so system design changes that enable a lower overall system pressure drop are potentially beneficial. The caveat is that we have assumed relatively aggressive pressure drop characteristics, so there is a potential for blower requirements to increase rather than decrease.

A final comment on the manufacturing process is appropriate. The scrap and reject rates used here are those recommended by our industry contacts as representative of the state of the art. Five percent rate of failure at final test, however, is an unacceptable rate for mass-produced hardware. It is essential to develop effective quality control measures and robust fabrication processes to reduce those rates to less than 0.5%.

## 8. Sensitivity Analysis

### 8.1 PEM System

The sensitivity analysis of the costs for the 100-kW PEM fuel cell systems at production volumes of 1,000 and 10,000 units per year explores the impact of specific variations to the assumptions for the major contributing cost factors and highlights their significance. The cost factors subjected to the sensitivity analysis were chosen because of their significant contribution to the cost and/or the difficulty associated with precisely assessing their magnitude, such as the cost of platinum. The analysis demonstrates the effect of varying each with all else held equal on the overall cost of the system based on reasonable variations to each factor. The results of the sensitivity analyses are shown in the following charts (Figures 8-1 and 8-2), which show the relative importance of the major cost drivers investigated.

The cost factors that were varied, along with the basis for the change and the overall effect for the PEM fuel cell system sensitivity analysis include:

- Replaced hybrid inverter with a DC/DC converter and a DC/AC inverter
  - Base system included the DC/AC hybrid inverter
  - Adjusted to include DC/DC converter and conventional DC/AC inverter to see effect
  - The three-port DC/AC hybrid inverter is relatively new technology and has not been proven in mass production for this application
  - The result of including (if needed) the DC/DC converter significantly increases the overall system cost
- Heat exchangers
  - Assumed total cost of \$50,797 at 1,000 units/year



- Assumed total cost of \$46,873 at 10,000 units/year
- Varied by -25%
- OTS heat exchangers are overdesigned for this application, yielding a conservative estimate for their cost; thus, a 25% reduction yields a significant effect
- DC/AC HYBRID INVERTER
  - Assumed to be \$33,600 at 1,000 units/year
  - Assumed to be \$26,400 at 10,000 units/year
  - Varied by -25%
  - Some of the cost estimates received for the DC/AC hybrid inverter suggested that even lower overall costs are possible at higher volumes; however, since the technology has not been proven for mass production, a more conservative estimate was employed
  - Despite the more conservative cost estimate, employing the DC/AC hybrid inverter yields significant savings that will be even greater if the lower costs at high volumes are achieved
- Current density
  - Assumed to be 0.4 amperes per square centimeter (A/cm<sup>2</sup>)
  - Adjusted to 0.6 A/cm<sup>2</sup> to see effect
  - The current density of 0.4A/cm<sup>2</sup> was chosen to achieve the desired 50,000 hours of durability
  - If the current density could be raised to 0.6 A/cm<sup>2</sup> while still maintaining durability, there is a slight positive impact on system cost
- Blowers
  - Selection dependent on system pressure drop
  - Assumed blower output pressure of ~2 psig
  - Varied to blower output pressure of ~5 psig (resulting in specification of different blowers)
  - There is a slightly negative impact on overall system cost if the assumed system pressure drop of 2 psig is not achieved
- Platinum loading
  - Assumed to be 0.4 milligrams per square centimeter (mg/cm<sup>2</sup>)
  - Varied by +0.1 mg/cm<sup>2</sup>, -0.25 mg/cm<sup>2</sup>
  - For past system studies on lower power systems, platinum loading has shown a significant cost impact
  - There is only a minor impact on overall system cost for a system of this size
- Platinum cost
  - Assumed to be \$1,294 per troy ounce (tr. oz.)
  - Varied by ±50%
  - The cost of platinum is highly variable
  - There is only a minor impact on overall system cost

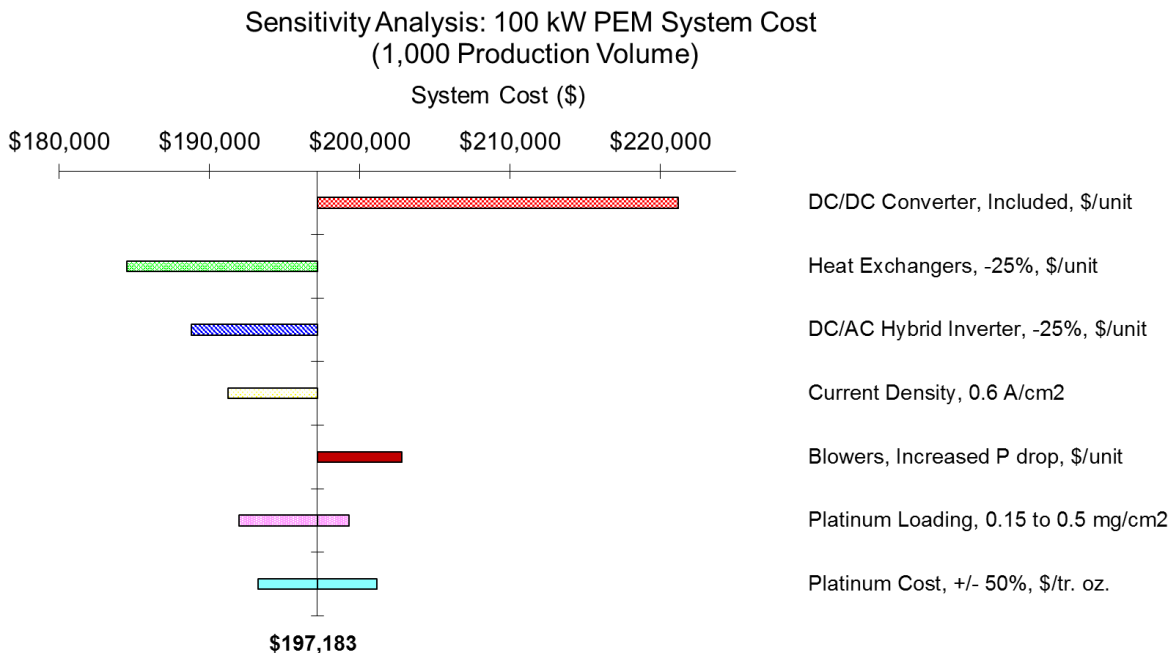


Figure 8-1. PEM sensitivity analysis: 100-kW system cost – 1,000 production volume.

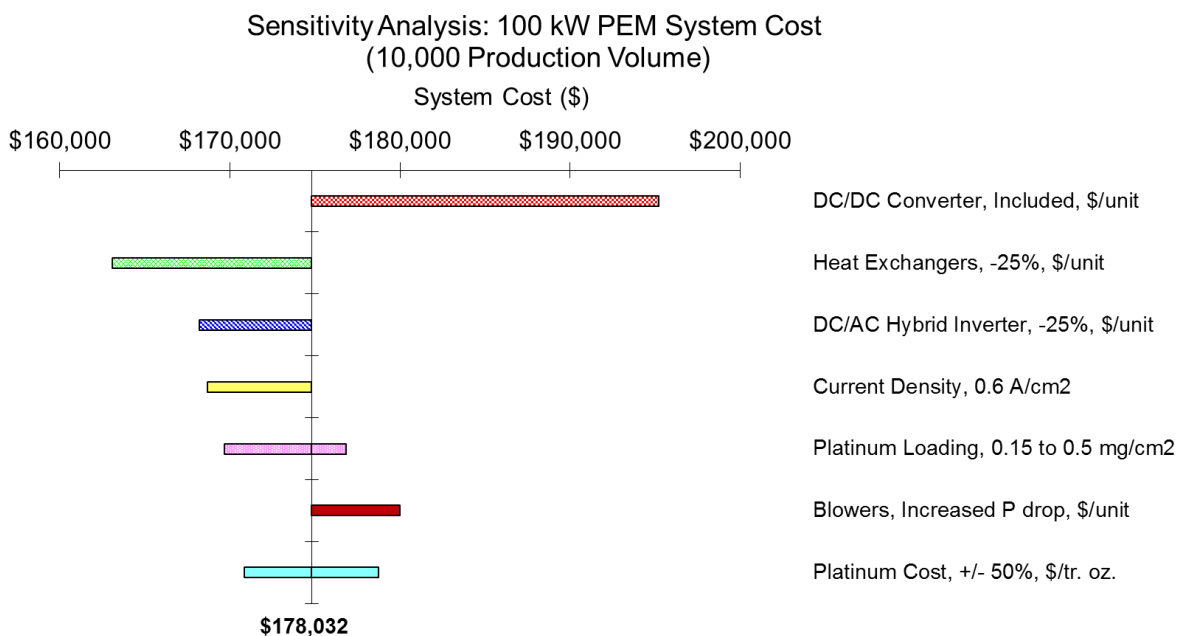


Figure 8-2. PEM sensitivity analysis: 100-kW system cost – 10,000 production volume.

## 8.2 SOFC System

The sensitivity analyses of the costs for the 100-kW systems at production volumes of 1,000 and 10,000 units per year explore the impact of specific variations to the assumptions for major contributing cost factors and highlights their significance. The cost factors were chosen because of their considerable contribution to system cost and/or the difficult nature of precisely assessing their magnitude; this is the case with non-commercial off-the-shelf (COTS) items such as high-temperature heat exchangers, and for specialty production items like grid-tied inverters. The analyses presented here demonstrate the effect of varying each factor over a reasonable range on the overall cost of the system. The results of the sensitivity analyses for the SOFC systems are illustrated in Figures 8-3 and 8-4, which show the relative importance of the major cost drivers investigated.

The cost factors that were varied, along with the basis and effect for the SOFC fuel cell system sensitivity analysis include:

- Replaced hybrid inverter with a DC/DC converter and a DC/AC inverter
  - Base system included the DC/AC hybrid inverter
  - Adjusted to include DC/DC converter and conventional DC/AC inverter to see effect
  - The three-port DC/AC hybrid inverter is relatively new technology and has not been proven in mass production for this application
  - The result of including (if needed) the DC/DC converter significantly increases the overall system cost
- DC/AC hybrid inverter
  - Assumed to be \$33,600 at 1,000 units/year
  - Assumed to be \$26,400 at 10,000 units/year
  - Varied by -25%
  - Some of the cost estimates received for the DC/AC hybrid inverter suggested that even lower overall costs are possible at higher volumes; however, since the technology has not been proven for mass production, a more conservative estimate was employed
  - Despite the more conservative cost estimate, employing the DC/AC hybrid inverter yields significant savings which will be even greater if the lower costs at high volumes are achieved
- SOFC stack
  - Assessed to be \$29,098 at 1,000 units/year
  - Assessed to be \$26,159 at 10,000 units/year
  - Varied by  $\pm 25\%$
  - Stack is a significant cost contributor
  - Varying the stack costs by 25% results in a moderate effect on system cost
- Cathode recuperator heat exchanger
  - Assumed to be \$17,580 at 1,000 units/year
  - Assumed to be \$16,439 at 10,000 units/year
  - Varied by  $\pm 25\%$
  - A COTS heat exchanger for this application was slightly overdesigned, yielding a conservative estimate for the cost; thus, a 25% reduction yields a slight positive effect
- Fuel processor
  - Assessed to be \$5,675 at 1,000 units/year
  - Assessed to be \$5,115 at 10,000 units/year
  - Varied by  $\pm 25\%$
  - Only a minor effect was seen by varying the fuel processor cost by 25%

- Blowers
  - Selection dependent on system pressure drop
  - Assumed blower output pressure of ~2 psig
  - Varied to blower output pressure of ~5 psig (resulting in specification of different blowers)
  - There is a slight negative impact on overall system cost if the assumed system pressure drop of 2 psig is not achieved

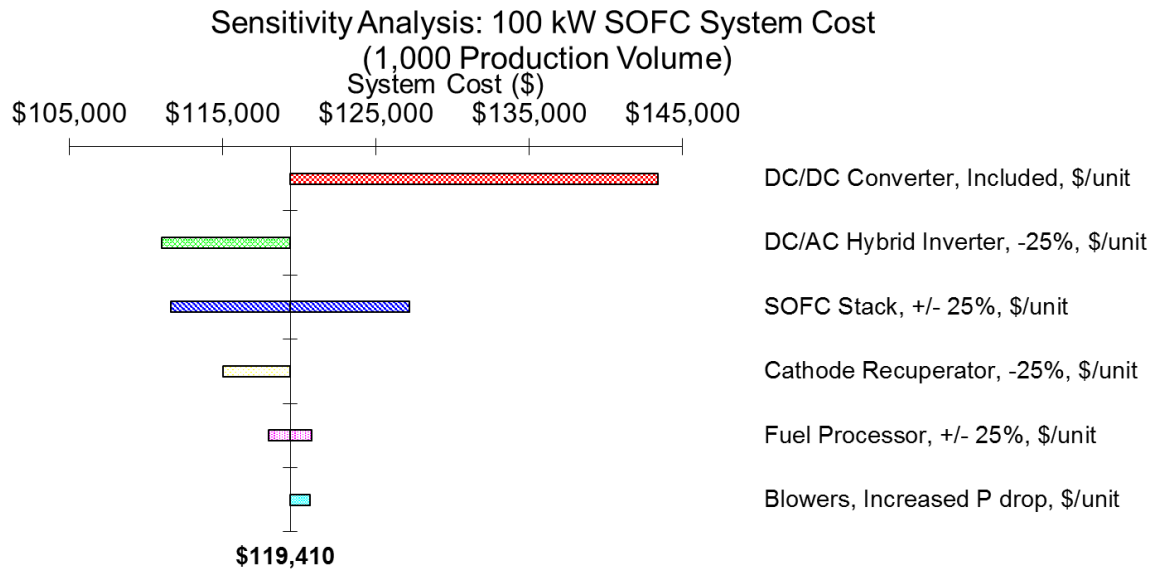


Figure 8-3. SOFC sensitivity analysis: 100-kW system cost – 1,000 production volume.

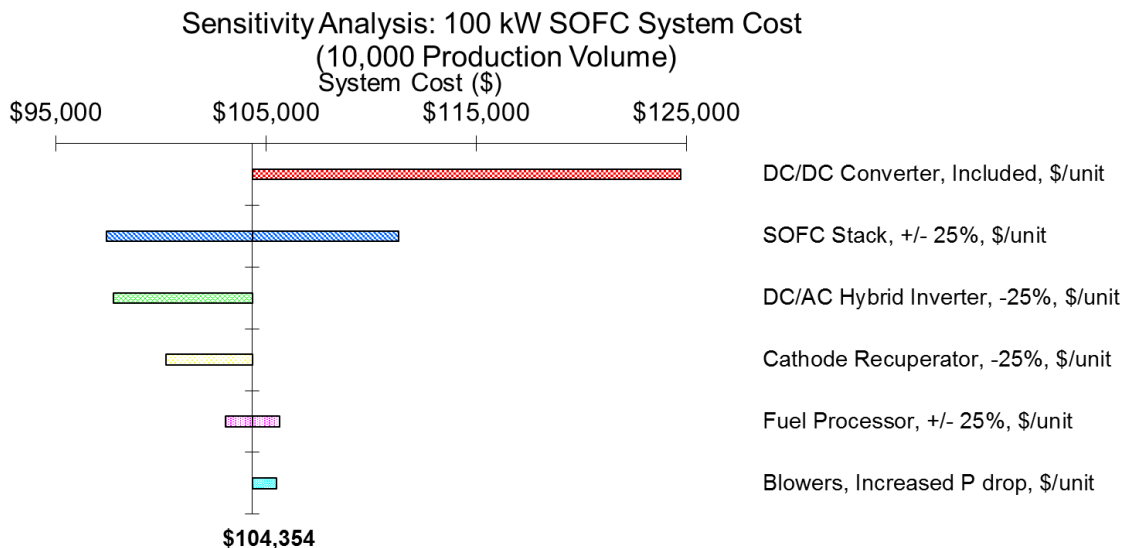


Figure 8-4. SOFC sensitivity analysis: 100-kW system cost – 10,000 production volume.

## 9.0. Life Cycle Cost Analyses of Fuel Cells

### 9.1 Introduction

Fuel cell systems may be configured to provide electricity only, or both electricity and thermal energy. As on-site electrical power generators, fuel cell systems would compete directly with the grid and against other standard power generation sources such as locally sited gas turbines or other engines. When designed to provide both electricity and thermal energy, waste heat is used for process heating and/or space heating or cooling to offset purchased energy that would otherwise be required for that purpose. Because utilization of waste heat requires the addition of capital equipment, the benefits are particularly site-specific and sensitive to natural gas price, natural gas-fired heating or cooling equipment being the likely alternative. For this life cycle cost analysis, we have focused on applications which derive their value from site-generated electricity with some consideration given to sites where the waste heat could be beneficially used, at least for a portion of the year.

It should be noted that all power generation alternatives would be expected to operate continuously, or nearly continuously, bringing them under any relevant environmental regulations related to total site emissions; however, fuel cell systems would have significantly lower emissions than the standard alternatives (with the obvious exception of solar and geothermal energy). However, for this analysis we have not included any environmental externality costs as they would vary widely with location, application, and site specifics.

### 9.2 Scenarios Evaluated

Rather than define a specific business application, we analyzed a generic commercial site with the following characteristics:

- Average electrical load of 400 kW for primary operations (e.g., lighting, information processing/servers, production equipment operation)
  - 400 kW was selected as a suitable demand load based on an assumed minimum electrical load at or near 100 kW or 250 kW, depending on the system being analyzed.
- Average heat load of 200 kW for space, water, or process heating
  - Usually provided by natural gas or electrically driven vapor-compression heat pump
    - The lower cost and lower maintenance requirement of natural gas fired heating equipment usually results in the selection of natural gas when available unless natural gas cost is exceptionally high.
    - For consistency we assumed natural gas heating at 85% efficiency as the basis for comparison.
    - We assume for the calculations shown below that the heating load is required for a full year. This is a convenience for comparison purposes.
- Average cooling load of 200 kW for space, water, or process cooling
  - Usually provided by either electrically driven vapor-compression equipment or natural gas fired absorption equipment.
    - Comparable equipment capital cost and maintenance requirement results in site specific choice.

- For consistency we have used an electrically driven heat pump with COP of 3 as the basis for comparison.
  - We assume for the calculations shown below that the heating load is required for a full year. This is a convenience for comparison purposes.
- 
- Natural gas provided at the site with rates based on Energy Information Agency ([www.eia.gov](http://www.eia.gov)) on-line reported cost for commercial sites (varies with location, e.g., \$0.811/therm in California)
  - Electric power provided at the site with rates based on Energy Information Agency ([www.eia.gov](http://www.eia.gov)) on-line reported costs for commercial sites (varies with location, e.g., \$0.173/kW-hr in California)

Using the conditions above, three discrete states were analyzed: California, New York, and Texas. We also considered the overall average rates for the United States.

The basic fuel cell system parameters used for the analysis are as follows:

## PEM

- Total system efficiency: 80%
- System electrical efficiency: 30%
- Net electrical output 100 kW and 250 kW
- Waste heat peak temperature ~80 C
- Recoverable waste heat
  - ~167 kW @ 100 kW electric output
  - ~417 kW @ 250 kW electric output
- System life = 6 years (~50,000 hours) based on assumed stack life

## SOFC

- Total system efficiency: 90%
- System electrical efficiency 40%
- Net electrical output 100 kW and 250 kW
- Waste heat peak temperature ~600 C
- Recoverable waste heat
  - ~125 kW @ 100 kW electric output
  - ~313 kW @ 250 kW electric output
- System life = 6 years (~50,000 hours) based on assumed stack life

The cost basis and operating cost assumptions for California are shown in Tables 9-1 and 9-2.

**Table 9-1. Cost Basis for California**

California Cost Basis		
Electricity	\$ 0.173	\$/kW-hr (Average 2014/2015 prices from EIA)
Natural gas	\$ 0.811	\$/therm (Average month 11/2014 to 10/2015 from EIA)
	\$ 0.0277	\$/kW-hr (based on higher heating value)

**Table 9-2. Operating Costs for California**

Operation	Net Power	Source	Gross Power	Yearly Cost Electric	Yearly Cost Natural Gas	Yearly Cost Assumed
System Required Electric	400 kW	From Grid	400 kW	\$605,842		\$605,842
Heating (if Natural Gas)	200 kW	@ 85% assumed efficiency, natural gas heating	235 kW		\$57,075	\$57,075
Heating (if Electric)	200 kW	@ COP=4 for Vapor Compression heat pump	50 kW	\$75,730		
Cooling (if Natural Gas)	200 kW	@ COP=1.0 natural gas absorption cooling	200 kW		\$48,514	
Cooling (if Electric)	200 kW	@ COP=3 for Vapor Compression heat pump	67 kW	\$100,974		\$100,974
Total Input Power	800 kW	Total Cost		\$782,545	\$711,431	\$763,891

The lifecycle cost analysis was performed for eight system configurations:

- PEM CHP system without waste heat recovery
  - 100 kW
  - 250 kW
- PEM CHP system with waste heat recovery
  - 100 kW
  - 250 kW
- SOFC CHP system without waste heat recovery
  - 100 kW
  - 250 kW
- SOFC CHP system with waste heat recovery
  - 100 kW
  - 250 kW

For the 100-/250-size range, we used mostly industrial equipment for BOP estimation purposes. This equipment generally has a 10- to 20-year life expectancy with adequate maintenance. The stack and the reformer have potentially shorter lifetimes. Therefore, it would potentially be possible to replace the stack and reformer periodically as needed and continue operation without replacing the remainder of the BOP. To investigate this possibility, we extended the analysis to 12 years for the California case. The PEM fuel cell stack and reformer are assumed to be replaced at the start of the 7<sup>th</sup> year (6-year life). The SOFC stack and reformer are assumed to be replaced at the beginning of years 4, 7, and 10 (3-year life). The choice to shorten the SOFC stack and reformer life for the 12-year analysis represents concern over the

maturity and total operating time achieved (at least in the published literature) for that technology. As will be noted below, even with the shortened stack/reformer life SOFC systems can be attractive. In calculating the stack replacement cost, we assumed that there would be significant scrap value in the PEM stack because the end plates, bipolar plates, and platinum catalyst could be recovered and reused. The recovered value varied by size and production volume but was generally between 18% and 24% of the original stack cost. Because the SOFC stack is brazed together and is a mixture of ceramic and refractory metals, we judged that the recovery value would not be significant.

### 9.3 Results

An example comparison is shown in Table 9-3 (in this case, the 100-kW SOFC system with waste heat recovery in California). The internal rate of return (IRR) assumes an initial cost to install the system followed by yearly savings which are applied at the beginning of each year following the initial outlay. For systems analyzed with waste heat recovery, additional cost is included to cover integration with facility heating/cooling infrastructure; this cost is outside the scope of the fuel cell CHP system, since every installation would be slightly different, but it is important when considering installation costs. The life of the system is presumed to be 6 years of operation at the nominal power level. The payback period is simply the total installed cost divided by the projected yearly savings.

Operating costs include:

- Annual electricity cost – cost of fuel-cell-generated electricity and electricity purchased from the grid to make up remainder of demand not covered by fuel cell CHP system
- Annual natural gas cost – cost of natural gas to provide heating/cooling
- Annual consumables – cost of consumed items (filters, elements, desulfurizer media, etc.)
- Annual operation and maintenance (O&M) – cost for estimated time and materials for routine maintenance

The annual savings is the difference between the annual total operating costs and the typical operating costs listed in Table 9-2.

For the case shown in Table 9-3, the IRR increased from 29% to 56% as the number of systems manufactured and installed increased from 100 to 50,000. While this case has an attractive return on investment (ROI), not all cases were found to be beneficial. For example, Table 9-4 shows the data for 100-kW PEM systems without waste heat recovery. Due to additional fuel costs (both for a reduced electrical efficiency compared to SOFC and for heating), the annual savings over grid electricity do not provide an ROI within the first 5 years at production volumes below 10,000 units/year.

Table 9-5 summarizes the IRR and payback period for all eight California cases considered using the base costs for electricity and natural gas shown in Table 9-1.



**Table 9-3. Annual Cash Flows, IRR and Payback Period (100-kW SOFC system with waste heat recovery)**

SOFC (with waste heat recovery)		100-kW Systems			
		100/year	1,000/year	10,000/year	50,000/year
System Production Rate		100/year	1,000/year	10,000/year	50,000/year
Fuel Cell CHP System Cost		\$222,087.09	\$176,229.20	\$154,251.93	\$142,008.95
Waste Heat Recovery Cost		\$5,000.00	\$4,750.00	\$4,513.00	\$4,287.00
Installation Cost		\$62,500.00	\$50,000.00	\$45,000.00	\$40,000.00
Total 1st Year Cost		\$289,587.09	\$230,979.20	\$203,764.93	\$186,295.95
Operating Costs					
Annual Electrical Cost		\$615,997.42	\$615,997.42	\$615,997.42	\$615,997.42
Annual Natural Gas Cost (Heating)		\$26,754.10	\$26,754.10	\$26,754.10	\$26,754.10
Annual Consumables		\$2,024.00	\$1,835.00	\$1,663.00	\$1,508.00
Annual O&M		\$2,000.00	\$2,000.00	\$2,000.00	\$2,000.00
Annual Total Operating Cost		\$646,775.51	\$646,586.51	\$646,414.51	\$646,259.51
Annual Savings		\$117,115.09	\$117,304.09	\$117,476.09	\$117,631.09
Annual Cash Flow	Year 1	-\$289,587.09	-\$230,979.20	-\$203,764.93	-\$186,295.95
	Year 2	\$117,115.09	\$117,304.09	\$117,476.09	\$117,631.09
	Year 3	\$117,115.09	\$117,304.09	\$117,476.09	\$117,631.09
	Year 4	\$117,115.09	\$117,304.09	\$117,476.09	\$117,631.09
	Year 5	\$117,115.09	\$117,304.09	\$117,476.09	\$117,631.09
	Year 6	\$117,115.09	\$117,304.09	\$117,476.09	\$117,631.09
Internal Rate of Return		29%	42%	50%	56%
Payback Period (years)		2.43	1.93	1.70	1.55

**Table 9-4. Annual Cash Flows, IRR and Payback Period (100-kW PEM system without waste heat recovery)**

PEM (No waste heat recovery)		100-kW Systems			
System Production Rate		100/year	1,000/year	10,000/year	50,000/year
System Cost		\$353,661.07	\$295,773.95	\$262,209.87	\$242,855.62
Waste Heat Recovery Cost		\$0.00	\$0.00	\$0.00	\$0.00
Installation Cost		\$62,500.00	\$50,000.00	\$45,000.00	\$40,000.00
Total 1st Year Cost		\$416,161.07	\$345,773.95	\$307,209.87	\$282,855.62
Operating Costs					
Annual Electrical Cost		\$636,211.62	\$636,211.62	\$636,211.62	\$636,211.62
Annual Natural Gas Cost (Heating)		\$57,075.40	\$57,075.40	\$57,075.40	\$57,075.40
Annual Consumables		\$4,048.00	\$3,670.00	\$3,326.00	\$3,016.00
Annual O&M		\$2,000.00	\$2,000.00	\$2,000.00	\$2,000.00
Annual Total Operating Cost		\$699,335.03	\$698,957.03	\$698,613.03	\$698,303.03
Annual Savings		\$64,555.58	\$64,933.58	\$65,277.58	\$65,587.58
Annual Cash Flow	Year 1	-\$416,161.07	-\$345,773.95	-\$307,209.87	-\$282,855.62
	Year 2	\$64,555.58	\$64,933.58	\$65,277.58	\$65,587.58
	Year 3	\$64,555.58	\$64,933.58	\$65,277.58	\$65,587.58
	Year 4	\$64,555.58	\$64,933.58	\$65,277.58	\$65,587.58
	Year 5	\$64,555.58	\$64,933.58	\$65,277.58	\$65,587.58
	Year 6	\$64,555.58	\$64,933.58	\$65,277.58	\$65,587.58
Internal Rate of Return		-8%	-2%	2%	5%
Payback Period (years)		6.45	5.33	4.71	4.31

**Table 9-5. IRR and Payback for Installations in California**

California Average Utility Rates for Commercial Installations					
	System Production rate	100/year	1,000/year	10,000/year	50,000/year
PEM (without waste heat recovery)	100 kW				
	Internal Rate of Return	-8%	-2%	2%	5%
	Payback Period (years)	6.45	5.33	4.71	4.31
	250 kW				
	Internal Rate of Return	2%	9%	15%	19%
	Payback Period (years)	4.67	3.85	3.39	3.08
PEM (with waste heat recovery heating)	100 kW				
	Internal Rate of Return	8%	15%	21%	25%
	Payback Period (years)	3.96	3.28	2.91	2.67
	250 kW				
	Internal Rate of Return	13%	21%	28%	32%
	Payback Period (years)	3.45	2.85	2.51	2.29
SOFC (without waste heat recovery)	100 kW				
	Internal Rate of Return	16%	27%	33%	39%
	Payback Period (years)	3.28	2.60	2.29	2.08
	250 kW				
	Internal Rate of Return	27%	38%	45%	52%
	Payback Period (years)	2.59	2.11	1.86	1.69
SOFC (with waste heat recovery heating)	100 kW				
	Internal Rate of Return	29%	42%	50%	56%
	Payback Period (years)	2.43	1.93	1.70	1.55
	250 kW				
	Internal Rate of Return	39%	51%	60%	67%
	Payback Period (years)	2.05	1.68	1.47	1.34

As illustrated in Table 9-5, 100-kW PEM systems without heat recovery are not profitable after the 6-year payback period until production volumes increase substantially, and these systems still do not offer significant financial benefit even at the highest production. The addition of heat recovery for all applications (in the Table 9-5 scenario) yields improved rates of return, particularly as production volumes increase for the 250-kW systems.

SOFC systems offer much better financial benefit, particularly in California, for most production volumes with or without heat recovery. The potential return in excess of 35% for the 250-kW system with waste heat recovery, even at low production volumes, provides a strong business case for the initial investment; this is significant as this application can provide an initial market entry for fuel cell systems that can support additional cost reduction and market expansion in the future. A caution is appropriate, however,

because this rate of return is based on a 6-year lifetime for the fuel cell system. Current SOFC technology has not yet been demonstrated to consistently achieve the required 50,000-hour life.

To address questions regarding SOFC lifetimes and look at the potential for periodic refurbishment of a fuel cell system, we considered extending the system lifetime to 12 years, thereby affording a longer time for recovery of the BOP investment. Table 9-6 provides the IRR values for the various options in California assuming stack and reformer replacement every 6 years for PEM and every 3 years for SOFC. As noted above, the PEM stack is considered to have roughly 20% recoverable value while the SOFC stack and both reformers are assumed to have no residual value. The payback period is the same as in Table 9-5 and is not repeated in Table 9-6. Table 9-6 shows that an attractive case can be made for most installations in California when a 12-year system life is considered. Even with the shortened lifespan on the SOFC stack and reformer the rate of return is higher than for the PEM systems.

**Table 9-6. IRR Summary for Installations in California**

California Average Utility Rates for Commercial Installations					
	System Production rate	100/year	1,000/year	10,000/year	50,000/year
PEM (without waste heat recovery)	100 kW				
	Internal Rate of Return	9%	14%	17%	19%
	250 kW				
	Internal Rate of Return	17%	23%	27%	30%
PEM (with waste heat recovery heating)	100 kW				
	Internal Rate of Return	21%	27%	32%	35%
	250 kW				
	Internal Rate of Return	26%	32%	37%	42%
SOFC (without waste heat recovery)	100 kW				
	Internal Rate of Return	23%	33%	39%	43%
	250 kW				
	Internal Rate of Return	33%	43%	49%	55%
SOFC (with waste heat recovery heating)	100 kW				
	Internal Rate of Return	35%	47%	54%	59%
	250 kW				
	Internal Rate of Return	43%	55%	63%	69%

The electric and gas prices shown in Table 9-1 are unique to California. Tables 9-7 and 9-8 provide cost comparisons using New York State utility rates and the average U.S. utility rate, respectively. The New York costs appear roughly comparable to the California installations because of the relatively higher electric costs compared to natural gas costs. However, when the national averages are considered, only 250 kW SOFC configurations offer a reasonable ROI because the ratio between electric and gas cost is too small. Evaluation of the above scenario using Texas and Illinois gas and electric rates yielded even worse results when using commercial gas and electric rates. Those results are not presented here but underscore the reason for the overall US averages showing poor payback for fuel cell installations. However, it is important to recognize that our analysis does not take any credit for cost avoidance associated with a power outage that can be partially offset by the fuel cell system. It is also relevant that this is a unique scenario developed for the purposes of a qualitative understanding of the factors that are

relevant to fuel cell deployment. Each potential installation should receive a similar analysis with credit taken for avoided losses during grid power failure. The system costs listed here include the capability to run during grid outage.

**Table 9-7. IRR and Payback for Installations in New York State**

New York Average Utility Rates for Commercial Installations					
	System Production rate	100/year	1,000/year	10,000/year	50,000/year
PEM (without waste heat recovery)	100 kW				
	Internal Rate of Return	-9%	-3%	1%	4%
	Payback Period (years)	6.68	5.52	4.87	4.47
	250 kW				
	Internal Rate of Return	1%	8%	13%	17%
	Payback Period (years)	4.84	3.99	3.51	3.19
PEM (with waste heat recovery heating)	100 kW				
	Internal Rate of Return	5%	12%	17%	21%
	Payback Period (years)	4.32	3.58	3.17	2.91
	250 kW				
	Internal Rate of Return	10%	18%	24%	29%
	Payback Period (years)	3.70	3.06	2.69	2.45
SOFC (without waste heat recovery)	100 kW				
	Internal Rate of Return	13%	23%	30%	35%
	Payback Period (years)	3.50	2.78	2.44	2.22
	250 kW				
	Internal Rate of Return	24%	34%	41%	47%
	Payback Period (years)	2.76	2.26	1.99	1.81
SOFC (with waste heat recovery heating)	100 kW				
	Internal Rate of Return	25%	37%	44%	50%
	Payback Period (years)	2.67	2.12	1.86	1.70
	250 kW				
	Internal Rate of Return	34%	45%	54%	61%
	Payback Period (years)	2.23	1.83	1.61	1.46

**Table 9-8. IRR and Payback for Installations Based on Overall US Energy Costs**

US Overall Average Utility Rates for Commercial Installations					
	System Production rate	100/year	1000/year	10,000/year	50,000/year
PEM (without waste heat recovery)	100 kW				
	Internal Rate of Return	-50%	-47%	-45%	-43%
	Payback Period (years)	61.29	48.24	40.90	36.16
	250 kW				
	Internal Rate of Return	-46%	-42%	-40%	-38%
	Payback Period (years)	43.70	34.32	29.25	25.77
PEM (with waste heat recovery heating)	100 kW				
	Internal Rate of Return	-16%	-11%	-8%	-5%
	Payback Period (years)	8.76	7.22	6.37	5.83
	250 kW				
	Internal Rate of Return	-20%	-15%	-12%	-9%
	Payback Period (years)	10.10	8.27	7.25	6.56
SOFC (without waste heat recovery)	100 kW				
	Internal Rate of Return	-19%	-13%	-9%	-6%
	Payback Period (years)	9.75	7.70	6.75	6.13
	250 kW				
	Internal Rate of Return	-13%	-7%	-3%	0%
	Payback Period (years)	7.68	6.25	5.49	4.97
SOFC (with waste heat recovery heating)	100 kW				
	Internal Rate of Return	-16%	-11%	-8%	-5%
	Payback Period (years)	8.76	7.22	6.37	5.83
	250 kW				
	Internal Rate of Return	5%	12%	18%	22%
	Payback Period (years)	4.30	3.51	3.09	2.80

Some states have natural gas to electric price ratios which are significantly disadvantageous to fuel cell installations, particularly for commercial customers. These ratios are really another way of looking at utility spark spread<sup>15</sup>, the margin of electricity pricing vs. price of fuel to produce the energy. Generally, the price of electricity is high enough to yield a small amount of savings from a relatively efficient fuel cell system, such as the 30% (PEM) and 40% (SOFC) efficient systems evaluated in this study. However, in some states (for example, Texas and Illinois), the commercial price for natural gas is greater than 30% of the price for commercial electricity. This commodity cost structure is such that the cost of electricity generated by a 30% efficient PEM fuel cell is greater than the price of electricity from the utility, so no yearly savings are possible. The higher efficiency of the SOFC system may still show yearly savings; but,

<sup>15</sup> "An introduction to spark spreads," Energy Information Administration, last modified February 8, 2013, <https://www.eia.gov/todayinenergy/detail.cfm?id=9911>.

the overall return will be low. However, “industrial” gas prices in these states may yield a potentially profitable price margin. Table 9-9 compares natural gas prices vs. electricity prices for four states and the overall U.S. average. Table 9-9 highlights the importance of considering the price structure when evaluating the installation of a fuel cell system. The states with red ratios indicate that PEM systems without heat recovery cannot be profitable without allowance for grid outage cost avoidance. Note that natural gas prices drop significantly in Texas under industrial rules, while electricity does not drop as much, moving Texas into the realm attractive for fuel cells. New York, on the other hand, shows the opposite effect, with industrial electric rates dropping more than industrial gas rates and potentially shifting New York away from an attractive return position for at least PEM fuel cells.

**Table 9-9: Direct Utility Price Comparison<sup>2</sup>**

	Commercial Prices					Industrial Prices			
	US	CA	IL	NY	TX	CA	IL	NY	TX
NG (\$/kW-hr)	0.0279	0.0277	0.0308	0.0232	0.0253	0.0221	0.0198	0.0225	0.0110
Electricity (\$/kW-hr)	0.1077	0.1729	0.0934	0.1555	0.0788	0.1388	0.0666	0.0620	0.0580
\$NG/\$Elect. (%)	26%	16%	33%	15%	32%	16%	30%	36%	19%

Using the 100-kW SOFC system with waste heat recovery (at the 100 units per year production level) as an example, Figure 9-1 provides a heat map for IRR indicating favorable utility prices for fuel cell CHP applications. Due to the significant impact of electricity costs, the IRR is more vertically aligned. For example, any location with electricity cost at or below \$0.08 per kWh will have a negative IRR regardless of natural gas pricing. However, at any gas price there is the potential to yield favorable returns, provided electricity costs for that area are relatively high compared to the natural gas price.

		IRR after 5 years												
		Electricity Cost (\$/kWh)												
		\$0.060	\$0.070	\$0.080	\$0.090	\$0.100	\$0.110	\$0.120	\$0.130	\$0.140	\$0.150	\$0.160	\$0.170	\$0.180
Natural Gas Cost (\$/kWh HHV)	\$0.010	-13%	-7%	-1%	4%	8%	13%	17%	21%	25%	29%	33%	37%	40%
	\$0.012	-14%	-8%	-3%	2%	7%	12%	16%	20%	24%	28%	32%	36%	39%
	\$0.014	-16%	-10%	-4%	1%	6%	10%	15%	19%	23%	27%	31%	35%	38%
	\$0.016	-18%	-11%	-5%	0%	5%	9%	14%	18%	22%	26%	30%	34%	38%
	\$0.018	-19%	-13%	-7%	-1%	4%	8%	13%	17%	21%	25%	29%	33%	37%
	\$0.020	-21%	-14%	-8%	-3%	2%	7%	12%	16%	20%	24%	28%	32%	36%
	\$0.022	-23%	-16%	-10%	-4%	1%	6%	10%	15%	19%	23%	27%	31%	35%
	\$0.024	-25%	-18%	-11%	-5%	0%	5%	9%	14%	18%	22%	26%	30%	34%
	\$0.026	-27%	-19%	-13%	-7%	-1%	4%	8%	13%	17%	21%	25%	29%	33%
	\$0.028	-29%	-21%	-14%	-8%	-3%	2%	7%	12%	16%	20%	24%	28%	32%
	\$0.030	-32%	-23%	-16%	-10%	-4%	1%	6%	10%	15%	19%	23%	27%	31%
\$0.032	-34%	-25%	-18%	-11%	-5%	0%	5%	9%	14%	18%	22%	26%	30%	

*Figure 9-1. IRR heat map for a 100-kW SOFC system with waste heat recovery at various costs of electricity and natural gas.*

Figure 9-2 uses the same example to illustrate the payback period in years based on a range of utility costs.

		Payback Period in years												
		Electricity Cost (\$/kWh)												
		\$0.060	\$0.070	\$0.080	\$0.090	\$0.100	\$0.110	\$0.120	\$0.130	\$0.140	\$0.150	\$0.160	\$0.170	\$0.180
Natural Gas Cost (\$/kWh HHV)	\$0.010	7.65	6.21	5.23	4.51	3.97	3.55	3.20	2.92	2.68	2.48	2.31	2.16	2.03
	\$0.012	8.11	6.52	5.44	4.67	4.09	3.64	3.28	2.99	2.74	2.53	2.35	2.19	2.06
	\$0.014	8.65	6.85	5.68	4.84	4.23	3.75	3.37	3.05	2.80	2.58	2.39	2.23	2.09
	\$0.016	9.25	7.23	5.93	5.03	4.36	3.86	3.45	3.13	2.86	2.63	2.44	2.27	2.12
	\$0.018	9.95	7.65	6.21	5.23	4.51	3.97	3.55	3.20	2.92	2.68	2.48	2.31	2.16
	\$0.020	10.75	8.11	6.52	5.44	4.67	4.09	3.64	3.28	2.99	2.74	2.53	2.35	2.19
	\$0.022	11.71	8.65	6.85	5.68	4.84	4.23	3.75	3.37	3.05	2.80	2.58	2.39	2.23
	\$0.024	12.84	9.25	7.23	5.93	5.03	4.36	3.86	3.45	3.13	2.86	2.63	2.44	2.27
	\$0.026	14.23	9.95	7.65	6.21	5.23	4.51	3.97	3.55	3.20	2.92	2.68	2.48	2.31
	\$0.028	15.94	10.75	8.11	6.52	5.44	4.67	4.09	3.64	3.28	2.99	2.74	2.53	2.35
	\$0.030	18.13	11.71	8.65	6.85	5.68	4.84	4.23	3.75	3.37	3.05	2.80	2.58	2.39
	\$0.032	21.00	12.84	9.25	7.23	5.93	5.03	4.36	3.86	3.45	3.13	2.86	2.63	2.44

Figure 9-2. Payback heat map for a 100-kW SOFC system with waste heat recovery at various costs of electricity and natural gas.

We chose to use commercial rates for the comparison since the scenarios evaluated for this analysis would probably be classified as commercial, rather than industrial. If the site has, or can negotiate, industrial gas rates, the financial benefits may be improved in those states with a notable difference between commercial and industrial rates. Additionally, our analysis only considered state average rates. Local gas and electric rates may vary significantly from state averages so that most installations will need to perform a similar economic analysis before investing in fuel cell systems.

## 9.4 Conclusions

The initial capital cost for PEM systems inhibits, but does not eliminate, development of attractive investment opportunities for CHP systems. The addition of waste heat recovery, for applications where the heat is useful, improves the ROI significantly. An SOFC systems that can achieve 6 year life (~50,000 hours operation) would provide attractive returns, particularly for sites with a use for heat. Lifecycle cost analysis depends significantly on local electric and gas rates and the rate structure associated with certain applications. Some states regulate industrial prices differently than commercial prices for both gas and electric. Although not discussed here, we observed that shifting from commercial to industrial utility rates could significantly shift the life cycle cost analysis results. Specifically, the industrial rates for gas and electric in New York result in less favorable return on fuel cell installations because the industrial electric rates drop more than the industrial gas rates in the switch from commercial to industrial rates.

# 10.0. Conclusions

## 10.1 System Cost Summary

Figures 10-1 and 10-2 show the summary pie charts for 1,000 units per year, repeated from Section 7, which emphasize that BOP costs dominate the final cost for both PEM and SOFC systems. The stack represents a maximum of 31% of the total system cost, with the stack contributing less cost as a percent



of total cost for most system production volumes. Within the BOP costs, the major contributor for all systems is the power electronics. Heat recovery and fuel processing contribute significantly to the PEM system, but less so to the SOFC system owing to the simpler BOP required for the SOFC system. For this size of equipment, the power electronics would represent an even greater portion of the cost if a more conventional DC/DC converter and DC/AC inverter were used to accommodate batteries for off-grid operation, rather than the hybrid inverter used in this analysis. The reduced cost of solar PV power is driving progress for grid-connected DC/AC inverters that can interface with storage. That progress will benefit fuel cell systems, with active management of fuel cell power (available 24 hours/day) eventually bringing the cost of this hardware below that for solar systems. Heat exchanger costs represent a significant area for evaluation and future cost reduction; particularly for the high-temperature heat exchangers that are required for both SOFC and PEM systems.

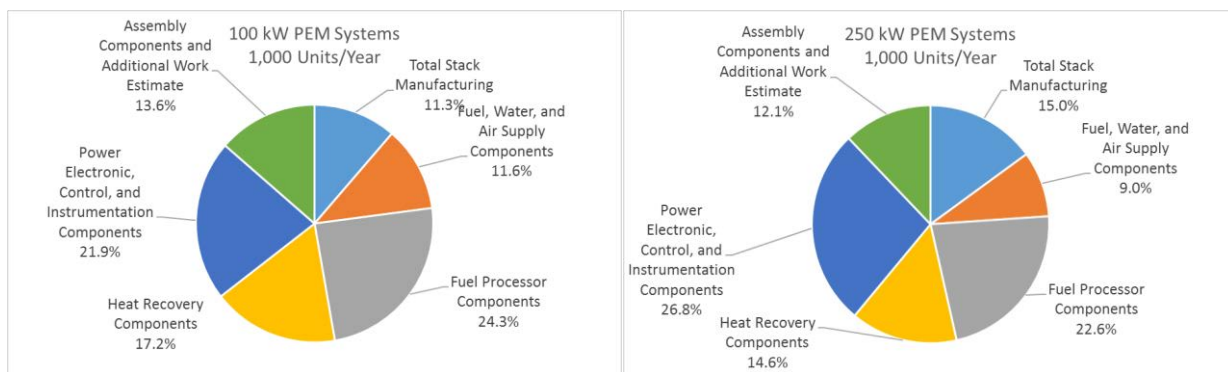


Figure 10-1. PEM system costs at 1,000 units per year.

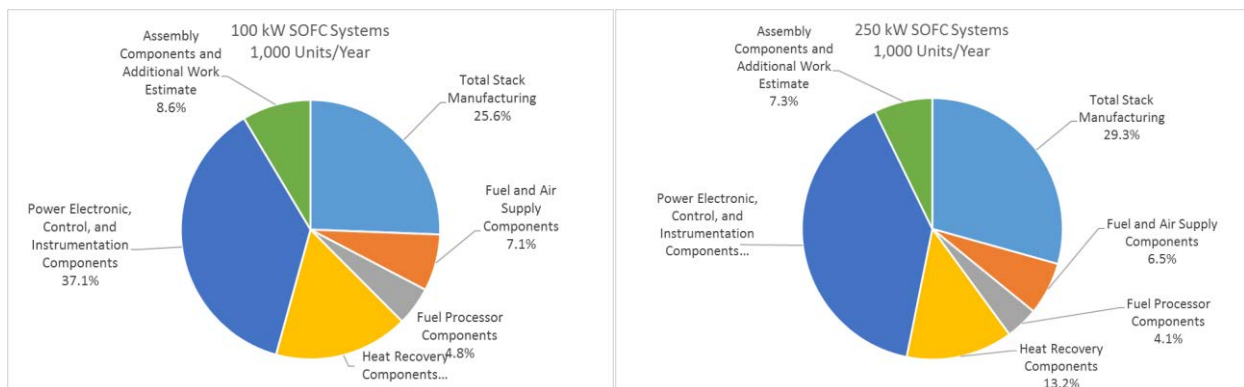


Figure 10-2. SOFC system costs at 1,000 units per year.

An important feature of primary power and CHP systems is that the space and weight requirements are less stringent than they are for mobile applications (e.g., material handling equipment [MHE]), therefore requiring less customization and enabling the use of more commercially available hardware and production equipment. However, at this early stage of system design, the industrial-grade components used may be oversized for the application, forcing costs up. Cost reduction efforts at the 100- and 250-kW scales must be mindful of codes and standards for industrial equipment and of local siting and permitting requirements which may apply at this scale—a topic not explored in this study.

Because of the number of stacks to be produced for each system (2 to 10), most stack fabrication processes are assumed to be brought in-house along with final assembly and testing. The calculation for determining whether to outsource versus produce in-house is shown in Appendix A-1. This ensures that the capital investment, once made, will be distributed across an appropriate number of systems.

The total costs for each size at two representative production volumes are shown in Tables 10-1 and 10-2. A sales markup of 50% was integrated into the overall cost and is called out separately. These tables emphasize the cost difference of the PEM and SOFC systems on an installed cost-per-kilowatt basis. PEM systems cost 37% to 65% more than SOFC. For continuous-power applications where the cyclic life concerns for SOFC are not realized, SOFC clearly appears to be the preferred choice, having both higher efficiency and lower initial cost. However, for applications where either operational characteristics or diurnal spark spread suggest turning down or turning off the fuel cell system, the PEM system may be the preferred choice. Applications with significant use for the waste heat may also favor PEM. As shown in Section 9, PEM systems may offer an attractive value proposition, so the choice between these technologies will be site-specific with SOFC generally being preferred when applicable. This is consistent with the expanding installed base of fuel cell systems designed for large-capacity (400 kW and greater) power offset and back-up power, like those being installed by Bloom Energy, for example. The life cycle cost analysis of Section 9 uses the **highlighted values** in Tables 10-1 and 10-2 for the 100-kW and 250-kW systems.

**Table 10-1. PEM System Cost**

Description	100 kW 1,000 Units/Yr	100 kW 10,000 Units/Yr	250 kW 1,000 Units/Yr	250 kW 10,000 Units/Yr
Total Stack Manufacturing, Testing & Conditioning Costs	\$34,850	\$22,315	\$20,078	\$19,856
Fuel, Water, and Air Supply Components	\$25,832	\$22,857	\$20,894	\$19,622
Fuel Processor Components	\$55,616	\$48,005	\$43,629	\$41,395
Heat Recovery Components	\$37,440	\$33,994	\$30,868	\$29,466
Power Electronic, Control, and Instrumentation Components	\$52,536	\$43,221	\$35,258	\$29,859
Assembly Components and Additional Work Estimate	\$29,500	\$26,790	\$24,080	\$21,705
Total system cost, pre-markup	\$235,774	\$197,183	\$174,807	\$161,904
System cost per kW <sub>net</sub> , pre-markup	\$2,358	\$1,972	\$1,748	\$1,619
Sales markup	50%	50%	50%	50%
Total system cost, with markup	\$353,661	\$295,774	\$262,210	\$242,856
System cost per kW <sub>net</sub> , with markup	\$3,537	\$2,958	\$2,622	\$2,429

**Table 10-2. SOFC System Cost**

Description	100 kW 1,000 Units/Yr	100 kW 10,000 Units/Yr	250 kW 1,000 Units/Yr	250 kW 10,000 Units/Yr
Total Stack Manufacturing, Testing & Conditioning Costs	\$44,555	\$30,081	\$27,017	\$26,746
Fuel and Air Supply Components	\$10,108	\$8,306	\$7,465	\$6,956
Fuel Processor Components	\$8,245	\$5,693	\$5,247	\$4,962
Heat Recovery Components	\$21,057	\$19,698	\$18,430	\$17,621
Power Electronic, Control, and Instrumentation Components	\$52,988	\$43,627	\$35,622	\$30,213
Assembly Components and Additional Work Estimate	\$11,105	\$10,080	\$9,055	\$8,175
Total system cost, pre-markup	\$148,058	\$117,486	\$102,835	\$94,673
System cost per kW <sub>net</sub> , pre-markup	\$1,481	\$1,175	\$1,028	\$947
Sales markup	50%	50%	50%	50%
Total system cost, with markup	\$222,087	\$176,229	\$154,252	\$142,009
System cost per kW <sub>net</sub> , with markup	\$2,221	\$1,762	\$1,543	\$1,420

Figures 10-3 and 10-4 show the after-markup cost per  $\text{kW}_{\text{electrical}}$  and for  $\text{kW}_{\text{total}}$  for PEM and SOFC systems assuming the waste heat is used for space, water, or process heating. Figure 10-3 considers only the electrical power delivered. Figure 10-4 includes the heat delivered to the CHP system; the installation costs for heat are the same as given in Section 9. The heat delivered may have more or less value, depending on how the water would otherwise have been heated (natural gas fired or electric heat pump water heater). A comparison of Figure 10-3 with Figure 10-4 shows a marked advantage of using the waste heat. However, some applications will not benefit directly from waste heat, having no use for hot water, space heating, or process heat. Data centers are an example of an application that requires cooling, essentially to remove the heat generated by the power supplied to the servers. To assess the potential for this application, we assumed that an absorption chiller would be operated with the waste heat from the fuel cell system. The heat collected from the fuel processor increases the temperature of the PEM system waste heat enabling its use in absorption chiller applications. The SOFC system clearly has sufficient temperature but has a lower net heat available because of the higher electrical efficiency. Figure 10-5 includes the cost per installed  $\text{kW}_{\text{total}}$  assuming that the waste heat is used for cooling. The estimate of cooling capacity and associated equipment cost was based on an online calculator<sup>16</sup> for a specific size and type of cooling. The available options were not optimized but provide some guidance on the possibilities. For both PEM and SOFC the chiller cost is a significant adder to the initial installed cost. The absorption chiller cost used in the calculations is discounted from the on-line estimate by 25%, for the SOFC systems on the assumption that the higher temperature would enable reduced system size. Figure 10-5 shows an improvement in the installed cost of fuel cell power compared to systems without waste heat recovery and some shift in the relative cost of total power provided between the two technologies. Figures 10-3, 10-4, and 10-5 show that installations with a use for the waste heat are the most attractive for fuel cell systems.

When considering the value of the heat delivered in terms of natural gas and electric costs avoided, the economic benefit of a continuously operating system versus a back-up power system becomes apparent if the difference between electric power and natural gas cost on a comparable energy basis (the “spark spread”) is characterized by electric prices higher than gas prices by at least \$0.10/kWh. A particular advantage of a fuel cell system over other alternatives (e.g., a natural gas reciprocating engine or gas turbine) is longer expected life in continuous operation coupled with simple maintenance requirements. Very low noise and emissions enable siting in urban and environmentally sensitive areas that would not allow most lower-cost power generation options.

---

<sup>16</sup> <http://www.ppiway.com/chillerperformance/index.html> (accessed on 11-6-2015, assuming model C-10 and temperatures/flows from the ChemCad system models.)

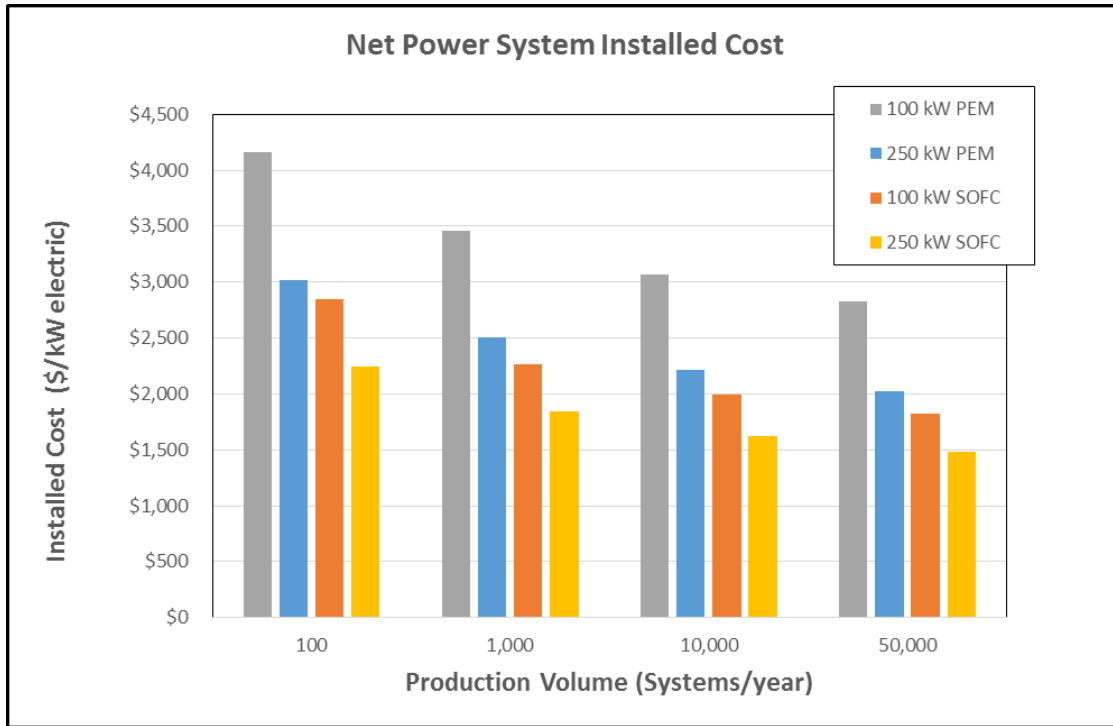


Figure 10-3. Net system installed cost (after mark-up).

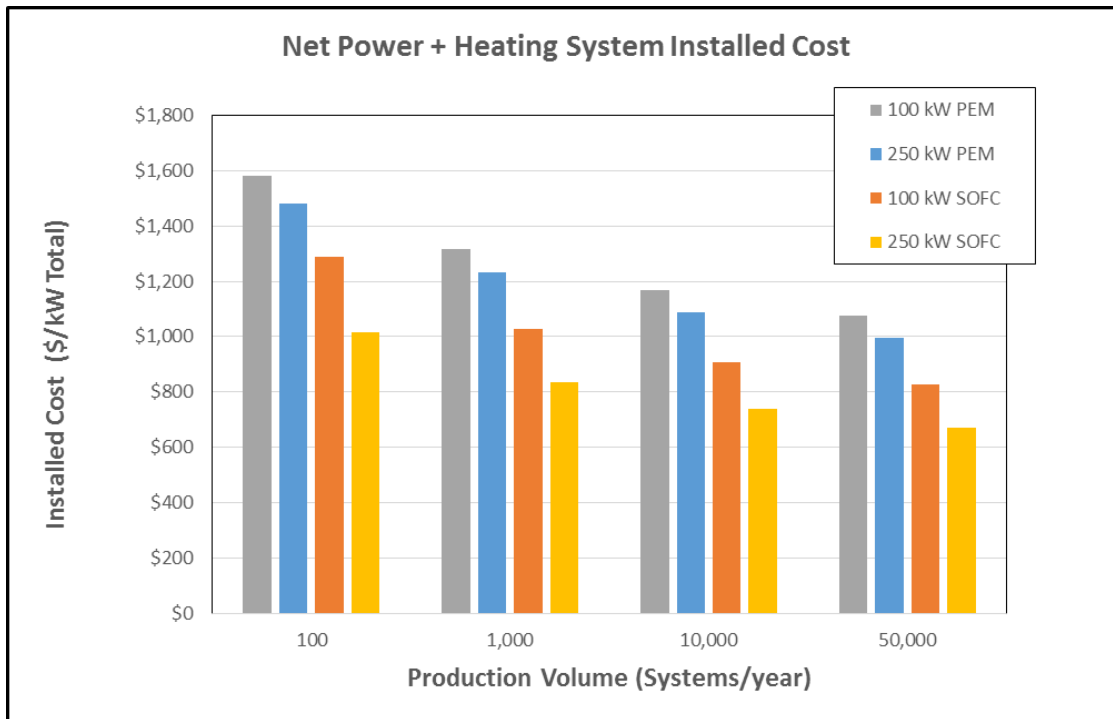


Figure 10-4. Final system cost of energy delivered (thermal and electric).

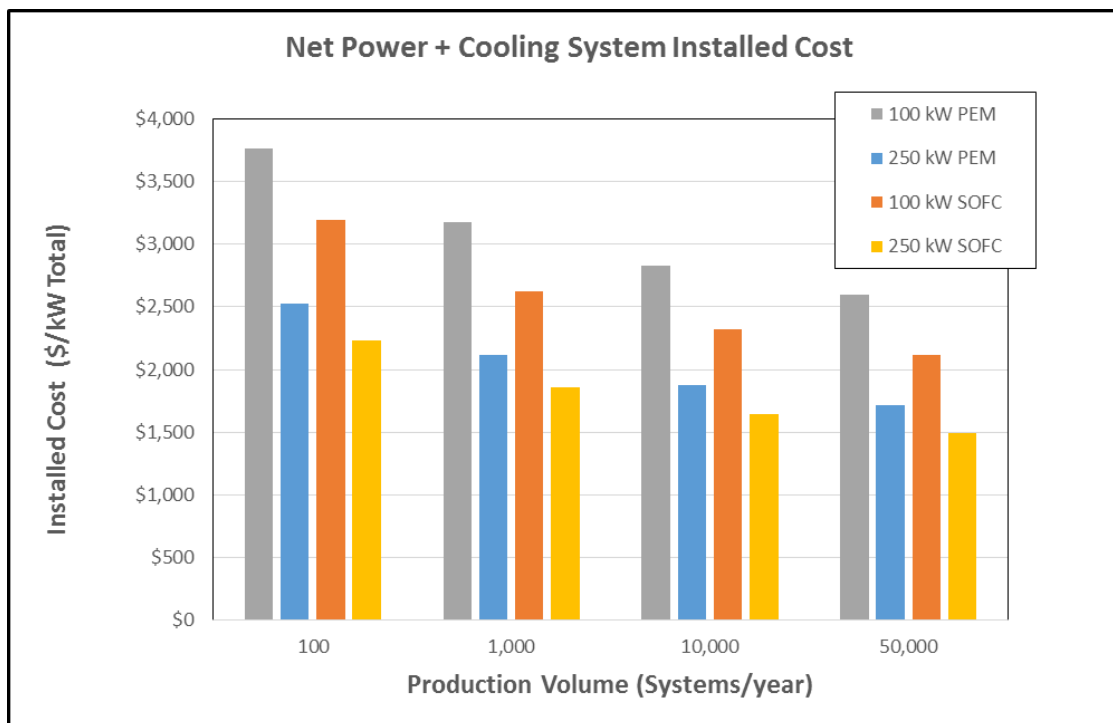


Figure 10-5. Total system cost of energy delivered including an absorption chiller.

## 10.2 Value Proposition

At locations where natural gas is inexpensive and electricity is expensive, the installation of a fuel cell primary power and/or CHP system offers attractive ROIs. Table 10-3, summarized from Table 9-5, shows the rates of return possible for various fuel cell system configurations.

Table 10-3. IRR in California Based on Average Commercial Rates

Internal Rate of Return for Commercial Installations in California					
Fuel Cell System Configuration		100 Units/Yr	1,000 Units/Yr	10,000 Units/Yr	50,000 Units/Yr
PEM (without waste heat recovery)	100 kW	-10%	-2%	4%	7%
	250 kW	1%	10%	17%	22%
PEM (with waste heat recovery for heating)	100 kW	5%	16%	23%	27%
	250 kW	12%	23%	31%	36%
SOFC (without waste heat recovery)	100 kW	15%	26%	33%	38%
	250 kW	26%	38%	45%	52%
SOFC (with waste heat recovery for heating)	100 kW	28%	42%	50%	56%
	250 kW	38%	51%	60%	67%

These returns/payback values do not incorporate any adjustment for environmental externalities or the value of continued operation during grid outages. For some businesses, the value of maintained operations during an extended grid outage may exceed the total system cost (e.g., avoided frozen food loss from a grocery store, or business loss for an on-line retailer). To the extent that electricity can be generated on-site for less than grid-purchased electricity, the payback and IRR become very attractive. Some sites in restrictive areas, like southern California, may be amenable only to fuel cell primary power and CHP installations because of the relatively low environmental footprint of fuel cells when compared to the available continuous-operation competitive options.

Although the investment appears attractive for many locations, there is risk in making the investment until fuel cell systems have been demonstrated to consistently achieve 40,000 hours of trouble-free operation in real-world applications. SOFC systems (typically somewhat higher capacity) are currently being installed in east and west coast locations. However, the financial arrangements, while proprietary, seem to provide some level of protection to the business. The designs apparently utilize a smaller stack configuration than used for this analysis, increasing system cost due to redundancy but also allowing a certain percentage of stack failures before system routine maintenance and repair are necessary. The analysis we have undertaken assumes that larger stacks can achieve the necessary lifetimes and therefore expand the opportunities for fuel cell system installations through lower system first cost.

### 10.3 Sensitivity and Future Market Impact

The sensitivity analysis indicates that a 50% change in the cost of platinum impacts PEM systems by less than 4%; SOFC systems are less sensitive to commodity material costs. Section 8 indicates that some factors (such as current density and platinum loading, which are likely to improve in the future) will have similar or greater overall cost benefits. Both system technologies show significant sensitivity to power electronics cost, suggesting that an additional, more detailed analysis of the core costs of power electronics would be beneficial. The PEM system in particular is affected by the cost of heat exchangers, placing it at a disadvantage to SOFC from a cost/kW-installed basis. Both the SOFC and PEM systems would benefit notably from improvements in heat exchanger cost.

The choice to define a dual-use system capable of both grid-connected and off-grid operation increases power electronics cost because batteries must be incorporated and coordinated with the fuel cell to permit safe and effective transient response. Requiring that the system operate with or without an applied thermal heat load also increases system cost slightly. For PEM systems, a full load radiator is required. For SOFC systems, high-temperature bypass valves are required, and provisions must be made for safe discharge of high-temperature combustion gas when a CHP heat load is not present. The components may not be appropriate for all applications, and some cost could be eliminated by assuming that the system would only operate when the grid is available. However, with a beneficial spark spread, the back-up power capable system pays for itself in a few years. For areas without a beneficial spark spread, the site-specific life cycle cost analysis should include the value of avoided losses associated with typical grid outage conditions. Grid outage operation will be more valuable in areas with lower grid reliability.

As fuel-cell-powered MHE increases market penetration and as automotive use of fuel cells increases, we expect that the CHP/primary power market will continue to develop, initially for areas with conducive utility pricing and critical grid outage conditions and then to applications where the waste heat can add sufficient value to provide acceptable payback times. We note, however, that the MHE and automotive developments only indirectly impact SOFC stationary applications because those markets require load-following, high-turn-down systems. Power electronics developments for MHE and automotive systems assist in reducing fuel cell system cost. Development of power electronics for the solar power industry may also provide future cost savings for fuel cell systems.

## Appendix A-1: Machine Rate with Make-Buy Calculations

The basic machine rate equation from James et al. (2014)<sup>17</sup> is:

$$R_M = C_{CAP} \frac{(F_{Inst} * F_{Cap} + F_{Maint} + F_{Misc})}{T_R + T_S} + C_P * P + C_L * L$$

where:

$$F_{Cap} = \left[ \frac{R_I(1 + R_I)^{T_L}}{(1 + R_I)^{T_L} - 1} \right] - \frac{R_{Tax}}{T_L} \Bigg/ [1 - R_{Tax}]$$

To calculate a baseline production station cost, we assume that the station is capable of operating three 8-hour shifts per day for 250 days per year. Therefore, total available production time for both operation and setup ( $T_R + T_S$ ) at 100% utilization is 6,000 hours per year. The actual production time based on utilization ( $U$ ) can be calculated as:

$$(TR + TS) = 6,000 * U$$

Input assumptions based on our previous work and on the assumptions shown in Table 3 of the James et al. paper<sup>17</sup> results in the following:

Expected equipment lifetime	20	yrs
Discount rate	7.00%	
Corporate income tax rate	38.90%	
Installation cost factor	1.4	
Annual maintenance cost factor	6.00%	of $C_{Cap}$
Annual miscellaneous cost factor	12.00%	of $C_{Cap}$
Energy cost	\$0.07	/kW-hr

$F_{Cap}$  is calculated as:

$$F_{Cap} = \left[ \frac{0.07(1 + 0.07)^{20}}{(1 + 0.07)^{20} - 1} \right] - \frac{0.389}{20} \Bigg/ [1 - 0.389] = 0.122656$$

Total capital cost over the assumed 20-year production life is calculated as:

$$C_{cap} = \sum_{i=1}^n N_i C_i \left( \left[ \frac{20}{L_i} \right] \right)$$

<sup>17</sup> James, B.D., Spisak, A.B., and Colella, W.G. 2014. Design for Manufacturing and Assembly (DFMA) Cost Estimates of Transportation Fuel Cell Systems, *ASME Journal of Manufacturing Science and Engineering*, New York, NY: ASME, Volume 136, Issue 2, p. 024503.



where:

$n$  = unique pieces of equipment making up production station

$N_i$  = number of item  $i$  required for production station

$C_i$  = capital cost of item  $i$

$L_i$  = expected life of item  $i$

As an example, the bipolar plate compression molding station consists of the following items:

		Cost	Units Per Station	Expected Life
Bipolar Plate Compression Molding				
1,000 ton fast-acting press	Wabash 1000H-48	\$650,000	1	20
Heated platens, 15"x12", 4.5 kW, controller	Custom Engineering	\$12,500	1	10
Arbor or hand-operated hydraulic pre-mold press	Central Hydraulics 6-ton bench-top press w/ pump	\$400	1	20
Electronic scale, industrial, gram resolution	Mettler-Toledo WM3002	\$6,000	1	10
Small industrial oven	Grieve NBS-400	\$1,000	1	20

Applying this information to the above equation yields the following:

	$N_i$	$C_i$	$L_i$	$C_{Cap}$
Bipolar Plate Compression Molding				
1,000-ton fast-acting press	1	\$650,000	20	\$600,000
Heated platens, 15"x12", 4.5 kW, controller	1	\$12,500	10	\$25,000
Arbor or hand-operated hydraulic pre-mold press	1	\$400	20	\$400
Electronic scale, industrial, gram resolution	1	\$6,000	10	\$12,000
Small industrial oven	1	\$1,000	20	\$1,000
Total				\$638,400

Energy costs to operate the station are a function of the power required to operate each piece of equipment. For cost estimating purposes, the total power draw of the production station can be calculated in similar fashion to the total capital cost as follows:

$$P = \sum_{i=1}^n N_i V_i A_i D_i$$

where:

n = unique pieces of equipment making up production station

N<sub>i</sub> = number of item i required for production station

V<sub>i</sub> = voltage supplied to item i

A<sub>i</sub> = current draw of item i

D<sub>i</sub> = duty cycle of item i

This yields the following:

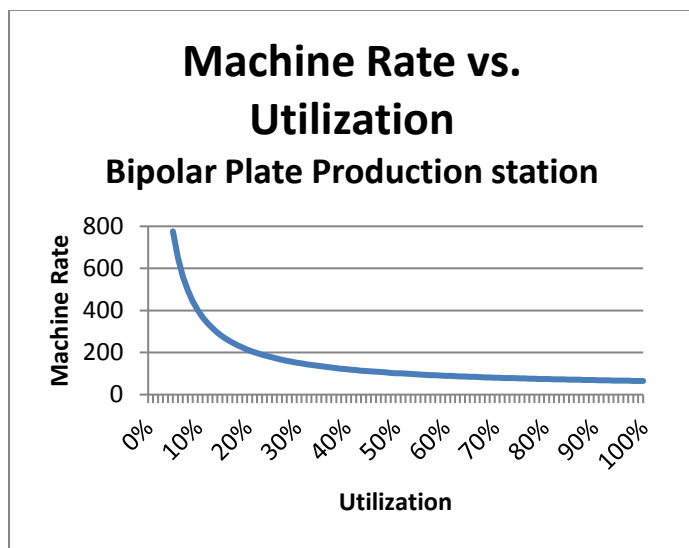
	N <sub>i</sub>	V <sub>i</sub>	A <sub>i</sub>	D <sub>i</sub>	P
Bipolar Plate Compression Molding					
1,000-ton fast-acting press	1	460	150	96%	66.24
Heated platens, 15"x12", 4.5 kW, controller	1	230	25	25%	1.44
Arbor or hand-operated hydraulic pre-mold press	1	0	0	10%	0.00
Electronic scale, industrial, gram resolution	1	120	1	100%	0.12
Small industrial oven	1	230	20	20%	0.92
Total					68.72

The machine rate is calculated as:

$$R_M = \$638,400 * \frac{(1.4 * 0.122656 + 0.06 + 0.12)}{6000 * U} + (0.07 * 68.72) + (45.00 * 0.5) = \frac{\$37.42}{U} + 27.31$$

where: U > 0

Graphically:



Applying the above to the remaining stack production stations yields the following:

PEM Production Station	Baseline Cost	Power Cost (/hr)	Labor Cost (/hr)	100% Utilization Machine Rate
Bipolar Plate Compression Molding	\$638,400	\$1.50	\$45.00	\$64.70
Platinum Catalyst Preparation	\$37,000	\$0.01	\$9.00	\$11.18
Slot Die Coating	\$661,800	\$0.90	\$22.50	\$62.20
Decal Transfer	\$58,400	\$0.74	\$22.50	\$26.66
GDL Slit and Cut	\$87,700	\$0.45	\$22.50	\$28.09
MEA Hot Pressing	\$499,400	\$0.80	\$22.50	\$52.58
Die Cutting	\$125,000	\$0.32	\$22.50	\$30.15
Gasket Injection Molding	\$48,000	\$0.72	\$45.00	\$26.04
End Plates	\$416,000	\$6.50	\$90.00	\$116.49
Stack Assembly	\$1,310	\$0.00	\$45.00	\$45.08
Testing and Conditioning	\$41,300	\$0.37	\$15.00	\$17.64

SOFC Production Station	Baseline Cost	Power Cost (/hr)	Labor Cost (/hr)	100% Utilization Machine Rate
High Volume Slurry Production	\$80,000	\$2.41	\$4.50	\$11.68
Low Volume Slurry Production	\$60,000	\$1.03	\$4.50	\$9.04
Tape Casting	\$343,600	\$1.06	\$67.50	\$88.70
Anode Pressing	\$58,400	\$0.74	\$22.50	\$26.66
Anode Blanking	\$125,000	\$0.00	\$22.50	\$29.83
Screen Printing	\$66,612	\$0.81	\$45.00	\$49.71
Kiln Firing	\$393,000	\$16.10	\$15.00	\$53.99
Sintering	\$500,000	\$16.10	\$15.00	\$60.26
Laser Cutting	\$35,000	\$9.26	\$15.00	\$33.81
Sheet Metal Stamping	\$150,000	\$1.61	\$15.00	\$55.40
Interconnect	\$365,860	\$2.98	\$90.00	\$114.43
End Plates	\$416,000	\$1.37	\$45.00	\$120.89
Sealing	\$27,500	\$1.59	\$45.00	\$48.21
Stack Assembly	\$550	\$0.00	\$45.00	\$45.03
Stack Brazing	\$500,000	\$16.10	\$15.00	\$60.26
Testing and Conditioning	\$41,300	\$0.37	\$15.00	\$17.64

### A-1.1 Make vs Buy Decision

As indicated in James et al. (2014)<sup>18</sup>, at low utilizations, job shops may make parts at a lower cost by pooling orders. Additional job shop costs include the profit charged by the job shop, and any overhead incurred by the manufacturer as a result of contract administration, shipping, and incoming parts inspection. Assuming a 65% minimum machine utilization and 40% markup for profit plus overhead, the job shop maximum machine rate becomes:

$$R_{Mjs} = 1.4 * \left[ C_{CAP} \frac{(F_{Inst} * F_{Cap} + F_{Maint} + F_{Misc})}{6000 * 0.65} + C_P * P + C_L * L \right]$$

Assuming labor, energy, and capital costs are the same, the maximum job shop machine rate for the bipolar plate station above would be:

$$R_{Mjsmax} = 1.4 * \left[ \frac{\$37.42}{0.65} + \$27.31 \right] = \$118.83$$

<sup>18</sup> B.D. James, A.B. Spisak, and W.G. Colella. 2014. Design for Manufacturing and Assembly (DFMA) Cost Estimates of Transportation Fuel Cell Systems, *ASME Journal of Manufacturing Science and Engineering*, New York, NY: ASME, Volume 136, Issue 2, p. 024503.

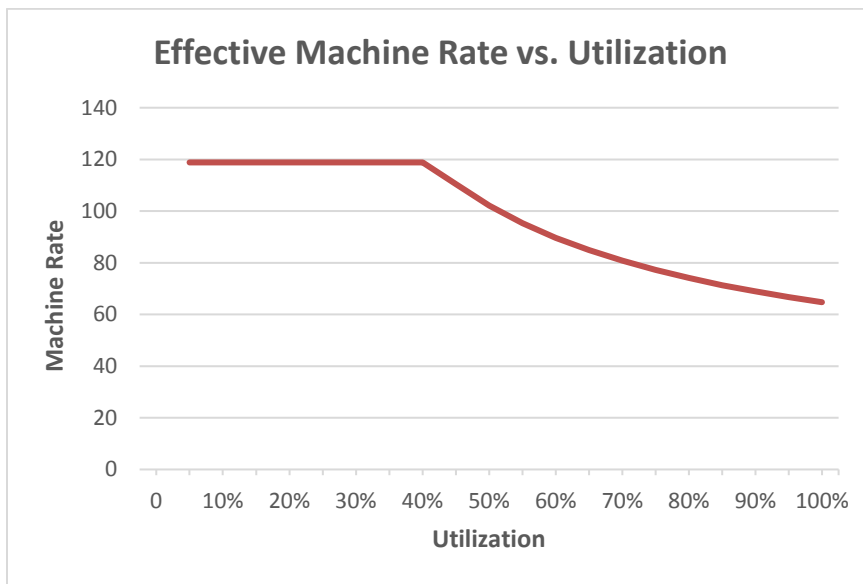
To achieve an equivalent in-house rate, the minimum utilization is:

$$R_{Mih} = \left[ \frac{\$37.42}{\frac{\text{hour}}{U}} + \$27.31 \right] = \$118.83$$

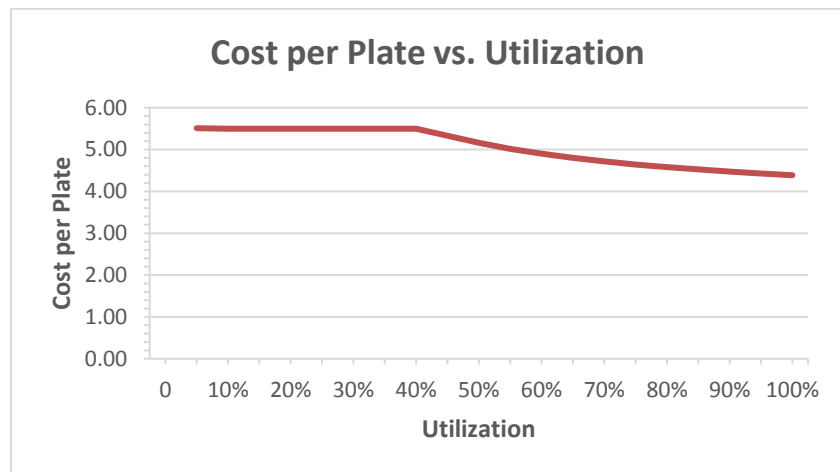
$$U = \frac{\$37.42}{(\$118.83 - \$27.31)} = 0.409$$

In other words, for utilization rates of less than 40.9%, bipolar plate manufacturing should be sub-contracted to a job shop instead of incurring the costs of manufacturing the plates in house.

It should be noted that the make-buy strategy outlined above results in a discontinuity in the machine rate curve (and, by extension, the total cost curve) since the job shop machine rate is unchanged up to the critical utilization rate of 40.9%, as shown below.



This can be further illustrated by estimating the production per unit for bipolar plates. Each plate contains 0.691 kg of BMC940 composite. Material cost for a purchase quantity Q is computed using the formula presented in Appendix A-2. The throughput of the process is 50 parts/hour, yielding a maximum annual capacity of 300,000 plates per year, and requires 0.5 operator time per machine. Using the above equations, the bipolar plate unit cost as a function of utilization is shown below:



Where multiple processes are closely coupled due to timing or handling constraints, the make-buy decision needs to consider the overall cost of the entire process train and not just the cost of individual processes within the train. In cases like these, the entire cost of the process train needs to be computed for both in-house and outsourced manufacturing costs using the following formula:

$$C_m = \sum_{i=1}^n R_{m_i} T_{m_i}$$

where:

$C_m$  = process train manufacturing cost

$R_{m_i}$  = machine rate for process i

$T_{m_i}$  = machine time for process i

n = number of processes

A similar situation arises when a single machine can be used for multiple processes, such as a slot die coater that can be used for both anode and cathode catalyst deposition. In this case, the utilization used in the machine rate calculation is total time required to complete all the processes divided by the total machine time available:

$$U_m = \frac{\sum_{i=1}^n T_{p_i}}{T_R + T_S}$$

where:

$U_m$  = utilization of machine m

$T_{pi}$  = time to complete process i

$T_R$  = total annual run time

$T_S$  = total annual setup time

n = number of processes using machine m

## Appendix A-2: Material Cost Learning Curve Calculations

### A-2.1 Background

In general, material cost on a per-unit basis (e.g. per kilogram, per square meter) decreases with increasing purchase volumes, due primarily to the manufacturer's ability to produce larger volumes of material from a single production run setup. It has been noted in previous work that material cost estimates at various discrete purchase volumes could be estimated for the intermediate volumes using a learning curve analysis.

From the *Cost Estimator's Reference Manual* (1995),<sup>19</sup> the general learning curve equation is:

$$Y = AX^b$$

where:

Y = time or cost per cycle or unit

A = time or cost for first cycle or unit

X = number of cycles or units

b =  $\log(m)/\log(2)$

m = slope of learning curve

If the material production is "learned" after 10,000 units (i.e., no substantial discounts are available for higher volume purchases), then the cost Y is the cost of the 10,000<sup>th</sup> unit.

### A-2.2 Preliminary Analysis

Where possible, quotes were obtained from both domestic and international suppliers for the materials. Other material costs were obtained from previous third-party fuel cell manufacturing analysis reports.

Some materials, such as the silicone gasket material, are considered commodity items for which manufacturing processes are well established and supplies are high enough to support most available demand. One supplier provided a quote for liquid silicone material of \$7.00 to \$7.50 per pound (\$15.40 to \$16.50 per kilogram) for quantities ranging from 250 to 25,000 pounds.

For these materials, the cost curve is very flat, which means the value of m in the learning curve equation is high. Iteration using the costs above led to a value of m=0.99, which results in:

$$b = \log(0.99)/\log(2) = -0.0154$$

Using a learned cost of \$15.40/kg for a volume of 55,000 kg, then the cost of the first unit is:

$$A = Y / X^b = 15.40 / 55,000^{(-0.0145)} = \$18.04$$

For a purchase of 250 kg of material, the calculated cost per unit is:

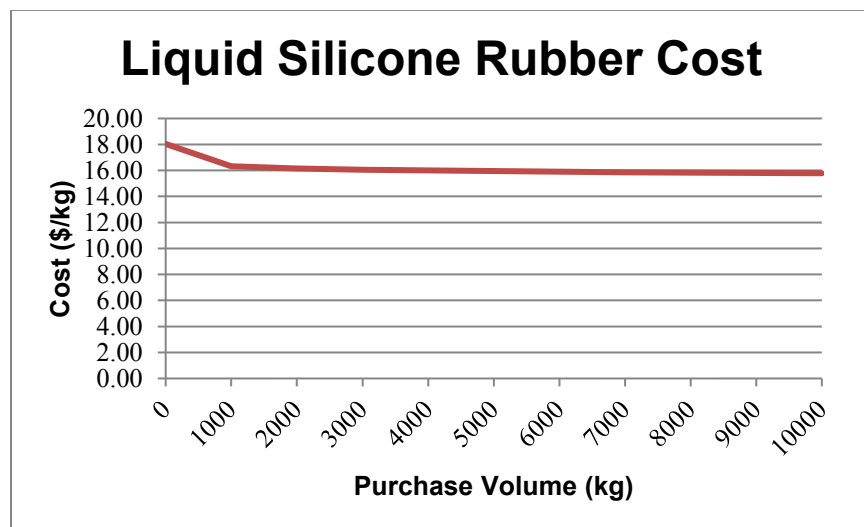
$$Y = A \times X^b = 18.04 \times 250^{(-0.0145)} = \$16.65$$

---

<sup>19</sup> R.D. Stewart, R.M. Wyskida, and J.D. Johannes (eds). 1995. *Cost Estimator's Reference Manual*, 2<sup>nd</sup> Ed. Wiley-Interscience, April 1995. 744 p.



The corresponding cost chart would appear as:



For specialty materials, like the polytetrafluoroethylene (PTFE)/ionomer membrane, the cost curve is steeper. One supplier provided low-volume quotes of \$535.63/square meter (m<sup>2</sup>) for 3 m<sup>2</sup>, and \$313.13/m<sup>2</sup> for 45 m<sup>2</sup>. Estimates obtained from previous fuel cell manufacturing cost analyses estimated high-volume costs to be in the range of \$50.00/m<sup>2</sup> for volumes up to 150,000 m<sup>2</sup>. Iteration using the costs above led to a value of m=0.86, which results in:

$$b = \log(0.86)/\log(2) = -0.21759$$

Using a learned cost of \$50.00/m<sup>2</sup> for a volume of 100,000 m<sup>2</sup>, then the cost of the first unit is:

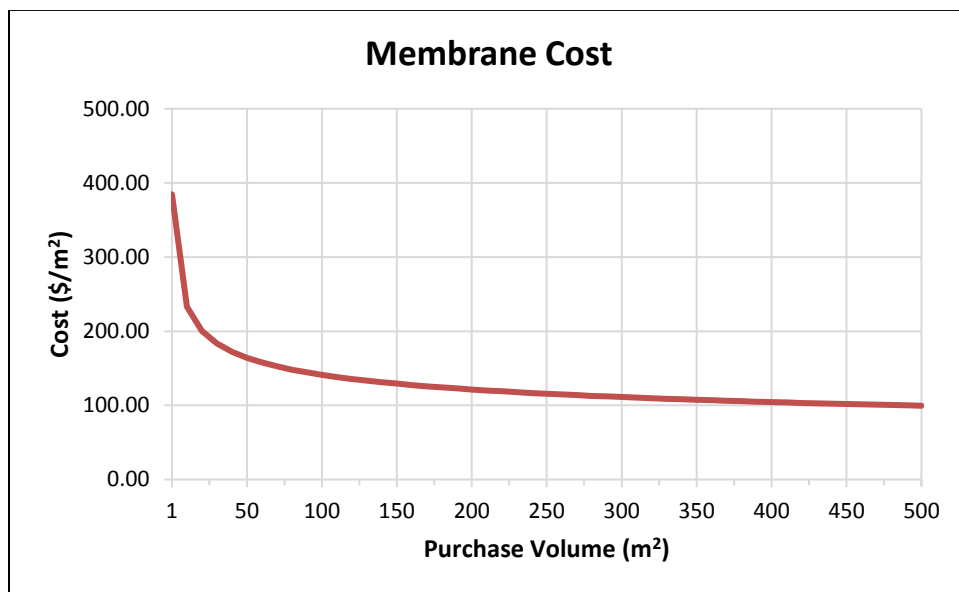
$$A = Y / X^b = 50.00 / 150,000^{(-0.21759)} = \$685.72$$

For a purchase of 3 and 45 m<sup>2</sup> of material, the calculated cost per unit is:

$$Y_3 = A \times X^b = 685.72 \times 3^{(-0.21759)} = \$526.53$$

$$Y_{45} = A \times X^b = 685.72 \times 45^{(-0.21759)} = \$292.09$$

The corresponding cost chart would appear as:



Using the above approach, the following learning curve parameters were used for the cost analysis of PEM material:

PEM Material	Units	Y	X	m	b	A
Platinum	kg	\$41,602.00	1	1.00	0.0000	\$41,602.00
XC-72	kg	\$0.90	1,000	0.95	-0.0740	\$1.50
DE-521	kg	\$90.00	100,000	0.85	-0.2345	\$1,338.35
DI Water	kg	\$0.10	160	0.85	-0.2345	\$0.33
Methanol	kg	\$0.55	10,000	0.95	-0.0740	\$1.09
Membrane	m²	\$28.76	150,000	0.86	-0.2176	\$384.65
Polyester Film	m²	\$0.32	30,000	0.55	-0.8625	\$2,289.88
GDL	m²	\$56.00	100,000	0.69	-0.5353	\$26,597.86
LSR	kg	\$15.40	55,000	0.99	-0.0145	\$18.04
BMC 940	kg	\$2.43	1,100	0.85	-0.2345	\$12.55
A356 Aluminum	kg	\$2.50	1,000	0.97	-0.0439	\$3.39
Hydrogen	m³	\$5.93	30,000	0.80	-0.3219	\$163.82
Natural Gas	m³	\$0.29	1,000	0.99	-0.0145	\$0.32

The following learning curve parameters were used for the cost analysis of SOFC material:

SOFC Material	Units	Y	X	m	b	A
NiO	kg	\$32.00	2,500	0.90	-0.1520	\$105.11
8YSZ	kg	\$40.00	2,500	0.90	-0.1520	\$131.39
LSM	kg	\$85.00	2,500	0.90	-0.1520	\$279.20
LSCF	kg	\$85.00	2,500	0.90	-0.1520	\$279.20
LO	kg	\$52.00	2,500	0.90	-0.1520	\$170.81
Ni-YSZ	kg	\$36.00	2,500	0.90	-0.1520	\$118.25
LSM-YSZ	kg	\$62.50	2,500	0.90	-0.1520	\$205.29
Perovskite Coating	kg	\$150.00	2,500	0.90	-0.1520	\$492.71
SS-441 Stainless Steel Sheet	kg	\$2.50	3,000	0.85	-0.2345	\$16.34
SS-441 Stainless Steel Mesh	kg	\$89.23	100,000	0.90	-0.1520	\$513.48
Hastelloy X	kg	\$30.36	2,000	0.90	-0.1520	\$96.40
Borosilicate glass	kg	\$2.00	2,500	0.85	-0.2345	\$12.52
DI Water	kg	\$0.10	160	0.85	-0.2345	\$0.33
Binder	kg	\$2.50	2,500	0.85	-0.2345	\$15.65
Dispersant	kg	\$1.27	2,500	0.85	-0.2345	\$7.95
A560 Stainless Steel	kg	\$2.50	3,000	0.97	-0.0439	\$3.55
Nitrogen	m <sup>3</sup>	\$0.53	30,000	0.80	-0.3219	\$14.64
Hydrogen	m <sup>3</sup>	\$5.93	30,000	0.80	-0.3219	\$163.82
Natural Gas	m <sup>3</sup>	\$0.29	1,000	0.99	-0.0145	\$0.32
Carrier Film	m <sup>2</sup>	\$0.32	30,000	0.55	-0.8625	\$2,326.22

### A-2.3 High Quantity Purchased Material Cost

For the annual system volumes used, the material purchase volume can be extremely large. For example, to manufacture bipolar plates for 50,000 100-kW systems requires over 60,000 metric tons of BMC940 material. According to the learning curve equation, a bulk purchase of this size would cost \$0.188/kg—a cost that is most likely unachievable and therefore unrealistic.

To address this problem, we have elected to assume that any additional volume discounts beyond the bulk pricing represented by the cost Y and quantity X in the above tables would be no more than that achieved by doubling the quantity X. Since the learning curve slope (m) represents the amount of reduction in Y when quantity X is doubled, the minimum material price is simply Y×m. Therefore, the material price for a given purchase quantity (q) is calculated as:

$$Y_q = \text{Max}(A \times X^b, Y \times m)$$

For the bipolar plate material, the equation above yields:

$$Y_q = \text{Max}(12.55 \times (60 \times 10^6)^{-0.2345}, 2.43 \times 0.85) = \text{Max}(0.188, 2.065) = \$2.065$$

## A-2.4 Special Cases

Platinum prices are dictated by the precious metals spot markets and are generally not subject to purchase volume reductions. This correlates to a learning curve slope value of  $m = 1$ .

The polyester film would seem to be a material that would have a commodity price profile like that of the silicone sheet. However, price quotes received showed relatively high cost at low purchase volumes of less than 100 m<sup>2</sup>, but falling by over 97% at bulk purchase volumes greater than 14,000 m<sup>2</sup>.

## Appendix A-3: Assembly Cost Learning Curve Calculations

### A-3.1 Background

The Boothroyd Dewhurst, Inc. (BDI) Design for Assembly (DFA) software produces assembly times based on hand assembly at its most efficient. Using the 60-kW PEM stack as an example, the assembly time was estimated to be 3.1 hours.

The learning curve analysis essentially backs that number up to a time when bugs are still being worked out of the assembly process.

From the *Cost Estimator's Reference Manual* (1995),<sup>20</sup> the general learning curve equation is:

$$Y = AX^b$$

where:

Y = time or cost per cycle or unit

A = time or cost for first cycle or unit

X = number of cycles or units

b = log(m)/log(2)

m = slope of learning curve

### A-3.2 Analysis

For stack assembly time, if we assume that m = 0.85 (typical for aerospace processes), then:

$$b = \log(0.85)/\log(2) = -0.23447$$

If the stack assembly process is "learned" after 100 units, and the assembly time for the X = 100<sup>th</sup> stack is the BDI DFA time, then the time to assemble the first unit is:

$$A = Y / X^b = 3.1 / 100^{(-0.23447)} = 9.12 \text{ hrs}$$

The average time to assemble the first 100 units ( $\bar{C}_{100}$ ) is calculated as:

$$\bar{C}_{100} = \frac{\left( \sum_{i=1}^{100} 9.12 * i^{(-0.23447)} \right)}{100} = 3.99 \text{ hrs}$$

---

<sup>20</sup> R.D. Stewart, R.M. Wyskida, and J.D. Johannes (eds). 1995. *Cost Estimator's Reference Manual*, 2<sup>nd</sup> Ed. Wiley-Interscience, April 1995. 744 p.

The time to assemble all subsequent units is assumed to be A. The average time to assemble n units (n > 100) is calculated as:

$$\bar{C}_n = \frac{\left( \left( \sum_{i=1}^{100} A * i^{(-0.23447)} \right) + (Y_{100} * (n - 100)) \right)}{n}$$

Using the above equations, the average stack assembly times are:

1 <sup>st</sup> Year Average Assembly Time (hrs)				
Stack Type	Stacks per year			
	100	1,000	10,000	50,000
60-kW PEM Stack	3.990	3.187	3.107	3.100
50-kW PEM Stack	3.350	2.676	2.608	2.602
30-kW SOFC Stack	4.546	3.631	3.540	3.531

The average system assembly times are:

1 <sup>st</sup> Year Average Assembly Time (hrs)				
System Type	Systems per year			
	100	1,000	10,000	50,000
100-kW PEM	3.611	2.884	2.812	2.805
250-kW PEM	4.121	3.291	3.208	3.201
100-kW SOFC	2.400	1.917	1.869	1.864
250-kW SOFC	2.986	2.385	2.325	2.319

## Appendix A-4: PEM Production Facility Estimation

The production facility estimation is based on the floor area required for production equipment, equipment operators, and support personnel. Primary space allowance guidelines used for this analysis were developed by Prof. Jose Ventura at Pennsylvania State University, and were downloaded on 10/18/2013 from <http://www.personal.psu.edu/jav1>.

### A-4.1 Equipment Footprint

Station utilization calculations provide the equipment count for a particular production station. Using the bipolar plate production as an example, each station consists of four pieces of equipment: the 1,000-ton fast acting press, the post-bake oven, the hydraulic pre-mold press, and the electronic material scale, which have the following footprint dimensions in inches:

- Compression molding press: 60 inches x 70 inches
- Post-bake oven: 40 inches x 40 inches
- Pre-mold press: 18 inches x 12 inches
- Material scale: 12 inches x 12 inches

Allowing a 3-foot (36-inch) margin on all sides for maintenance access makes the total machine footprints in square feet (ft<sup>2</sup>):

$$\text{Compression molding press: } (60 + (2 \times 36)) \times (70 + (2 \times 36)) / 144 \text{ in}^2/\text{ft}^2 = 130 \text{ ft}^2$$

$$\text{Post-bake oven: } (40 + (2 \times 36)) \times (40 + (2 \times 36)) / 144 \text{ in}^2/\text{ft}^2 = 87 \text{ ft}^2$$

$$\text{Pre-mold press: } (18 + (2 \times 36)) \times (12 + (2 \times 36)) / 144 \text{ in}^2/\text{ft}^2 = 53 \text{ ft}^2$$

$$\text{Material scale: } (12 + (2 \times 36)) \times (12 + (2 \times 36)) / 144 \text{ in}^2/\text{ft}^2 = 49 \text{ ft}^2$$

Three additional space allowances are made for each station for material, personnel, and aisles. The production stations will require space for material receiving and part pickup, typically done using pallets. We will assume one standard 40-inch by 48-inch pallet for receiving and pickup, adding to the required area by:

$$\text{Material allowance} = 2 \times (40 \times 48) / 144 = 27 \text{ ft}^2$$

Ventura recommends personnel space of 20 ft<sup>2</sup> per person to allow for movement within the work station during equipment operation. The bipolar plate pressing requires a single operator, adding:

$$\text{Personnel allowance} = 1 \times 20 \text{ ft}^2 = 20 \text{ ft}^2$$

Aisle allowance is based on the largest transported load. Because we intend to transport material and finished parts on standard pallets, our anticipated load size is 27 ft<sup>2</sup>, for which Ventura recommends a 30% to 40% allowance for the net area required, which include personnel and material. Using a value of 35% makes the aisle allowance for the bipolar plate station:

$$\text{Aisle allowance: } (130 + 87 + 53 + 49 + 27 + 20) \times 0.35 = 128 \text{ ft}^2$$

The total floor space allocation for the bipolar plate station is:

$$\text{Floor space allocation} = 130 + 87 + 53 + 49 + 27 + 20 + 128 = 494 \text{ ft}^2$$

The PEM fuel cell stack production was broken up into 12 primary work stations with total floor space allocations calculated using the above formulas as:

Production Station	Floor Space Allocation (ft <sup>2</sup> )
Catalyst	262
Slot die coating	759
Decal transfer	551
Hot press	426
Die cutting	178
Bipolar plate	494
End plate	1,261
Seal injection molding	178
Stack assembly	522
Stack test and conditioning	439
System assembly	356
System test	439

In addition to equipment, industrial facility space must be allocated for offices, food service, restrooms, and parking, all of which depend on the number of people present during operation. For most automated or semi-automated production equipment, one operator can cover multiple machines. In addition, some operations have long periods of unsupervised operation (e.g., the 10-hour milling time in catalyst production). Ventura estimates the number of required machine operators using the formula:

$$n' = (a + t) / (a + b)$$

where

a = machine-operator concurrent activity time (load, unload)

b = independent operator activity time (inspect, package)

t = independent machine activity time

n' = maximum number of machines per operator



The reciprocal of  $n'$  would represent the minimum number of operators per machine. Using time data (in seconds) extracted from the DFM process analyses for  $a$  and  $t$ , and estimating time for  $b$ , resulted in the following:

PEM Production Station	a	b	t	$n'$	$1/n'$
Catalyst	1,907	600	36,000	15.12	0.07
Slot Die Coating	1,800	600	2,666	1.86	0.54
Decal Transfer	1,800	600	2,933	1.97	0.51
Slit and Cut	1,800	600	10,547	5.14	0.19
Hot Press	1,800	600	10,547	5.14	0.19
Die Cutting	1,800	600	1,316	1.30	0.77
Bipolar Plate	20	84	240	2.50	0.40
End Plate	60	60	306	3.05	0.33
Seal Injection Molding	1,800	60	1,480	1.76	0.57
Stack Assembly	11,051	0	0	1.00	1.00
Stack Test and Conditioning	1,800	600	9,000	4.50	0.22
System Assembly	11,051	0	0	1.00	1.00
System Test	1,800	600	9,000	4.50	0.22

In general, we assume that a single operator is capable of operating a maximum of three machines in a cell arrangement. We also assume that stations requiring multiple operators can utilize a floating operator working between three machines. The exception is catalyst production: we assume that the 10-hour milling time per catalyst batch permits one operator to operate five machines.

To obtain a rough estimate of the number of operators required during any one shift, we multiply the required number of operators per station (combinations of either 1.0, 0.5, 0.33) by the number of stations required to produce a particular annual volume and the station utilization (assuming a single operator is trained to perform multiple tasks). Using the station utilization numbers for 2,000 60-kW stacks per year, we have:

PEM Production Station	Stations	Utilization	Operators per station	Operators Per Shift
Catalyst	1	0.021	0.10	0.00
Slot Die Coating	1	0.127	0.50	0.06
Decal Transfer	1	0.062	0.33	0.02
Slit and Cut	1	0.139	0.50	0.07
Hot Press	1	0.649	0.33	0.22
Die Cutting	1	0.098	1.00	0.10
Bipolar Plate	8	0.867	0.50	3.47
End Plate	1	0.073	0.33	0.02
Seal Injection Molding	1	0.794	0.50	0.79
Stack Assembly	1	0.524	1.00	1.05
Stack Test and Conditioning	2	0.583	0.33	0.19
System Assembly	1	0.495	1.00	0.49
System Test	1	0.667	0.33	0.22
Total				6.71

Rounding up to seven machine operators per shift, and assuming approximately one support staff per four operators for purchasing, quality control (QC), and maintenance, the facility needs to support a total of nine employees. Ventura provides estimates for the following additional facilities:

Food service: 15 ft<sup>2</sup>/employee

Restrooms: 2 toilets + 2 sinks per 15 employees (estimated at 25 ft<sup>2</sup> per fixture)

Parking: 276 ft<sup>2</sup>/employee

In addition, office space for support personnel is estimated at 72 ft<sup>2</sup>/employee based on the State of Wisconsin Facility Design Standard. Therefore, additional space requirements are:

Facility	Space Required (ft <sup>2</sup> )
Food Service	105
Restrooms	100
Parking	1932
Office	144

Estimated total factory building floor space can be estimated as:

$$\text{Equipment} + \text{Food service} + \text{Restrooms} + \text{Office} = 7,887 \text{ ft}^2$$

Assuming a construction cost of \$250/ ft<sup>2</sup>, the estimated cost of factory construction is approximately \$1,971,750.

Total real estate required can be estimated as building floor space plus parking and building set-back (distance from building to streets and other structures). Assuming a 30-foot set-back on all sides of a reasonably square facility gives a total real estate requirement of:

$$((\text{Factory space} + \text{Parking space})^{1/2} + 60)^2 = 25,310 \text{ ft}^2 = 0.58 \text{ acre}$$

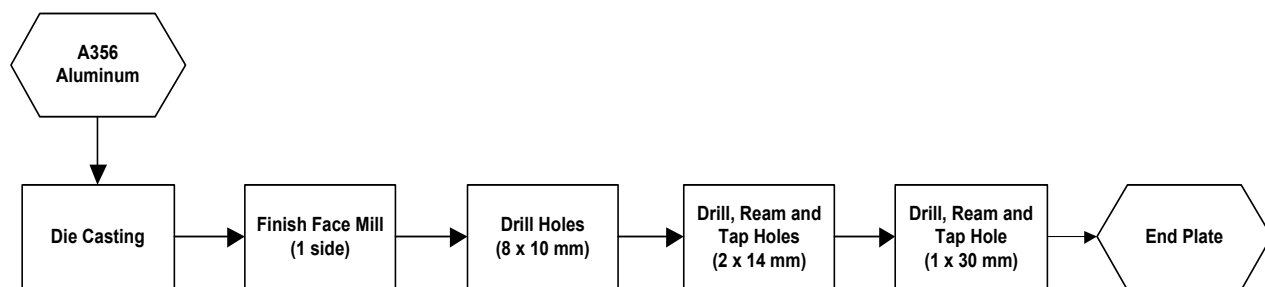
Assuming a real estate cost of \$125,000/acre, the estimated total real estate cost is approximately \$72,629.

## Appendix A-5: PEM End Plate Manufacturing Process

### A-5.1 Model Approach

- Use standard Boothroyd Dewhurst, Inc. (BDI) cell machining cost analysis
  - Near net shape workpiece
  - Face mill bottom
  - Drill tie rod holes
  - Drill, ream, and tap gas connector mounting holes

### A-5.2 Process Flow

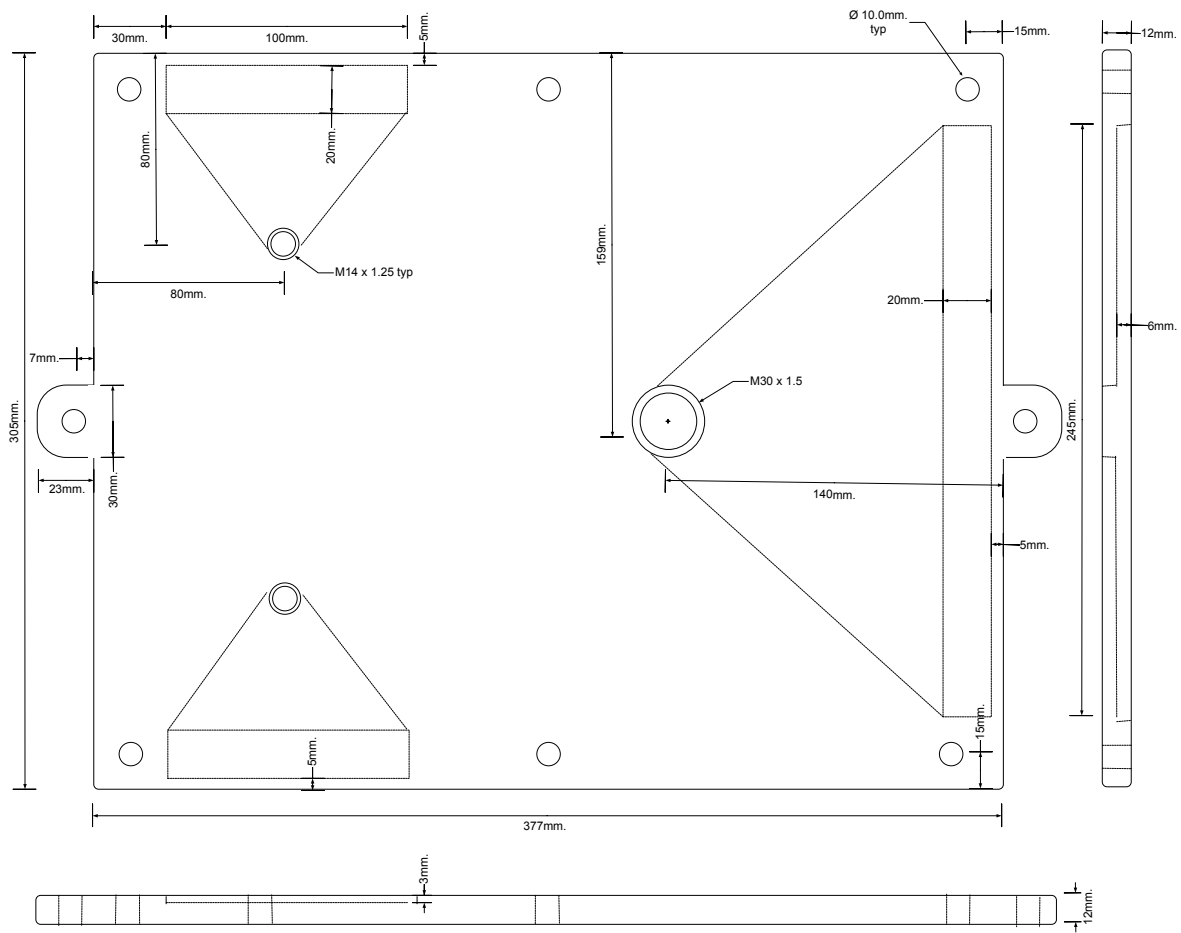


### A-5.3 Background

The BDI software provides preprogrammed cost models for the casting and cell machining operations used to manufacture the fuel cell stack end plates. The end plates need to be rigid in order to apply even pressure across the face of the stack. The process selection for the PEM end plate was sand casting of A356 cast aluminum to near net shape, followed by finish machining of the stack contact face, drilling the tie rod holes, and drilling, reaming and tapping the holes for fuel, exhaust, and cooling flows.

### A-5.4 Preliminary Analysis

The 60-kW stack end plate features and dimensions are shown below:



## A-5.5 DFM Software Analysis

The screenshot shows the DFM Concurrent Costing 2.4 software interface. The main window displays a tree view of manufacturing processes for a part named 'A356 cast aluminum sand cast part'. The processes listed include Automatic sand casting process, Milltronics MB18 bed mill, and Sugino V6 CNC drilling center. The software also shows a 3D model of the part with dimensions: 12 mm average thickness, 305 mm length, and 377 mm width. A cost results table is visible at the bottom left, comparing previous and current costs for various components.

Cost results, \$	Previous	Current
material	8.71	8.71
setup	0.10	0.10
process	5.69	5.84
rejects	0.32	0.32
piece part	14.81	14.97
tooling	0.20	0.20
total	15.01	15.17
Tooling investment	19,786	19,786

The BDI software estimates an 18.35-hour machine setup time and calculates the total manufacturing time for the end plates as 375 seconds, making the total machine time for annual production of 1,000 100-kW systems:

$$\text{Machine time} = (375 \text{ sec/part} / 3,600) \times 4,000 \text{ parts} + 18.35 = 435.0 \text{ hours}$$

Machine utilization is:

$$\text{Utilization} = 435.0 / 6,000 = 7.3\%$$

Machine rate was determined in accordance with Appendix A-1 as:

$$\begin{aligned} \text{In-house rate} &= \$116.79 / 0.073 = \$1,606.75 \\ \text{Job shop rate} &= 1.4 \times (\$116.79 / 0.65) = \$250.91 \end{aligned}$$

Assuming two full-time operators (one for casting, one for machining) per station, the total machine labor time is equal to twice the machine time = 881.2 hours.

Material cost was determined in accordance with Appendix A-2 as:

$$\text{Material cost} = \$2.425/\text{kg}$$

Tooling cost is \$19,786 and is assumed to be capable of producing 180,000 parts. Amortizing over a 5-year production life, the total annual tooling cost is:

$$\text{Annual tooling cost} = \frac{1}{5}(\text{Tooling cost} \times \text{Number of tools purchased})$$

where:

$$\text{Number of tools purchased} = \text{Roundup}(\text{Total production} / \text{Tool life})$$

$$\text{Total production} = \text{Annual production} \times 5$$

$$\text{Annual tooling cost} = (\$19,786 / 5 \text{ yrs}) \times \text{Roundup}((4,000 \text{ parts/yr} \times 5 \text{ yrs}) / 180,000 \text{ parts/tool}) = \$3,957.20$$

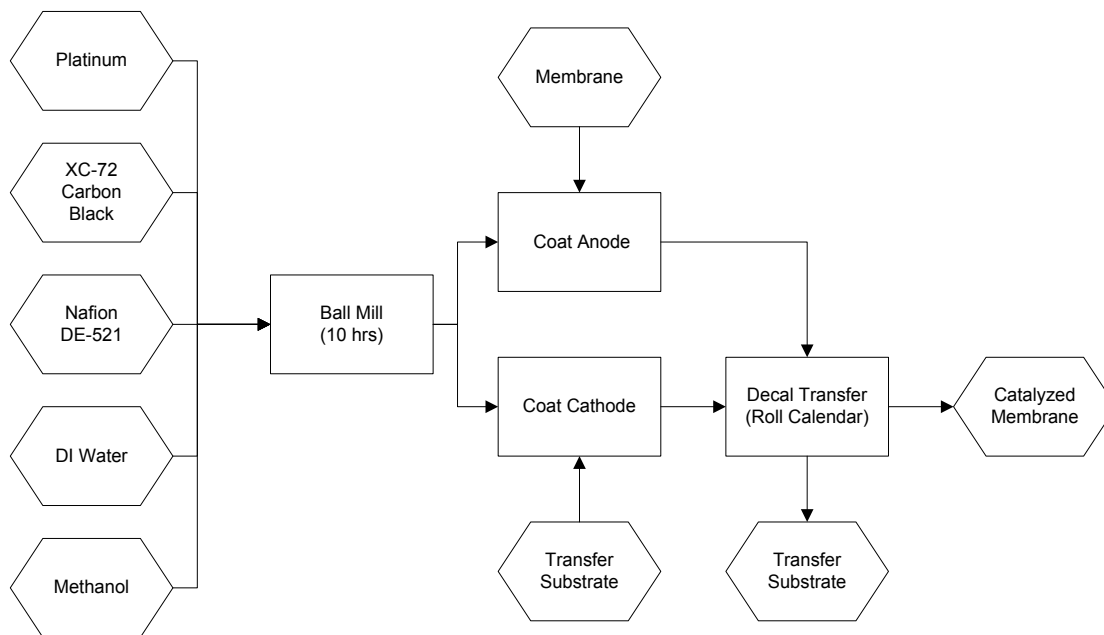
## Appendix A-6: PEM Platinum Catalyst Coating Process

### A-6.1 Model Approach

- Catalyst ink preparation operation
  - Compute machine setup labor time based on user input
  - Compute required batch size based on part batch size and catalyst loading
  - Compute catalyst ink material unit cost based on usage
  - Compute catalyst ink processing time and machine utilization
  
- Anode catalyst ink slot die deposition to membrane operation
  - Compute processing time based on production size and substrate speed
  - Compute number of setups based on purchased roll length
  - Compute setup labor time based on user input and number of setups required
  - Compute material unit cost based on usage
  - Compute required heater area based on drying time and substrate speed
  - Compute total anode ink deposition processing time and machine utilization
  
- Cathode catalyst ink slot die deposition to transfer substrate operation
  - Compute processing time based on batch size and substrate speed
  - Compute number of setups based on purchased roll length
  - Compute setup labor time based on user input and number of setups required
  - Compute material unit cost based usage
  - Compute required heater area based on drying time and substrate speed
  - Compute total cathode ink deposition processing time and machine utilization
  
- Cathode catalyst ink decal transfer calendaring operation
  - Compute processing time based on batch size and substrate speed
  - Compute number of setups based on purchased roll length
  - Compute setup labor time based on user input and number of setups required
  - Compute required heater area based on heating time and substrate speed
  - Compute decal transfer processing time and machine utilization



## A-6.2 Process Flow



## A-6.3 Background

U.S. patent no. 7,141,270 reported that the wet platinum catalyst composition consists of:

- 6 wt% Pt
- 9 wt% Vulcan XC-72 (carbon black)
- 72 wt% Nafion DE-521 solution (5 wt% Nafion)
- 6.5 wt% deionized (DI) water
- 6.5 wt% methanol

Assuming that all solvents are driven off during the drying process, the dry catalyst consists of:

- 48.4 wt% Vulcan XC-72 (carbon black)
- 32.3 wt% Pt
- 19.4 wt% Nafion

Technical literature and conversations with stack manufacturers indicate that ball milling is used as the primary means of grinding and homogenizing the catalyst ink, with milling times reported in the range of 4 hours to “overnight.” U.S. patent no. 6,187,468 details a two-step preparation process of mixing (milling) for 60 to 300 minutes, followed by 30 to 300 minutes in a “three-dimensional vibrating stirrer.” Constant processing in a regular or planetary ball mill for 8 to 10 hours may suffice for both the mixing and stirring parts of the process.

Manufacturers noted that there are significant losses during the ink production process, which tends to occur when handling ink/slurry from one part of the process to the next (e.g., transfer of final composition from mixing vessel to catalyst application method apparatus), but that much of the platinum was subsequently recovered, reducing the platinum scrap rate to 1% or less.

In the past, low-volume catalyst application was performed using screen printing, but the current process is generally done roll-to-roll. At least one approach involves a two-step process. One catalyst layer is applied directly to the membrane, and the other catalyst layer is applied to a low-cost substrate material. The membrane is then turned over, and the second catalyst layer is applied by hot press decal transfer.

Gore has proposed a three-step MEA manufacturing process that involves sequential roll-to-roll coating. (see [https://www.hydrogen.energy.gov/pdfs/progress14/vi\\_2\\_busby\\_2014.pdf](https://www.hydrogen.energy.gov/pdfs/progress14/vi_2_busby_2014.pdf) for details) The catalyst ink is applied to a backing material, dried and re-rolled. The membrane is then applied to the first catalyst layer using a co-extrusion deposition, which is dried and re-rolled. Catalyst ink is then applied to the membrane layer, dried and re-rolled. The three-layer MEA would then move to the hot-pressing operation to apply the gas diffusion layer (GDL).

All the above methods pay a material cost penalty by applying catalyst to the entire MEA surface, including the non-active areas. A more economical approach may involve using a slot-die patch coating process (see <http://www.frontierindustrial.com/>), where anode catalyst is applied to the membrane and the cathode catalyst applied to a transfer substrate in rectangular patches sized to the active area. The cathode catalyst patches are then bonded to the membrane using hot press decal transfer, followed by the hot-pressing operation to apply the GDL.

## A-6.4 Preliminary Analysis

### A-6.4.1 Batch Volume

Catalyst batch volume depends on the coated area, catalyst loading, and maximum catalyst batch size.

The cells for this analysis will have an active area size of:

$$245.0 \text{ mm width} \times 318.4 \text{ mm length} = 780.0 \text{ cm}^2$$

Material densities for the catalyst components are as follows:

- $\rho(\text{Pt}) = 21.45 \text{ g/cm}^3$
- $\rho(\text{XC-72}) = 0.264 \text{ g/cm}^3$
- $\rho(\text{Nafion DE-521}) = 1.05 \text{ g/cm}^3$
- $\rho(\text{DI water}) = 1.0 \text{ g/cm}^3$
- $\rho(\text{methanol}) = 0.792 \text{ g/cm}^3$

Based on the wet platinum catalyst composition as specified above, 100 grams of wet catalyst contains 6 grams of Pt and has a volume of:

$$v = (6/21.45) + (9/0.264) + (72/1.05) + (6.5/0.792) + (6.5/1) = 117.6 \text{ cm}^3$$

Yielding a wet catalyst density of:

$$\rho(\text{wet catalyst}) = (100/117.6) = 0.85 \text{ g/cm}^3$$

The Pt content of the wet catalyst is:

$$m(\text{Pt})/v(\text{wet catalyst}) = 6/117.6 = 0.051 \text{ g/cm}^3 = 51 \text{ mg/cm}^3$$

To obtain a loading of 1 mg/cm<sup>2</sup>, the depth of the wet catalyst layer is:

$$d(\text{wet catalyst}) = 1/51 = 0.02 \text{ cm} = 200 \text{ microns}$$

Based on the dry platinum catalyst composition as specified above, 100 grams of dry catalyst contains 32.3 grams of Pt and has a volume of:

$$v = (32.3/21.45) + (48.4/0.264) + (19.4/2.05) = 194.3 \text{ cm}^3$$

Yielding a dry catalyst density of:

$$\rho(\text{dry catalyst}) = (100/194.3) = 0.515 \text{ g/cm}^3$$

The Pt content of the dry catalyst is:

$$m(\text{Pt})/v(\text{dry catalyst}) = 32.3/194.3 = 0.166 \text{ g/cm}^3 = 166 \text{ mg/cm}^3$$

To obtain a loading of 1 mg/cm<sup>2</sup>, the depth of the dry catalyst layer is:

$$d(\text{dry catalyst}) = 1/166 = 0.006 \text{ cm} = 60 \text{ microns}$$

The total Pt loading for this design is 0.4 mg/cm<sup>2</sup> with cathode loading in a 2:1 ratio relative to anode loading, making the loadings 0.27 mg/cm<sup>2</sup> and 0.13 mg/cm<sup>2</sup> for the cathode and anode, respectively, which will require wet deposition to depths of 53 and 27 microns, respectively, resulting in dry layer depths of 16 and 8 microns. Therefore, to coat both sides of the membrane with a total loading 0.4 mg/cm<sup>2</sup> will require a total coated depth of 80 microns (0.008 cm):

$$\text{Wet catalyst weight} = 0.85 \text{ g/cm}^3 \times (780.0 \times 0.008) \text{ cm}^3 = 5.304 \text{ g/part}$$

The 60-kW stack requires 283 cells. Based on producing 2,000 stacks per year, the required annual production before scrap is:

$$\text{Annual production} = 283 \text{ parts/stack} \times 2,000 \text{ stacks} = 566,000 \text{ parts}$$

$$\text{Catalyst batch size} = 566,000 \text{ parts} \times 5.304 \text{ g/part} \times 0.001 \text{ kg/g} = 3,002 \text{ kg}$$

#### A-6.4.2 Catalyst Ink Material Cost

Material cost of the ink is calculated using the weight percents of the slurry constituents multiplied by the raw material cost to determine a cost per kilogram. Material pricing was obtained from suppliers and supplier web sites in February 2014. Platinum cost is very volatile, with a 3-year monthly range of \$1,677/tr.oz. to \$832/tr.oz. For this analysis, we will assume a price equal to the 3-year average of \$1,294/tr.oz. (\$41,602/kg) for April 2016 delivery. Bulk costs for DE-521 were estimated at \$160, which translates to a price of about \$1,344/kg. Bulk costs for XC-72 catalyst grade carbon black were quoted by WeiKu Information and Technology and others at around \$900/MT (\$0.90/kg). Bulk costs for Methanol were quoted by Methanex and others at around \$630/MT (\$0.63/kg). The cost of DI water is based on amortized distillation costs obtained from [www.apswater.com](http://www.apswater.com).

The weight of each material contained in the catalyst is:

- Platinum:  $0.06 \times 3,002 \text{ kg} = 180.12 \text{ kg}$
- Nafion DE-521:  $0.72 \times 3,002 \text{ kg} = 2,161.44 \text{ kg}$
- Vulcan XC-72:  $0.09 \times 3,002 \text{ kg} = 270.18 \text{ kg}$
- Methanol:  $0.065 \times 3,002 \text{ kg} = 195.13 \text{ kg}$
- DI Water:  $0.065 \times 3,002 \text{ kg} = 195.13 \text{ kg}$

Using the above quotes, learning curve analysis in accordance with Appendix A-2 was applied to determine the following material costs:

- Platinum = \$41,602/kg
- Nafion DE-521 = \$219.84/kg
- Vulcan XC-72 = \$0.990/kg
- Methanol = \$0.735/kg
- DI water = \$0.094/kg

The cost of the ink is:

$$\text{Material cost} = (0.06 \times 44,368) + (0.72 \times 219.84) + (0.09 \times 0.990) + (0.065 \times 0.735) + (0.065 \times 0.094)$$

$$\text{Material cost} = \$2,820.51/\text{kg} = \$2.821/\text{g}$$

Total annual catalyst material cost before scrap is:

$$\$2,820.51/\text{kg} \times 3,002 \text{ kg} = \$8,467,171$$

### A-6.4.3 Catalyst Ink Processing

The first step is to weigh the materials out and place them in the mill. We will assume a manual process consisting of a measurement step and a material handling step. The BDI DFMA software contains an analogous operation for off-line precision measurement with a default value of 17.4 seconds for the measurement, and a minimum of 4 seconds for material handling. The catalyst ink is made up of five materials, so that total handling time for material preparation can be estimated as:

$$\text{Material prep time} = 5 \times 21.4 \text{ sec} = 107 \text{ sec} = 1.8 \text{ min}$$

The primary cost for operating the ball mill is the energy input to the motor running the mill. Some studies have looked into the cost of operating large ball mills used for cement and powder metallurgy material processing, where the target parameter is the amount of energy required to process a given amount of material, usually expressed in kW-hr/ton. The calculations are complex owing to the large number of inputs to the calculations.

In "Technical Notes 8, Grinding," R.P. King develops a relationship based on fundamental physical models of ball mill processing (see <http://www.mineraltech.com/MODSIM/ModsimTraining/Module6/Grinding.pdf>). He assumes a 35% volumetric loading ratio, of which milling balls represents 10% of the total charge volume. Given a mill with diameter  $d$  and length  $l$ , the total catalyst charge volume is:

$$\text{Catalyst charge volume} = (\pi \times d^2 / 4) \times l \times 0.35 \times 0.9 = 0.079 \pi d^2 l \text{ m}^3$$

Patterson Industries offers simple torque drive batch ball mills in 42-inch diameter × 48-inch length (1.067-m diameter × 1.219-m length), and 48-inch diameter × 60-inch length (1.219-m diameter × 1.524-m length). These provide maximum catalyst charge volumes of:

$$V = 0.079 \times \pi \times (1.067)^2 \times 1.219 = 295 \text{ kg}$$

$$V = 0.079 \times \pi \times (1.219)^2 \times 1.524 = 482 \text{ kg}$$

We note that production levels of 2,000 stacks per year will require 3,002 kg of catalyst production per year, or about 11 batches per year in the smaller mill. At less than one batch per month, the smaller mill would seem to be the prudent choice.

King presents a log-log plot showing that a mill with a diameter of 1 meter will consume about 10 kW of power, where a mill with a diameter of 2 meters consumes about 100 kW. These two values yield the equation:

$$\text{Power} = 10d^{3.32} \text{ kW}$$

To estimate the power required to process a batch of catalyst with a density of 850 kg/m<sup>3</sup>, we plug the mill diameter into the power equation to obtain:

$$\text{Power} = 10 \times (1.067)^{3.32} = 12.4 \text{ kW}$$

Once processing is complete, the catalyst ink will need to be separated from the milling balls and transferred to the coating machine. While we presently have no information about this part of the process, one approach would be to use a vacuum sieve (e.g., Farleygreene, Ltd. SM950 Sievmaster Vacu-siev) to remove and separate the catalyst ink from the mill, and transfer the ink to a transport container or directly to the coater reservoir.

ShopVac reports a sealed suction of 54 in-H<sub>2</sub>O (13.4 kPa) for their 2-HP (1.5-kW) unit. Using an equivalent vacuum sieve with a 1.5-in (0.038-m) diameter hose and 80% transfer efficiency, the flow rate is:

$$\text{Flow rate} = 0.8 \times (\pi \times (0.038)^2 / 4) \times (2 \times 13.4 / 850)^{1/2} = 0.00016 \text{ m}^3/\text{sec}$$

Since the catalyst forms 90% of the charge volume, the total charge volume is:

$$\text{Charge volume (m}^3\text{)} = 1.11 \times (\text{Catalyst weight (kg)} / \text{Catalyst density (kg/m}^3\text{)})$$

$$\text{Charge volume (m}^3\text{)} = 0.0013 \times \text{Catalyst weight}$$

Therefore, the optimal time required to remove the charge volume is:

$$\text{Material removal time (sec)} = \text{Charge volume} / \text{Flow rate} = 8.1 \times \text{Catalyst weight}$$

The optimal time to remove a full charge of catalyst from the mill would be:

$$\text{Material removal time} = 8.1 \times 295 = 2389.5 \text{ sec} = 39.8 \text{ minutes}$$

We estimate the total transfer time to remove the ink from the mill and transfer it to the coater as twice the ink removal time.

The estimated total processing time is calculated as the sum of the setup time, material prep time, milling time, and transfer time, multiplied by the total number of batches processed for annual production of 149.6 kg of catalyst:

$$\text{Process time} = 11 \text{ batches} \times (10 + (1.8 / 60) + (2 \times (39.8 / 60))) \text{ hrs} = 124.92 \text{ hrs}$$

Given an availability of 6,000 hours per year per machine, the number of mills required is:

$$\text{Roundup}(124.92 / 6,000) = 1 \text{ mill}$$

Machine utilization is:

$$124.92 / 6,000 = 2.08\%$$

Machine rate was determined in accordance with Appendix A-1 as:

$$\text{In-house rate} = \$11.18 / 0.0208 = \$537.50$$

$$\text{Job shop rate} = 1.4 \times (\$11.18 / 0.65) = \$24.08$$

#### A-6.4.4 Catalyst Ink Deposition

As indicated previously, one approach to catalyst deposition involves a two-step process. The anode catalyst is applied to the membrane and the cathode catalyst is applied to a transfer substrate in rectangular patches sized to the active area. The cathode catalyst patches are then bonded to the membrane using hot press decal transfer. Both the membrane application and decal creation are direct deposition processes to a substrate material, one being to the membrane itself, and the other to a carrier substrate (commonly a polyester or polyimide material). The patches will be centered in the full cell size envelope of 305 millimeters (mm)  $\times$  378 mm.

We will assume a roll-to-roll slot die application process. Depending on the roll length and width, multiple machine setups may be required to process the material for an entire production run. The length of material being processed is a function of the batch size and the number of parts that can be produced across the material width. Assuming no cutting margin for rectangular MEAs, the optimal part orientation can be determined based on the fraction of material width left over as waste as:

$$\text{Number of lengthwise parts} = \text{floor}(\text{Roll width} / \text{Part length})$$

$$\text{Lengthwise waste fraction} = (\text{Roll width} / \text{Part length}) - \text{Number of lengthwise parts}$$

##### A-6.4.4.1 Material Cost

Membrane material is sold in widths of 12-inch (0.305-m) and 24-inch (0.610-m) widths with lengths of 50 or 100 meters. Common thin films (polyimide, polyethylene) used as transfer media tend to be either 0.4 or 0.8 meter, while lengths can be found up to a maximum of about 1,000 meters. GDL material is typically sold in either 0.4- or 0.8-meter widths, and is available up to a maximum of 800-meter lengths.

The membrane roll has the smallest standard widths and is the most expensive, so it will be used to determine the maximum coating width with minimum scrap. Because the 60-kW cells are rectangular, orientation is an important issue in terms of minimizing scrap. Sizing the cells across the 305.0-mm dimension, two cells will take up 610 mm of membrane width, leaving a 0.0-mm edge margin on a 610-mm roll width for the membrane. Sizing across the 378.4-mm dimension, one cell will take up

378.4 mm, leaving a 231.6-mm edge margin. Since two cell widths across results in lower scrap, the material length required will be:

$$\text{Material length} = (566,000 \text{ parts} / 2 \text{ part widths/part length}) \times 378 \text{ mm part length} / 1,000 = 106,974 \text{ m}$$

The total material area required before scrap is:

$$\text{Membrane area} = 106,974 \text{ m} \times 0.610 \text{ m} = 65,254 \text{ m}^2$$

$$\text{Transfer substrate area} = 106,974 \text{ m} \times 0.8 \text{ m} = 85,579 \text{ m}^2$$

Using learning curve analysis in accordance with Appendix A-2, the material cost before scrap can be estimated as:

$$\text{Membrane cost} = \$34.27/\text{m}^3$$

$$\text{Transfer substrate cost} = \$0.17/\text{m}^3$$

Slot die coating machine setup consists of loading and threading the substrate, and loading the catalyst ink into the reservoir. For costing purposes, we will take the setup time as a user input and assume a value of 0.5 hour. Bulk roll stock is available in 100-meter length for the membrane, and 1,000-meter length for the transfer substrate, so the number of setups required to run 566,000 parts is:

$$\text{Number of setups} = \text{Roundup}(\text{Carrier length (m)} / \text{Roll length (m)})$$

$$\text{Membrane: Number of setups} = \text{Roundup} (106,974 / 100) = 1,070$$

$$\text{Transfer substrate: Number of setups} = \text{Roundup} (106,974 / 1,000) = 107$$

#### **A-6.4.4.2 Slot Die Coating**

Slot die coating is capable of very thin coating thicknesses. The coated material passes the slot die at a speed determined by the rheology of the coating material and the thickness of the application. While the precise rheology of the catalyst ink is not known, we can estimate the substrate speed using the tape casting estimating formula as follows:

$$\text{Maximum coating speed} = 157.18 \times 0.987^{\text{coating thickness } (\mu\text{m})} \text{ mm/sec}$$

The wet coating thickness was calculated above as 200 microns per 1 mg/cm<sup>2</sup> of platinum loading. The cathode/anode coating ratio is assumed to be 2:1, for a total loading of 0.4 mg/cm<sup>2</sup> of platinum; the anode will be coated to a depth of 27 microns, while the cathode will be coated to a depth of 53 microns, making the maximum coating speeds:

$$\text{Anode maximum coating speed} = 157.18 \times 0.987^{27} = 110.4 \text{ mm/sec} = 6.62 \text{ m/min}$$

$$\text{Cathode maximum coating speed} = 157.18 \times 0.987^{53} = 78.56 \text{ mm/sec} = 4.71 \text{ m/min}$$

Part throughput is calculated as:

$$\text{Throughput (parts/hour)} = \text{Coating speed (m/min)} \times \text{Parts per part length (parts)} / \text{Part length (m)} \times 60 \text{ min/hour}$$

$$\text{Anode: Throughput} = 6.62 \times 2 / (318.4 / 1,000) \times 60 = 2,495.0 \text{ parts/hour}$$

$$\text{Cathode: Throughput} = 4.71 \times 2 / (318.4 / 1,000) \times 60 = 1,775.1 \text{ parts/hour}$$

Total machine time to set up and produce 566,000 parts is:

$$\text{Anode machine time} = (1,070 \text{ setups} \times 0.5 \text{ hr/setup}) + (566,000 \text{ parts} / 2,495.0 \text{ parts/hr}) = 761.9 \text{ hrs}$$

$$\text{Cathode machine time} = (107 \text{ setups} \times 0.5 \text{ hr/setup}) + (566,000 \text{ parts} / 1,775.1 \text{ parts/hr}) = 372.4 \text{ hrs}$$

Given an availability of 6,000 hours per year per machine, the number of coating systems required is:

$$\text{Roundup}((60.72 + 33.17) / 6,000) = 1 \text{ coater}$$

Machine utilization is:

$$(761.9 + 372.4) / 6,000 = 18.9\%$$

Machine rate was determined in accordance with Appendix A-1 as:

$$\text{In-house rate} = \$62.20 / 0.189 = \$329.10$$

$$\text{Job shop rate} = 1.4 \times (\$62.2 / 0.65) = \$133.96$$

#### A-6.4.4.3 Tooling Cost

Slot dies are precision machined and assembled to provide uniform coating thickness. The cost can vary widely depending on the coating fluid properties and die size. Frontier Industries estimates a stainless steel fixed die cost of \$14,000, and is capable of delivering approximately 100,000 parts before refurbishment at a cost of around \$3,500. Assuming four refurbishments before scrapping, and amortizing over a 5-year production life, the total annual tooling cost is:

$$\text{Annual tooling cost} = \frac{1}{5} (\text{Tooling cost} \times \text{Number of tools purchased})$$

where:

$$\text{Number of tools purchased} = \text{Roundup}(\text{Total production} / \text{Tool life})$$

$$\text{Total production} = \text{Annual production} \times 5$$

$$\text{Anode annual tooling cost} = \frac{1}{5} ((\$14,000 + (4 \times \$3,500)) \times \text{Roundup}((566,000 \text{ parts/yr} \times 5 \text{ yrs}) / 500,000 \text{ parts/tool})) = \$33,600$$

$$\text{Cathode annual tooling cost} = \frac{1}{5} ((\$14,000 + (4 \times \$3,500)) \times \text{Roundup}((566,000 \text{ parts/yr} \times 5 \text{ yrs}) / 500,000 \text{ parts/tool})) = \$33,600$$

#### A-6.4.5 Catalyst Ink Drying

Following deposition, the catalyst ink is dried, usually by means of a tunnel dryer positioned directly after the deposition step. The drying can be done by either radiant or convective heating. For the cost analysis, we will assume radiant (infrared) heating and compute the cost of drying by determining the required heater area based on the substrate speed and the drying time.

Infrared heating panels are generally sold with various energy watt densities and in standard-sized units and assembled to provide the necessary heating area. Using the Casso Solar Type FB as an example, standard watt densities are 15 and 25 W/in<sup>2</sup> (23 and 39 kW/m<sup>2</sup>) with standard width of 12 inches



(0.305 m) and lengths in 12-inch increments up to 60 inches (1.524 m). They note that 25 W/in<sup>2</sup> corresponds to an emitter temperature of 880°C, and that the conversion efficiency of electrical power to usable radiant energy is up to 80%.

Drying time is a function of the evaporation rate of the solvent and is inversely and exponentially proportional to the coating thickness. Experiments conducted by Mistler et al. (1978)<sup>21</sup> indicate drying rates of  $1.35 \times 10^{-5}$  g/cm<sup>2</sup>-sec at room temperature for an air flow rate of 2 liters per minute (l/min), and  $2.22 \times 10^{-5}$  g/cm<sup>2</sup>-sec at room temperature for an air flow rate of 75 l/min.

The change in density from wet to dry catalyst is 0.335 g/cm<sup>3</sup>, making the liquid removed per unit area a function of coating thickness as follows:

$$\text{Anode liquid removed per area} = 0.335 \text{ g/cm}^3 \times 0.0027 \text{ cm} = 0.0009 \text{ g/cm}^2$$

$$\text{Cathode liquid removed per area} = 0.335 \text{ g/cm}^3 \times 0.0053 \text{ cm} = 0.0018 \text{ g/cm}^2$$

For costing purposes, we will take drying time as an input and use the substrate speed and part width to compute the theoretical required heater area.

$$\text{Heater area} = \text{Drying time (min)} \times \text{Substrate speed (m/min)} \times (\text{Part width (mm)} / 1,000) \times \text{Parts across width}$$

At a rate of  $2.0 \times 10^{-5}$  g/cm<sup>2</sup>-sec drying rate, the estimated drying time is:

$$\text{Anode drying time} = 0.0009 \text{ g/cm}^2 / 2.0 \times 10^{-5} \text{ g/cm}^2\text{-sec} = 45 \text{ sec} = 0.75 \text{ min}$$

$$\text{Cathode drying time} = 0.0018 \text{ g/cm}^2 / 2.0 \times 10^{-5} \text{ g/cm}^2\text{-sec} = 90 \text{ sec} = 1.50 \text{ min}$$

The required dryer length is:

$$\text{Anode dryer length} = 0.75 \text{ min} \times 6.65 \text{ m/min} = 5.0 \text{ m}$$

$$\text{Cathode dryer length} = 1.50 \text{ min} \times 4.69 \text{ m/min} = 7.0 \text{ m}$$

Sizing for the maximum dryer length, and assuming 12-inch × 36-inch panels fitted two across the drying conveyor, we calculate 14 total infrared panels required.

#### A-6.4.6 Catalyst Layer Decal Transfer

The roll-to-roll decal transfer operation can be either by a semi-continuous process where the material is indexed into a standard heated platen press (see James et al. [2010], Section 4.4.6.1)<sup>22</sup> or by preheating and passing through heated rollers in a calendaring process. For the preliminary analysis, we will assume a calendaring process.

##### A-6.4.6.1 Setup

Decal transfer setup consists of loading, threading, and aligning the anode and cathode into the calendaring rollers. For costing purposes, we will take the setup time as a user input and assume a value

<sup>21</sup> R.E. Mistler, D.J. Shanefield, and R.B. Runk. 1978. Tape casting of ceramics, in *Ceramic Processing Before Firing*, G.Y. Onoda, Jr. and L.L. Hench (eds). John Wiley and Sons, New York.

<sup>22</sup> B.D. James, J.A. Kalinoski, and K.N. Baum. 2010. *Mass Production Cost Estimation for Direct H<sub>2</sub> PEM Fuel Cell Systems for Automotive Applications: 2010 Update*. NREL Report No. SR-5600-49933. Directed Technologies, Inc. Available at [https://www1.eere.energy.gov/hydrogenandfuelcells/pdfs/dti\\_80kW\\_fc\\_system\\_cost\\_analysis\\_report\\_2010.pdf](https://www1.eere.energy.gov/hydrogenandfuelcells/pdfs/dti_80kW_fc_system_cost_analysis_report_2010.pdf).

of 0.5 hour. The number of setups is a function of the shortest roll stock length, so that the number of required setups to run 36,000 parts is the same as the number of setups for the anode slot die coating:

$$\text{Number of setups} = 1,070$$

#### **A-6.4.6.2 Calendaring**

The calendaring process consists of two main steps: preheating and rolling. We will assume that the coated membrane and decal catalyst layers are brought together and passed through an infrared tunnel oven for preheating. Assuming that the two layers need to reach 100°C, we can estimate the oven dwell time as (noting that 1 W = 1 J/sec):

$$\text{Oven dwell time} = \frac{\text{Part weight (g)} \times \text{Part specific heat (J/g-}^\circ\text{C)} \times \text{Temperature rise (}^\circ\text{C)}}{\text{Energy input (W)}}$$

If we assume that the same infrared heaters used for drying are used for preheating, the energy rate impinging on the part is:

$$\text{Energy input} = \text{Heater watt density (W/cm}^2\text{)} \times \text{Part area (cm}^2\text{)} \times \text{Energy transfer efficiency}$$

$$\text{Energy input} = 2.3 \text{ W/cm}^2 \times 780 \text{ cm}^2 \times 0.80 = 1,435 \text{ W/part}$$

Common polymers (polytetrafluoroethylene [PTFE], polyester, polyimide) have specific heats in the range of 1.1 to 1.3 J/g-°C and densities around 2.2 g/cm<sup>3</sup>. Specific heat capacities of the dry catalyst constituents are:

- Nafion: 4.2 J/g-°C
- Platinum: 0.13 J/g-°C
- Carbon black: 4.18 J/g-°C

The specific heat of the catalyst is:

$$\text{Catalyst specific heat} = (0.194 \times 4.2) + (0.323 \times 0.13) + (0.484 \times 4.18) = 2.88 \text{ J/g-}^\circ\text{C}$$

The volumes of dry catalyst for the anode and cathode per part are:

$$\text{Anode dry catalyst volume} = 780 \text{ cm}^2 \times 0.0008 \text{ cm} = 0.62 \text{ cm}^3$$

$$\text{Cathode dry catalyst volume} = 780 \text{ cm}^2 \times 0.0017 \text{ cm} = 1.33 \text{ cm}^3$$

The volume of substrate material (75-micron thickness) per part is:

$$\text{Membrane volume} = 780 \text{ cm}^2 \times 0.0075 \text{ cm} = 5.85 \text{ cm}^3$$

The heating dwell time for each is then (dry catalyst density = 0.515 g/cm<sup>3</sup>):

$$\text{Anode oven dwell time} = \frac{((2.2 \text{ g/cm}^3 \times 5.85 \text{ cm}^3 \times 1.2 \text{ J/g-}^\circ\text{C}) + (0.515 \text{ g/cm}^3 \times 0.62 \text{ cm}^3 \times 2.88 \text{ J/g-}^\circ\text{C})) \times 75^\circ\text{C}}{368 \text{ W}} = 3.33 \text{ sec/part}$$

$$\text{Cathode oven dwell time} = \frac{((2.2 \text{ g/cm}^3 \times 5.85 \text{ cm}^3 \times 1.2 \text{ J/g-}^\circ\text{C}) + (0.515 \text{ g/cm}^3 \times 1.33 \text{ cm}^3 \times 2.88 \text{ J/g-}^\circ\text{C})) \times 75^\circ\text{C}}{368 \text{ W}} = 3.55 \text{ sec/part}$$

For the calendaring process, the layers will be moving together, so the worst case heating time of 3.55 seconds is used to determine the required oven length. At a substrate speed of 5 m/min (8.33 cm/sec), the required heating length of about 0.30 meters, which can be accomplished using four 12-inch by 24-inch infrared panels (two for each layer).

At 5 m/min (300 m/hr), part throughput is:

$$\text{Parts per hour} = 300 \text{ m/hr} / 0.318 \text{ m} \times 2 \text{ parts per width} = 1,887 \text{ parts/hr}$$

Once the material layers are preheated, they are compressed between steel rollers that bond the catalyst decal layer to the membrane. The decal substrate is then peeled away from the decal layer and collected on a roll or in a bin. Total machine time to set up and produce 566,000 parts is:

$$\text{Anode machine time} = (1,070 \text{ setups} \times 0.5 \text{ hr/setup}) + (566,000 \text{ parts} / 1,887 \text{ parts/hr}) = 835.0 \text{ hrs}$$

Given an availability of 6,000 hours per year per machine, the number of coating systems required is:

$$\text{Roundup}(835.0 / 6,000) = 1 \text{ calendar machine}$$

Machine utilization is:

$$67.38 / 6,000 = 13.9\%$$

Machine rate was determined in accordance with Appendix A-1 as:

$$\text{In-house rate} = \$26.66 / 0.139 = \$191.80$$

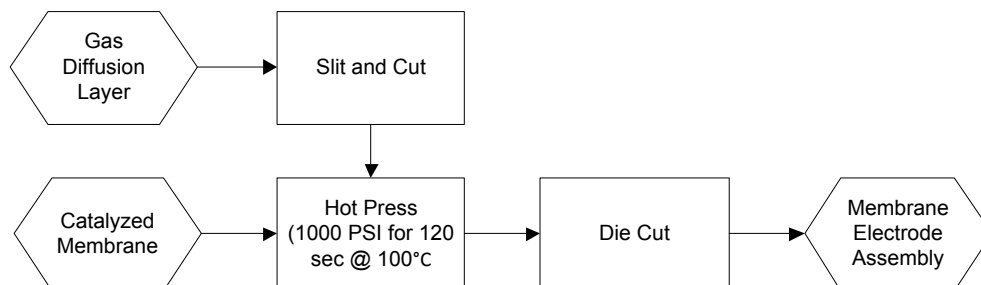
$$\text{Job shop rate} = 1.4 \times (\$26.66 / 0.65) = \$57.43$$

## Appendix A-7: PEM MEA Hot Pressing Process

### A-7.1 Model Approach

- GDL slit and cut
  - Machine setup labor cost based on number of setups required to process material and input labor time; default = 0.5 hour
  - Slit and cut in single machine operation
  - Operation cost based on parts per cutting operation and cutter cycle time
- Hot press operation
  - Machine setup labor cost based on number of setups required to process material and input labor time; default = 0.5 hour
  - Tooling cost based on input platen cost and life
  - Press cost based on part size, cycle time, platen energy, and standard machine rate

### A-7.2 Process Flow



### A-7.3 Background

Directed Technologies, Inc. (DTI) (James et al., 2010)<sup>23</sup> reported hot pressing conditions for MEA fabrication as 160°C for 90 seconds using heated platens of 0.5 meter wide by 1.5 meters long for processing 0.5-meter wide roll materials. They estimated a reset period of 3 seconds to open the press, index the materials, and reclose the press.

Therdthianwong et al. (2007)<sup>24</sup> found the most suitable hot pressing conditions for MEA fabrication to be 100°C and 1,000 psi (70 kg/cm<sup>2</sup>) for 2 minutes, stating that these conditions "...provided the highest maximum power density from the MEA and the best contact at the interfaces between the gas diffusion layer, the active layer, and the electrolyte membrane."

<sup>23</sup> B.D. James, J.A. Kalinoski, and K.N. Baum. 2010. *Mass Production Cost Estimation for Direct H<sub>2</sub> PEM Fuel Cell Systems for Automotive Applications: 2010 Update*. NREL Report No. SR-5600-49933. Directed Technologies, Inc. Available at [https://www1.eere.energy.gov/hydrogenandfuelcells/pdfs/dti\\_80kW\\_fc\\_system\\_cost\\_analysis\\_report\\_2010.pdf](https://www1.eere.energy.gov/hydrogenandfuelcells/pdfs/dti_80kW_fc_system_cost_analysis_report_2010.pdf).

<sup>24</sup> A. Therdthianwong, P. Manamayidthidarn, and S. Therdthianwong. 2007. Investigation of membrane electrode assembly (MEA) hot-pressing parameters for proton exchange membrane fuel cell. *Energy*, 32(12): 2401–2411.

## A-7.4 Preliminary Analysis

The 60-kW stack cells for this analysis will have a total active area of:

$$245 \text{ mm width} \times 318 \text{ mm length} = 780 \text{ cm}^2$$

The 60-kW stack cells for have a total MEA area of:

$$305 \text{ mm width} \times 378 \text{ mm length} = 1,153 \text{ cm}^2$$

The parts for this analysis were coated two across the 305 mm width for a total width of 610 mm.

### A-7.4.1 Material

GDL material is typically sold in either 0.4- or 0.8-meter widths and will be cut to the size of the active area plus a 2.5-mm margin on all sides, making the final dimensions 250 mm wide by 323 mm long. Three widthwise cells will take up 750 mm of GDL width, while two lengthwise cells will take up 646 mm of membrane width, so the widthwise orientation will result in less overall scrap. Assuming two GDL layers per MEA, the material length required will be:

$$\text{Material length} = ((2 \times 566,000 \text{ parts}) / 3 \text{ part widths/part width}) \times 323 \text{ mm part length} / 1,000 = 121,879 \text{ m}$$

The GDL material usage is calculated as:

$$\text{Material usage} = 0.8 \text{ m} \times 121,879 \text{ m} = 97,502 \text{ m}^2$$

The cost of the membrane is accounted for in a previous process step, and is not included as part of the hot pressing operation. GDL material cost is computed in accordance with Appendix A-2 as:

$$\text{Material cost} = \$55.81/\text{m}^2$$

### A-7.4.2 Setup

GDL material is available up to a maximum of 800-meter lengths, so that the number of setups required to run 1,132,000 parts is:

$$\text{Number of setups} = \text{Roundup}(\text{Carrier length (m)} / \text{Roll length (m)})$$

$$\text{Membrane: Number of setups} = \text{Roundup}(121,879 / 800) = 153$$

### A-7.4.3 GDL Slit and Cut

The GDL is cut to shape by slitting the 800-mm-wide bulk roll into strips of the pre-determined width of 250 mm, then cutting the strips to the required length of 323 mm. We assume a single machine operation with one full-time operator. The limiting rate is the shearing operation, which is estimated to be 50 cuts/minute, or 3,000 cuts per hour. Each shearing operation produces three parts, making the total number of required operations:

$$\text{Number of cuts} = \text{Roundup}((2 \times 566,000 \text{ parts}) / 3 \text{ parts/operation}) = 377,334 \text{ cuts}$$

At a rate of 300 cuts/hour, the total slitting and cutting time is:

$$\text{Total operation time} = 377,334 \text{ cuts} / 300 \text{ cuts/hr} = 126 \text{ hrs}$$

Given an availability of 6,000 hours per year per machine, the number of cutting stations required is:

$$\text{Roundup}(126 / 6,000) = 1 \text{ machine}$$

Machine utilization is:

$$126 / 6,000 = 2.1\%$$

Machine rate was determined in accordance with Appendix A-1 as:

$$\text{In-house rate} = \$28.09 / 0.021 = \$1,337.62$$

$$\text{Job shop rate} = 1.4 \times (\$28.09 / 0.65) = \$60.50$$

#### A-7.4.4 MEA Hot Press Tooling

Tooling consists of the heated platens, which generally consist of 2-inch to 2.5-inch-thick aluminum plates loaded with electric cartridge heaters spaced 3 inches (7.6 cm) apart. In 2010, A quote from Custom Engineering Co. (<http://www.customeng.com/platens/>) for heated platens used for compression molding of bipolar plates estimated the cost at approximately \$13,500/m<sup>2</sup> of platen area and included platen, base plate, and heater control electronics, estimated to be approximately \$15,650 in 2015 dollars. Standard platen widths are in 0.5 meter increments based on standard cartridge heater sizes. For the size and orientation of the parts, the platen width will be 1 meter. Due to the indexing and alignment required for the patch coated MEAs, the die length should be at least 1 meter long, and as close to a multiple of 378 mm as possible while allowing for proper cartridge heater spacing. Six cells arranged two widthwise by three lengthwise take up 114 cm of length. The number of heaters is calculated as:

$$\begin{aligned} \text{Number of heaters} &= \text{Roundup}(\text{Required length} / \text{Heater spacing}) = \\ &\text{Roundup}(114 \text{ cm} / 7.6 \text{ cm}) = 15 \end{aligned}$$

The overall die length is:

$$\text{Die length} = \text{Number of heaters} \times \text{Heater spacing} = 15 \times 7.6 \text{ cm} = 114 \text{ cm} = 1.14 \text{ m}$$

An engineering estimate for tool life based on heater life would be around 100,000 cycles. Using \$15,600/m<sup>2</sup> as a basis, and amortizing over a 5 year production life, the total annual tooling cost is:

$$\text{Annual tooling cost} = \frac{1}{5}(\text{Tooling cost} \times \text{Number of tools purchased})$$

where:

$$\text{Number of tools purchased} = \text{Roundup}(\text{Total production} / \text{Tool life})$$

$$\text{Total production} = \text{Annual production} \times 5$$

$$\begin{aligned} \text{Annual tooling cost} &= \frac{1}{5}((\$15,600/\text{m}^2 \times 1.14 \text{ m}^2) \times \text{Roundup}(((566,000 \text{ parts/yr} / 6 \text{ parts/cycle}) \times \\ &5 \text{ yrs}) / 100,000 \text{ cycles/tool})) = \$17,784.00 \end{aligned}$$

### A-7.4.5 MEA Hot Press

The hot press occurs in two steps: the material is moved into the press (handling time) and the press operation (clamp time). The material handling time is computed using an empirical formula developed by Boothroyd Dewhurst, Inc. (BDI) for automated handling with 2.8-second minimum as follows:

$$\text{Handling time} = \text{Layers placed} \times \text{Max}((0.012 \times (\text{Platen length (cm)} + \text{Platen width (cm)}) + 1.6), 2.8)$$

$$\text{Handling time} = 3 \text{ layers} \times \text{Max}((0.012 \times (114 + 100) + 1.6), 2.8) = 12.50 \text{ sec}$$

Omega (<http://www.omega.com/prodinfo/cartridgeheaters.html>) estimates 0.5-inch cartridge heaters to have a watt density of 50W per inch of heater length (about 20W per cm length). Calculating the total input heater power for the platen:

$$\text{Platen power input} = \text{Number of heaters} \times (\text{Platen width (cm)} \times 20 \text{ (W/cm)})$$

$$\text{Platen power input} = 15 \text{ heaters} \times (100 \text{ cm} \times 20 \text{ W/cm}) = 30 \text{ kW}$$

The heated platens need to maintain a temperature during pressing of about 100°C. A study conducted by the food service industry, indicates that 3-foot electric griddles with rated energy inputs of 8 to 16 kW demonstrate a 25% duty cycle in actual use.

Platen sizing allows for processing six parts per press cycle (two parts wide × three parts long). Throughput can be computed as:

$$\text{Parts/hr} = 6 \text{ parts/cycle} / ((124 + 12.5) / 3,600) \text{ hrs/cycle} = 158.2 \text{ parts/hr}$$

The total machine time for processing and setup is:

$$\text{Machine processing time} = (566,000 \text{ parts} / 158.2 \text{ parts/hr}) + (1,070 \text{ setups} \times 0.5 \text{ hr/setup}) = 318.6 \text{ hrs}$$

Total machine labor time for processing and setup:

$$\text{Machine labor time} = 1 \text{ operator/machine} \times 318.6 \text{ hrs} = 4,112.7 \text{ hrs}$$

Machine utilization is:

$$4,112.7 / 6,000 = 68.5\%$$

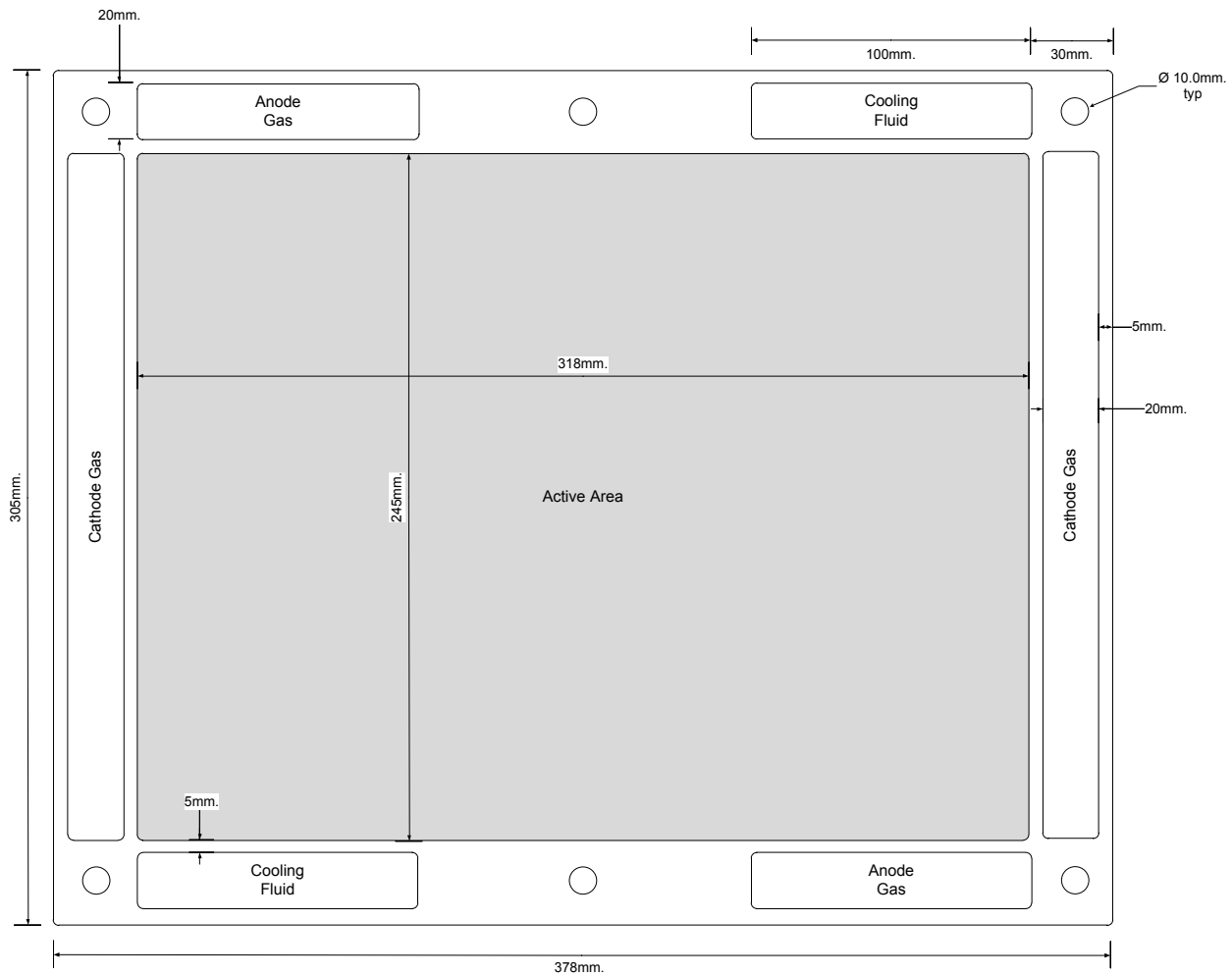
Machine rate was determined in accordance with Appendix A-1 as:

$$\text{In-house rate} = \$52.58 / 0.685 = \$76.71$$

$$\text{Job shop rate} = 1.4 \times (\$52.58 / 0.65) = \$113.25$$

### A-7.4.6 MEA Die Cutting

Following hot pressing, the MEA is die cut to final shape as shown:



### A-7.4.7 Tooling

The primary factor contributing to steel rule die cost is the total cutting length of the die. Assuming a platen size equal to that of the hot pressing operation, the total number of cavities is six (two widthwise by three lengthwise). The outer cell perimeters will require a total length of :

$$\text{Outer perimeter length} = 2 \times (2 \times 378.4) + 2 \times (3 \times 305) = 3,343.6 \text{ mm}$$

The inner perimeters are shared and will require a total length of:

$$\text{Inner perimeter length} = 2 \times (2 \times 305) + 1 \times (3 \times 378.4) = 2,355.1 \text{ mm}$$



Internal features are unique to each cell cavity and include the fluid and gas openings, and the tie rod holes, which require a total die length of:

$$\text{Feature length} = 4 \times (2 \times (100 + 20)) + 2 \times (2 \times (245 + 20)) + 6 \times (\pi \times 10) = 2,208.5 \text{ mm}$$

Therefore the total die cutting length is:

$$\text{Die cutting length (mm)} = 3,343.6 + 2,425.6 + (6 \times 2,208.5) = 18,949 \text{ mm}$$

A rough quote of approximately \$230 was obtained from steel-rule-dies.com for a two-cavity die with a similar configuration.

$$\text{Tooling rate} = \$230 / (2 \times 2,706) \text{ mm} = \$0.04/\text{mm}$$

Information obtained from Mag-Knight ([www.mag-knight.com/diecutting/Steel\\_Rule\\_Dies.htm](http://www.mag-knight.com/diecutting/Steel_Rule_Dies.htm)) indicates that dies used to cut softer materials have an expected life of about 30,000 hits. For a six-cavity die (six parts per cycle) and amortizing over a 5-year production life, the total annual tooling cost is:

$$\text{Annual tooling cost} = \frac{1}{5}(\text{Tooling cost} \times \text{Number of tools purchased})$$

where:

$$\text{Number of tools purchased} = \text{Roundup}(\text{Total production} / \text{Tool life})$$

$$\text{Total production} = \text{Annual production} \times 5$$

$$\text{Annual tooling cost} = (18,949 \text{ mm/die} \times \$0.04/\text{mm}) / 5 \text{ years} \times \text{Roundup}(((566,000 \text{ parts/year} / 6 \text{ parts/cycle}) \times 5 \text{ years}) / 30,000 \text{ cycles/tool}) = \$2,425.47$$

#### A-7.4.8 Setup

The total number of setup operations will be dictated by the length of the membrane at 100 meters. As shown above, the number of roll setups is 1,070. Assuming 0.5 hour per setup, the total setup time is:

$$\text{Setup time} = 1,070 \times 0.5 \text{ hr} = 535 \text{ hrs}$$

#### A-7.4.9 Die Cutting

The primary energy input to run the press is hydraulic pump motor power. The total force required to cut the material is the total shear area (cutting length  $\times$  material thickness) multiplied by the material shear strength. Shear strength data for Nafion is not readily available, but polymer-based materials typically range from 8,000 to 11,000 pounds per square inch (psi) (55 to 76 N/mm<sup>2</sup>). Assuming the worst case shear strength, and using the material thickness of 0.7 mm, the total required press force per part is calculated as:

$$\text{Press force} = \text{Die cutting length (mm)} \times \text{Material thickness (mm)} \times \text{Shear strength (N/mm}^2\text{)}$$

$$\text{Press force} = 19,020 \text{ mm/die} \times 0.7 \text{ mm} \times 76 \text{ N/mm}^2 = 1,012 \text{ kN}$$

A survey of 15- to 100-ton (150- to 1,000-kN) fast-acting die cutting presses found that the motor power required to operate the press fell in the range of 0.015 – 0.025 kW/kN. Assuming a 50% capacity margin and using the upper end of the motor power rating, the maximum required press energy input is:

$$\text{Press energy} = 1,012 \text{ kN} \times 1.5 \times 0.025 \text{ kW/kN} = 37.95 \text{ kW}$$

Typical die cutting press speed ranges from 30 to 60 cycles/min (1,800 to 3,600 cycles/hour). Assuming the slower speed, the time to process a batch of parts is calculated as

$$\text{Processing time} = 566,000 \text{ parts} / 6 \text{ parts/cycle} / 1,800 \text{ cycles/hour} = 52.41 \text{ hours}$$

The total machine time for processing and setup is:

$$\text{Machine processing time} = 52.41 + 535.5 = 587.9 \text{ hours}$$

Given an availability of 6,000 hours per year per machine, the number of presses required is:

$$\text{Roundup}(587.9 / 6,000) = 1 \text{ machine}$$

Machine utilization is:

$$587.9 / 6,000 = 9.8\%$$

Machine rate was determined in accordance with Appendix A-1 as:

$$\text{In-house rate} = \$30.15 / 0.098 = \$307.65$$

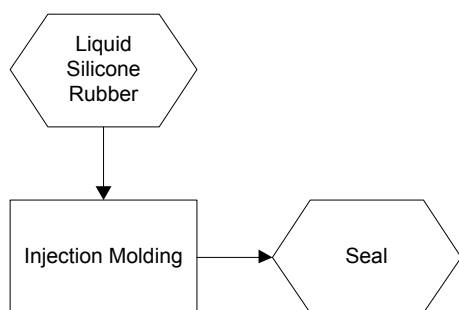
$$\text{Job shop rate} = 1.4 \times (\$30.15 / 0.65) = \$64.94$$

## Appendix A-8: PEM Seal Injection Molding Process

### A-8.1 Model Approach

- Use standard Boothroyd Dewhurst, Inc. (BDI) injection molding cost analysis

### A-8.2 Process Flow



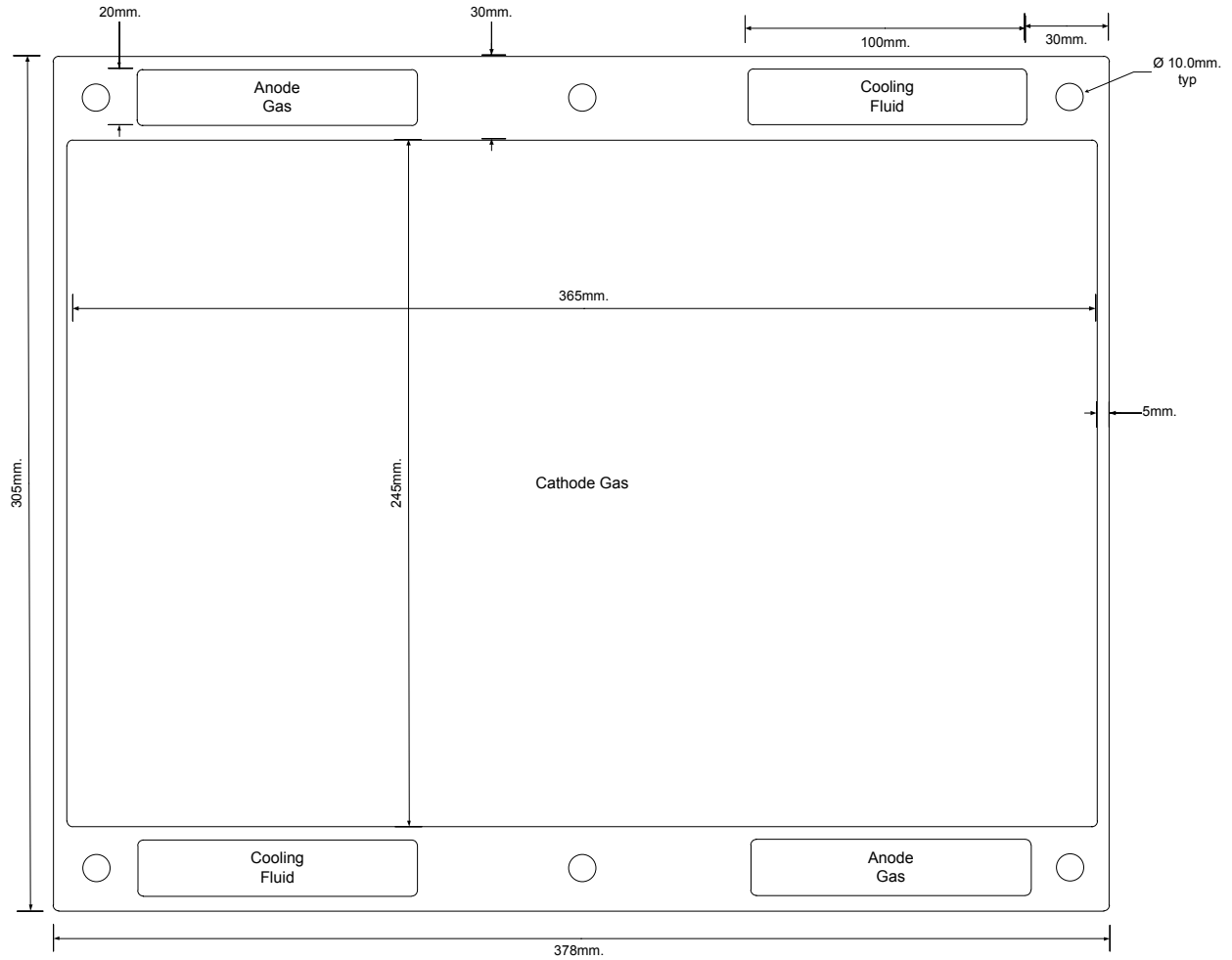
### A-8.3 Background

The BDI software provides preprogrammed cost models for the injection molding process used to manufacture the fuel cell stack coolant seals. The process selection was liquid silicon injection molding.

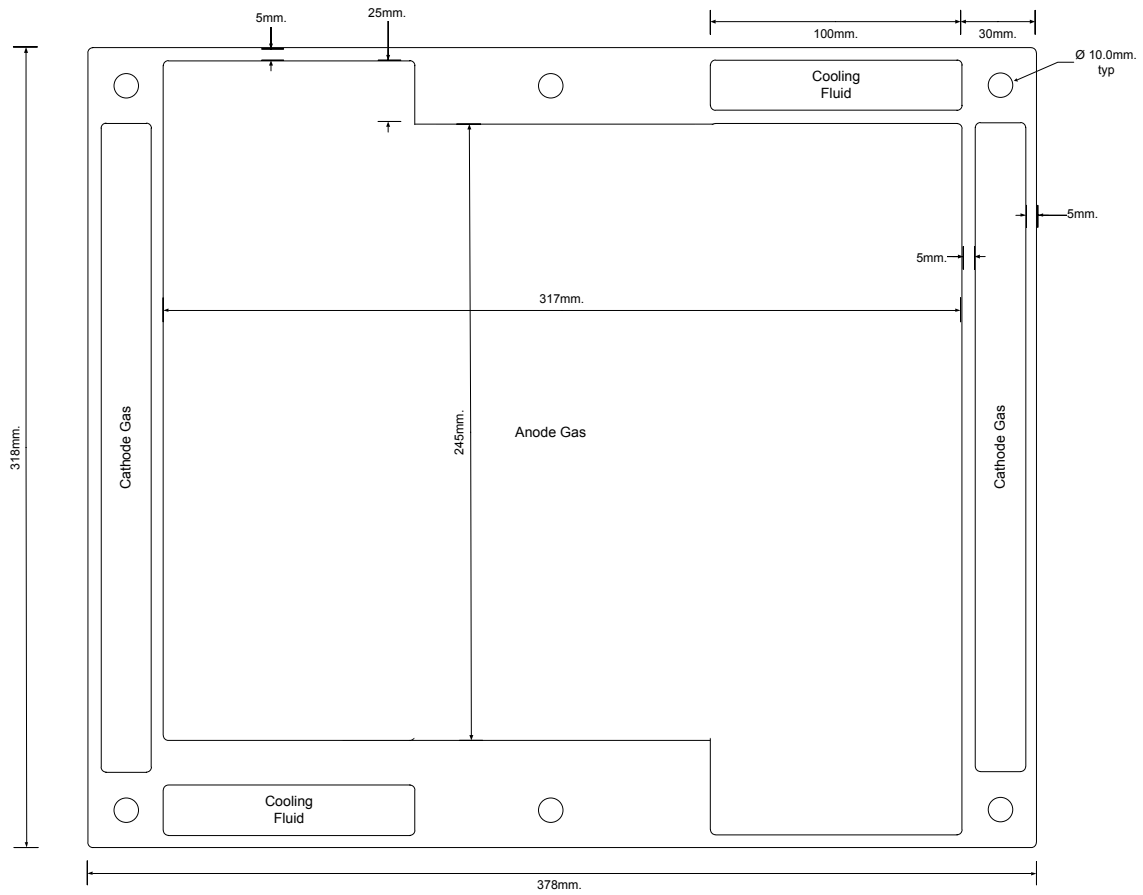
### A-8.4 Preliminary Analysis

The stack contains three seals (cathode, anode and cooling) per cell plus two cathode seals on each end of the stack. To manufacture 1,000 60-kW stacks consisting of 283 cells each requires a total of 566,000 each anode and cooling seals, and 570,000 cathode seals. The seal features and dimensions are shown below for reference.

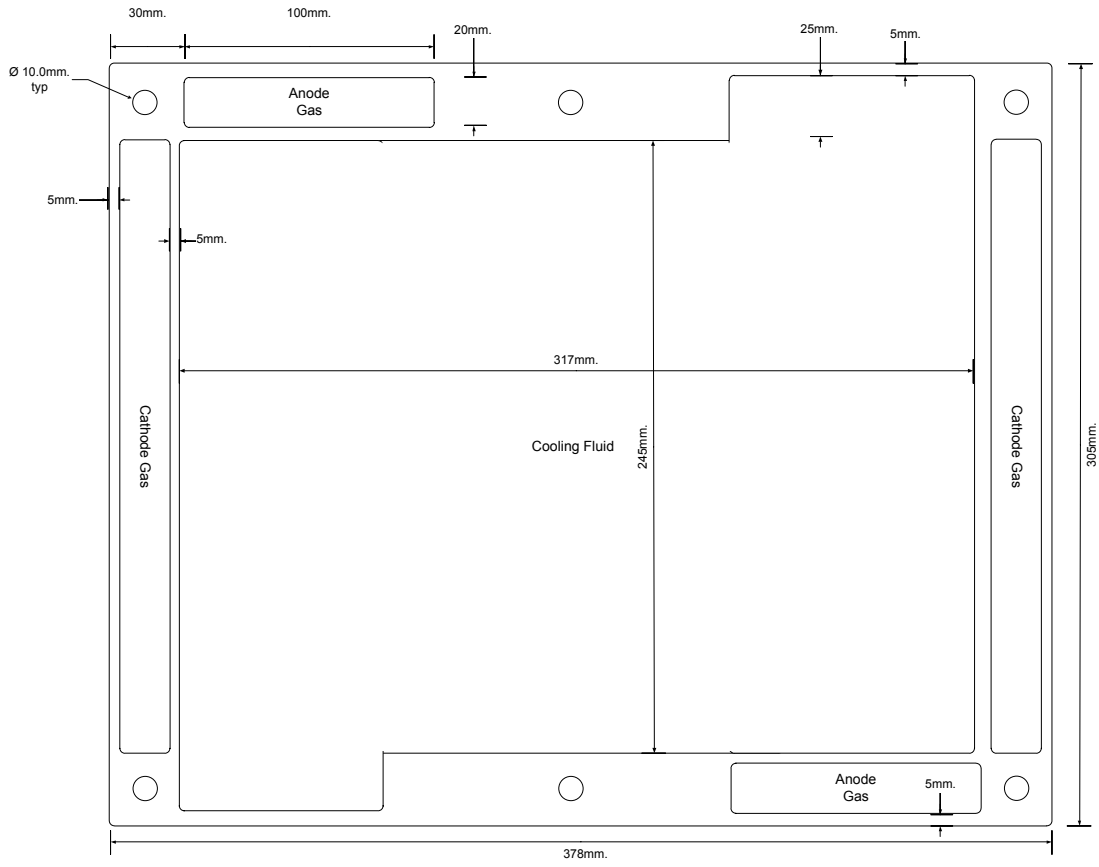
### A-8.4.1 Cathode Seal



### A-8.4.2 Anode Seal

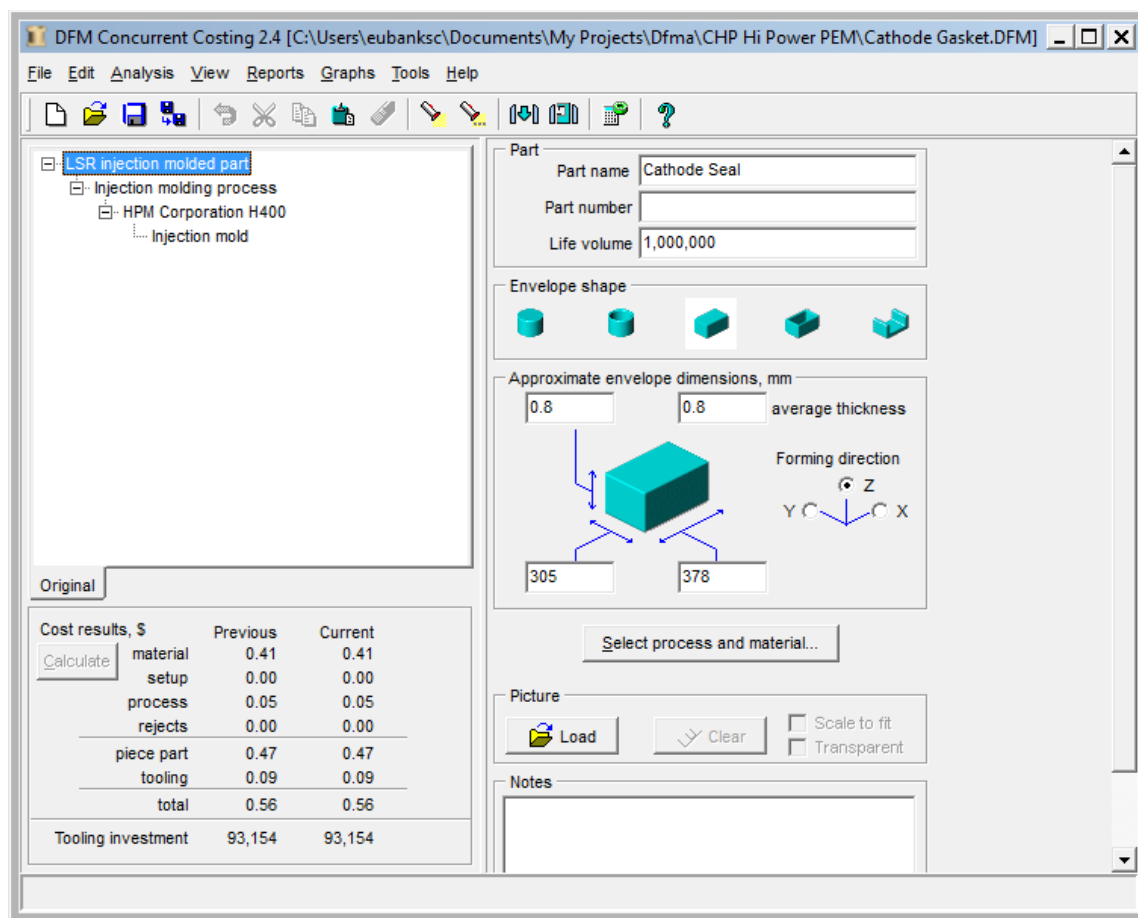


### A-8.4.3 Cooling Seal



## A-8.5 DFM Software Analysis

### A-8.5.1 Cathode Seal



The BDI estimate for the 60-kW cathode seal is a 1.5-hour machine setup time, and calculates the total manufacturing cycle time as 9.16 sec for a four-cavity mold, making the total machine time for annual production of 1,000 stacks:

$$\text{Machine time} = (9.16 \text{ sec/cycle} / 4 \text{ parts/cycle} / 3,600) \times 570,000 \text{ parts} + 1.5 = 364.1 \text{ hrs}$$

Assuming one full-time operator per two molding machines, the total machine labor time is equal to half the machine time = 364.1 hours.

The BDI estimate for material weight per part is 0.019 kg, making total annual material usage:

$$\text{Material usage} = 0.019 \text{ kg/part} \times 570,000 \text{ parts} = 10,830 \text{ kg}$$

Tooling cost is \$93,154 and is assumed to be capable of producing 1 million parts. Amortizing over a 5-year production life, the total annual tooling cost is:

$$\text{Annual tooling cost} = \frac{1}{5}(\text{Tooling cost} \times \text{Number of tools purchased})$$

where:

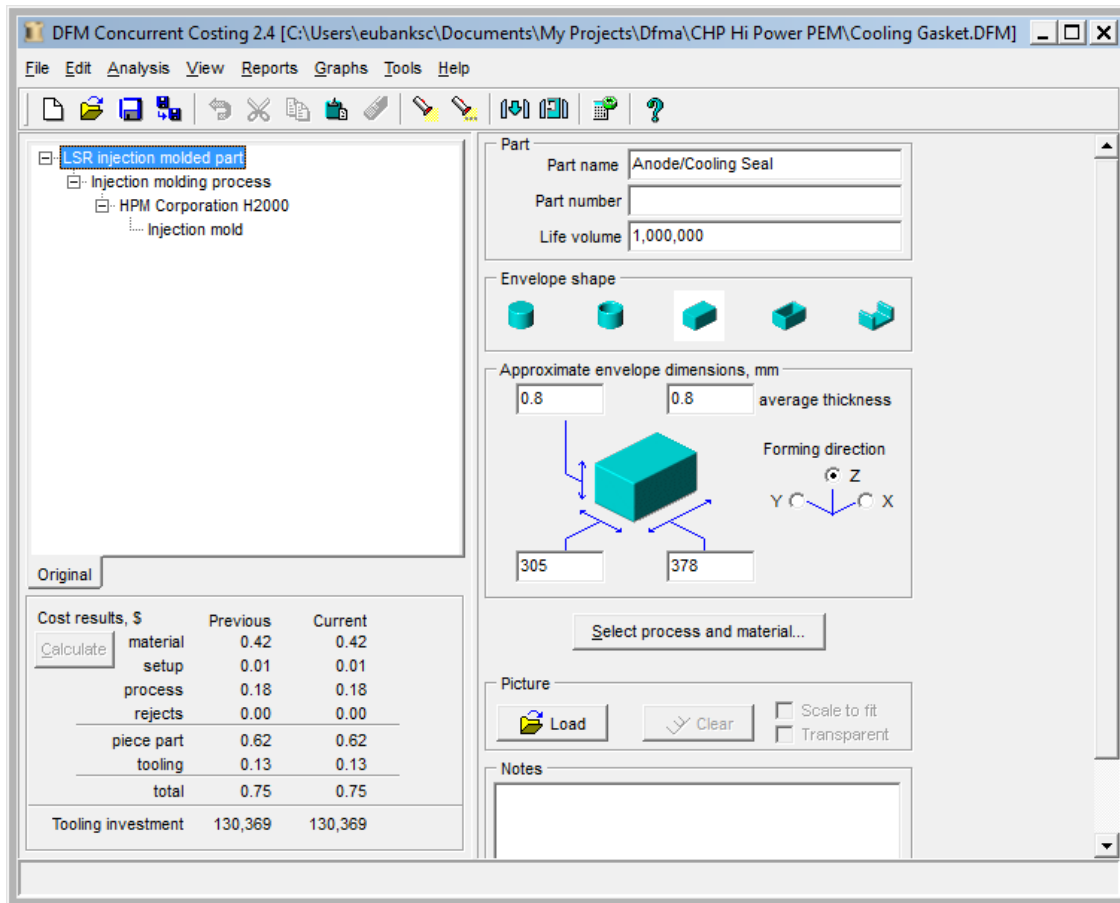
$$\text{Number of tools purchased} = \text{Roundup}(\text{Total production} / \text{Tool life})$$

$$\text{Total production} = \text{Annual production} \times 5$$

$$\text{Annual tooling cost} = \frac{1}{5} (\$93,154 \times \text{Roundup}((570,000 \text{ parts/yr} \times 5 \text{ yrs}) / 1,000,000 \text{ parts/tool})) = \$55,892.4$$

### A-8.5.2 Anode/Cooling Seal

Note that the anode and cooling seals are the same design, but are installed by flipping along the vertical center axis and are therefore analyzed by the DFM software as the same seal, as shown below:





The BDI estimate for the anode/cooling seal is a 2.5-hour machine setup time, and calculates the total manufacturing cycle time as 10.28 seconds for a four-cavity mold, making the total machine time for annual production of 1,000 stacks:

$$\text{Machine time} = (10.28 \text{ sec/cycle} / 4 \text{ parts/cycle} / 3,600) \times 1,132,000 \text{ parts} + 2.5 = 810.6 \text{ hrs}$$

Tooling cost for the anode/cooling seal is \$132,369 and is assumed to be capable of producing 1 million parts. Amortizing over a 5-year production life, the total annual tooling cost is:

$$\text{Annual tooling cost} = \frac{1}{5}(\text{Tooling cost} \times \text{Number of tools purchased})$$

where:

$$\text{Number of tools purchased} = \text{Roundup}(\text{Total production} / \text{Tool life})$$

$$\text{Total production} = \text{Annual production} \times 5$$

$$\begin{aligned} \text{Annual tooling cost} &= \frac{1}{5}((\$132,369) \times \text{Roundup}((1,132,000 \text{ parts/yr} \times 5 \text{ yrs}) / \\ &1,000,000 \text{ parts/tool})) = \$158,842.80 \end{aligned}$$

Total machine time to mold the three seals is 1,174.7 hours, making the machine utilization:

$$\text{Utilization} = 1,174.7 / 6,000 = 19.6\%$$

Machine rate was determined in accordance with Appendix A-11 as:

$$\text{In-house rate} = \$26.04 / 0.196 = \$132.99$$

$$\text{Job shop rate} = 1.4 \times (\$26.04 / 0.65) = \$56.09$$

Assuming one full-time operator per two molding machines, the total machine labor time is equal to half the machine time = 587.4 hours.

The BDI estimate for the anode/cooling seal material weight per part is 0.020 kilogram (kg), making total annual material usage:

$$\text{Material usage} = 0.020 \text{ kg/part} \times 1,132,000 \text{ parts} = 22,640 \text{ kg}$$

The three gaskets require a total of 33,470 kg of material. The material cost was determined in accordance with Appendix A-12 as:

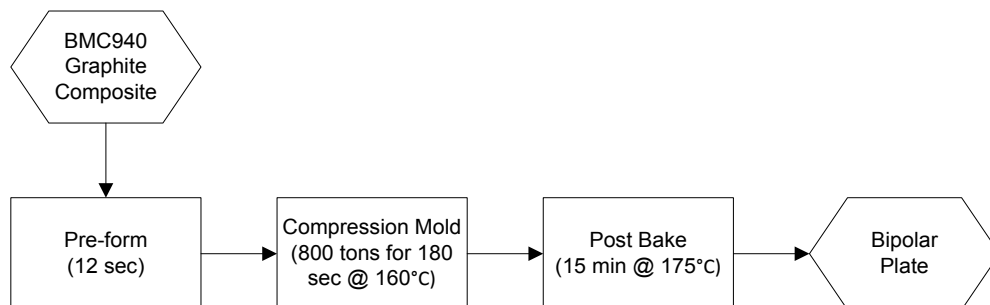
$$\text{Material cost} = \$15.51/\text{kg}$$

## Appendix A-9: PEM Bipolar Plate Compression Molding Process

### A-9.1 Model Approach

- Setup operation
  - Machine setup labor time based on user input
  - Tooling cost based on input insert and platen cost and life
- Pre-form operation
  - Measure and pre-form labor time based on user input labor time
  - Part material unit cost based on usage
- Compression mold
  - Part handling time based on part size per BDI formula; 4 second minimum
  - Press processing time based on part size and cycle time
  - Compute machine utilization
- Post bake
  - Part handling time based on part size per BDI formula and throughput; 4-second minimum

### A-9.2 Process Flow



### A-9.3 Background

A supplier of composite bipolar plates for PEM fuel cell stacks provided the following information regarding their process:

- Process requires a special press
  - High speed – 30 inches per second (ips)
  - High tonnage – 800-ton capacity to produce one part per cycle
  - Cure time in the press is 120 to 230 seconds
  - Allow 5% material overage

- Tooling costs
  - Inserts: \$45,000 to \$50,000 produces about 100,000 parts
  - Base: \$50,000 (reusable)
- Molding material supplied by Bulk Molding Compounds (BMC)
  - Has a consistency like sand
  - From BMC940 specification sheet
    - Cure time: 30 to 60 seconds
    - Mold temp: 300 to 320°F (149 to 160°C)
    - Recommended tonnage: >40MPa on projected part area
    - Press close speed: <2 seconds after material begins flowing
    - Post-mold bake at 350°F for 15 minutes

### A-9.4 Preliminary Analysis

Unlike injection molding, compression molding requires that a pre-measured, usually pre-formed, and generally preheated amount of material be loaded into the mold insert prior to pressing. Given the stated consistency of the material, we will assume a manual weighing process followed by a manual packing process to get the material into the rough rectangular shape of the plate. No material preheating was mentioned by the manufacturer or the material spec sheet.

The bipolar plates for this analysis will be:

$$305 \text{ mm width} \times 378.4 \text{ mm length} = 1,154 \text{ cm}^2$$

Process values will be calculated based on annual production of 1,000 60-kW stacks per year. The 60-kW stack requires 284 anode bipolar plates and 284 cathode bipolar plates, requiring annual production of 568,000 of each type of plate.

#### A-9.4.1 Setup

We will assume one full setup per run of parts. This would include such things as platen and die installation, die alignment, work station setup and maintenance, and operational checks. An analogous setup operation in the BDI DFMA<sup>®</sup> software is for a powder metallurgy compaction press, for which the default value is 4 hours.

#### A-9.4.2. Material Cost

Flow channels cut into the plates are generally 1 mm deep. The cathode bipolar plate has flow channels cut into one side of the plate, indicating a plate depth of around 2 mm. The anode bipolar plate has flow channels cut into both sides of the plate to accommodate anode gas flow on one side, and cooling fluid flow on the other, indicating a plate depth of around 3 mm. Given a material density of 1.9 g/cm<sup>3</sup> (BMC940 spec sheet) and 5% overage allowance, the total annual material required before scrap is:

$$\text{Cathode plate material required} = 1.9 \text{ g/cm}^3 \times 0.001 \text{ kg/g} \times (1154 \times .2) \text{ cm}^3 \times 1.05 \times 568,000 \text{ parts} = 261,533 \text{ kg}$$

$$\text{Anode plate material required} = 1.9 \text{ g/cm}^3 \times 0.001 \text{ kg/g} \times (1154 \times .3) \text{ cm}^3 \times 1.05 \times 568,000 \text{ parts} = 392,300 \text{ kg}$$

Based on quotes from BMC, the material cost can be estimated in accordance with Appendix A-2 as:

$$\text{Material cost} = \$2.066/\text{kg}$$

### A-9.4.3. Compression Molding Press Time

The material specification recommends molding pressure in excess of 40 MPa (0.4 tons/cm<sup>2</sup>) on the projected part area:

$$\text{Tonnage} = 0.4 \text{ tons/cm}^2 \times 1154 \text{ cm}^2 = 461.6 \text{ tons}$$

Discussions with a bipolar plate manufacturer indicate the use of a special fast-acting 800-ton press. Moving the capacity up to 1,000 tons, it is feasible to mold two plates per cycle (923.2 tons).

The primary energy input to run the press is hydraulic motor power. Surveying press manufacturers Wabash, Beckwood, and Karunanand, the hydraulic motor size for 800-ton presses appears as either 30 or 50 HP, but lists pressing speeds of only 20 inches per minute (ipm) (0.3 inches per second [ips]). Cylinder bore sizes are listed as 26-inch to 30-inch diameter. To move a 30-inch diameter cylinder at 30 ips requires a pump delivery of:

$$\text{Flow rate} = (30 \text{ in})^2 \times (\pi / 4) \times 30 \text{ in/sec} \times 60 \text{ sec/min} \times 0.004 \text{ gal/in}^3 = 5,089 \text{ gpm}$$

This is beyond the practical limit of most high-performance hydraulic gear pumps, which tend to have maximum flow rates of 90 gallons per minute (gpm) at 100-HP input power and 2,500 pounds per square inch (psi) working output pressure (reference Commercial Intertech P365 series hydraulic pumps).

To supply 1,000 tons of force using a 30-inch cylinder requires a delivery pressure of:

$$\text{Pressure} = 1,000 \text{ tons} \times 2,240 \text{ lbs/long ton} / ((30 \text{ in})^2 \times (\pi / 4)) = 3,169 \text{ psi}$$

For this analysis, we will assume two 100-HP (75-kW) pumps feeding a set of staged cylinders (e.g., two smaller-diameter cylinders to provide the necessary pressing speed, and one larger cylinder to develop the required pressure). To provide some limited scalability, we assume that 150 kilowatts (kW) of input power is required to mold two 1,154-cm<sup>2</sup> bipolar plates, giving a factor of approximately 0.130 kW/cm<sup>2</sup> of plate area.

Total press cycle time is the sum of part handling time, press actuation time, and press dwell time. An empirical formula developed by Boothroyd Dewhurst, Inc. (BDI) calculates a quantity called part girth, then calculates a theoretical total handling time (both load and unload) with a minimum value of 4 seconds, as follows:

$$\text{Part girth} = \text{Part length} + \text{Part width} + \text{part depth}$$

$$\text{Handling time} = \text{Max}((0.60714 \times (\text{Part girth} / 25.4) - 4.57143), 4)$$

$$\text{Cathode plate handling time} = \text{Max}((0.60714 \times ((305 + 378.4 + 3) / 25.4) - 4.57143), 4) = 11.8 \text{ sec}$$

$$\text{Anode plate handling time} = \text{Max}((0.60714 \times ((305 + 378.4 + 6) / 25.4) - 4.57143), 4) = 11.9 \text{ sec}$$

For an actuation time of 10 seconds, dwell time of 230 seconds, and handling times shown above, the total cycle time is:

$$\text{Cathode plate cycle time} = ((2 \times 11.8) + 230 + 10) = 263.6 \text{ sec/cycle} = 0.0732 \text{ hours/cycle}$$

$$\text{Anode plate cycle time} = ((2 \times 11.9) + 230 + 10) = 263.8 \text{ sec/cycle} = 0.0732 \text{ hours/cycle}$$

Throughput is calculated as:

$$\text{Parts/hr} = 2 \text{ parts/cycle} / 0.0732 \text{ hrs/cycle} = 26.57 \text{ parts/hr}$$

Since throughput for each type of plate is essentially the same, we can calculate the total time required to process both sets of plates (222,000 parts) as:

$$\text{Press machine time} = 1,136,000 \text{ parts} / 26.57 \text{ parts/hr} + (2 \times 4) \text{ hr setup} = 42,763 \text{ hrs}$$

Given an availability of 6,000 hours per year per machine, the number of presses required is:

$$\text{Roundup}(42,763 / 6,000) = 8 \text{ machines}$$

Machine utilization across the 8 machines is:

$$42,763 / (8 \times 6,000) = 89.1\%$$

Machine rate was determined in accordance with Appendix A-1 as:

$$\text{In-house rate} = \$64.70 / 0.891 = \$65.31$$

$$\text{Job shop rate} = 1.4 \times (\$64.70 / 0.65) = \$139.35$$

#### A-9.4.4 Tooling Cost

Tooling consists of the mold inserts and the heated platens. Contact with Custom Engineering Co. (platens.com) indicates that platens in the size range required will generally consist of 2-inch to 2.5-inch-thick aluminum plates loaded with electric cartridge heaters spaced 3 inches (7.6 cm) apart. Costs will be in the range of \$10,000 for a 7,500-cm<sup>2</sup> platen (\$1.333/cm<sup>2</sup>), and \$3,500 for the controller. No life was provided for the platens. An engineering estimate based on heater life would be around 500,000 cycles.

Assuming two plates per cycle with 50-mm margin between and around each plate, the total platen area is:

$$\text{Platen width} = ((2 \times 305 \text{ mm}) + 150 \text{ mm}) = 760 \text{ mm}$$

$$\text{Platen length} = ((2 \times 378.4 \text{ mm}) + 150 \text{ mm}) = 907 \text{ mm}$$

$$\text{Platen area} = 760 \text{ mm} \times 907 \text{ mm} = 6893 \text{ cm}^2$$

$$\text{Platen cost} = (6893 \text{ cm}^2 \times \$1.333/\text{cm}^2) + \$3,500 = \$12,688$$

Using the BDI DFMA® software, the tooling cost for a two-part insert was estimated at \$150,000 with a 100,000-cycle life. Amortizing over a 5-year production life, the total annual tooling cost is:

$$\text{Annual tooling cost} = \frac{1}{5}(\text{Tooling cost} \times \text{Number of tools purchased})$$

where:

$$\text{Number of tools purchased} = \text{Roundup}(\text{Total production} / \text{Tool life})$$

$$\text{Total production} = \text{Annual production} \times 5$$

$$\text{Annual insert tooling cost} = \frac{1}{5} ((\$150,000) \times \text{Roundup}((1,136,000 \text{ parts/year} / 2 \text{ parts/cycle} \times 5 \text{ years}) / 100,000 \text{ parts/tool})) = \$870,000$$

$$\text{Annual insert tooling cost} = \frac{1}{5} ((\$12,668) \times \text{Roundup}((1,136,000 \text{ parts/year} / 2 \text{ parts/cycle} \times 5 \text{ years}) / 500,000 \text{ parts/tool})) = \$15,202$$

#### A-9.4.5 Heated Platen Energy

Omega (<http://www.omega.com/prodinfo/cartridgeheaters.html>) estimates 0.5-inch cartridge heaters to have a watt density of 50 watts (W) per inch of heater length (about 20 W per centimeter length). Calculating the total input heater power for the platen based on 3-inch (7.6-cm) heater spacing:

$$\text{Number of heaters} = \text{Ceiling}(\text{Platen width (cm)} / 7.6)$$

$$\text{Platen power input} = \text{Number of heaters} \times (\text{Platen width (cm)} \times 20 \text{ (W/cm)})$$

$$\text{Number of heaters} = \text{Ceiling}(76.0 \text{ cm} / 7.6 \text{ cm}) = 10$$

$$\text{Platen power input} = 10 \text{ heaters} \times (90.7 \text{ cm} \times 20 \text{ W/cm}) = 18.2 \text{ kW}$$

The mold insert will be attached to heated platens that are capable of maintaining the proper mold temperature of up to 160°C. A study conducted by the food service industry indicates that 3-foot electric griddles with rated energy inputs of 8 to 16 kW demonstrate a 25% duty cycle in actual use. Given that the surface areas, power densities, and manual work flow are comparable, we will assume a similar usage profile.

#### A-9.4.6 Post Bake Cycle

The BMC940 material spec sheet calls for a post bake at 350°F (177°C) for 15 minutes after the part reaches temperature. For a batch-type oven, the strategy is to rack parts in quantities that permit racks to be interchanged in 15-minute intervals. Given a throughput of 26.57 parts/hour and that we are molding parts in pairs, we can expect a rack size of:

$$\text{Parts per bake cycle} = (26.57 \text{ parts/hr} \times 0.25 \text{ hr}) = 6.64 \text{ parts per bake cycle} \cong 6 \text{ parts/rack}$$

For this level of production, we will assume that an industrial bench oven will provide sufficient capacity. One example is the Grieve NBS-400 with 4-kW heating capacity capable of reaching 400°F (204°C), 28-inch x 24-inch x 18-inch (0.2-m<sup>3</sup>) working volume with seven-shelf capacity, and 2-inch (5-cm) rockwool insulation ( $k = 0.045 \text{ W/m}^\circ\text{C}$ ) on 304 stainless steel construction. A study conducted by the food service industry indicates that “deck ovens” demonstrate a 20% duty cycle in actual use. Given that the usage scenarios are comparable, we will assume a similar usage profile.

For the post bake step, we assume that parts will be racked to facilitate swapping parts at intervals equal to the bake time in order to minimize oven heat loss. A rack of two parts will fit onto one shelf. Assuming a rack depth of 10 mm and 50 mm part margin, an estimate of the rack handling time is:

$$\text{Rack girth} = (\text{Parts per rack} \times (\text{Part width (mm)} + 50)) + (\text{Part length (mm)} + 50) + 10$$

$$\text{Rack girth} = (2 \times (305 + 50)) + (378.4 + 50) + 10 = 1,149$$

$$\text{Rack handling time} = \text{Max}((0.60714 \times ((1,149) / 25.4) - 4.57143), 4) = 22.9 \text{ sec}$$

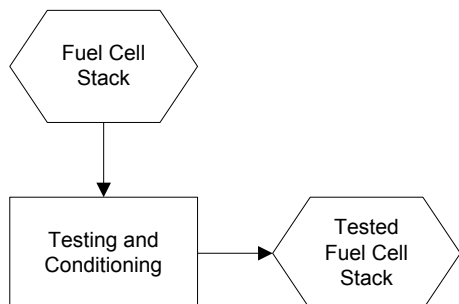
Given that the rack handling time is about 10% of the press dwell time, no additional labor time is incurred by the press operator to complete the tasks associated with the post-bake operation.

## Appendix A-10: PEM Stack Testing and Conditioning Process

### A-10.1 Model Approach

- Test and condition fuel cell stack

### A-10.2 Process Flow



### A-10.3 Background

Following assembly, the PEM stack is tested and conditioned to determine its fitness for installation into the system. The total test time is assumed to be 2.5 hours. Total H<sub>2</sub> consumption at full power is determined from the equation:

$$\text{H}_2 \text{ consumption mol/sec} = (\text{Current} \times \text{Cells}) / (2 \times \text{H}_2 \text{ Cal/mol})$$

For a 60-kW stack current of 312 amperes (A) and a cell count of 283 cells, we have:

$$\text{H}_2 \text{ consumption g/sec} = 312 \text{ A} \times 283 \text{ Cells} / (2 \times 96,485 \text{ Cal/mol}) = 0.458 \text{ mol/sec}$$

Converting to liters per minute (l/min):

$$\text{H}_2 \text{ consumption l/min} = 1.2 \times 0.0456 \text{ mol/sec} \times 60 \times 2.016 / 0.0899 = 73.63 \text{ l/min}$$

Air is supplied in a stoichiometric ratio of 1.2:2, resulting in required air flow of:

$$\text{Air flow l/min: } (2 / 1.2) \times 73.63 \text{ l/min} = 1231 \text{ l/min}$$

### A-10.4 Preliminary Analysis

Assuming setup and teardown of the stack test stand requires 0.5 hour for one operator per run, the setup time per production run of 2,000 stacks is:

$$\text{Setup labor time} = 0.5 \text{ hours/stack} \times 2,000 \text{ stacks} = 1,000 \text{ hrs}$$



The Fuel Cell and Hydrogen Energy Association placed the 2010 nation-wide average cost of hydrogen in bulk liquid form at about \$7.83 per kilogram (kg) for usage levels of 700 to 1,400 kg/month. Internet quotes indicate a price of about \$5.93/kg for bulk purchases of 30,000 kg or more. The mass of 1 mole hydrogen gas (H<sub>2</sub>) = 2 grams (g), so the mass of 22.4 liters (stp) of H<sub>2</sub> is 2 g.

$$1 \text{ kg of H}_2 = (1,000 / 2) \times 22.4 \text{ liters} = 11,200 \text{ liters} = 11.2 \text{ m}^3$$

At 100% rated power, the total material usage of the hydrogen is:

$$\text{Full power material usage} = ((73.63 \text{ l/min} / 1,000 \text{ l/m}^3) / 11.2 \text{ m}^3/\text{kg}) \times 60 \text{ min/hr} = 0.394 \text{ kg/hr}$$

During the 2.5-hour test, we assume a conditioning and test regimen as follows:

25% rated power for 1 hr

100% rated power for 0.5 hr

25% rated power for 1 hr

Therefore, the total material usage of the hydrogen is:

$$\text{H}_2 \text{ usage} = 3.958 \text{ kg/hr} \times ((0.25 \times 1.0 \text{ hr}) + (1.0 \times 0.5 \text{ hr}) + (0.25 \times 1.0 \text{ hr})) \times 2,000 \text{ stacks} = 7,916 \text{ kg}$$

The material cost before scrap can be estimated in accordance with Appendix A-2 as:

$$\text{Material cost} = \$8.96/\text{kg}$$

We will assume that one test station (150-kW load bank) is capable of supporting two stacks during testing, making the total machine time for setup and test:

$$\text{Testing machine time} = ((2.5 \text{ hrs/stack} / 2) + (0.5 \text{ hrs/stack})) \times 2,000 \text{ stacks} = 3,500 \text{ hrs}$$

We will assume that one operator can cover three testing stations, making the total labor time:

$$\text{Testing labor time} = (2.5 \text{ hrs/stack} / 3) \times 2,000 \text{ stacks} = 1,667 \text{ hrs}$$

Machine utilization is:

$$3,500 / 6,000 = 58.3\%$$

Machine rate was determined in accordance with Appendix A-1 as:

$$\text{In-house rate} = \$17.64 / 0.583 = \$30.26$$

We will assume that one operator can cover three testing stations, making the total labor time:

$$\text{Testing labor time} = (2.5 \text{ hrs/stack} / 3) \times 2,000 \text{ stacks} = 833.3 \text{ hrs}$$

The testing process is subject to a failure rate estimated at around 5%. Stacks failing test are reworked by disassembling the stack, replacing the defective part (assumed to be an MEA), and reassembling the stack. Using the Boothroyd Dewhurst, Inc. (BDI) Design for Assembly software, the 60-kW stack assembly labor time was estimated to be 2.8 hours.

The formula for scrap value is based on the total amount of additional production necessary to make up for the value of the scrapped items as:

$$\text{Scrap value} = (\text{Unit value} / (1 - \text{Scrap rate})) - \text{Unit value}$$

Assuming a scrap rate of 5%, the total loss associated with disassembly and reassembly labor is:

$$\text{Scrap labor time} = (((2 \times 3.1 \text{ hrs/stack}) / (1-0.05)) - (2 \times 3.1 \text{ hrs/stack})) \times 2,000 \text{ stacks} = 652.6 \text{ hrs}$$

Assuming that the part requiring replacement is a membrane electrode assembly (MEA), the total loss associated with replacement parts is:

$$\text{Scrap value (\$)} = ((\$31.01/\text{stack} / (1-0.05)) - \$31.01/\text{stack}) \times 2,000 \text{ stacks} = \$3,264.21$$

## Appendix A-11: SOFC Production Facility Estimation

The production facility estimation is based on the floor area required for production equipment, equipment operators, and support personnel. Primary space allowance guidelines used for this analysis were developed by Prof. Jose Ventura at Pennsylvania State University, and were downloaded on 10/18/2013 from <http://www.personal.psu.edu/jav1>.

### A-11.1 Equipment Footprint

The machine utilization calculations provide the equipment count for a particular production station. Using the application of the cathode layer as an example, each station consists of two pieces of equipment: the screen printer, and a heated conveyor for slurry drying, which have the following footprint dimensions:

Screen printer: 63 in x 55 in

Heated conveyor: 24 in x 36 in

Allowing a 3-foot (36-in) margin on all sides for maintenance access makes the total machine footprints:

Screen printer:  $(63 + (2 \times 36)) \times (55 + (2 \times 36)) / 144 \text{ in}^2/\text{ft}^2 = 119 \text{ ft}^2$

Heated conveyor:  $(24 + (2 \times 36)) \times (36 + (2 \times 36)) / 144 \text{ in}^2/\text{ft}^2 = 72 \text{ ft}^2$

Three additional space allowances are made for each station for material, personnel, and aisles. The production stations will require space for material receiving and part pickup, typically done using pallets. We will assume one standard 40-inch by 48-inch pallet for receiving and pickup, adding to the required area by:

Material allowance =  $2 \times (40 \text{ in} \times 48 \text{ in}) / 144 = 27 \text{ ft}^2$

Ventura recommends personnel space of 20 square feet (ft<sup>2</sup>) per person to allow for movement within the work station during equipment operation. The bipolar plate pressing requires a single operator, adding:

Personnel allowance =  $1 \times 20 \text{ ft}^2 = 20 \text{ ft}^2$

Aisle allowance is based on the largest transported load. Because we intend to transport material and finished parts on standard pallets, our anticipated load size is 27 ft<sup>2</sup>, for which Ventura recommends a 30% to 40% allowance for the net area required, which include personnel and material. Using a value of 35% makes the aisle allowance for the bipolar plate station:

Aisle allowance:  $(119 + 72 + 27 + 20) \times 0.35 = 83 \text{ ft}^2$

The total floor space allocation for the screen printing station is:

Floor space allocation =  $119 + 72 + 27 + 20 + 83 = 321 \text{ ft}^2$

SOFC fuel cell stack production was broken up into 20 primary work stations with total floor space allocations calculated using the above formulas as:

Production Station	Floor Space Allocation (ft <sup>2</sup> )
High Volume Slurry Preparation	457
Low Volume Slurry Preparation	336
Tape Casting	1,027
Anode Pressing	551
Anode Blanking	318
Screen Printing	321
Kiln Firing	622
Sintering	598
Final Trim	221
Laser Cutting	221
Sheet Metal Stamping	185
Interconnects	589
End Plates	1,234
Laser Weld	221
Sealing Line	395
Stack Assembly	422
Stack Brazing	598
Stack Test and Conditioning	252
System Assembly	356
System Test	252

In addition to equipment, industrial facility space must be allocated for offices, food service, restrooms and parking, all of which depend on the number of people present during operation. For most automated or semi-automated production equipment, one operator can cover multiple machines. In addition, some operations have long periods of unsupervised operation (e.g. the 10-hour milling time in catalyst production).

Ventura estimates the number of required machine operators using the formula:

$$n' = (a + t) / (a + b)$$

where

a = machine-operator concurrent activity time (load, unload)

b = independent operator activity time (inspect, package)

t = independent machine activity time

n' = maximum number of machines per operator

The reciprocal of  $n'$  would represent the minimum number of operators per machine. Using time data (in seconds) extracted from the DFM process analyses for a and t, and estimating time for b, resulted in the following:

SOFC Production Station	a	b	t	$n'$	$1/n'$
High Volume Slurry Preparation	1,907	600	36,000	15.12	0.07
Low Volume Slurry Preparation	1,887	600	36,000	15.23	0.07
Tape Casting	1,800	600	12,780	6.08	0.16
Anode Pressing	1,800	600	13,805	6.50	0.15
Anode Blanking	1,800	600	3,135	2.06	0.49
Screen Printing	4	4	23	3.38	0.30
Kiln Firing	4	4	15	2.38	0.42
Sintering	4	4	34	4.75	0.21
Final Trim	4	4	6.85	1.36	0.74
Laser Cutting	4	4	6.85	1.36	0.74
Sheet Metal Stamping	4	4	2	0.75	1.33
Interconnects	10	10	179	9.45	0.11
End Plates	30	30	295	5.42	0.18
Laser Weld	4	4	6.85	1.36	0.74
Sealing Line	10	10	98.6	5.43	0.18
Stack Assembly	12,742	0	0	1.00	1.00
Stack Brazing	13	10	1,290	56.65	0.02
Stack Test and Conditioning	1,800	600	21,600	9.75	0.10
System Assembly	21,600	0	0	1.00	1.00
System Test	1,800	600	21,600	9.75	0.10

In general, we assume that a single operator is capable of operating a maximum of three machines in a cell arrangement. We will also assume that stations requiring multiple operators can utilize a floating operator working between three machines.

To obtain a rough estimate of the number of operators required during any one shift, we multiply the required number of operators per station (combinations of either 1.0, 0.5, 0.33) by the number of stations required to produce a particular annual volume and the station utilization (assuming a single operator is trained to perform multiple tasks). Using the station utilization numbers for 4,000 30-kW stacks per year we have:

Production Station	Stations	Utilization	Operators per station	Operators Per Shift
High Volume Slurry Preparation	1	0.249	0.10	0.02
Low Volume Slurry Preparation	1	0.038	0.10	0.00
Tape Casting	4	0.760	1.50	4.56
Anode Pressing	1	0.124	0.50	0.06
Anode Blanking	1	0.040	0.50	0.02
Screen Printing	7	0.900	1.00	6.30
Kiln Firing	5	0.823	0.33	1.36
Sintering	4	0.807	0.33	1.07
Final Trim	1	0.566	0.50	0.28
Laser Cutting	1	0.692	0.50	0.35
Sheet Metal Stamping	1	0.169	1.00	0.17
Interconnects	3	0.696	2.00	4.18
End Plates	2	0.637	1.00	1.27
Laser Weld	2	0.944	0.33	0.62
Sealing Line	4	0.990	1.00	1.36
Stack Assembly	3	0.790	1.00	2.37
Stack Brazing	1	0.232	0.33	0.08
Stack Test and Conditioning	2	0.722	0.33	0.48
System Assembly	1	0.329	1.00	0.33
System Test	1	0.694	0.33	0.23
Total				27.70

Rounding up to 28 machine operators per shift, and assuming approximately one support staff per four operators for purchasing, quality control (QC), and maintenance, the facility needs to support 35 employees. Ventura provides estimates the following additional facilities:

Food service: 15 ft<sup>2</sup>/employee

Restrooms: 2 toilets + 2 sinks per 15 employees (estimated at 25 ft<sup>2</sup> per fixture)

Parking: 276 ft<sup>2</sup>/employee

In addition, office space for support personnel is estimated at 72 ft<sup>2</sup>/employee based on the State of Wisconsin Facility Design Standard. Therefore, additional space requirements are:

Facility	Space Required (ft <sup>2</sup> )
Food Service	420
Restrooms	200
Parking	7,728
Office	504

Estimated total factory building floor space can be calculated as:

$$\text{Equipment} + \text{Food service} + \text{Restrooms} + \text{Office} = 22,809 \text{ ft}^2$$

Assuming a construction cost of \$250/ft<sup>2</sup>, the estimated cost of factory construction is approximately \$570,225.

Total real estate required can be estimated as building floor space plus parking and building set-back (distance from building to streets and other structures). Assuming a 30-foot set-back on all sides of a reasonably square facility gives a total real estate requirement of:

$$((\text{Factory space} + \text{Parking space})^{1/2} + 60)^2 = 55,107 \text{ ft}^2 = 1.27 \text{ acre}$$

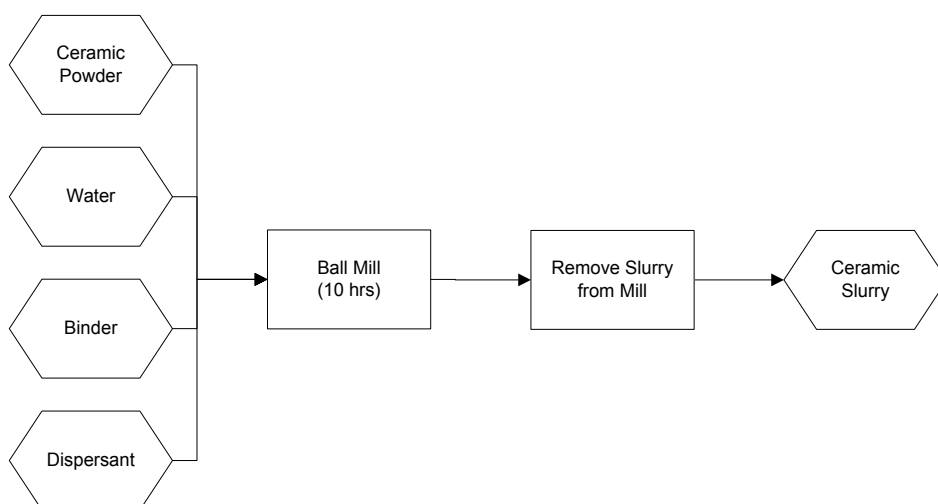
Assuming a real estate cost of \$125,000/acre, the estimated total real estate cost is approximately \$158,134.

## Appendix A-12: SOFC Ceramic Slurry Production Process

### A-12.1 Model Approach

- Ceramic slurry preparation operation
  - Machine setup labor time based on user input
  - Compute required batch size based on part batch size and ceramic layer thickness
  - Compute ceramic slurry material unit cost based on usage
  - Compute ceramic slurry processing time and machine utilization

### A-12.2 Process Flow



### A-12.3 Background

The composition of typical SOFC ceramic slurries used in industry is not directly reported, and fundamental work seems to be continuing in the area of ceramic powder characterization.

In *Modern Ceramic Engineering* (2006),<sup>25</sup> D.W. Richerson lists a typical solvent-based slurry as:

- 70 wt% ceramic powder
- 14 wt% organic solvent (MEK/EtOH)
- 9 wt% binder (ethyl methacrylate)
- 1 wt% dispersant (fish oil)
- 6 wt% plasticizer (BBP/PEG)

<sup>25</sup> D.W. Richerson. 2006. *Modern Ceramic Engineering: Properties, Processing, and Use in Design*. CRC Press, Taylor & Francis Group, LLC. 707 p.



In their study of sintering and deformation, Cologna et al. (2010)<sup>26</sup>, report using a water-based slurry in tape casting experiments as follows:

- Electrolyte: blade gap = 30  $\mu\text{m}$ ; dry thickness =  $12 \pm 2 \mu\text{m}$ ; 60% reduction
  - 59 wt% YSZ (8% mol)
  - 14 wt% water
  - 26 wt% binder (Dow Duramax B-1000/B-1014)
  - 2 wt% dispersant (ammonium polyacrylate)
  
- Anode: blade gap = 500  $\mu\text{m}$ ; dry thickness =  $270 \pm 5 \mu\text{m}$ ; 46% reduction
  - 26 wt% YSZ (8% mol)
  - 37 wt% NiO
  - 12 wt% water
  - 24 wt% binder
  - 1 wt% dispersant

Cologna's values are consistent with general "rule-of-thumb" thickness reduction of 50% seen on several web sites and used on some technical papers. Therefore, for cost purposes, we will assume that wet ceramic deposition will be twice the thickness of the required final ceramic layer thickness.

## A-12.4 Preliminary Analysis

### A-12.4.1 Anode Batch Volume

Slurry batch volume depends on the part size, casting width, and ceramic layer thickness.

The cells for this analysis are for a 100-kilowatt (kW) system at a production rate of 4,000 stacks per year (1,000 systems with four stacks per system). The deposition area for the anode will be:

$$187 \text{ mm width} \times 268 \text{ mm length} = 501.16 \text{ cm}^2$$

Material densities for the anode slurry components are as follows:

- $\rho(\text{YSZ}) = 6.1 \text{ g/cm}^3$
- $\rho(\text{NiO}) = 6.7 \text{ g/cm}^3$
- $\rho(\text{water}) = 1.0 \text{ g/cm}^3$
- $\rho(\text{binder}) = 1.05 \text{ g/cm}^3$
- $\rho(\text{dispersant}) = 1.16 \text{ g/cm}^3$

---

<sup>26</sup> M. Cologna, V. Sglavo, and M. Bertoldi. 2010. *Sintering and Deformation of Solid Oxide Fuel Cells Produced by Sequential Tape Casting*. International Journal of Applied Ceramic Technology 7(6): 803-813.

Based on the slurry composition as specified above, 100 grams of wet slurry has a volume of:

$$v = (26/6.1) + (37/6.7) + (12/1.0) + (25/1.05) + (1/1.16) = 45.50 \text{ cm}^3$$

Yielding a wet slurry density of:

$$\rho(\text{wet slurry}) = (100/45.50) = 2.20 \text{ g/cm}^3 = 2,200 \text{ kg/m}^3$$

The required dried depth of 500 microns requires a deposited wet depth of 1,000 microns. (Note that final anode depth will be achieved by casting two 250-micron tapes and pressing the tapes together to achieve the final desired thickness.) The weight of slurry material required per part is:

$$\text{Wet slurry weight} = 2 \times (2.2 \text{ g/cm}^3 \times (501.16 \times 0.10) \text{ cm}^3 \times 0.001 \text{ kg/g}) = 0.220 \text{ kg/part}$$

Batch sizes will be calculated based on a production schedule producing 4,000 stacks per year. The 30-kW stack requires 259 cells, requiring total slurry production of:

$$\text{Annual slurry production: } 259 \text{ parts/stack} \times 4,000 \text{ stacks} \times 0.220 \text{ kg/part} = 228,201 \text{ kg}$$

#### A-12.4.2 Anode Ceramic Slurry Material Cost

Material cost of the slurry is calculated using the weight percents of the slurry constituents multiplied by the raw material cost to determine a cost per kilogram. Ceramic material pricing was obtained from Inframat Advanced Materials in December 2013. Bulk cost for the dispersant was obtained from web quotes at around \$2.50 for 2,500 kg. The cost of deionized (DI) water is based on amortized distillation costs obtained from [www.apswater.com](http://www.apswater.com).

Summarizing, the weight of each material contained in the slurry is:

- YSZ =  $0.26 \times 228,201 \text{ kg} = 59,332 \text{ kg}$
- NiO =  $0.37 \times 228,201 \text{ kg} = 84,434 \text{ kg}$
- Water =  $0.12 \times 228,201 \text{ kg} = 27,384 \text{ kg}$
- Binder =  $0.24 \times 228,201 \text{ kg} = 54,768 \text{ kg}$
- Dispersant =  $0.01 \times 228,201 \text{ kg} = 2,282 \text{ kg}$

Material costs were determined in accordance with Appendix A-2 as:

- YSZ = \$36.00
- NiO = \$28.80
- Water = \$0.084
- Binder = \$2.125
- Dispersant = \$1.268

The raw material cost of the slurry is:

$$\text{Raw material cost} = (0.26 \times \$36.00) + (0.37 \times \$28.80) + (0.12 \times \$0.084) + (0.24 \times \$2.125) + (0.01 \times \$1.268)$$

$$\text{Raw material cost} = \$20.55/\text{kg}$$

The annual anode slurry cost before scrap is:

$$\$20.55/\text{kg} \times 228,201 \text{ kg} = \$4,689,530$$

### A-12.4.3 Anode Ceramic Slurry Processing

The first step is to weigh the materials out and place them in the mill. We will assume a manual process consisting of a measurement step and a material handling step. The Boothroyd Dewhurst, Inc. (BDI) DFMA® software contains an analogous operation for off-line precision measurement with a default value of 17.4 seconds for the measurement, and a minimum of 4 seconds for material handling. The slurry is made up of five materials, so that total handling time for material preparation can be estimated as:

$$\text{Material prep time} = 5 \times 21.4 \text{ sec} = 107 \text{ sec} = 1.8 \text{ min} = 0.03 \text{ hr}$$

The primary cost for operating the ball mill is the energy input to the motor running the mill. Some studies have looked into the cost of operating large ball mills used for cement and powder metallurgy material processing, where the target parameter is the amount of energy required to process a given amount of material, usually expressed in kilowatt-hours per ton (kW-hr/ton). The calculations are complex owing to the large number of inputs to the calculations.

In “Technical Notes 8, Grinding,” R.P. King develops a relationship based on fundamental physical models of ball mill processing (see <http://www.mineraltech.com/MODSIM/ModsimTraining/Module6/Grinding.pdf>). He assumes a 35% volumetric loading ratio, of which milling balls represents 10% of the total charge volume. Given a mill with diameter  $d$  and length  $l$ , the total catalyst charge volume is:

$$\text{Catalyst charge volume} = (\pi \times d^2 / 4) \times l \times 0.35 \times 0.9 = 0.079 \pi d^2 l \text{ m}^3$$

We note that production levels of 1,000 systems (4,000 stacks) per year will require a total of 264,900 kg of catalyst production per year across all layers, or a little over 1 MT per working day. A volume of 50,000 (200,000 stacks) systems per year will require about 13,245 MT per year of slurry, or about 4 MT per day.

A web search identified a batch ball mill capable of 5 MT loading weight measuring 2.8 meters diameter and 2.6 meters long and consuming 37 kW of power. For 4,000 30-kW stacks, the total number of batches processed will be:

$$\text{Roundup}(228,201 / 5,000) = 46 \text{ batches}$$

For other SOFC layers, the slurry volumes required will be smaller due to thinner deposition layers, ranging from 5 to 30 microns. The total depth of all subsequent layers is around 80 microns across six additional layers. Assuming similar density and composition profiles, we can expect slurry production for the remaining layers to be around 370 MT per year, or about 1.5 MT per day.

A web search identified a batch ball mill capable of 1.5 MT loading weight measuring 2.0 meters diameter and 1.8 meters long and consuming 15 kW of power.

Once the milling process is complete, the slurry will need to be separated from the milling balls and transferred to the coating machine. While we presently have no information about this part of the process, one approach would be the use of a vacuum sieve (e.g., Farleygreene, Ltd. SM950 Sievmaster Vacu-siev) to remove and separate the slurry from the mill, and transfer the slurry to a transport container or directly to the coater reservoir.

ShopVac reports a sealed suction of 54 in-H<sub>2</sub>O (13.4 kPa) for their 2-HP (1.5-kW) unit. Using an equivalent vacuum sieve with a 1.5-inch (0.038-m) diameter hose and 80% transfer efficiency, the flow rate is:

$$\text{Flow rate} = 0.8 \times (\pi \times (0.038)^2 / 4) \times (2 \times 13.4 / 850)^{1/2} = 0.00016 \text{ m}^3/\text{sec}$$

Since the slurry forms 90% of the charge volume, the total charge volume is:

$$\text{Charge volume (m}^3\text{)} = 1.11 \times (\text{Slurry weight (kg)} / \text{Slurry density (kg/ m}^3\text{)})$$

$$\text{Charge volume (m}^3\text{)} = 0.0013 \times \text{Slurry weight}$$

Therefore, the optimal time required to remove the charge volume is:

$$\text{Material removal time (sec)} = \text{Charge volume} / \text{Flow rate} = 8.1 \times \text{Slurry weight}$$

We will estimate the total transfer time to remove the slurry from the mill and transfer it to the coater as twice the slurry removal time. The total time required to remove the slurry from the mill would be:

$$\text{Material removal time} = 2 \times 8.1 \times 5,000 \text{ kg} = 54,800 \text{ sec} = 22.5 \text{ hrs}$$

Total machine time is:

$$(\text{Setup time} + \text{Material prep time} + \text{Milling time} + \text{Material removal time}) \times \text{Number of batches} = (0.5 + 0.03 + 10.0 + 22.5) \times 46 = 1,519 \text{ hrs}$$

Machine utilization is:

$$1,519 / 6,000 = 25.3\%$$

Machine rate was determined in accordance with Appendix A-1 as:

$$\text{In-house rate} = \$11.68 / 0.253 = \$46.17$$

$$\text{Job shop rate} = 1.4 \times (\$11.68 / 0.65) = \$25.16$$

For computing machine labor time, we assume one dedicated operator for the setup, material prep, and material removal operations, but only minimal labor time required during milling. The total machine labor time is then:

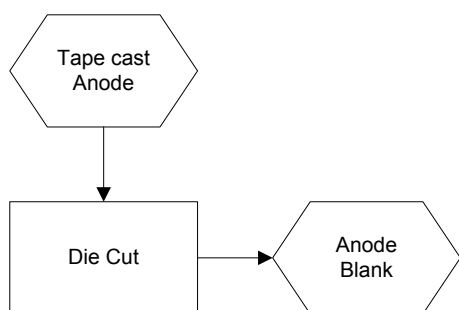
$$((0.5 + 0.03 + 22.5) \times 1 \text{ operator} + (10 \times 0.1 \text{ operator})) \times 46 \text{ batches} = 1,105.4 \text{ hrs}$$

## Appendix A-13: SOFC Anode Blanking Process

### A-13.1 Model Approach

- Anode blanking operation
  - Machine setup labor time based on number of setups required to process material and input labor time
  - Tooling cost based on die cutting length and die life
  - Press machine time based on cutting force, cutting time, and throughput

### A-13.2 Process Flow



### A-13.3 Background

We will assume that the pre-fired anode tape has similar physical properties to those of elastomeric materials. The primary method for blanking elastomeric materials with standard features and tolerances is steel rule die cutting. The outline of the gasket is laid out and cut into a board. Strip steel is embedded into the board at a uniform height and mounted on a small stroke, fast acting press. The anode material is fed into the press where the steel rule die shears the material. The cutout areas of the blank are pushed out of the bulk material and the blanks stacked.

### A-13.4 Preliminary Analysis

The cells for this analysis are for a 100 kW<sub>net</sub> system at a production rate of 4,000 stacks per year (1,000 systems with 4 stacks per system). The deposition area for the anode will be:

$$187 \text{ mm width} \times 268 \text{ mm length} = 501.16 \text{ cm}^2$$

The 30 kW stack requires 259 cells, requiring total annual production of:

$$\text{Annual production} = 259 \text{ parts/stack} \times 4,000 \text{ stacks} = 1,036,000 \text{ parts}$$

#### A-13.4.1 Setup

The number of setups for anode blanking will be the same as that for anode tape pressing, which is 15.

### A-13.4.2 Tooling Cost

The primary factor contributing to steel rule die cost is the total cutting length of the die. For the anode, the cutting length (mm) is:

$$\text{Cutting length} = 2 \times (268 + 187) = 910 \text{ mm}$$

The total number of cavities is four (one widthwise by four lengthwise). A steel-rule-die will have  $(2 \times (1 + 5)) = 10$  outer edges, leaving  $((5 \times 4) - 16) = 4$  common sides, yielding four inner cutting edges of 268 millimeters (mm). Therefore, the die cutting length is:

$$\text{Die cutting length (mm)} = ((4 - 1) \times 268) + ((4 \times 2) \times 187) + (2 \times 268) = 2,836 \text{ mm}$$

A rough quote of approximately \$230 was obtained from steel-rule-dies.com for a two-cavity die with a similar configuration.

$$\text{Tooling rate} = \$230 / (2 \times 2,706) \text{ mm} = \$0.04/\text{mm}$$

Information obtained from Mag-Knight ([www.mag-knight.com/diecutting/Steel\\_Rule\\_Dies.htm](http://www.mag-knight.com/diecutting/Steel_Rule_Dies.htm)) indicates that dies used to cut softer materials have an expected life of about 30,000 hits. Assuming a shorter die life of 20,000 cycle for the ceramic material, the total tooling cost per part for a four-cavity die (four parts per stroke) amortizing over a 5 year life can be calculated as:

$$\text{Annual tooling cost} = \frac{1}{5}(\text{Tooling cost} \times \text{Number of tools purchased})$$

where:

$$\text{Number of tools purchased} = \text{Roundup}(\text{Total production} / \text{Tool life})$$

$$\text{Total production} = \text{Annual production} \times 5$$

$$\text{Annual tooling cost} = \frac{1}{5}((2,836 \text{ mm/die} \times \$0.04/\text{mm}) \times \text{Roundup}((1,036,000 \text{ parts/yr} / 4 \text{ parts/cycle} \times 5 \text{ yrs}) / 20,000 \text{ parts/tool})) = \$1,474.72$$

### A-13.4.3 Die Cutting

The primary energy input to run the press is hydraulic pump motor power. The total force required to cut the material is the total shear area (cutting length  $\times$  material thickness) multiplied by the material shear strength. Assuming that the unfired anode material has the approximate consistency of high-density polyethylene (HDPE), we will use 23 N/mm<sup>2</sup> as the shear strength, giving the total required press force as:

$$\text{Press force} = \text{Cutting length (mm)} \times \text{Material thickness (mm)} \times \text{Shear strength (N/mm}^2)$$

$$\text{Press force} = 4 \text{ dies} \times 2836 \text{ mm/die} \times 0.25 \text{ mm} \times 23 \text{ N/mm}^2 = 65.23 \text{ kN} = 6.55 \text{ tons}$$

A survey of 15- to 100-ton (150- to 1,000-kN) fast-acting die-cutting presses found that the motor power required to operate the press fell in the range of 0.015 to 0.025 kW/kN. Assuming a 50% capacity margin and using the upper end of the motor power rating, the required press energy input is:

$$\text{Press energy} = 65.23 \text{ kN} \times 1.5 \times 0.025 \text{ kW/kN} = 2.45 \text{ kW}$$

Typical die cutting press speed ranges from 30 to 60 cycles/minute (1,800 to 3,600 cycles/hour). Assuming the slower speed, part throughput is calculated as

$$\text{Throughput} = 4 \text{ parts per cycle} \times 1,800 \text{ cycles per hr} = 7,200 \text{ parts/hr}$$

The total machine time required to produce 1,000 30-kW stacks is:

$$\begin{aligned} \text{Machine time} &= \text{Setup time} + \text{Machine time} = (0.5 \text{ hours/setup} \times 194 \text{ setups}) + \\ &(1,036,000 \text{ parts} / 7200 \text{ parts/hour}) = 241 \text{ hours} \end{aligned}$$

Machine utilization is:

$$\text{Machine utilization} = 241 / 6,000 = 4.02\%$$

Machine rate was determined in accordance with Appendix A-1 as:

$$\text{In-house rate} = \$29.83 / 0.0402 = \$742.04$$

$$\text{Job shop rate} = 1.4 \times (\$29.83 / 0.65) = \$64.24$$

Assuming one operator per casting machine for both setup and operation, the machine labor time is equal to the total machine time of 241 hours.

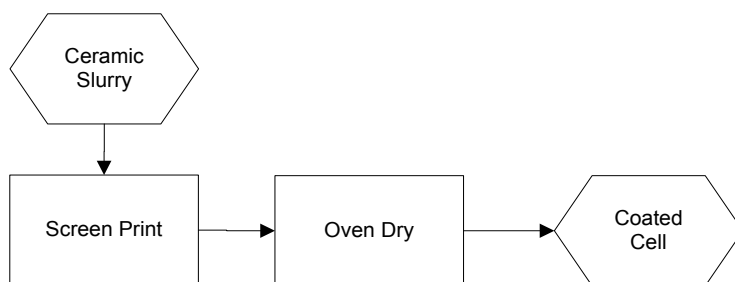
## Appendix A-14: SOFC Screen Printing Process

### Ceramic Screen Printing Process

#### A-14.1 Model Approach

- Screen Preparation
  - Compute tooling cost
  - Compute labor time for screen cleaning
  - Compute labor time and material cost for emulsion coating based on required ceramic layer thickness
  - Compute energy, machine time and labor time for masking and emulsion exposure
  - Compute energy, machine time and labor time for emulsion rinse and post-cure
- Screen Printing
  - Compute time for machine setup
  - Compute labor time for substrate load/unload
  - Compute machine time for screen printing operation
- Oven Drying
  - Compute required heater area based on drying time and required conveyor speed
  - Compute heater energy on energy watt density and heater area

#### A-14.2 Process Flow



#### A-14.3 Background

The mechanics of the screen preparation and printing process are described in several on-line sources, as well as a series of instructional videos produced by Cat Spit Productions found on YouTube. The calculations used for the screen preparation process were based on material and process specifications for Ulano QT-THIX emulsion and the article "Screen Coating Techniques" available from emulsion manufacturer Kiwo at <http://www.kiwo.com/articles/>. Technical details of the printing process were based on the article "Screen and Stencil Printing" available at <http://archive.is/www.ami.ac.uk>, and "The Basics of Printing Thick Film Inks" available at from DuPont Microcircuit Materials at [http://www2.dupont.com/MCM/en\\_US/techtip/basics.html](http://www2.dupont.com/MCM/en_US/techtip/basics.html).



## A-14.4 Preliminary Analysis

The cells for this analysis are for a 100 kW<sub>net</sub> system comprised of four 30-kW stacks. The deposition area for the anode will be:

$$187 \text{ mm width} \times 268 \text{ mm length} = 501.16 \text{ cm}^2$$

To develop the analysis, we will assume that the screen printing operation is being used to apply the anode active layer, which has a finished depth of 15 microns. Annual production rate is 4,000 stacks per year (1,000 systems with four stacks per system). The 30-kW stack requires 259 cells, requiring annual production of:

$$\text{Annual production} = 259 \text{ parts/stack} \times 4,000 \text{ stacks} = 1,036,000 \text{ parts}$$

### A-14.4.1 Screen Tooling Cost

Screen size is determined based on pattern area. Dupont recommends a squeegee length of 10-20 mm beyond the pattern area (part width) on both sides, and squeegee travel of 50-80 mm beyond the pattern area (part length) on both ends. Bopp, a printing mesh manufacturer, recommends a screen width of 3 times the squeegee width and screen length of 2 times the squeegee travel. The minimum screen size can be calculated as:

$$\text{Screen width} = 3 \times (\text{Part width} + 20)$$

$$\text{Screen length} = 2 \times (\text{Part length} + 100)$$

For the two part sizes, the screen sizes are:

$$\text{Screen width} = 3 \times (187 + 20) = 621 \text{ mm}$$

$$\text{Screen length} = 2 \times (268 + 100) = 736 \text{ mm}$$

$$\text{Screen area} = 621 \times 736 = 4,571 \text{ cm}^2$$

The two primary wear items are the screen and the squeegee. Atlas screen supply company quotes triple durometer squeegee material for \$2.05/inch (\$0.81/cm). Squeegee cost is:

$$\text{Squeegee cost} = \$0.81/\text{cm} \times (187 + 20) / 10 = \$16.77$$

AMI indicates that polymer squeegees may be changed daily in high volume production applications, indicating a useful life of around 5,000 to 6,000 parts. The squeegee tooling cost is:

$$\text{Squeegee tooling cost} = \$16.77 \times \text{Roundup}(1,036,000 \text{ parts} / 5,000 \text{ parts/squeegee}) = \$3,487.74$$

Web quotes for fine mesh precision metal screens in 24-inch x 30-inch size ranged from \$50 to \$100, equating to about \$0.02/cm<sup>2</sup>, giving estimated screen costs of:

$$\text{Screen cost} = \$0.02/\text{cm}^2 \times 4,571 \text{ cm}^2 = \$91.42$$

AMI reports screen lives between 5,000 and 50,000 cycles. Given the nature of the ceramic inks used, we will assume the lower value of 5,000 cycles. Total screen tooling cost based on a life of 5,000 cycles and amortizing over a 5-year life is:

$$\text{Annual tooling cost} = \frac{1}{5}(\text{Tooling cost} \times \text{Number of tools purchased})$$

where:

$$\text{Number of tools purchased} = \text{Roundup}(\text{Total production} / \text{Tool life})$$

$$\text{Total production} = \text{Annual production} \times 5$$

$$\text{Annual tooling cost} = \frac{1}{5}((\$91.41) \times \text{Roundup}((1.036,000 \text{ parts/yr} \times 5 \text{ yrs}) / 5,000 \text{ parts/screen})) = \$18,940.15$$

#### A-14.4.2 Screen Preparation

Screen preparation is a manual process that consists of cleaning, emulsion coating, emulsion masking and exposure to high intensity light, emulsion rinsing and post cure using high intensity light. The primary cost component will be the labor involved in handling and coating the screen. An empirical formula developed by Boothroyd Dewhurst, Inc. (BDI) calculates a quantity called part girth, then calculates a theoretical total handling time (both load and unload) with a minimum value of 4 seconds. Adapting the formula for dimensions in millimeters (mm) and handling of large, light-weight parts, the handling time is calculated as follows:

$$\text{Part girth} = \text{Part length} + \text{Part width} + \text{Part depth}$$

$$\text{Handling time} = \text{Max}((0.3 \times (\text{Part girth} / 25.4) - 4.6), 4)$$

Common screen frames are 1 inch (25.4 mm) thick, so that the handling time for the screen is:

$$\text{Screen handling time} = \text{Max}((0.3 \times (1,382 / 25.4) - 4.6), 4) = 11.73 \text{ sec}$$

Cleaning is assumed to be accomplished by brushing the screen mesh and spray rinsing with water. The time to accomplish the tasks will consist of a tool acquisition time (e.g., brush, hose) and operation time. The general default time for acquisition of tools within easy reach is 3 seconds, and is applicable to a wash station set-up. Brush and rinse operation time will depend on the treatment area. No general area-based guidelines could be found, so we will assume that the operation time per screen side can be estimated using an adaptation of the formula as the total handling time. The calculation for a combination clean and rinse operation for both sides of a screen becomes:

$$\text{Cleaning time} = 4 \times (3 + \text{Handling time})$$

$$\text{Screen cleaning time} = 4 \times (3 + 11.73) = 58.91 \text{ sec}$$

The emulsion coating is applied with a hand-held trough coater with width equal to the screen width. This allows the emulsion to be applied in one fluid motion from the bottom to the top of the screen. Observations of video recordings of the process indicate that a single coat can be applied to a 1-meter length in approximately 5 seconds. Using 3 seconds for tool acquisition, the time to apply a single coat can be estimated as:

$$\text{Emulsion application time} = 3 + (\text{Screen length} / 1,000) \times 5$$

$$\text{Emulsion application time} = 3 + (736 / 1,000) \times 5 = 6.68 \text{ sec}$$

The number of emulsion coats depends on the desired coating depth. Dupont suggests that fine mesh screens provide a dry print depth for thick film inks of approximately 16 microns. Further reductions in film thickness is achieved through calendar rolling of the screen. Kiwo recommends two coats of emulsion on the squeegee side of the screen, followed by at least one coat up to as many coats on the print side as necessary to provide the proper coating depth. The number of emulsion coats can be estimated as:

$$\text{Number of coats} = 3 + \text{Max}((\text{Coating depth} - 16), 0)$$

$$\text{Number of coats} = 3 + \text{Max}((15 - 16), 0) = 3 \text{ coats}$$

Screens are air-dried for about 1 hour following coating. Consequently, no additional labor time is accumulated for the drying operation. Total emulsion coating time is calculated as:

$$\text{Emulsion coating time} = \text{Number of coats} \times (\text{Emulsion application time} + \text{Handling time})$$

$$\text{Emulsion coating time} = 3 \times (6.68 + 11.73) = 55.22 \text{ sec}$$

The emulsion is developed by applying the pattern mask and exposing the coated screen to 4,500-watt light for a period equal to approximately 1 minute per 1 micron of emulsion depth and a minimum of 15 minutes. Assuming approximately 4 seconds to place the mask, the handling time for the applying the mask is 10.95 seconds. The required power for the light source can be calculated as:

$$\text{Exposure power} = ((15 + \text{Max}((\text{Coating depth} - 15), 0)) / 60) \text{ hrs} \times 4.5 \text{ kW}$$

$$1 \text{ Exposure power cost} = (15 / 60) \times 4.5 = 1.125 \text{ kW}$$

The unexposed emulsion is rinsed from the screen in a manner similar to the cleaning step, air-dried, and re-exposed to the light source to harden the emulsion coating on the squeegee side of the screen. Using the cost equations developed previously:

$$\text{Rinsing time} = 2 \times (3 + \text{Handling time})$$

$$\text{Rinsing time} = 2 \times (3 + 11.73) = 29.46 \text{ sec}$$

Summarizing screen preparation by step:

100 kW	
Labor Time (sec)	
Cleaning	58.91
Coating	55.22
Exposure	10.95
Rinsing	29.46
Post-cure	10.95
Total	165.49

### A-14.4.3 Screen Printing

The screen printing operation consists of a part load/unload, which may be manual or robotic, but will be driven by overall part size. Using the handling time formula developed previously, the load/unload time is:

$$\text{Handling time} = \text{Max}((0.3 \times ((187 + 268 + 1) / 25.4) - 4.6), 4) = 4.0 \text{ sec}$$

The time to perform the printing operation is a function of the flood blade speed, which can be estimated to move at four times the squeegee speed. Setting L to the squeegee travel length and S to the squeegee speed:

$$\text{Substrate coating time} = (L/S) + (L/4S) = 1.25 \times (L/S)$$

Observations of SOFC screen printing operations suggest that the squeegee speed is approximately 25 millimeters per second (mm/sec). Using these values, the time to coat the substrate is:

$$\text{Substrate coating time} = 1.25 \times (368 / 25) = 18.4 \text{ sec}$$

Total machine time for screen printing is:

$$\text{Setup time} + (\text{Handling time} + \text{Coating time}) \times \text{Number of parts} = 0.5 \text{ hr} + ((4.0 + 18.4) / 3,600) \times 1,036,000 \text{ parts} = 6,446 \text{ hrs}$$

Machine utilization is:

$$\text{Machine utilization} = 6,446 / (6,000 \times 2 \text{ machines}) = 53.71\%$$

Machine rate was determined in accordance with Appendix A-1 as:

$$\text{In-house rate} = \$49.71 / 0.537 = \$92.57$$

$$\text{Job shop rate} = 1.4 \times (\$49.71 / 0.65) = \$107.07$$

Assuming one operator per screen printing machine, the machine labor time is equal to the total machine time of 6,446 hours.

#### A-14.4.4 Ceramic Slurry Drying

Following deposition, the ceramic slurry is dried, usually by means of a tunnel dryer positioned directly after the deposition step. The drying can be done by either radiant or convective heating. For the cost analysis, we will assume radiant (infrared) heating and compute the cost of drying by determining the required heater area based on throughput and the drying time.

Drying time is a function of the evaporation rate of the solvent and is inversely and exponentially proportional to the coating thickness. Experiments conducted by Mistler et al. (1978)<sup>27</sup> indicate drying rates of  $1.35 \times 10^{-5}$  g/cm<sup>2</sup>-sec at room temperature for an air flow rate of 2 l/min, and  $2.22 \times 10^{-5}$  g/cm<sup>2</sup>-sec at room temperature for an air flow rate of 75 l/min.

Previous analysis assumed that the screen printed slurry material was formulated with aqueous components as follows:

- 12 wt% water
- 24 wt% binder (Dow Duramax B-1000/B-1014)
- 1 wt% dispersant

The binder consists of approximately 45% solids. Roughly estimating the volume of liquid per gram of slurry by multiplying the material density by the material weight percent:

$$\text{Liquid density} = (0.12 \times 1.0) + ((0.24 \times 0.55) \times 1.05) + (0.01 \times 1.16) = 0.270 \text{ g/cm}^3$$

The weight of liquid to be removed per unit area is a function of slurry thickness. As with tape casting, we assume a 50% thickness reduction after drying. Using the anode active layer (15-micron green thickness; 30-micron wet thickness) as an example:

$$\text{Liquid removed per area} = 0.270 \text{ g/cm}^3 \times 0.003 \text{ cm} = 0.0008 \text{ g/cm}^2$$

At a rate of  $2.0 \times 10^{-5}$  g/cm<sup>2</sup>-sec drying rate, the estimated drying time is:

$$\text{Drying time} = 0.0008 \text{ g/cm}^2 / 2.0 \times 10^{-5} \text{ g/cm}^2\text{-sec} = 40.5 \text{ sec} = 0.675 \text{ min}$$

The conveyor speed is a function of part throughput and belt length required to transport the part. Using the results above, the throughput is:

$$\text{Throughput} = 1,036,000 \text{ parts} / 6,446 \text{ hrs} = 160.7 \text{ parts/hr}$$

Assuming a 50-mm gap between parts on the belt, the conveyor speed can be calculated as:

$$\text{Conveyor speed} = \text{Belt length per part (mm/part)} * \text{Throughput (parts/min)}$$

$$\text{Conveyor speed} = (187 + 50) * (237 / 60) = 634.8 \text{ mm/min} = 0.635 \text{ m/min}$$

---

<sup>27</sup> R.E. Mistler, D.J. Shanefield, and R.B. Runk. 1978. Tape casting of ceramics, in *Ceramic Processing Before Firing*, G.Y. Onoda, Jr. and L.L. Hench (eds). John Wiley and Sons, New York.

Infrared heating panels are generally sold with various energy watt densities and in standard sized units and assembled to provide the necessary heating area. Using the Casso Solar Type FB as an example, standard watt densities are 15 and 25 W/in<sup>2</sup> (23 and 39 kW/m<sup>2</sup>) with standard width of 12 inches (0.305 meter) and lengths in 12-inch increments up to 60 inches (1.524 meter). They note that 25 W/in<sup>2</sup> corresponds to an emitter temperature of 880°C, and that the conversion efficiency of electrical power to usable radiant energy is up to 80%.

For a drying time of 0.675 minutes, the required heater area is:

$$\text{Heater area} = \text{Drying time (min)} \times \text{Conveyor speed (m/min)} \times (\text{Belt length per part (mm)} / 1,000)$$

$$\text{Heater area} = 0.675 \times 0.635 \times (237 / 1,000) = 0.102 \text{ m}^2$$

While the heater energy density will be taken as an input, the drying temperatures for the ceramic slurry are fairly moderate (150°C or less), so that the 23 kW/m<sup>2</sup> should be sufficient to maintain the drying area temperature. Using an energy cost of \$0.07/kW-hr, the hourly energy cost to power the heaters will be:

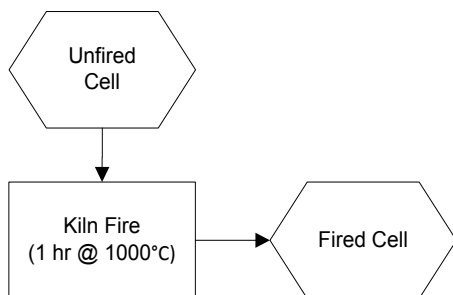
$$\text{Heating energy} = 0.102 \text{ m}^2 \times 23 \text{ kW/m}^2 = 2.35 \text{ kW}$$

## Appendix A-15: SOFC Kiln Firing Process

### A-15.1 Model Approach

- Kiln Firing
  - Compute part handling labor time
  - Compute machine time

### A-15.2 Process Flow



### A-15.3 Preliminary Analysis

The cells for this analysis are for a 100 kW<sub>net</sub> system at a production rate of 4,000 stacks per year (1,000 systems with four stacks per system). The deposition area for the anode will be:

$$187 \text{ mm width} \times 268 \text{ mm length} = 501.16 \text{ cm}^2$$

The 30 kW stack requires 259 cells, requiring total annual production of:

$$\text{Annual production} = 259 \text{ parts/stack} \times 4,000 \text{ stacks} = 1,036,000 \text{ parts}$$

#### A-15.3.1 Kiln Firing

The SOFC process calls for kiln firing at 1,000°C (1,832°F) for 1 hour after the part reaches temperature. The moderate temperatures required allow for the use of a mesh belt furnace to accomplish the kiln firing process.

Large mesh belt furnaces manufactured by AFC-Holcroft feature a 66-inch (167-centimeter [cm]) wide belt, 6-inch (15.24-cm) workspace clearance, and effective load length of 456 inches (1,158 cm) for a total load volume of  $2.95 \times 10^6 \text{ cm}^3$ . The maximum part thickness following the last screen printing operation is 328 microns (0.0328 cm). Adding 1 cm on all sides for part spacing in the furnace and assuming optimal racking, the total part envelope is:

$$\text{Part envelope} = (18.7 + (2 \times 1.0)) \times (26.8 + (2 \times 1.0)) \times (0.0328 + (2 \times 1.0)) = 1,212 \text{ cm}^3$$

The maximum furnace loading is then:

$$\text{Furnace loading} = 2.95 \times 10^6 \text{ cm}^3 / 1212 \text{ cm}^3 = 2,435 \text{ parts}$$

The firing schedule is based on the firing schedule suggested in PNNL-22732<sup>28</sup>:

Segment	Rate/Time	Temp.
Ramp	3°C/min	1,000°C
Hold	1 hr	1,000°C
Ramp	5°C/min	Ambient

Using 25°C as the ambient temperature, the required preheat time is:

$$(1,000 - 25)^\circ\text{C} / (3^\circ/\text{min}) = 325 \text{ min} = 5.42 \text{ hrs}$$

The required cooling time is:

$$(1,000 - 25)^\circ\text{C} / (5^\circ/\text{min}) = 195 \text{ min} = 3.25 \text{ hrs}$$

Therefore, total furnace time is 9.67 hours, making furnace throughput:

$$\text{Throughput} = 2,435 \text{ parts} / 9.67 \text{ hrs} = 252 \text{ parts/hr}$$

Total machine time to fire the cells is:

$$\text{Machine time} = 1,036,000 \text{ parts} / 252 \text{ parts/hr} = 4,111 \text{ hrs}$$

Machine utilization is:

$$\text{Utilization} = 4,111 / 6,000 = 68.5\%$$

Machine rate was determined in accordance with Appendix A-1 as:

$$\text{In-house rate} = \$53.99 / 0.685 = \$78.82$$

$$\text{Job shop rate} = 1.4 \times (\$53.99 / 0.65) = \$116.29$$

Part load/unload, which may be manual or robotic, will be driven by overall part size. To determine if a single operator can load and unload parts while the machine is operating, we use the handling time formula adapted from the Boothroyd Dewhurst, Inc. (BDI) Design for Manufacture and Assembly (DFMA)<sup>®</sup> software to determine the total load/unload time required per hour of machine time as:

$$\text{Part handling time} = \text{Max}((0.3 \times ((187 + 268 + 1) / 25.4) - 4.6), 4) \times 252 \text{ parts/hr} = 0.243 \text{ hr per hr of machine time}$$

Given that part handling time is a small percentage of the total firing time, we assume one operator is capable of covering three machines, making the labor time:

$$\text{Machine labor time} = 4,111 / 3 = 1,370 \text{ hrs}$$

<sup>28</sup> M.R. Weimar, L.A. Chick, D.W. Gotthold, and G.A. Whyatt. 2013. Cost Study for Manufacturing of Solid Oxide Fuel Cell Power Systems (PNNL-22732). Pacific Northwest National Laboratory, September 2013.

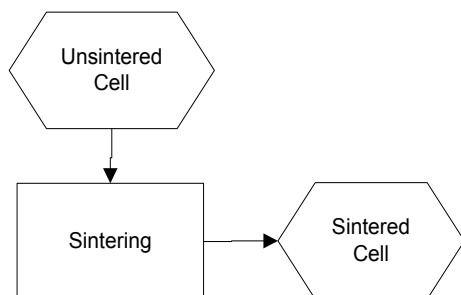


## Appendix A-16: SOFC Sintering Process

### A-16.1 Model Approach

- Sintering
  - Part handling time labor cost based on part size per Boothroyd Dewhurst, Inc. (BDI) formula and throughput; 4-second minimum
  - Process cost based on furnace energy cost plus standard machine rate

### A-16.2 Process Flow



### A-16.3 Preliminary Analysis

The cells for this analysis are for a 100-kW<sub>net</sub> system at a production rate of 4,000 stacks per year (1,000 systems with four stacks per system). The deposition area for the anode will be:

$$187 \text{ mm width} \times 268 \text{ mm length} = 501.16 \text{ cm}^2$$

The 30 kW stack requires 259 cells, requiring total annual production of:

$$\text{Annual production} = 259 \text{ parts/stack} \times 4,000 \text{ stacks} = 1,036,000 \text{ parts}$$

#### A-16.3.1 Sintering Process

The sintering process schedule is based on the bilayer sintering schedule suggested in PNNL-22732<sup>29</sup> :

Segment	Rate/Time	Temp.
Ramp	0.5°C/min	190°C
Hold	2 hrs	190°C
Ramp	0.5°C/min	450°C
Hold	1 hr	450°C
Ramp	3°C/min	1,375°C
Hold	1 hr	1,375°C
Ramp	5°C/min	Ambient

<sup>29</sup> M.R. Weimar, L.A. Chick, D.W. Gotthold, and G.A. Whyatt. 2013. Cost Study for Manufacturing of Solid Oxide Fuel Cell Power Systems (PNNL-22732). Pacific Northwest National Laboratory, September 2013.

Generally, the high sintering temperatures require the use of either pusher, walking beam, or rotary hearth continuous furnaces. A used Surface Combustion rotary hearth furnace supports 60 5-inch × 21-inch (12.7-cm × 53.3-cm) trays with a workspace clearance of 35 inches (88.9 cm), for a total load volume of  $3.61 \times 10^6 \text{ cm}^3$ . The maximum part thickness following the last screen printing operation is 328 microns (0.0328 cm). Adding 1 cm on all sides for part spacing in the furnace and assuming optimal racking, the total part envelope is:

$$\text{Part envelope} = (18.7 + (2 \times 1.0)) \times (26.8 + (2 \times 1.0)) \times (0.0328 + (2 \times 1.0)) = 1,212 \text{ cm}^3$$

The maximum furnace loading is then:

$$\text{Furnace loading} = 3.61 \times 10^6 \text{ cm}^3 / 1,212 \text{ cm}^3 = 2,978 \text{ parts}$$

Using 25°C as the ambient temperature, the required heating times are:

$$(190 - 25)^\circ\text{C} / (0.5^\circ/\text{min}) = 330 \text{ min} = 5.5 \text{ hrs}$$

$$(450 - 190)^\circ\text{C} / (0.5^\circ/\text{min}) = 520 \text{ min} = 8.67 \text{ hrs}$$

$$(1,375 - 450)^\circ\text{C} / (3^\circ/\text{min}) = 308 \text{ min} = 5.14 \text{ hrs}$$

The required cooling time is:

$$(1,375 - 25)^\circ\text{C} / (5^\circ/\text{min}) = 270 \text{ min} = 4.5 \text{ hrs}$$

Adding the 4 hours of hold time, the total furnace time is 27.81 hours, making furnace throughput:

$$\text{Throughput} = 2,978 \text{ parts} / 27.81 \text{ hrs} = 107 \text{ parts/hr}$$

Total machine time to fire the cells is:

$$\text{Machine time} = 1,036,000 \text{ parts} / 107 \text{ parts/hr} = 9,682 \text{ hrs}$$

Total number of furnaces required is:

$$\text{Roundup}(9682 / 6,000) = 2$$

Machine utilization is:

$$\text{Utilization} = 9,682 / (2 \times 6,000) = 80.7\%$$

Machine rate was determined in accordance with Appendix A-1 as:

$$\text{In-house rate} = \$60.26 / 0.807 = \$74.67$$

$$\text{Job shop rate} = 1.4 \times (\$60.26 / 0.65) = \$129.79$$

Part load/unload, which may be manual or robotic, will be driven by overall part size. To determine if a single operator can load and unload parts while the machine is operating, we use the handling time formula developed previously, to determine the total load/unload time required per hour or machine time as:

$$\text{Part handling time} = \text{Max}((0.3 \times ((187 + 268 + 1) / 25.4) - 4.6), 4) \times 107 \text{ parts/hr} = 0.044 \text{ hr per hr of machine time}$$

Given that part handling time is a small percentage of total firing time, we assume one operator is capable of covering three machines, making the labor time:

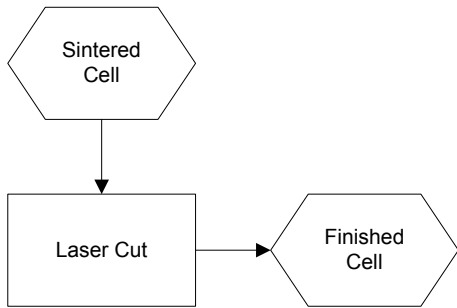
$$\text{Machine labor time} = 9,682 / 3 = 3,227 \text{ hrs}$$

## Appendix A-17: SOFC Final Trim Process

### A-17.1 Model Approach

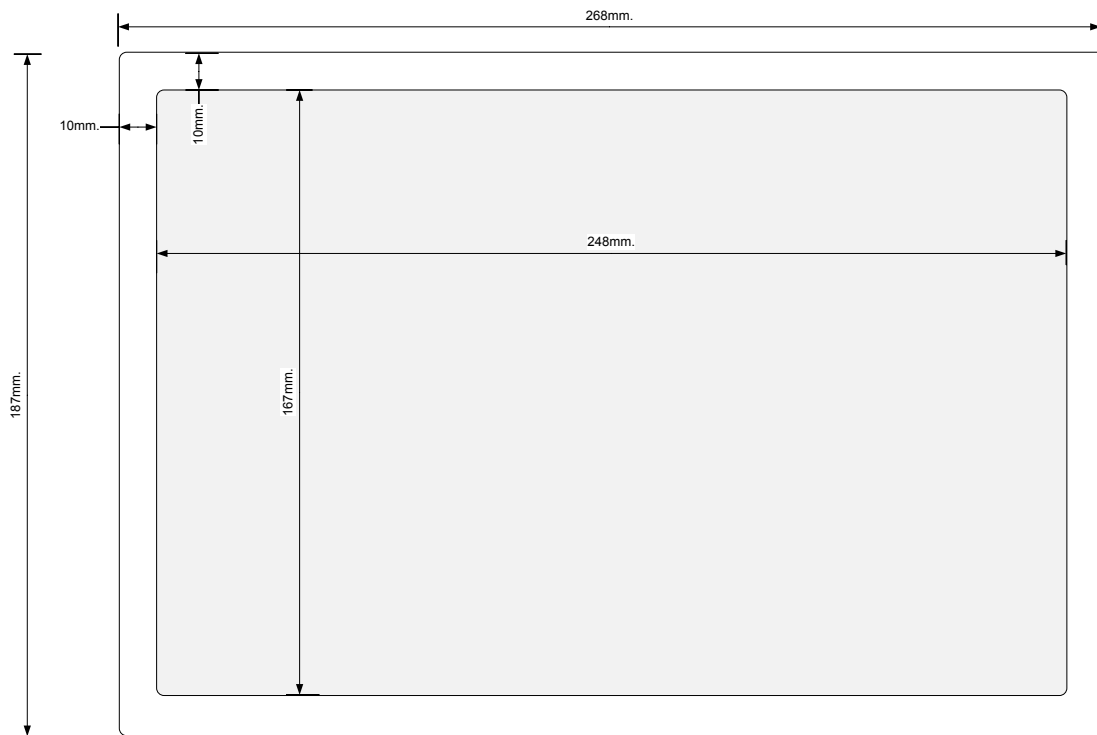
- Laser cut final cell shape

### A-17.2 Process Flow



### A-17.3 Background

Following sintering, the SOFC cells are laser cut to final dimensions as shown:



## A-17.4 Preliminary Analysis

The cells for this analysis are for a 100 kW<sub>net</sub> system at a production rate of 4,000 stacks per year (1,000 systems with 4 stacks per system). The deposition area for the anode will be:

$$187 \text{ mm width} \times 268 \text{ mm length} = 501.16 \text{ cm}^2$$

The 30-kW stack requires 259 cells, requiring total annual production of:

$$\text{Annual production} = 259 \text{ parts/stack} \times 4,000 \text{ stacks} = 1,036,000 \text{ parts}$$

### A-17.4.1 Laser Cutting Cost

Assuming a single setup operation requiring one operator per batch of parts, the final trim setup time will be 0.5 hour.

Part load/unload, which may be manual or robotic, will be driven by overall part size. Using the handling time formula adapted from the Boothroyd Dewhurst, Inc. (BDI) Design for Manufacture and Assembly (DFMA)<sup>®</sup> software, the total handling time is:

$$\text{Part handling time} = \text{Max}((0.3 \times ((187 + 268 + 3.5) / 25.4) - 4.6), 4) = 4.0 \text{ sec/part}$$

The total cutting length for the cell is:

$$\text{Cutting length} = (2 \times (187 + 268)) = 910 \text{ mm}$$

Linde suggests that laser cutting of 1-mm-thick stainless steel be performed using a 1,500-W YAG laser under pure nitrogen flow of 8.0 cubic meters per hour (m<sup>3</sup>/hr) at a maximum speed of 7.0 meters per minute (m/min) (0.117 m/sec). Assuming that the sintered ceramic has similar properties, the time required to cut the cells is:

$$\text{Cutting time} = 0.91 \text{ m} / 0.117 \text{ m/sec} = 7.8 \text{ sec/part}$$

The total machine time required is:

$$\text{Total machine time} = (7.8 + 4) \text{ sec/part} \times 1,036,000 \text{ parts} / 3,600 = 3,396 \text{ hrs}$$

Machine utilization is:

$$\text{Utilization} = 3,396 / 6,000 = 56.6\%$$

Machine rate was determined in accordance with Appendix A-1 as:

$$\text{In-house rate} = \$33.81 / 0.566 = \$59.73$$

$$\text{Job shop rate} = 1.4 \times (\$33.81 / 0.65) = \$72.82$$

Given that the operator required time for load/unload is nearly the same as the total part processing time, we will assume one operator is capable of operating one machine, making the machine labor hours the same as the machine hours of 3,396 hours.

At a consumption rate of 8.0 m<sup>3</sup>/hr, the nitrogen material usage is:

$$\text{Etching material cost} = 8.0 \text{ m}^3/\text{hr} \times 7.8 \text{ sec/part} / 3,600 \text{ sec/hr} \times 1,036,000 \text{ parts} = 17,957 \text{ m}^3$$

Material cost before scrap was determined in accordance with Appendix A-2 as:

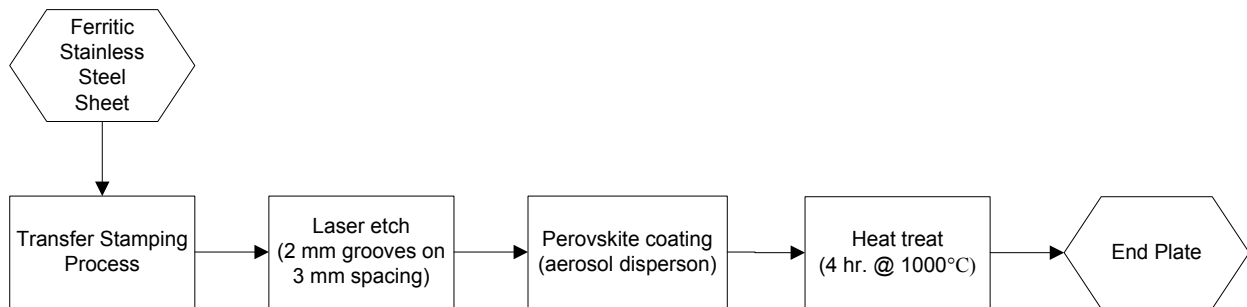
$$\text{Material cost} = \$0.423/\text{m}^3$$

## Appendix A-18: SOFC Interconnect Production Process

### A-18.1 Model Approach

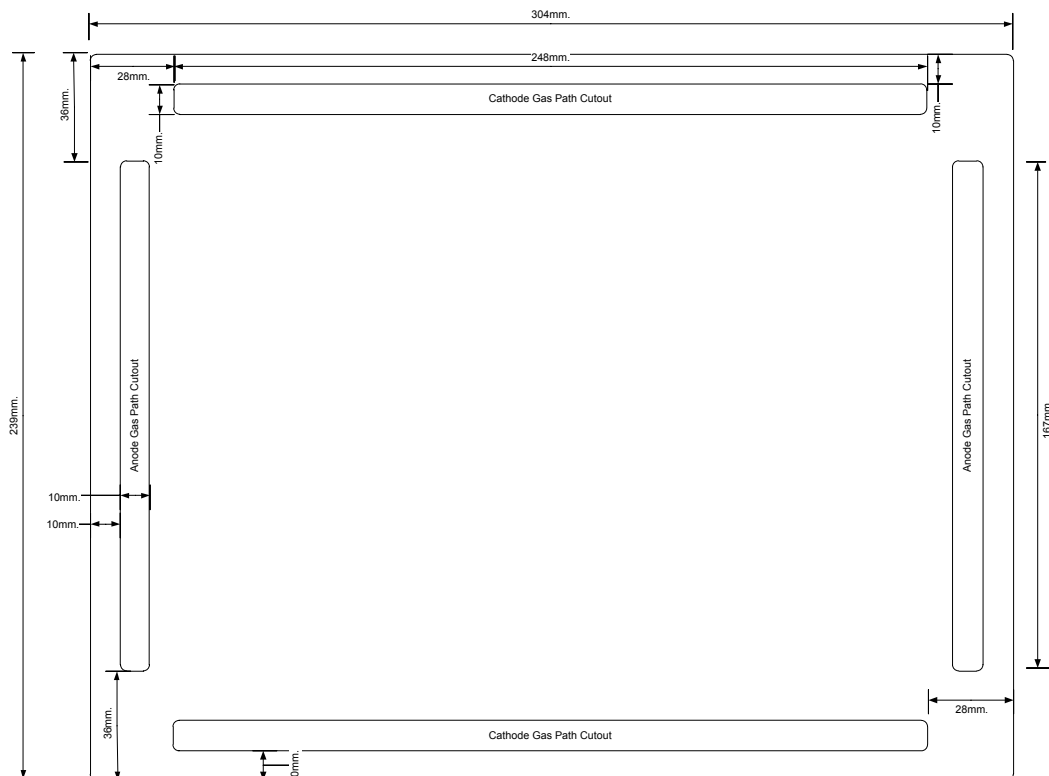
- Ferritic stainless steel stamping operation
- Laser etching operation
- Perovskite coating operation
- Heat treating operation

### A-18.2 Process Flow



### A-18.3 Background

The interconnect plates are dimensioned as shown:



## A-18.4 Preliminary Analysis

The interconnects for this analysis will be working in a 30-kW stack for which the part size is:

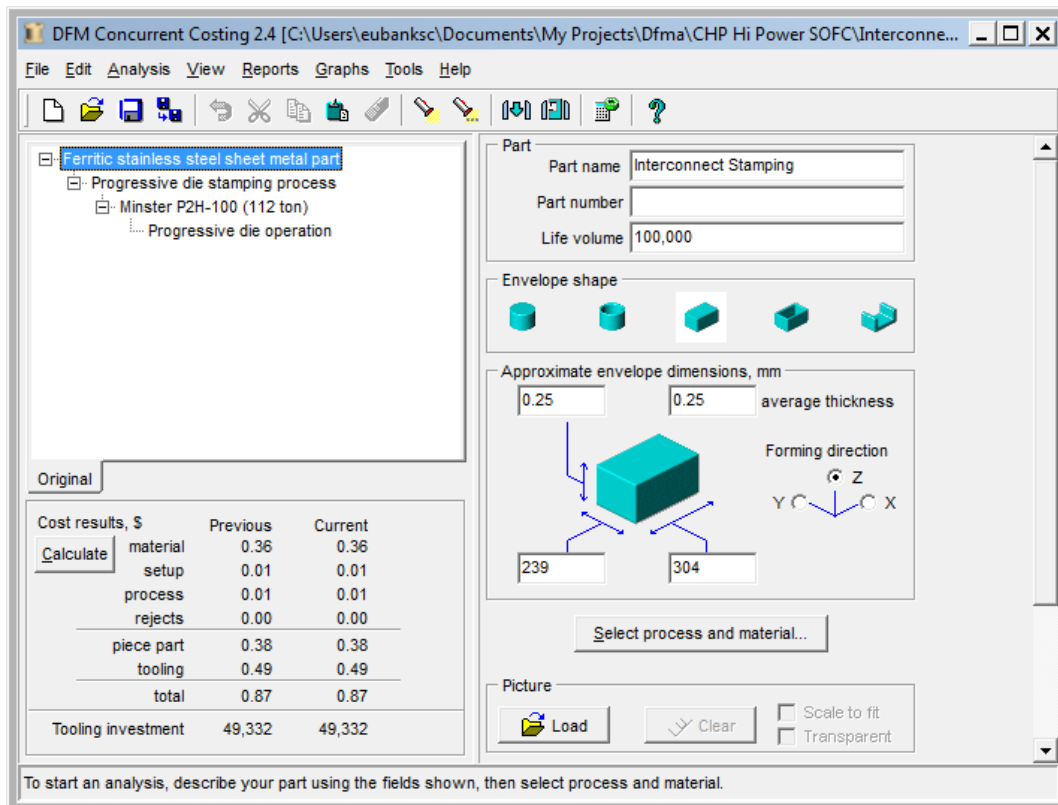
$$239 \text{ mm width} \times 304 \text{ mm length} = 726.6 \text{ cm}^2$$

The interconnects will be manufactured from 0.25-mm-thick ferritic stainless steel (SS-441) plate. The 30-kW stack requires 268 interconnects. The 100-kW<sub>net</sub> system utilizes four stacks, so annual production of 1,000 systems requires annual production of:

$$\text{Annual production} = 268 \text{ parts/stack} \times 4,000 \text{ stacks} = 1,072,000 \text{ parts}$$

### A-18.4.1 Transfer Stamping Processing Cost

The Boothroyd Dewhurst, Inc. (BDI) software provides pre-programmed cost models for the transfer stamping operations used to manufacture the interconnect plate blanks, as shown below:



$$\text{Machine time} = (1 \text{ sec/part} / 3,600) \times 1,072,000 \text{ parts} + 2.0 = 300 \text{ hrs}$$

Machine utilization is:

$$\text{Utilization} = 300 / 6,000 = 5.0\%$$



Machine rate was determined in accordance with Appendix A-1 as:

$$\text{In-house rate} = \$55.40 / 0.05 = \$1,108.00$$

$$\text{Job shop rate} = 1.4 \times (\$55.40 / 0.65) = \$119.32$$

Assuming one full-time operator per machine, the total machine labor time is equal to the machine time of 300 hours.

Tooling cost is \$49,332 and is assumed to be capable of producing 400,000 parts. Amortizing over a 5-year life, the total annual tooling cost:

$$\text{Annual tooling cost} = \frac{1}{5}(\text{Tooling cost} \times \text{Number of tools purchased})$$

where:

$$\text{Number of tools purchased} = \text{Roundup}(\text{Total production} / \text{Tool life})$$

$$\text{Total production} = \text{Annual production} \times 5$$

$$\text{Annual tooling cost} = \frac{1}{5} (\$49,332) \times \text{Roundup}((1,072,000 \text{ parts/yr} \times 5 \text{ yrs}) / 400,000 \text{ parts/tool}) = \$138,129.60$$

#### A-18.4.2 Aerosol Coating Processing Cost

Assuming a single setup operation requiring one operator per production run of parts, the setup time will be 0.5 hour.

Part load/unload, which may be manual or robotic, will be driven by overall part size. Because the part will be turned in order to coat both sides, additional time equal to half of the load/unload time will be added. Using the handling time formula developed previously, the total handling time is:

$$\text{Part handling time} = 1.5 \times \text{Max}((0.3 \times ((239 + 304 + 0.25) / 25.4) - 4.6), 4) = 6.0 \text{ sec/part}$$

The perovskite coating is deposited via aerosol spray to a depth of 3 microns (0.003 mm) and has a material density of approximately 6.1 g/cm<sup>3</sup>. Assuming a 90% spray efficiency, and allowing for 5 mm overspray on the four edges, the total deposited material per coated side is:

$$\text{Deposited material} = 2 \times ((23.9 + 0.5) \text{ cm} \times (30.4 + 0.5) \text{ cm} \times 0.0003 \text{ cm}) = 0.452 \text{ cm}^3/\text{part}$$

Total coating material usage is:

$$\text{Coating material usage} = 6.1 \text{ g/cm}^3 \times 0.452 \text{ cm}^3/\text{part} \times 1,072,000 \text{ parts} = 2,955 \text{ kg}$$

The material cost before scrap was determined in accordance with Appendix A-2 as:

$$\text{Material cost} = \$146.29/\text{kg}$$

Deposited depth is a function of flow rate, spray width and nozzle speed:

$$\text{Coating depth} = \text{Flow rate (mm}^3/\text{sec)} / (\text{Spray width (mm)} \times \text{Nozzle speed (mm/sec)})$$

Spray nozzle manufacturers will generally specify a maximum flow rate associated with a particular nozzle. Therefore, given a flow rate, coated width and coating depth, the nozzle speed is calculated as:

$$\text{Nozzle speed (mm/sec)} = \text{Flow rate (mm}^3\text{/sec)} / (\text{Spray width (mm)} \times \text{Coating depth (mm)})$$

Using the SonoTek Flexicoat Impact nozzle system as an example, the maximum precision spray width is approximately 50 mm and maximum nozzle speed is 400 mm/sec. Assuming a maximum coating flow rate of 333 mm<sup>3</sup>/sec (20 ml/min), the nozzle speed is:

$$\text{Nozzle speed} = \text{Min}(333 / (50 \times 0.003), 400) = 400 \text{ mm/sec}$$

The time to coat both sides of the interconnect plate, and allowing for 25 mm overspray on the four edges is:

$$\text{Coating time per part} = 2 \times ((239 + 50) \text{ mm} \times (304 + 50) \text{ mm} / (50 \text{ mm} \times 400 \text{ mm/sec})) = 10.23 \text{ sec/part}$$

Total machine time required for annual production is:

$$\text{Machine time} = (10.23 + 6.0) \text{ sec/part} / 3,600 \times 1,072,000 \text{ parts} = 4,833 \text{ hrs}$$

Machine utilization is:

$$\text{Utilization} = 4,833 / 6,000 = 80.5\%$$

Machine rate was determined in accordance with Appendix A-1 as:

$$\text{In-house rate} = \$31.06 / 0.805 = \$38.58$$

$$\text{Job shop rate} = 1.4 \times (\$31.06 / 0.65) = \$66.90$$

Given that the operator required time for load/unload is approximately equal to the total part processing time, we will assume one operator per machine, making the machine labor time equal to the machine time of 375.7 hours.

### A-18.4.3 Heat Treating Processing Cost

The interconnect coating process calls for heat treatment at 1,000°C (1,472°F) for 4 hours after the part reaches temperature. Large mesh belt furnaces manufactured by AFC-Holcroft feature a 66-inch (167-cm) wide belt, 6-inch (15.24-cm) workspace clearance, and effective load length of 456 inches (1,158 cm), for a total load volume of  $2.95 \times 10^6$  cm<sup>3</sup>. The maximum part thickness following the last screen printing operation is 328 microns (0.0328 cm). Adding 1 cm on all sides for part spacing in the furnace and assuming optimal racking, the total part envelope is:

$$\text{Part envelope} = (23.9 + (2 \times 1.0)) \times (30.4 + (2 \times 1.0)) \times (0.025 + (2 \times 1.0)) = 1,699 \text{ cm}^3$$

The maximum furnace loading is then:

$$\text{Furnace loading} = 2.95 \times 10^6 \text{ cm}^3 / 1,699 \text{ cm}^3 = 1,737 \text{ parts}$$

The firing schedule is based on the metallization schedule suggested in PNNL-22732<sup>30</sup>:

Segment	Rate/Time	Temp.
Ramp	3°C/min	1,000°C
Hold	4 hr	1,000°C
Ramp	5°C/min	Ambient

Using 25°C as the ambient temperature, the required preheat time is:

$$(1,000 - 25)^\circ\text{C} / (3^\circ/\text{min}) = 325 \text{ min} = 5.42 \text{ hrs}$$

The required cooling time is:

$$(1,000 - 25)^\circ\text{C} / (5^\circ/\text{min}) = 195 \text{ min} = 3.25 \text{ hrs}$$

Therefore, total furnace time is 12.67 hours, making furnace throughput:

$$\text{Throughput} = 1,737 \text{ parts} / 12.67 \text{ hrs} = 137 \text{ parts/hr}$$

Total machine time to fire the interconnects is:

$$\text{Machine time} = 1,072,000 \text{ parts} / 137 \text{ parts/hr} = 7,825 \text{ hrs}$$

The machine utilization is:

$$\text{Utilization} = 7,825 / (2 \times 6,000) = 65.2\%$$

Machine rate was determined in accordance with Appendix A-1 as:

$$\text{In-house rate} = \$53.99 / 0.652 = \$82.81$$

$$\text{Job shop rate} = 1.4 \times (\$53.99 / 0.65) = \$116.29$$

Part load/unload, which may be manual or robotic, will be driven by overall part size. To determine if a single operator can load and unload parts while the machine is operating, we use the handling time formula developed previously, to determine the total load/unload time required per hour or machine time as:

$$\text{Part handling time} = \text{Max}((0.3 \times ((239 + 304 + 0.28) / 25.4) - 4.6), 4) = 4 \text{ sec/part}$$

$$\text{Total part handling time} = (4 \text{ sec/part} / 3,600) \times 137 \text{ parts/hr} = 0.152 \text{ hrs per hour of machine time}$$

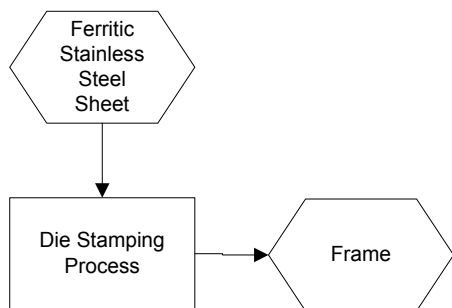
<sup>30</sup> M.R. Weimar, L.A. Chick, D.W. Gotthold, and G.A. Whyatt. 2013. Cost Study for Manufacturing of Solid Oxide Fuel Cell Power Systems (PNNL-22732). Pacific Northwest National Laboratory, September 2013.

## Appendix A-19: SOFC Picture Frame Production Process

### A-19.1 Model Approach

- Ferritic stainless steel stamping operation

### A-19.2 Process Flow



### A-19.3 Background

The SOFC cell contains three frames:

- The anode frame supports the interconnect on the anode side and provides space for the anode mesh
- The picture frame provides space for the cathode side of the cell
- The cathode frame supports the interconnect on the cathode side and provides space for the cathode mesh

The Boothroyd Dewhurst, Inc. (BDI) Design for Manufacture and Assembly (DFMA)<sup>®</sup> software provides pre-programmed cost models for the transfer stamping operations used to manufacture the frames. Labor and machine times will be aggregated to determine number of presses required and utilization. Material usage will be aggregated to compute material cost.

### A-19.4 Preliminary Analysis

The frames for this analysis will be working in a 30-kW stack for which the overall part size is:

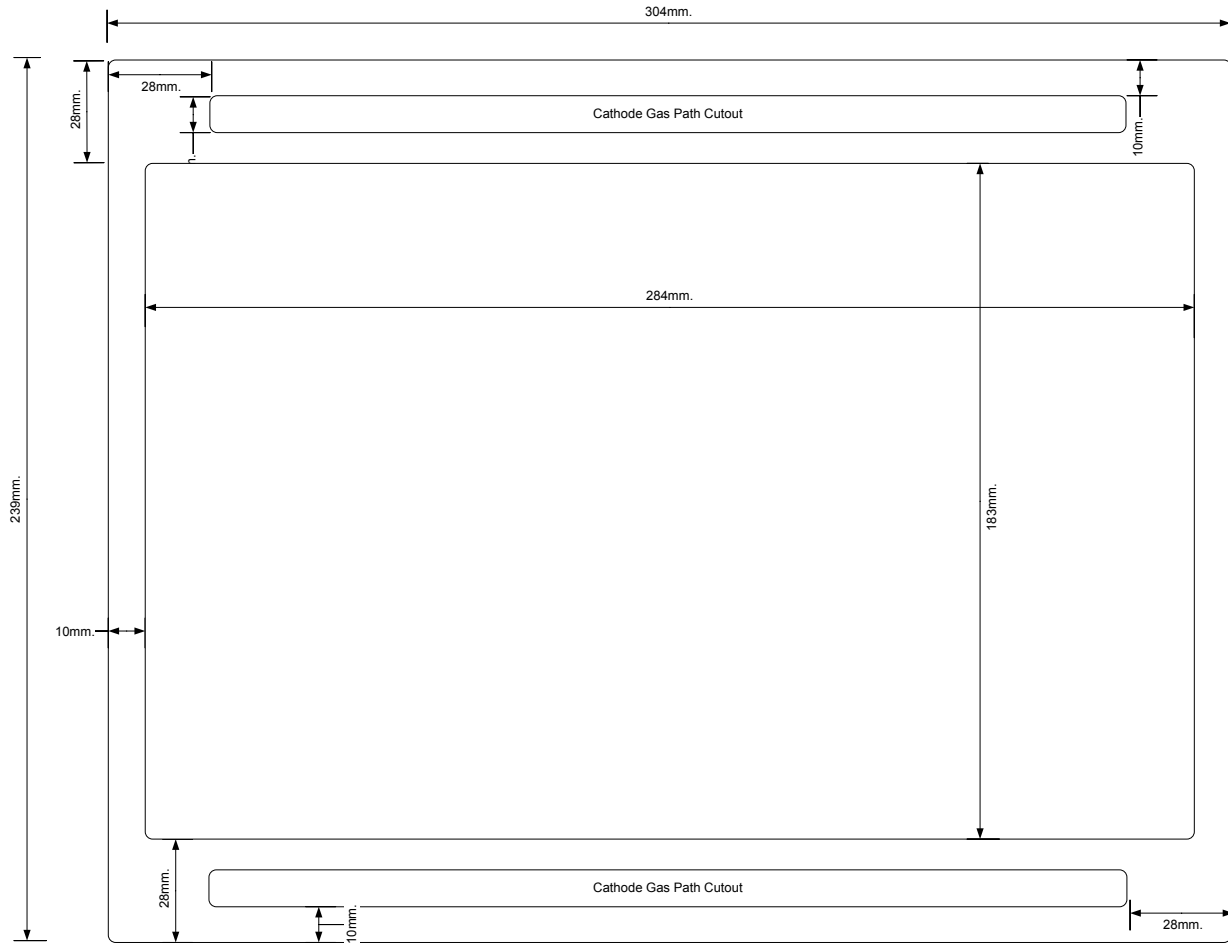
$$239 \text{ mm width} \times 304 \text{ mm length} = 726.6 \text{ cm}^2$$

Machine and labor time will be calculated based on an annual production of 1,000 100-kW<sub>net</sub> systems per year, with each system requiring four stacks. The 30-kW stack requires 259 of each type of frame, requiring production of:

$$\text{Annual production} = 259 \text{ parts/stack} \times 4,000 \text{ stacks} = 1,036,000 \text{ parts/frame}$$

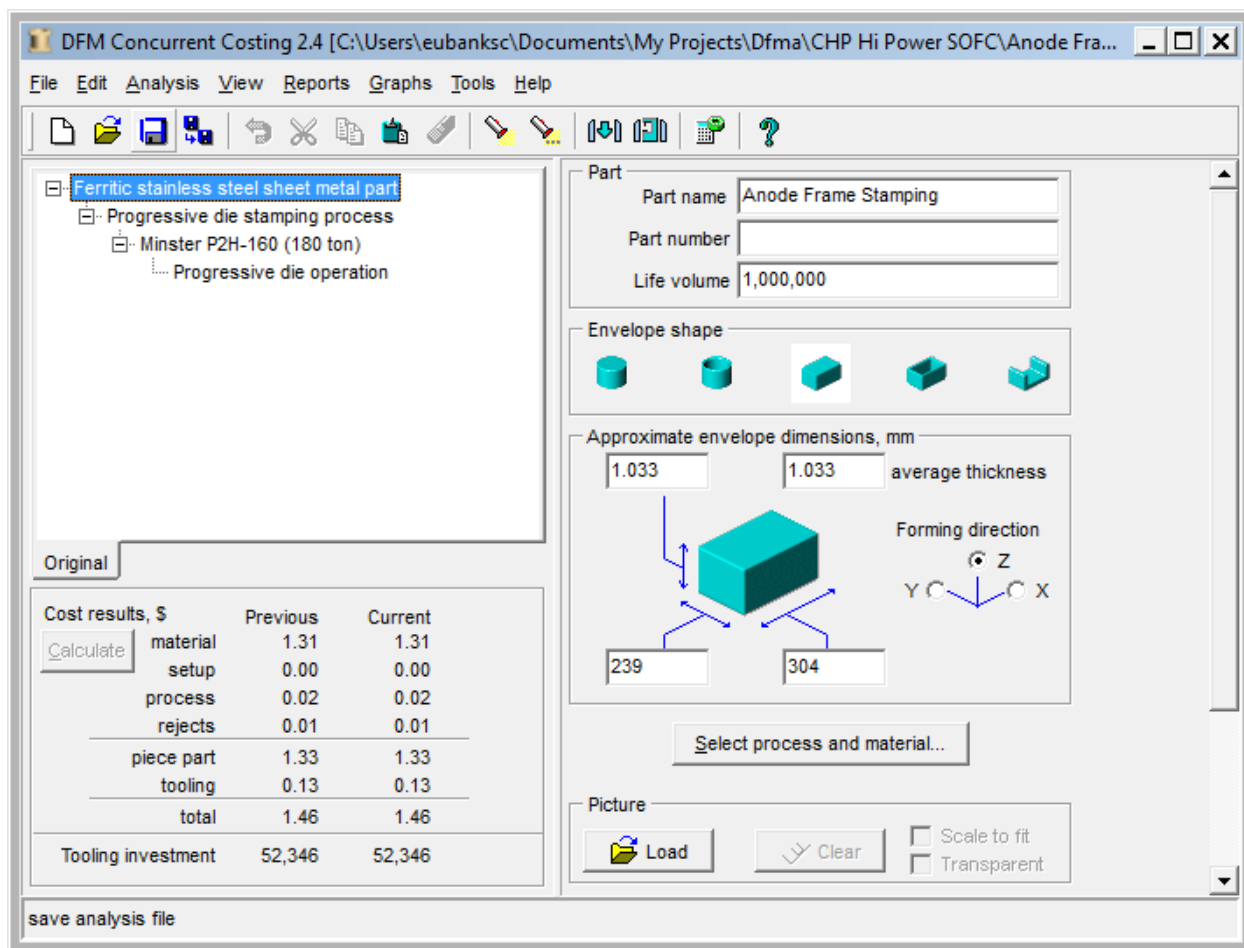
## A-19.5 Anode Frame

### A-19.5.1 Frame Dimensions



## A-19.5.2 Die Stamping Processing Cost

The resulting BDI DFMA software analysis is shown in the following screen shot:



The BDI software estimates a 2-hour machine setup time and calculates the total manufacturing time for the stamped part as 1.5 seconds, making the total machine time for annual production:

$$\text{Machine time} = (1.5 \text{ sec/part} / 3,600) \times 1,036,000 \text{ parts} + 2.0 = 433.7 \text{ hrs}$$

Assuming one full-time operator per machine, the total machine labor time is equal to the machine time of 433.7 hours.

Tooling cost is \$52,346 and is assumed to be capable of producing 400,000 parts. Amortizing over a 5-year life, the total annual tooling cost is:

$$\text{Annual tooling cost} = \frac{1}{5}(\text{Tooling cost} \times \text{Number of tools purchased})$$

where:

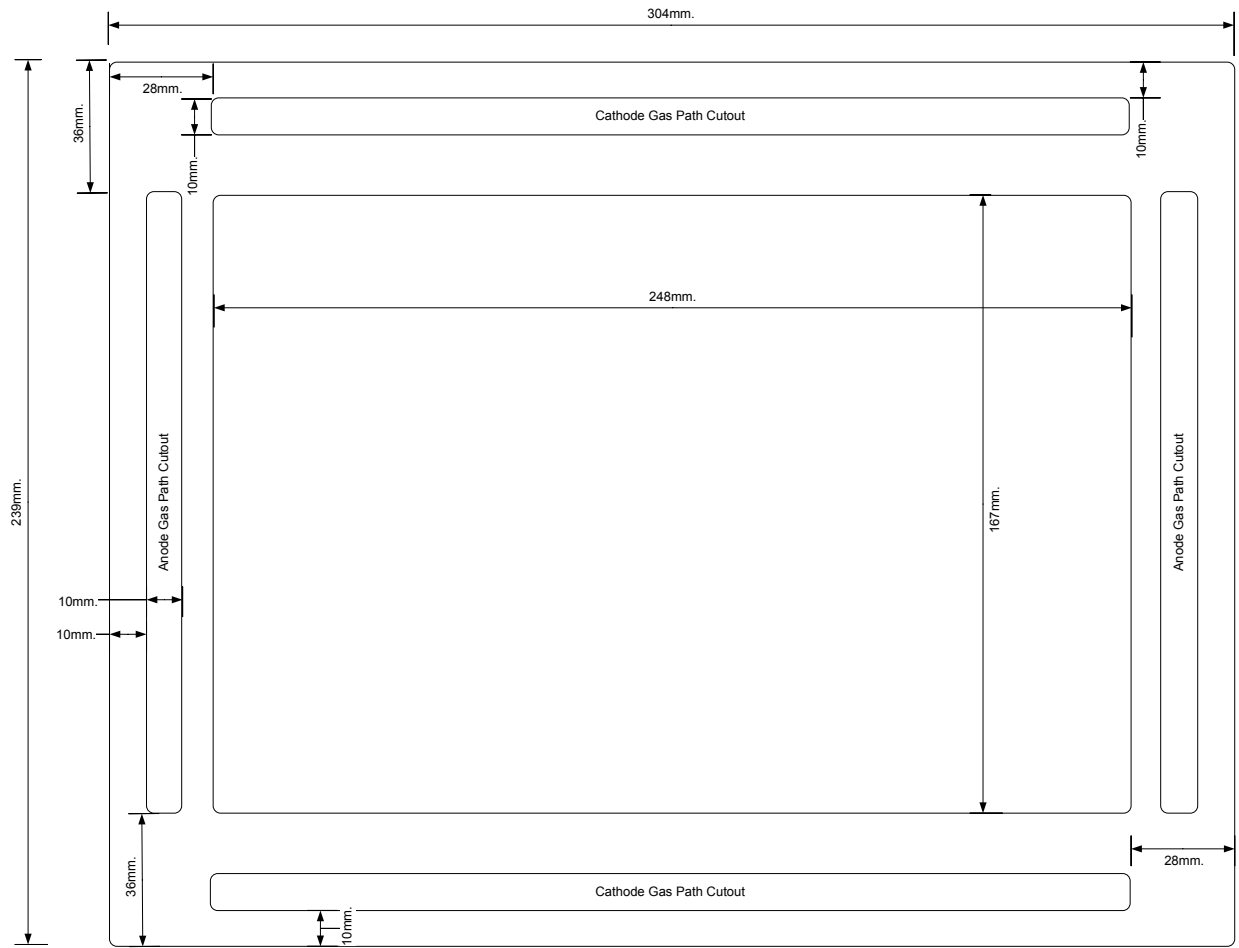
$$\text{Number of tools purchased} = \text{Roundup}(\text{Total production} / \text{Tool life})$$

$$\text{Total production} = \text{Annual production} \times 5$$

$$\text{Annual tooling cost} = \frac{1}{5}((\$52,346) \times \text{Roundup}((1,036,000 \text{ parts/yr} \times 5 \text{ yrs}) / 400,000 \text{ parts/tool})) = \$136,100$$

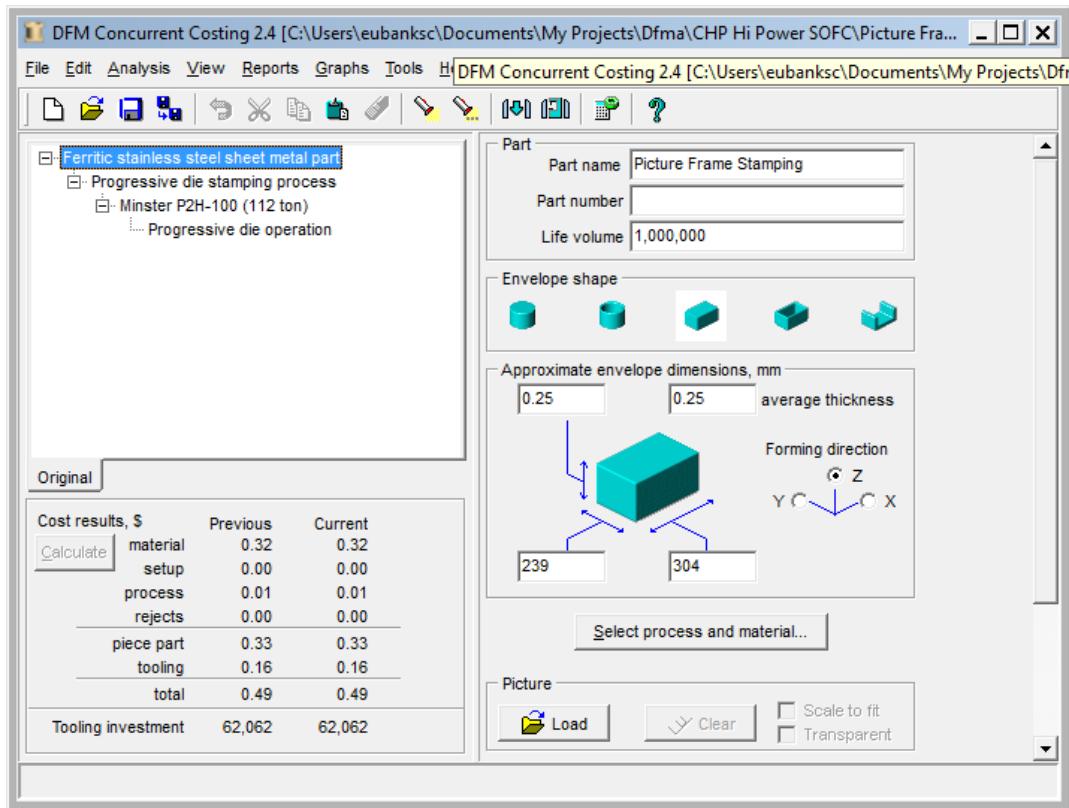
## A-19.6 Picture Frame

### A-19.6.1 Frame Dimensions



## A-19.6.2 Die Stamping Processing Cost

The resulting BDI DFMA<sup>®</sup> software analysis is shown in the following screen shot:



The BDI software estimates a 2-hour machine setup time and calculates the total manufacturing time for the stamped part as 1.0 second, making the total machine time for annual production:

$$\text{Machine time} = (1.0 \text{ sec/part} / 3,600) \times 1,036,000 \text{ parts} + 2.0 = 289.8 \text{ hrs}$$

Assuming one full-time operator per machine, the total machine labor time is equal to the machine time of 289.8 hours.

Tooling cost is \$62,062 and is assumed to be capable of producing 400,000 parts. Amortizing over a 5 year life, the total annual tooling cost is:

$$\text{Annual tooling cost} = \frac{1}{5}(\text{Tooling cost} \times \text{Number of tools purchased})$$

where:

$$\text{Number of tools purchased} = \text{Roundup}(\text{Total production} / \text{Tool life})$$

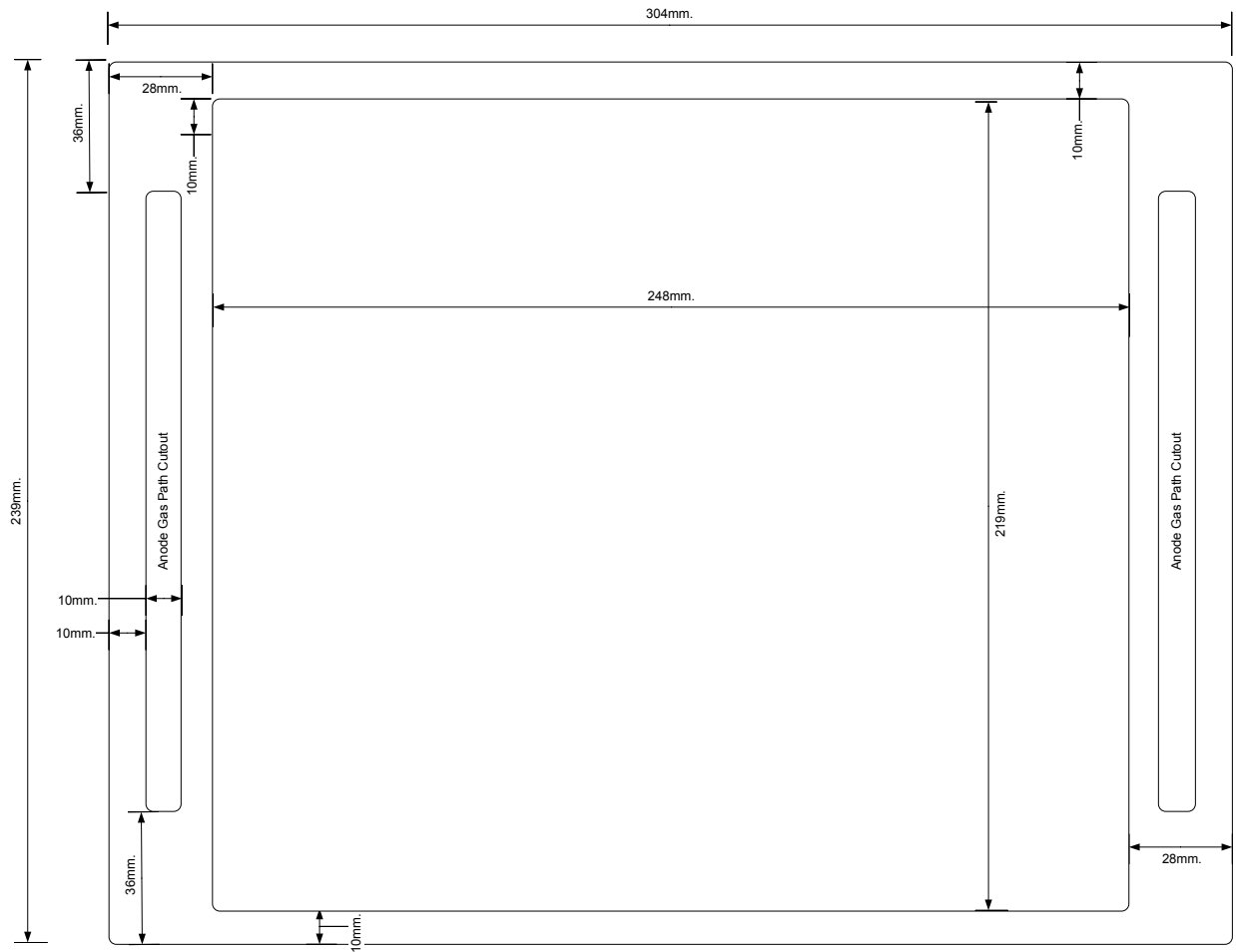
$$\text{Total production} = \text{Annual production} \times 5$$

$$\text{Annual tooling cost} = \frac{1}{5}((\$62,062) \times \text{Roundup}((1,036,000 \text{ parts/yr} \times 5 \text{ yrs}) / 400,000 \text{ parts/tool})) = \$161,361$$



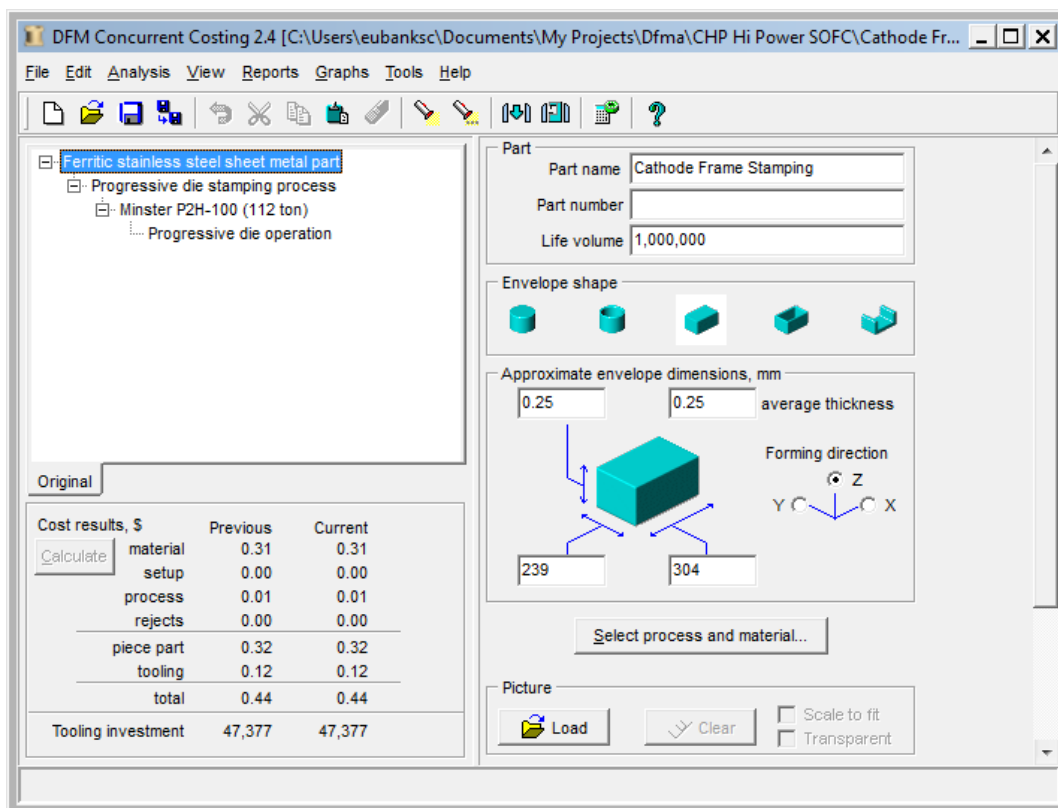
## A-19.7 Cathode Frame

### A-19.7.1 Frame Dimensions



## A-19.7.2 Die Stamping Processing Cost

The resulting BDI DFMA software analysis is shown in the following screen shot:



The BDI software estimates a 2-hour machine setup time and calculates the total manufacturing time for the stamped part as 1.0 second, making the total machine time for annual production:

$$\text{Machine time} = (1.0 \text{ sec/part} / 3,600) \times 1,036,000 \text{ parts} + 2.0 = 289.8 \text{ hrs}$$

Assuming one full-time operator per machine, the total machine labor time is equal to the machine time of 289.8 hours.

Tooling cost is \$47,377 and is assumed to be capable of producing 400,000 parts. Amortizing over a 5-year life, the total annual tooling cost is:

$$\text{Annual tooling cost} = \frac{1}{5}(\text{Tooling cost} \times \text{Number of tools purchased})$$

where:

$$\text{Number of tools purchased} = \text{Roundup}(\text{Total production} / \text{Tool life})$$

$$\text{Total production} = \text{Annual production} \times 5$$

$$\text{Annual tooling cost} = \frac{1}{5}((\$47,377) \times \text{Roundup}((1,036,000 \text{ parts/yr} \times 5 \text{ yrs}) / 400,000 \text{ parts/tool})) = \$123,180$$

## A-19.8 Machine Utilization

Total machine time to produce the three frames is:

$$\text{Stamping machine time} = 433.7 + 289.8 + 289.8 = 1,013 \text{ hrs}$$

Machine utilization is:

$$\text{Utilization} = 1,013 / 6,000 = 16.9\%$$

Machine rate was determined in accordance with Appendix A-1 as:

$$\text{In-house rate} = \$55.40 / 0.169 = \$327.81$$

$$\text{Job shop rate} = 1.4 \times (\$55.40 / 0.65) = \$119.32$$

## A-19.9 Material Cost

The BDI DFMA software estimated the part weights as:

Anode frame: 0.524 kg

Picture frame: 0.128 kg

Cathode frame: 0.124 kg

Total annual material usage for the three frames is:

$$\text{Annual material usage} = (0.524 + 0.128 + 0.124) \text{ kg/cell} \times 259 \text{ cells/stack} \times 4,000 \text{ stacks} = 803,936 \text{ kg}$$

Material cost is computed in accordance with Appendix A-2 as:

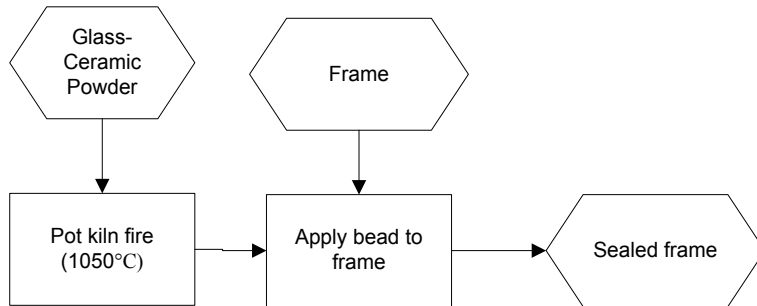
$$\text{Material cost} = \$2.250/\text{kg}$$

## Appendix A-20: SOFC Glass-Ceramic Sealant Production Process

### A-20.1 Model Approach

- Calculate glass-ceramic sealant batch size
- Calculate glass-ceramic sealant production time
- Calculate glass-ceramic sealant application time

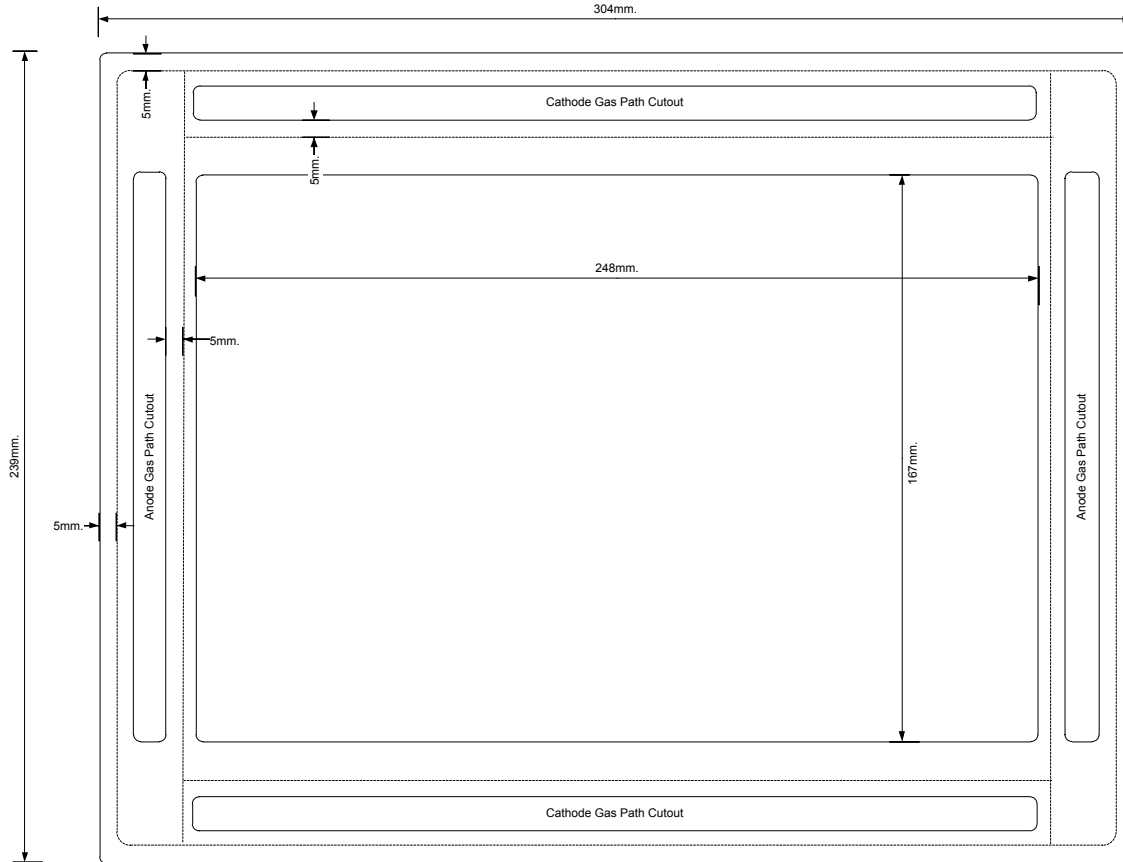
### A-20.2 Process Flow



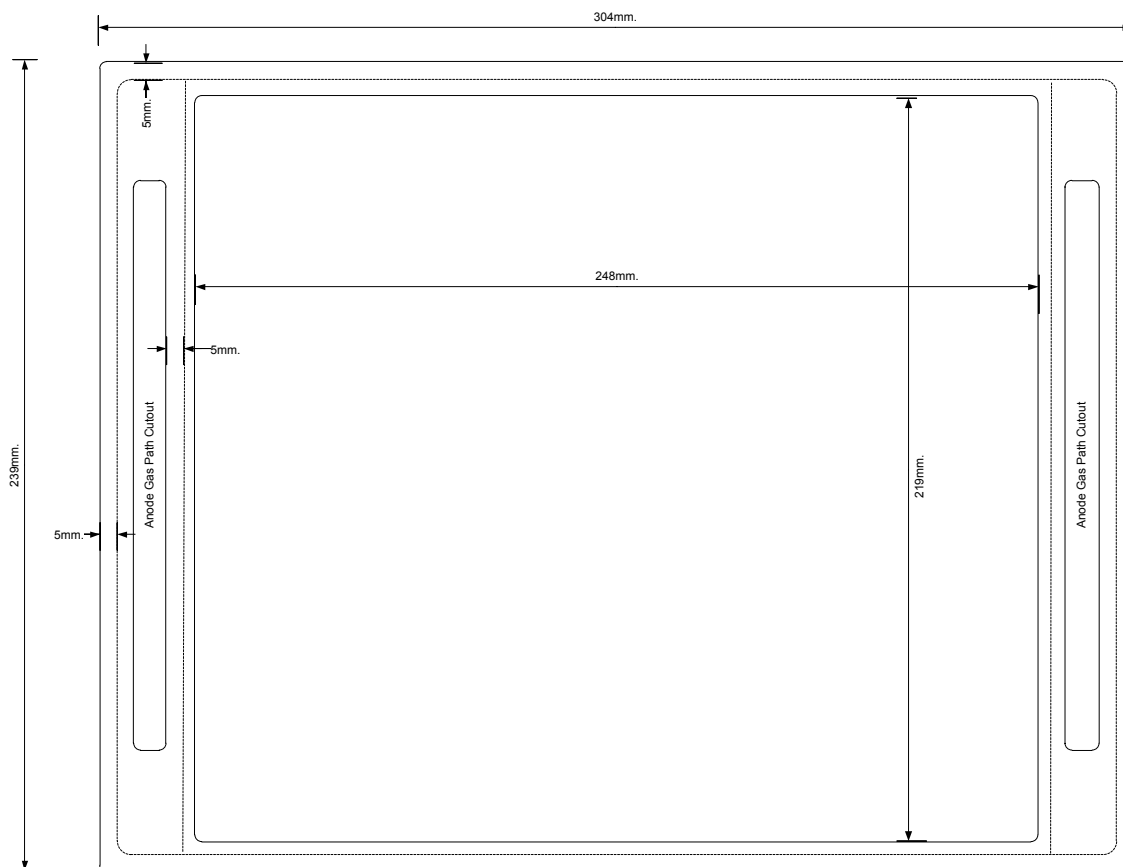
### A-20.3 Background

The sealant bead (dashed lines) is applied to the picture frame and cathode frame as shown:

#### A-20.3.1 Picture Frame



### A-20.3.2 Cathode Frame



### A-20.4 Preliminary Analysis

Machine and labor time will be calculated based on an annual production of 4,000 30-kW stacks. The 30-kW stack requires 259 of each type of frame.

#### A-20.4.1 Sealant Material

The sealant will be applied to areas that are 10 mm wide and needs to fill a gap of about 148 microns on both sides of the interconnect plates and one side of the picture frame with the same seal length as the cathode side. Assuming a maximum finished seal width of 8 mm, the total seal cross-sectional area is:

$$\text{Seal cross sectional area} = 8 \text{ mm wide} \times 0.148 \text{ mm high} = 1.184 \text{ mm}^2$$

Assuming application in a round bead, the required bead diameter that will yield the same cross sectional area is:

$$\text{Seal dispense diameter} = 2 \times (1.184/\pi)^{1/2} = 1.23 \text{ mm}$$

The total seal length per side based on the above drawings is:

$$\text{Picture frame seal length: } (2 \times (304 - 10)) + (4 \times (239 - 10)) + (2 \times (304 - 50)) = 2012 \text{ mm}$$

$$\text{Cathode frame seal length: } (2 \times (304 - 10)) + (4 \times (239 - 10)) = 1504 \text{ mm}$$

The total volume of seal material required per cell (sealing both parts) is:

$$1.184 \text{ mm}^2 \times (2012 + 1504) \text{ mm} = 4163 \text{ mm}^3 = 4.163 \text{ cm}^3$$

The total sealant batch size (cm<sup>3</sup>) for 4,000 stacks is:

$$4.163 \text{ cm}^3/\text{cell} \times 259 \text{ cells/stack} \times 4,000 \text{ stacks} = 4,312,868 \text{ cm}^3$$

A typical sealant is the Ceredyne VIOX V1649 glass ceramic sealant, consisting of 50/50 borosilicate glass (BSG) / lanthanum oxide (LO) by volume. The density of the mixture is:

$$\text{Sealant density} = (2.23 \text{ g/cm}^3 + 6.51 \text{ g/cm}^3) / 2 = 4.37 \text{ g/cm}^3$$

Therefore, the required sealant by weight is:

$$\text{Sealant weight: } 4,312,868 \text{ cm}^3 \times 4.37 \text{ g/cm}^3 / 1,000 = 18,847 \text{ kg}$$

The weight of each material in the sealant mixture is:

$$\text{LO: } (6.51 / 8.74) \times 18,847 \text{ kg} = 14,038 \text{ kg}$$

$$\text{BSG: } (2.23 / 8.74) \times 18,847 \text{ kg} = 4,809 \text{ kg}$$

Material costs before scrap were determined in accordance with Appendix A-2 as:

$$\text{LO material cost} = \$46.80/\text{kg}$$

$$\text{BSG material cost} = \$1.70/\text{kg}$$

To create the paste, the borosilicate glass/lanthanum oxide mixture is fired at 1,050°C in a pot furnace for 3 hours. The Trent PF-1000 17-kW pot furnace with a total pot size of 44,480 cm<sup>3</sup> is capable of holding 145 kg of sealant material at 75% fill volume. At the highest anticipated volume, the 25-kW stack will require annual production 13.4 million cells, requiring about 12.5 times as much material, so this furnace should be sufficient for all anticipated levels of production.

The number of batches is:

$$\text{Roundup}(18,847 / 145) = 130$$

Assuming that one operator can set up a sealant batch in 0.5 hour results in a total furnace machine time of:

$$\text{Machine time} = (0.5 + 3) \text{ hrs} \times 130 \text{ batches} = 455 \text{ hrs}$$

Given that the operator-required time for batch setup represents a small percentage of the total part processing time, we will assume one operator is capable of operating three machines, making the machine labor hours:

$$\text{Machine labor hrs} = 130 \text{ batches} \times (0.5 + (3.0 / 3)) = 195 \text{ hrs}$$

## A-20.4.2 Sealant Application Cost

Assuming a single setup operation requiring one operator per batch of parts, the sealant application station setup time is 0.5 hour.

Part load/unload (two total part movements), which may be manual or robotic, will be driven by overall part size. Using the handling time formula developed based on the Boothroyd Dewhurst, Inc. (BDI) Design for Manufacture and Assembly (DFMA)<sup>®</sup> software, the total handling time for each part is:

$$\text{Part handling time: } \text{Max}((0.3 \times ((188 + 229 + 0.25) / 25.4) - 4.6), 4) = 4.0 \text{ sec/part}$$

The BDI DFMA software tool estimate for the bead application rate of viscous sealants is 2 inches per second (in/sec) (51 mm/sec) with an applicator positioning time of 0.4 second. For the picture frame, we assume that the bead is applied to the part perimeter in a single bead, followed by the two beads between the anode gas path and the ceramic cell, followed by the two beads between the anode gas path and the ceramic cell. Consequently, there will be six total repositionings: move applicator to start of perimeter bead, move applicator to start of each of the four gas path beads, move applicator to second gas path bead, move applicator to home position. The total application time is:

$$\text{Picture frame application time} = 4.0 \text{ sec} + (6 \times 0.4) \text{ sec} + (2,012 \text{ mm} / 51 \text{ mm/sec}) = 45.85 \text{ sec/part}$$

For the cathode frame, we assume that the bead is applied to the part perimeter in a single bead, followed by the two beads between the anode gas path and the ceramic cell for four total repositionings. The total application time is:

$$\text{Cathode frame application time} = 4.0 \text{ sec} + (4 \times 0.4) + (1,154 \text{ mm} / 51 \text{ mm/sec}) = 35.09 \text{ sec/part}$$

Total application time per cell is:

$$\text{Total application time} = 45.85 + 35.09 = 80.94 \text{ sec}$$

Total sealant machine time is:

$$\text{Machine time} = 0.5 \text{ hr} + ((80.94 \text{ sec} / 3,600) \text{ hrs/cell} \times 259 \text{ cells/stack} \times 4,000 \text{ stacks}) = 23,293 \text{ hrs}$$

Given that the operator required time for load/unload represents a small percentage of the total part processing time, we will assume one operator is capable of operating three sealant machines, making the machine labor hours:

$$\text{Machine labor hrs} = 23,293 / 3 = 7,764 \text{ hrs}$$

Machine utilization is:

$$\text{Utilization} = 23,293 / (4 \times 6,000) = 97.1\%$$



Machine rate was determined in accordance with Appendix A-1 as:

$$\text{In-house rate} = \$48.21 / 0.971 = \$48.72$$

$$\text{Job shop rate} = 1.4 \times (\$48.21 / 0.65) = \$103.84$$

Total station labor time is:

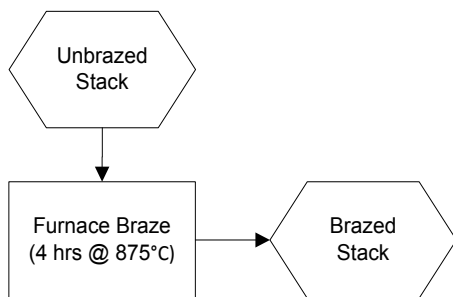
$$\text{Machine labor hrs} = 195 + 7,764 = 7,959 \text{ hrs}$$

## Appendix A-21: SOFC Stack Brazing Process

### A-21.1 Model Approach

- Stack Brazing
  - Part handling time labor cost based on part size per Boothroyd Dewhurst, Inc. (BDI) formula and throughput; 4-second minimum
  - Process cost based on oven energy cost plus standard machine rate

### A-21.2 Process Flow



### A-21.3 Preliminary Analysis

The cells for this analysis are for a 100-kW<sub>net</sub> system at a production rate of 4,000 stacks per year (1,000 systems with four stacks per system).

The overall part envelope is bounded by the end plate length and width and the stack height. The 30-kW stack height is estimated based on a thickness of about 2.1 millimeters (mm) per repeat cell, 259 cells per stack, plus 12 mm each for the two end plates. The total stack envelope is estimated as:

$$36.4 \text{ cm width} \times 29.9 \text{ cm length} \times ((0.21 \times 259) + (1.2 \times 2)) \text{ cm high} = 61,808 \text{ cm}^3$$

#### A-21.3.1 Stack Brazing

The brazing schedule is based on the metallization schedule suggested in PNNL-22732<sup>31</sup>:

Segment	Rate/Time	Temp.
Ramp	3°C/min	600°C
Hold	1 hr	600°C
Ramp	5°C/min	875°C
Hold	4 hrs	875°C
Ramp	5°C/min	750°C
Hold	2 hrs	750°C
Ramp	5°C/min	Ambient

<sup>31</sup> M.R. Weimar, L.A. Chick, D.W. Gotthold, and G.A. Whyatt. 2013. Cost Study for Manufacturing of Solid Oxide Fuel Cell Power Systems (PNNL-22732). Pacific Northwest National Laboratory, September 2013.

The 30-kW stack dimensions require that the furnace have a workspace clearance of at least 30 centimeters (cm) (11.8 inches), an unusually large size for conveyor-type continuous furnaces. A used Surface Combustion rotary hearth furnace supports 60 5-inch × 21-inch (12.7-cm × 53.3-cm) trays with a workspace clearance of 35 inches (88.9 cm) for a total load volume of  $3.61 \times 10^6 \text{ cm}^3$ . Allowing 5-cm separation between stacks creates an effective part volume of:

$$41.4 \text{ cm width} \times 34.9 \text{ cm length} \times 61.8 \text{ cm high} = 89,292 \text{ cm}^3$$

The maximum furnace loading is then:

$$\text{Furnace loading} = \text{Rounddown} (3.61 \times 10^6 \text{ cm}^3 / 89,292 \text{ cm}^3) = 40 \text{ parts}$$

Using 25°C as the ambient temperature, the required heating times are:

$$(600 - 25)^\circ\text{C} / (3.0^\circ/\text{min}) = 192 \text{ min} = 3.2 \text{ hrs}$$

$$(875 - 600)^\circ\text{C} / (5.0^\circ/\text{min}) = 55 \text{ min} = 0.917 \text{ hrs}$$

The required cooling times are:

$$(875 - 750)^\circ\text{C} / (5.0^\circ/\text{min}) = 25 \text{ min} = 0.417 \text{ hrs}$$

$$(750 - 25)^\circ\text{C} / (5.0^\circ/\text{min}) = 145 \text{ min} = 2.417 \text{ hrs}$$

Adding the 7-hour hold times, total furnace time is 13.95 hours, making furnace throughput:

$$\text{Throughput} = 40 \text{ stacks} / 13.95 \text{ hrs} = 2.88 \text{ stacks/hr}$$

Total machine time to fire the cells is:

$$\text{Machine time} = 4,000 \text{ stacks} / 2.88 \text{ stacks/hr} = 1,389 \text{ hrs}$$

Machine utilization is:

$$\text{Utilization} = 1,389 / 6,000 = 23.1\%$$

Machine rate was determined in accordance with Appendix A-1 as:

$$\text{In-house rate} = \$60.26 / 0.231 = \$260.87$$

$$\text{Job shop rate} = 1.4 \times (\$60.26 / 0.65) = \$129.79$$

Part load/unload, which may be manual or robotic, will be driven by overall part size. To determine if a single operator can load and unload parts while the machine is operating, we use the handling time formula adapted from the BDI Design for Manufacture and Assembly (DFMA)<sup>®</sup> software to determine the total load/unload time required per hour or machine time as:

$$\text{Part handling time} = \text{Max}((0.3 \times ((299 + 364 + 567.9) / 25.4) - 4.6), 4) = 9.94 \text{ sec}$$

Total part loading time per batch is:

$$\text{Part loading time} = (9.94 / 3,600) * 40 \text{ parts} = 0.11 \text{ hr}$$

Given that part handling time is a small fraction of total firing time, we assume one operator is capable of covering three machines, making the labor time:

$$\text{Machine labor time} = 1,389 / 3 = 463 \text{ hrs}$$

During the final hold at 750°C, reducing gas (2% hydrogen in nitrogen) is flowed through the anode cavities to reduce the NiO to Ni metal. Using the required testing flow rate for 30-kW stacks of 358.86 l/min:

$$\text{Total flow rate} = 358.86 \text{ l/min} \times 60 \text{ min/hr} / 1,000 \text{ l/m}^3 = 21.53 \text{ m}^3/\text{hr}$$

During the 2-hour reduction phase, the total reducing gas usage before scrap is:

$$\text{Nitrogen} = (21.53 \times 0.98) \text{ m}^3/\text{hr} \times 2 \text{ hrs/stack} \times 4,000 \text{ stacks} = 168,811 \text{ m}^3$$

$$\text{Hydrogen} = (21.53 \times 0.02) \text{ m}^3/\text{hr} \times 2 \text{ hrs/stack} \times 4,000 \text{ stacks} = 3,445 \text{ m}^3$$

Material cost before scrap was determined in accordance with Appendix A-2 as:

$$\text{Nitrogen cost} = \$0.423/\text{m}^3$$

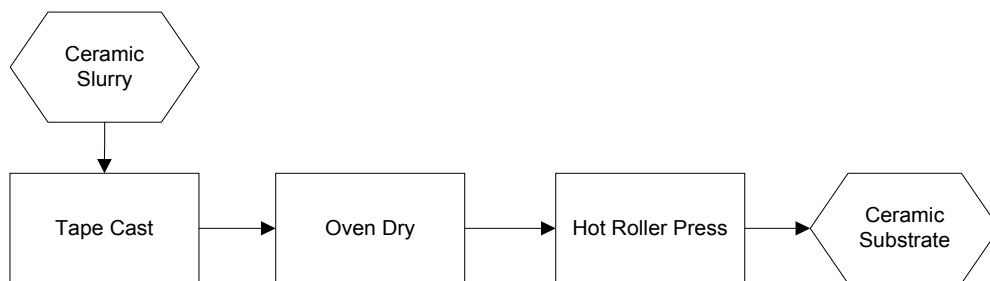
$$\text{Hydrogen cost} = \$4.744/\text{m}^3$$

## Appendix A-22: SOFC Tape Casting Process

### A-22.1 Model Approach

- Tooling Cost
  - Compute tooling cost
- Tape Casting
  - Compute machine time for machine setup
  - Compute material cost for tape casting substrate
  - Compute casting speed/throughput
  - Compute machine and labor time for tape casting operation
- Oven Drying
  - Compute drying time and dryer length
  - Compute radiant heater area
  - Compute heater energy based on energy watt density and dryer area

### A-22.2 Process Flow



### A-22.3 Background

The total required anode thickness is 500 microns, which will be achieved via hot roller pressing of two 250-micron tapes.

### A-22.4 Preliminary Analysis

The cells for this analysis are for a 30-kW system at a production rate of 4,000 stacks per year. The deposition area for the anode will be:

$$187 \text{ mm width} \times 268 \text{ mm length} = 501.16 \text{ cm}^2$$

The 30-kW stack requires 107 cells, requiring total annual production of:

$$\text{Annual production} = 259 \text{ parts/stack} \times 4,000 \text{ stacks} = 1,036,000 \text{ parts}$$

### A-22.4.1 Cost

In a personal communication with Richard Mistler, co-author of *Tape Casting: Theory and Practice*,<sup>32</sup> he estimates that a doctor blade for this application would cost approximately \$2,050 and would “last for years.” Using 100,000 parts as a life approximation and amortizing over a 5-year production life, the total annual tooling cost is:

$$\text{Annual tooling cost} = \frac{1}{5}(\text{Tooling cost} \times \text{Number of tools purchased})$$

where:

$$\text{Number of tools purchased} = \text{Roundup}(\text{Total production} / \text{Tool life})$$

$$\text{Total production} = \text{Annual production} \times 5$$

$$\text{Annual tooling cost} = \frac{1}{5}((\$2,050) \times \text{Roundup}((1,036,000 \text{ parts/yr} \times 2 \text{ tapes/part} \times 5 \text{ yrs}) / 100,000 \text{ parts/tool})) = \$42,476$$

### A-22.4.2 Tape Casting

Since the slurry cost is calculated separately, the material cost will consist of the cost of the tape casting carrier film. The carrier film is usually Mylar or polyethylene. For roll stock in 2-mil thickness, these materials cost approximately \$2.00/m<sup>2</sup> in bulk. Assuming that the casting width will be equal to the longest part dimension (i.e., the part length), the required casting length is determined by the part width as:

$$\text{Carrier length} = (187 \text{ mm} / 1,000) \times 1,036,000 \times 2 \text{ tapes/part} = 387,464 \text{ m}$$

Tape casting machine setup consists of loading and threading the casting substrate, and loading the ceramic slurry into the reservoir. Bulk roll stock is available in 1,000-meter lengths. Therefore, the number of setups required to run a batch of parts is:

$$\text{Number of setups} = \text{Roundup}(387,464 / 1,000) = 388 \text{ setups}$$

Allowing a 25-mm casting margin on each side, the required minimum roll widths are:

$$\text{Minimum carrier width} = 318 \text{ mm}$$

Rolls commonly appear in 6-inch (152.4-mm) incremental widths, requiring a 18-inch (457.2-mm) roll width. The total material required is:

$$\text{Material required} = 0.457 \text{ m} \times 387,464 \text{ m} = 177,149 \text{ m}^2$$

For roll stock in 2-mil thickness, these materials cost approximately \$0.32/m<sup>2</sup> in bulk. Material cost was determined in accordance with Appendix A-2 as:

$$\text{Material cost} = \$0.173/\text{m}^2$$

---

<sup>32</sup> R.E. Mistler and E.R. Twiname. 2000. Wiley – American Ceramic Society. 298 p.

Casting speed is limited by the slurry material properties, since running too fast can result in non-uniform deposition. Tok et al. (1999)<sup>33</sup> plotted experimental data relating maximum green tape thickness to casting speed, which shows a roughly exponential shape. Using the Excel function LOGEST for estimating an exponential curve fit produced the following relationship with maximum 3% error in the range of 150 to 300 microns:

$$\text{Casting speed (mm/sec)} = 157.18 \times 0.987^{\text{Green tape thickness (microns)}}$$

For a green tape thickness of 250 microns, the resulting casting speed is:

$$\text{Casting speed} = 157.18 \times 0.987^{250} = 5.97 \text{ mm/sec} = 0.358 \text{ m/min}$$

Part throughput is calculated as:

$$\text{Throughput (parts/hr)} = \text{Casting speed (m/min)} / \text{Part width (m/part)} / \text{Tapes/part} * 60 \text{ min/hr}$$

$$\text{Throughput} = 0.358 / (187 / 1,000) / 2 \times 60 = 57.43 \text{ parts/hr}$$

The total machine time required to produce 4,000 30-kW stacks is:

$$\text{Machine time} = \text{Setup time} + \text{Machine time} = (0.5 \text{ hr/setup} \times 388 \text{ setups}) + (1,036,000 \text{ parts} / 57.43 \text{ parts/hr}) = 18,234 \text{ hrs}$$

The number of tape casting machines required is:

$$\text{Number of machines} = \text{Roundup}(1,370 / 6,000) = 4 \text{ machines}$$

Machine utilization is:

$$\text{Machine utilization} = 18,234 / (4 \times 6,000) = 76.0\%$$

Machine rate was determined in accordance with Appendix A-1 as:

$$\text{In-house rate} = \$88.70 / 0.760 = \$116.71$$

$$\text{Job shop rate} = 1.4 \times (\$88.70 / 0.65) = \$191.06$$

Assuming one operator per casting machine for both setup and operation, the machine labor time is equal to the total machine time of 18,234 hours.

Casting speed is also a function of required drying time and available dryer length. HED® International's PRO-CAST® series features systems ranging in length from 12 to 100 feet (3.66 to 30.5 meters).

### A-22.4.3 Ceramic Slurry Drying

Following deposition, the ceramic slurry is dried, usually by means of a tunnel dryer positioned directly after the deposition step. The drying can be done by either radiant or convective heating. For the cost analysis, we will assume radiant (infrared) heating and compute the cost of drying by determining the required heater area.

---

<sup>33</sup> A.I.Y. Tok, F.Y.C. Boey, and M.K.A. Khor. Tape casting of high dielectric ceramic composite substrates for microelectronics applications. *Journal of Materials Processing Technology* 89-90: 508-512.

Drying time is a function of the evaporation rate of the solvent and is inversely and exponentially proportional to the coating thickness. Experiments conducted by Mistler et al. (1978)<sup>34</sup> indicate drying rates of  $1.35 \times 10^{-5}$  g/cm<sup>2</sup>-sec at room temperature for an air flow rate of 2 l/min, and  $2.22 \times 10^{-5}$  g/cm<sup>2</sup>-sec at room temperature for an air flow rate of 75 l/min.

Previous analysis assumed that the anode slurry material was formulated as follows:

- 26 wt% YSZ (8% mol)
- 37 wt% NiO
- 12 wt% water
- 24 wt% binder (Dow Duramax B-1000/B-1014)
- 1 wt% dispersant

The binder consists of approximately 45% solids. Roughly estimating the volume of liquid per gram of slurry by multiplying the material density by the material weight percent:

$$\text{Liquid density} = (0.12 \times 1.0) + ((0.24 \times 0.55) \times 1.05) + (0.01 \times 1.16) = 0.270 \text{ g/cm}^3$$

The weight of liquid to be removed per unit area is a function of slurry thickness:

$$\text{Liquid removed per area} = 0.270 \text{ g/cm}^3 \times 0.05 \text{ cm} = 0.0135 \text{ g/cm}^2$$

At a rate of  $2.0 \times 10^{-5}$  g/cm<sup>2</sup>-sec drying rate, the estimated drying time is:

$$\text{Drying time} = 0.0135 \text{ g/cm}^2 / 2.0 \times 10^{-5} \text{ g/cm}^2\text{-sec} = 675 \text{ sec} = 11.25 \text{ min}$$

At a casting speed of 0.358 m/min, the required dryer length is:

$$\text{Dryer length} = 0.358 \text{ m/min} \times 11.25 \text{ min} = 4.03 \text{ meters}$$

Infrared heating panels are generally sold with various energy watt densities and in standard sized units and assembled to provide the necessary heating area. Using the Casso Solar Type FB as an example, standard watt densities are 15 and 25 W/in<sup>2</sup> (23 and 39 kW/m<sup>2</sup>) with standard width of 12 inches (0.305 m) and lengths in 12-inch increments up to 60 inches (1.524 m). They note that 25 W/in<sup>2</sup> corresponds to an emitter temperature of 880°C, and that the conversion efficiency of electrical power to usable radiant energy is up to 80%.

The theoretical required heater area is calculated as:

$$\text{Heater area} = \text{Dryer length (meters)} \times (\text{Part width (mm)} / 1,000)$$

$$\text{Heater area} = 4.03 \times (268 / 1,000) = 1.079 \text{ m}^2$$

---

<sup>34</sup> R.E. Mistler, D.J. Shanefield, and R.B. Runk. 1978. Tape casting of ceramics, in *Ceramic Processing Before Firing*, Onoda, G.Y. Jr. and Hench, L.L. (eds). John Wiley and Sons, New York.



While the heater energy density will be taken as an input, the drying temperatures for the green tape are fairly moderate (150°C or less), so the 23 kW/m<sup>2</sup> should be sufficient to maintain the drying area temperature. While researching the tape casting process, the manufacturing specifications for the 1-kW parts were provided to HED International, a manufacturer of coaters, dryers, kilns, and furnaces. They recommended their TCM-251M tape casting machine with 12-inch (300-mm) casting width and 25-foot (7.7-meter) casting length with counter-flow heated-air dryer. The total machine power rating is 24 kW, the bulk of which would be consumed by the drying system. This is consistent with our estimate of  $25 \text{ kW/m}^2 \times 1.079 \text{ m}^2 = 27 \text{ kW}$ .

#### A-22.4.4 Anode Roll Pressing

The roll-to-roll pressing operation can be either a semi-continuous process where the material is indexed into a standard heated platen press (see James et al. [2010], Section 4.4.6.1)<sup>35</sup> or by preheating and passing through heated rollers in a calendaring process. For the preliminary analysis, we will assume a calendaring process.

##### A-22.4.1 Setup

Setup consists of loading, threading, and aligning the anode tapes into the calendaring rollers. For costing purposes, we will take the setup time as a user input and assume a value of 0.5 hour. Tapes were cast in 1,000-meter lengths totaling 387,464 meters, so that the number of setups required is:

$$\text{Number of setups} = \text{Roundup}(387,464 / 1,000) / 2 \text{ tapes} = 194 \text{ setups}$$

##### A-22.4.2 Calendaring

The calendaring process consists of two main steps: preheating and rolling. We will assume that the anode layers are brought together and passed through an infrared tunnel oven for preheating. Assuming that the two layers need to reach 500°C, we can estimate the oven dwell time as (noting that 1 W = 1 J/sec):

$$\text{Oven dwell time} = \frac{\text{Part weight (g)} \times \text{Part specific heat (J/g-}^\circ\text{C)} \times \text{Temperature rise (}^\circ\text{C)}}{\text{Energy input (W)}}$$

If we assume that the same infrared heaters used for drying are used for preheating, the energy rate impinging on the part is:

$$\text{Energy input} = \text{Heater watt density (W/cm}^2\text{)} \times \text{Part area (cm}^2\text{)} \times \text{Energy transfer efficiency}$$

$$\text{Energy input} = 2.3 \text{ W/cm}^2 \times 501.16 \text{ cm}^2 \times 0.80 = 922 \text{ W}$$

The cast anode material has a density of approximately 4.6 g/cm<sup>3</sup> and specific heat capacity of 0.590 J/g-°C.

The volume of anode material per part is:

$$\text{Anode volume} = 501.16 \text{ cm}^2 \times 0.05 \text{ cm} = 25.058 \text{ cm}^3$$

---

<sup>35</sup> B.D. James, J.A. Kalinoski, and K.N. Baum. 2010. *Mass Production Cost Estimation for Direct H<sub>2</sub> PEM Fuel Cell Systems for Automotive Applications: 2010 Update*. NREL Report No. SR-5600-49933. Directed Technologies, Inc. Available at [https://www1.eere.energy.gov/hydrogenandfuelcells/pdfs/dti\\_80kW\\_fc\\_system\\_cost\\_analysis\\_report\\_2010.pdf](https://www1.eere.energy.gov/hydrogenandfuelcells/pdfs/dti_80kW_fc_system_cost_analysis_report_2010.pdf).

The heating dwell time for each is:

$$\text{Anode oven dwell time} = (4.6 \text{ g/cm}^3 \times 13.124 \text{ cm}^3 \times 0.590 \text{ J/g-}^\circ\text{C}) \times 475^\circ\text{C} / 482.9 \text{ W} = 35.0 \text{ sec}$$

For the calendaring process, the layers will be moving together, so the heating time of 35 seconds (0.583 min) is used to determine the required oven length. At a substrate speed of 5 m/min, the required heating length is about 2.92 meters, which can be accomplished using eight 12-inch by 36-inch infrared panels (four for each layer).

At 5 m/min (300 m/hour), part throughput is:

$$\text{Parts per hour} = 300 \text{ m/hr} / 0.187 \text{ m} = 1,604.3 \text{ parts/hr}$$

Once the material layers are preheated, they are compressed between steel rollers that bond the anode layers together. Total machine time to setup and produce 107,000 parts is:

$$\text{Machine time} = (194 \text{ setups} \times 0.5 \text{ hr/setup}) + (1,036,000 \text{ parts} / 1,064.3 \text{ parts/hr}) = 742.8 \text{ hrs}$$

Given an availability of 6,000 hours per year per machine, the number of coating systems required is:

$$\text{Roundup}(742.8 / 6,000) = 1 \text{ machine}$$

Machine utilization is:

$$742.8 / 6,000 = 12.4\%$$

Machine rate was determined in accordance with Appendix A-1 as:

$$\text{In-house rate} = \$26.66 / 0.124 = \$215.00$$

$$\text{Job shop rate} = 1.4 \times (\$26.66 / 0.65) = \$57.43$$

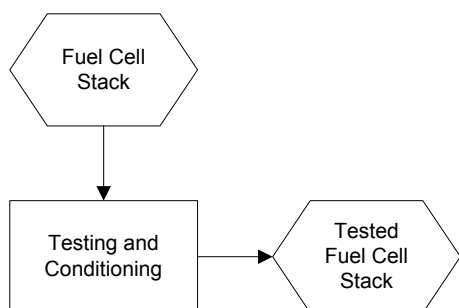
Assuming one operator per casting machine for both setup and operation, the machine labor time is equal to the total machine time of 742.8 hours.

## Appendix A-23: SOFC Testing and Conditioning Process

### A-23.1 Model Approach

- Test and condition fuel cell stack

### A-23.2 Process Flow



### A-23.3 Background

Following assembly, the SOFC stack is tested and conditioned to determine its fitness for installation into a CHP system. The total test time is assumed to be 6 hours, consisting of a 2-hour warm-up at 5% hydrogen (H<sub>2</sub>)/95% nitrogen (N<sub>2</sub>), a 2-hour test at 50% H<sub>2</sub>/50% N<sub>2</sub>, and 2-hour cool-down at 100% N<sub>2</sub>. Total H<sub>2</sub> consumption for a 30-kW stack at full power is 359 l/min. Machine and labor time and material usage will be calculated for production of 4,000 30-kW stacks.

### A-23.4 Preliminary Analysis

The mass of 1 mole hydrogen gas (H<sub>2</sub>) = 2 grams, so the mass of 22.4 liters (stp) of H<sub>2</sub> is 2 g.

$$1 \text{ kg of H}_2 = (1,000 / 2) \times 22.4 \text{ liters} = 11,200 \text{ liters} = 11.2 \text{ m}^3$$

Total gas flow rate is:

$$\text{Total flow rate} = 359 \text{ l/min} \times 60 \text{ min/hr} / 1,000 \text{ l/m}^3 = 21.54 \text{ m}^3/\text{hr}$$

During the 2-hour warm-up, the total material usage is:

$$\text{Hydrogen: Warm-up material usage} = (21.54 \times 0.05) \text{ m}^3/\text{hr} \times 2 \text{ hrs} = 2.154 \text{ m}^3$$

$$\text{Nitrogen: Warm-up material usage} = (21.54 \times 0.95) \text{ m}^3/\text{hr} \times 2 \text{ hrs} = 40.926 \text{ m}^3$$

During the 2-hour full power test, the total material usage is:

$$\text{Hydrogen: Full power material usage} = (21.54 \times 0.50) \text{ m}^3/\text{hr} \times 2 \text{ hrs} = 21.54 \text{ m}^3$$

$$\text{Nitrogen: Full power material usage} = (21.54 \times 0.50) \text{ m}^3/\text{hr} \times 2 \text{ hrs} = 21.54 \text{ m}^3$$

During the 2-hour cool-down, the total material usage is:

$$\text{Nitrogen: Cool-down material usage} = 21.54 \text{ m}^3/\text{hr} \times 2 \text{ hrs} = 43.08 \text{ m}^3$$

Total material cost for a full test and conditioning cycle of 4,000 stacks is:

$$\text{Hydrogen: Testing material usage} = (2.154 + 21.54) \times 4,000 \text{ stacks} = 94,776 \text{ m}^3$$

$$\text{Nitrogen: Testing material usage} = (40.926 + 21.54 + 43.08) \times 4,000 \text{ stacks} = 422,184 \text{ m}^3$$

Material costs we determined in accordance with Appendix A-2 as:

$$\text{Hydrogen cost} = \$4.74/\text{m}^3$$

$$\text{Nitrogen cost} = \$0.423/\text{m}^3$$

We will assume that one operator takes 0.5 hour to for setup and tear-down of each stack on the test stand, and can cover three testing stations, making the total labor time:

$$\text{Testing labor cost} = (0.5 + (0.33 \times 6) \text{ hrs/stack}) \times 4,000 \text{ stacks} = 10,000 \text{ hrs}$$

We will assume that each test stand can support three stacks simultaneously, making the total machine time:

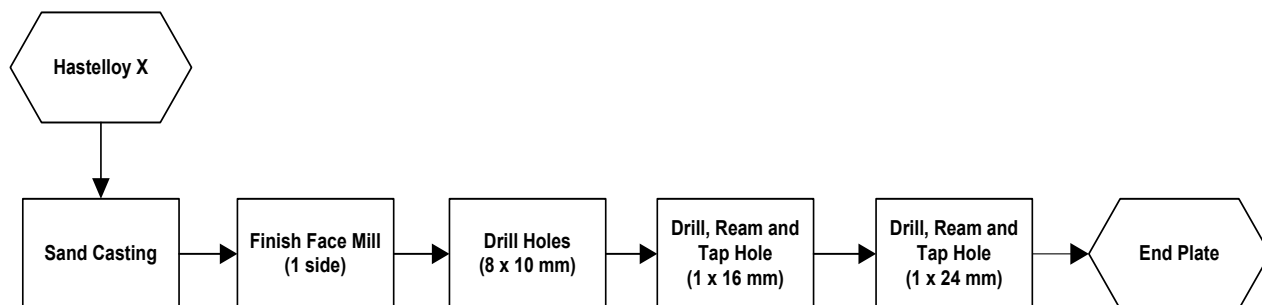
$$\text{Testing machine time} = (0.5 + 6) \text{ hrs/stack} \times 4,000 \text{ stacks} / 3 \text{ stacks/test stand} = 8,667 \text{ hrs}$$

## Appendix A-24: SOFC End Plate Manufacturing Process

### A-24.1 Model Approach

- Use standard Boothroyd Dewhurst, Inc. (BDI) cell machining cost analysis
  - Near net shape workpiece
  - Face mill bottom
  - Ream, and tap gas connector mounting holes

### A-24.2 Process Flow

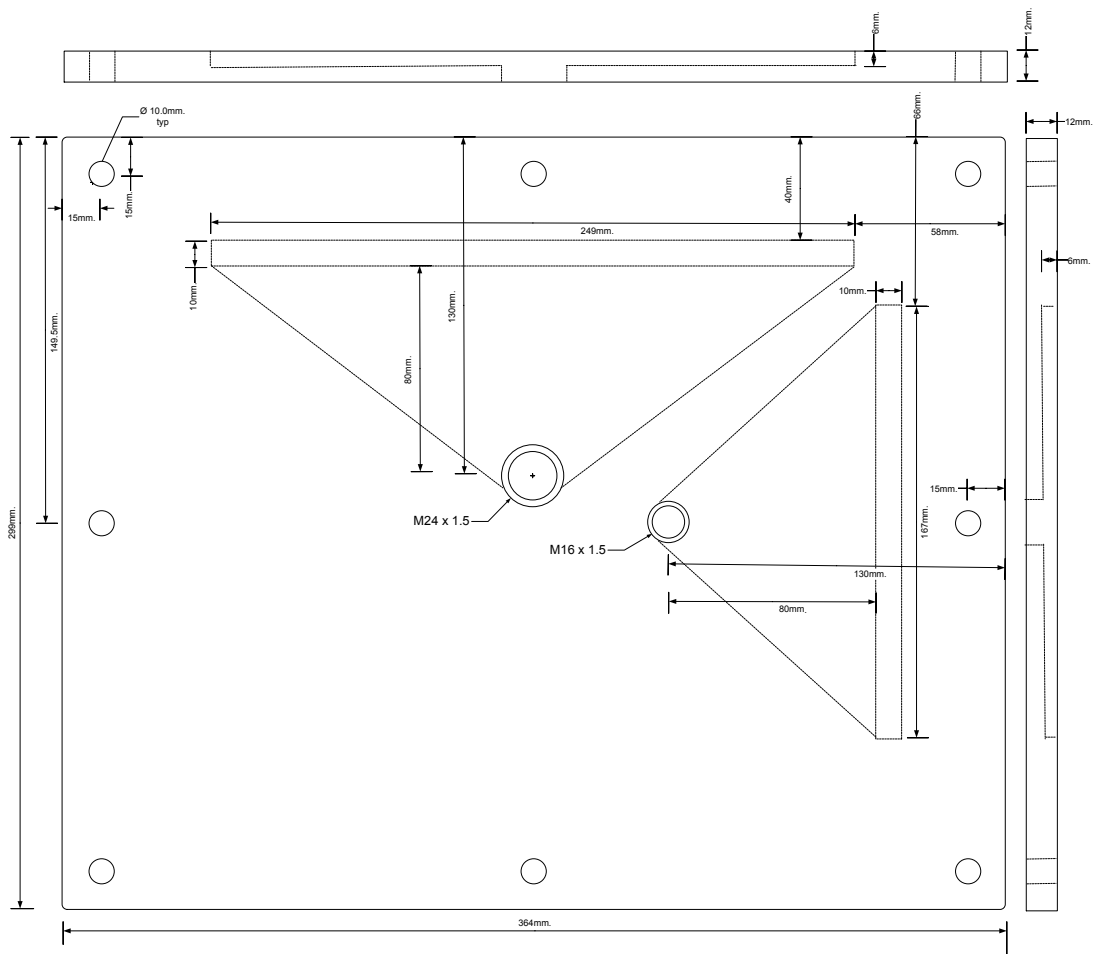


### A-24.3 Background

The BDI software provides pre-programmed cost models for the casting and cell machining operations used to manufacture the fuel cell stack end plates. The end plates need to be rigid in order to apply even pressure across the face of the stack. The process selection for the SOFC end plate was automatic sand casting of A356 cast aluminum to near net shape, followed by finish machining of the stack contact face on a Haas VF-3B vertical machining center, drilling the tie rod holes, and drilling, reaming and tapping the holes for fuel and exhaust.

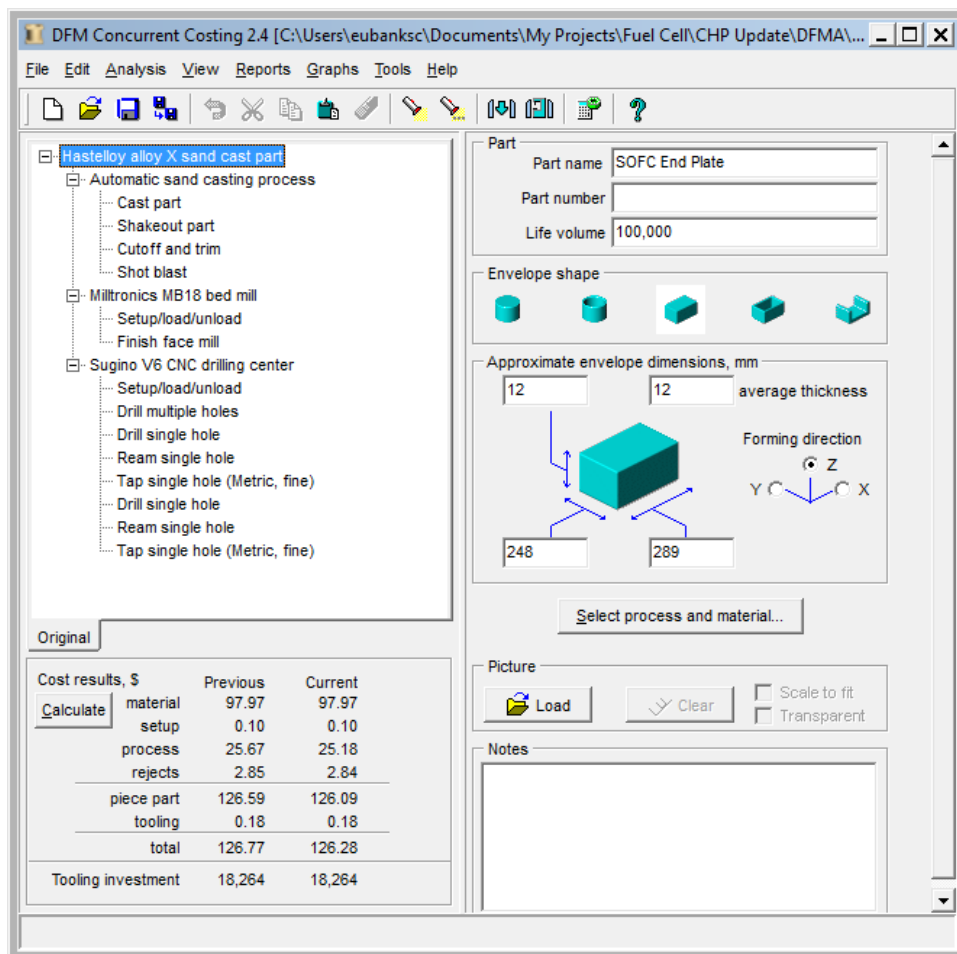
## A-24.4 Preliminary Analysis

The end plate features and dimensions are show below:



## A-24.5 DFM Software Analysis

### A-24.5.1 End Plate



The BDI software estimates a 17.78-hour machine setup time and calculates the total manufacturing time for the end plates as 3,669 seconds, making the total machine time for annual production of 4,000 30-kW systems:

$$\text{Machine time} = (3,669 \text{ sec/part} / 3,600) \times 8,000 \text{ parts} + 17.78 = 8,171 \text{ hrs}$$

Because total time exceeds available single machine time, machine utilization is:

$$\text{Utilization} = 8,171 / (2 \times 6,000) = 68.1\%$$

Machine rate was determined in accordance with Appendix A-1 as:

$$\text{In-house rate} = \$53.89 / 0.681 = \$79.13$$

$$\text{Job shop rate} = 1.4 \times (\$53.89 / 0.65) = \$116.07$$

Assuming two full-time operators (one for casting, one for machining) per station, the total machine labor time is equal to twice the machine time = 16,342 hours.

Tooling cost is \$15,042 and is assumed to be capable of producing 180,000 parts. Amortizing over a 5 year production life, the total annual tooling cost is:

$$\text{Annual tooling cost} = \frac{1}{5}(\text{Tooling cost} \times \text{Number of tools purchased})$$

where:

$$\text{Number of tools purchased} = \text{Roundup}(\text{Total production} / \text{Tool life})$$

$$\text{Total production} = \text{Annual production} \times 5$$

$$\text{Annual tooling cost} = \frac{1}{5}((\$15,042) \times \text{Roundup}((8,000 \text{ parts/yr} \times 5 \text{ yrs}) / 180,000 \text{ parts/tool})) = \$3,008.40$$

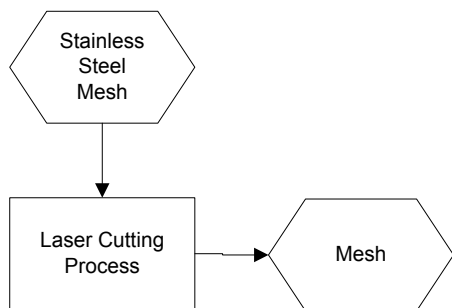


## Appendix A-25: Mesh Production Process

### A-25.1 Model Approach

- Stainless steel mesh laser cutting operation

### A-25.2 Process Flow



### A-25.3 Background

The SOFC cell contains two meshes:

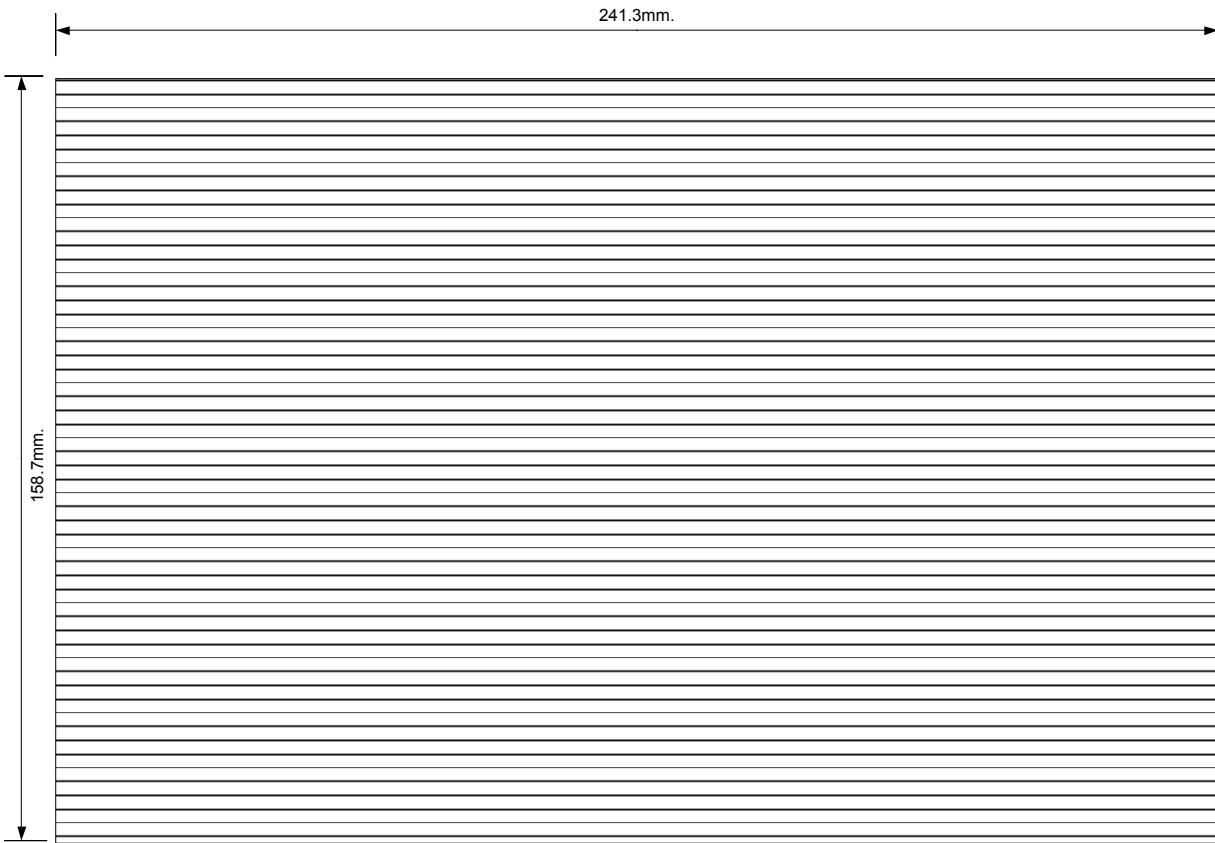
- The anode mesh is 0.5 mm thick and provides directed anode gas flow and electrical contact between the anode contact layer and interconnect.
- The cathode mesh is 0.75 mm thick and provides directed cathode gas flow and electrical contact between the cathode contact layer and interconnect.

### A-25.4 Preliminary Analysis

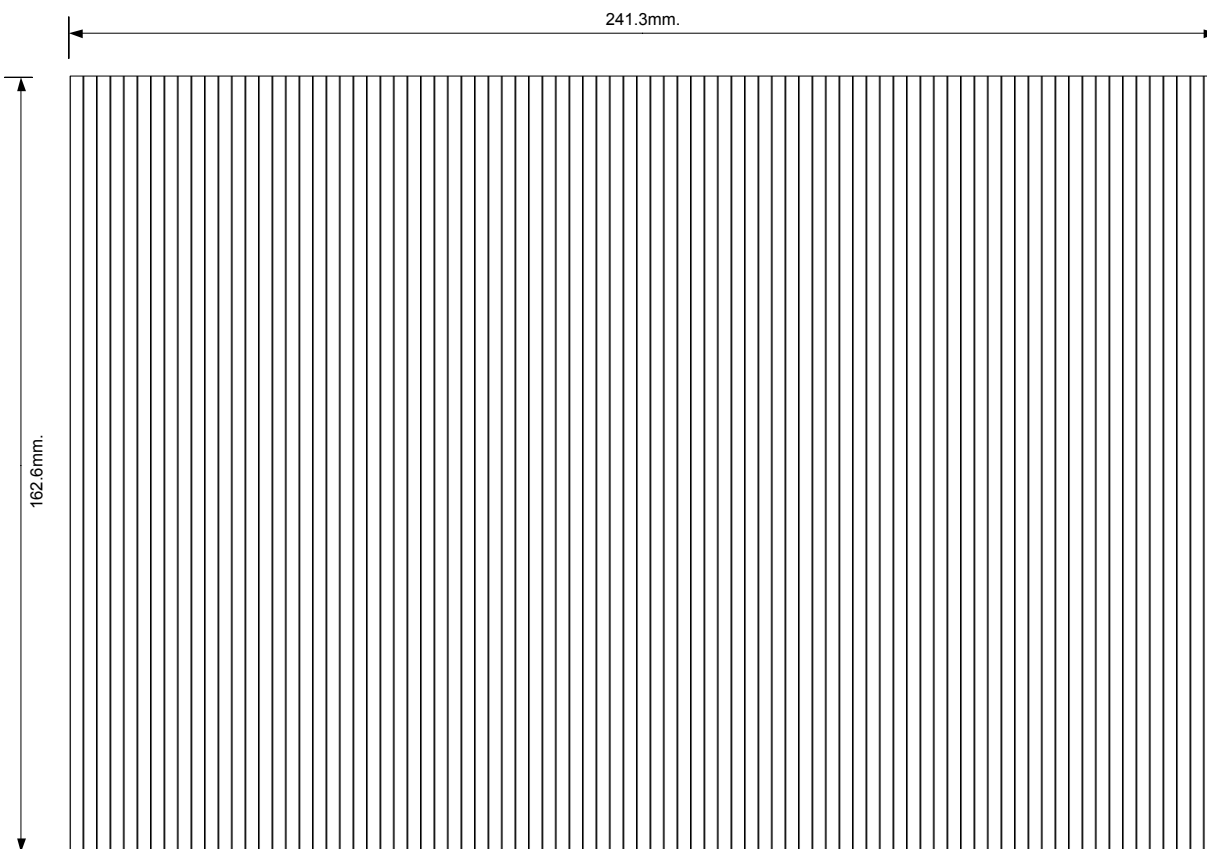
Machine and labor time will be calculated based on an annual production of 4,000 30-kW stacks. The 30-kW stack requires 259 of each type of mesh, requiring production of:

$$\text{Annual production} = 259 \text{ parts/stack} \times 4,000 \text{ stacks} = 1,036,000 \text{ parts/mesh}$$

### A-25.4.1 Anode Mesh Dimensions



### A-25.4.2 Cathode Mesh Dimensions



### A-25.4.3 Laser Cutting Cost

Assuming a single setup operation requiring one operator per batch of parts, the laser cutting setup time will be 0.5 hour.

Part load/unload, which may be manual or robotic, will be driven by overall part size. Using the handling time formula adapted from the Boothroyd Dewhurst, Inc. (BDI) Design for Manufacture and Assembly (DFMA)<sup>®</sup> software, the total handling time is:

$$\text{Anode mesh handling time} = \text{Max}((0.3 \times ((241.3 + 158.7 + 0.5) / 25.4) - 4.6), 4) = 4.0 \text{ sec/part}$$

$$\text{Cathode mesh handling time} = \text{Max}((0.3 \times ((241.3 + 162.6 + 0.75) / 25.4) - 4.6), 4) = 4.0 \text{ sec/part}$$

The total cutting length for the meshes is:

$$\text{Anode mesh cutting length} = (2 \times (241.3 + 158.7)) = 800 \text{ mm}$$

$$\text{Cathode mesh cutting length} = (2 \times (241.3 + 162.6)) = 808 \text{ mm}$$

Research suggests that laser cutting of 0.75 mm thick stainless steel can be performed using a 1,500-W YAG laser under pure nitrogen flow of 8.0 m<sup>3</sup>/hr at a maximum speed of approximately 15.0 m/min (250 mm/sec). Assuming that the mesh has similar cutting properties as stainless steel plate, the time to cut the mesh is:

$$\text{Anode mesh cutting time} = 800 \text{ mm} / 250 \text{ mm/sec} = 3.20 \text{ sec/part}$$

$$\text{Cathode mesh cutting time} = 808 \text{ mm} / 250 \text{ mm/sec} = 3.23 \text{ sec/part}$$

The total machine time required is:

$$\text{Total machine time} = ((3.20 + 4) + (3.23 + 4)) \text{ sec/part} / 3600 \times 259 \text{ cells/stack} \times 4,000 \text{ stacks} = 4,153 \text{ hrs}$$

Machine utilization is:

$$\text{Utilization} = 4,153 / 6,000 = 69.2\%$$

Machine rate was determined in accordance with Appendix A-1 as:

$$\text{In-house rate} = \$33.81 / 0.692 = \$48.86$$

$$\text{Job shop rate} = 1.4 \times (\$33.81 / 0.65) = \$72.82$$

Given that the operator required time for load/unload is about the same as the total part processing time, we will assume one operator per machine, making the machine labor hours equal to 4,153 hours.

At a consumption rate of 8.0 m<sup>3</sup>/hr, the nitrogen material usage is:

$$\text{Material usage} = 8.0 \text{ m}^3/\text{hr} \times ((3.20 + 3.23) \text{ sec} / 3,600) \times 259 \text{ cells/stack} \times 4,000 \text{ stacks} = 14,803 \text{ m}^3$$

Material cost was determined in accordance with Appendix A-2 as:

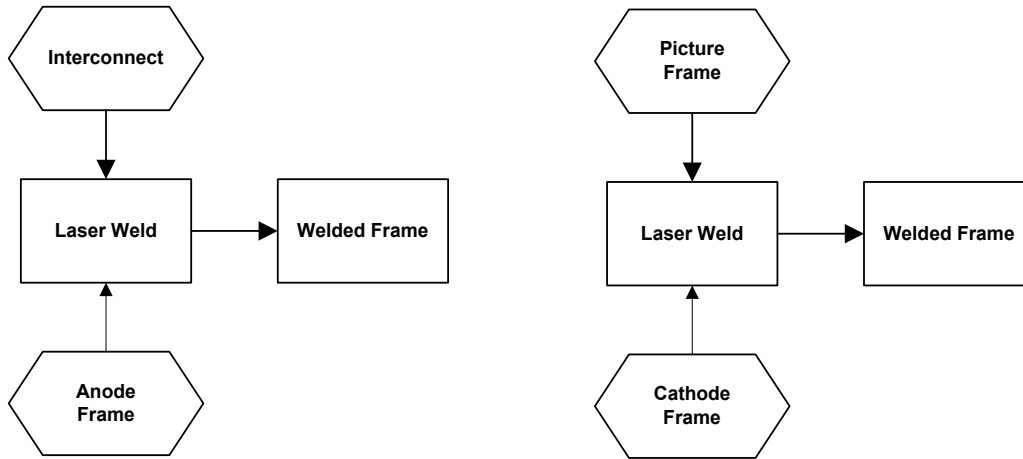
$$\text{Material cost} = \$0.423/\text{m}^3$$

## Appendix A-26: Laser Welding Process

### A-26.1 Model Approach

- Laser weld anode frame to interconnect
- Laser weld picture frame to cathode frame

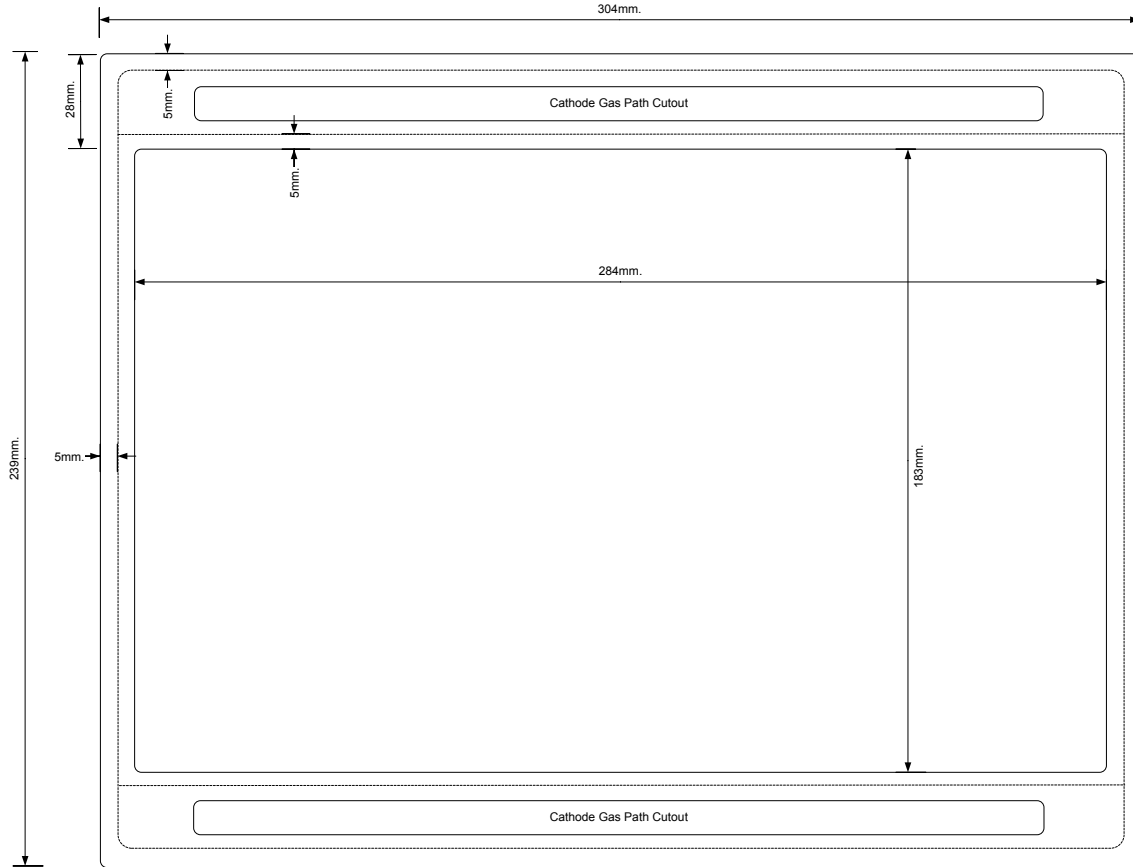
### A-26.2 Process Flow



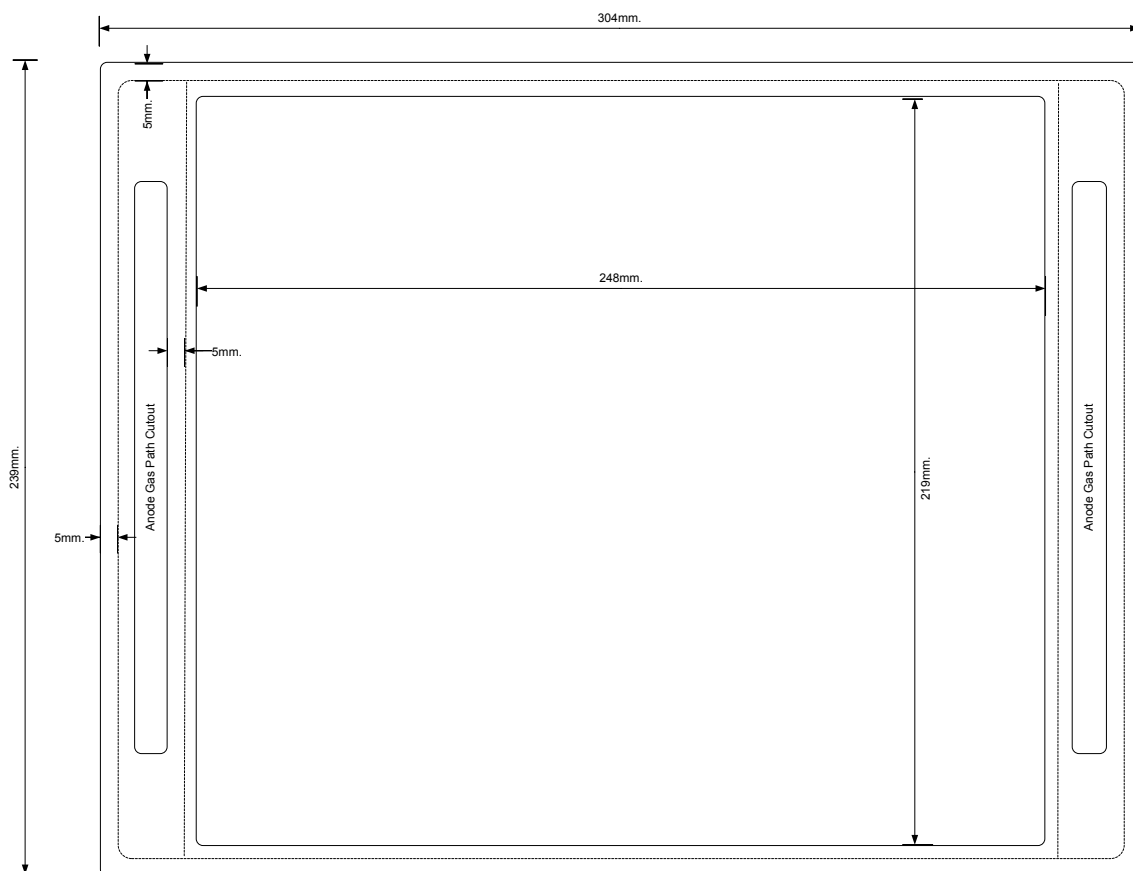
## A-26.3 Background

Prior to final assembly and sealing of each SOFC cell, the SOFC frames are laser-welded as shown:

### A-26.3.1 Anode Frame to Interconnect Welding Path



### A-26.3.2 Picture Frame to Cathode Frame Welding Path



### A-26.4 Preliminary Analysis

The cells for this analysis are for a 100-kW<sub>net</sub> system at a production rate of 4,000 stacks per year (1,000 systems with four stacks per system).

The 30-kW stack requires 259 cells, requiring total annual production of:

$$\text{Annual production} = 259 \text{ parts/stack} \times 4,000 \text{ stacks} = 1,036,000 \text{ parts}$$

#### A-26.4.1 Laser Welding Cost

Assuming a single setup operation requires one operator per batch of parts, the final trim setup time will be 0.5 hour.

Part load/unload, which may be manual or robotic, will be driven by overall part size. Using the handling time formula adapted from the Boothroyd Dewhurst, Inc. (BDI) Design for Manufacture and Assembly (DFMA)<sup>®</sup> software, the total handling time is:

$$\text{Part handling time} = \text{Max}((0.3 \times ((239 + 304 + 0.50) / 25.4) - 4.6), 4) = 4.0 \text{ sec/part}$$

The total welding length for the frames is:

$$\text{Anode frame weld length} = (2 \times (239 - 10)) + (4 \times (304 - 10)) = 1,634 \text{ mm}$$

$$\text{Cathode frame weld length} = (2 \times ((304 - 10) + (239 - 10))) + (4 \times (239 - 10)) = 1,504 \text{ mm}$$

Dilas suggests that laser welding to a depth of 0.5 mm in stainless steel can be achieved using a 500-W YAG laser at a maximum speed of 6.0 m/min (0.10 m/sec). The time to weld the frames is:

$$\text{Anode frame weld time} = 1.634 \text{ m} / 0.10 \text{ m/sec} = 16.34 \text{ sec/part}$$

$$\text{Cathode frame weld time} = 1.504 \text{ m} / 0.10 \text{ m/sec} = 15.04 \text{ sec/part}$$

The total machine time required for welding both sets of frames is:

$$\text{Total machine time} = ((16.34 + 4) + (15.04 + 4)) \text{ sec/part} \times 1,036,000 \text{ parts} / 3,600 = 11,333 \text{ hrs}$$

Machine utilization is:

$$\text{Utilization} = 11,333 / (2 \times 6,000) = 94.4\%$$

Machine rate was determined in accordance with Appendix A-1 as:

$$\text{In-house rate} = \$16.80 / 0.944 = \$17.80$$

$$\text{Job shop rate} = 1.4 \times (\$16.80 / 0.65) = \$36.18$$

Given that the operator required time for load/unload represents about 34% of the total part processing time, we will assume one operator is capable of operating two machines, making the machine labor hours:

$$\text{Machine labor hrs} = 11,333 / 2 = 5,666.5 \text{ hrs}$$